

University of Washington

Abstract

Spatial and Temporal Models of Migrating Juvenile Salmon with Applications

by Richard W. Zabel

Chairperson of the Supervisory Committee: Professor James J. Anderson
Fisheries Research Institute

The downstream migration of juvenile salmon is a critical phase of salmon life history. Individuals are susceptible to mortality from a variety of sources, and in the Columbia River system, hydroelectric dams are a further source of mortality. Models that describe the spatial and temporal distribution of populations of fish can aid in the understanding of juvenile salmon behavior and can be used as management tools. This dissertation presents several models of the distribution of migrating juvenile salmonids. The models are derived from diffusion equations and are expressed as probability density functions. Likelihood functions are formulated from the probability densities and data, and parameter estimation and alternative model comparison are based on the likelihoods.

A two parameter travel time model is effective at describing the arrival time distributions of run-of-the-river, yearling chinook. One of the parameters determines the rate of downstream migration; the other parameter determines the rate of population spreading. After model parameters are related to date of release and river flow in a nonlinear regression equation, the model is used predictively. With subyearling chinook, a delay term, which represents delay in the initiation of migration, substantially improves the travel time model. In addition, fish length is determined to be important in modeling sockeye and subyearling chinook travel time. The vertical distribution of juvenile salmonids in the forebay is modeled based on a chemotaxis equation, where the fish cue on light intensity. The correspondence between the model and data is good.

Table of Contents

1	Introduction	4
1.1.	Anadromous salmonid biology	8
2	Overview of models of dispersing animals	16
2.1.	Introduction	16
2.2.	Models of individual movements	17
2.3.	Group movements	19
2.4.	Waiting time, Poisson process	25
3	General statistical treatment of spatio-temporal models	27
3. 1.	Introduction	27
3. 2.	Forms of data	27
3. 3.	Forms of the models	28
3. 4.	Parameter estimation	29
3. 5.	Confidence intervals	31
3. 6.	Goodness-of-fit	32
3. 7.	Model discrimination, model selection, generalized likelihood ratio test	37
3. 8.	Statistical simulations	41
3. 9.	Types of data	42
4	Basic travel time model	45
4.1.	Introduction	45
4.2.	Development of basic model	46
4.3.	Statistical methods	53
4.4.	Simulations	59
4.5.	Application to discrete time data	64
4.6.	Application to continuous data	70
4.7.	Appendices	81
5	Extensions of the travel time model	98
5.1.	Introduction	98
5.2.	Time dependent mortality	99
5.3.	Delay in migration	104
5.4.	Predicting model parameters and travel times	118
6	Travel time model with individual covariates	135
6.1.	Introduction	135
6.2.	Development of model and statistical technique	136
6.3.	Applications with length covariate	137
6.4.	Multiple covariate model	143
7	Movements of individuals	151
7.1.	Introduction and motivation	151
7.2.	Models	152
7.3.	Statistical analysis	157
7.4.	Application to radio-tracking data	160

8 Vertical distribution models	165
8.1. Introduction	165
8.2. The model	168
8.3. Example – light gradient	169
8.4. Application to data	171
8.5. Discussion	175
9 Summary	177
9.1. Overview	177
9.2. Summary by chapter	177
9.3. Recommendations for salmon population management	180
References	184
Appendix 1. PIT tag release groups	198
Appendix 2. Cohort covariates	212
Appendix 3. Computer code	217
A3.1. Introduction	217
A3.2. Analysis of continuous travel time data	217
A3.3. inverse Gaussian random variate	224

1. Introduction

Salmon populations in the Columbia River system have declined dramatically in the past century. A century ago, an estimated 8 - 16 million adult salmon and steelhead returned to the Columbia River each year (Chapman, 1986; NPPC, 1992). A current estimate of adult returns is 2.5 million, and many of these returnees are hatchery stock (NPPC, 1992). In addition to reduction in numbers, the elimination of runs associated with particular tributaries has resulted in a loss of genetic diversity. This alarming reduction in salmon runs prompted Congress to pass the Pacific Northwest Electric Power Planning and Conservation Act in 1980, which dictates that a certain percentage of revenues generated from hydroelectricity be directed to restoring salmon populations. In addition, in 1991 Snake River sockeye were listed under the Endangered Species Act, and Snake River chinook were also listed as threatened in 1992. Currently, other stocks are being considered for this status.

The Columbia Basin is an extensive region extending into the states of Washington, Oregon, Idaho, and Montana, and the province of British Columbia (Figure 1.1). In addition to the Columbia River and its major tributary, the Snake River, many tributaries, including the Yakima, Wenatchee, Methow, Clearwater and Salmon Rivers, comprise the Columbia River system. Several species of anadromous¹ salmonids² inhabit the Columbia River system – sockeye (*Oncorhynchus nerka*), coho (*O. kisutch*), chinook (*O. tshawytscha*), and steelhead

1. Anadromous fish are reared in freshwater habits, migrate to saltwater habitats, and return as adults to freshwater habitats to spawn.

2. Salmonids are salmon and their close relatives, including trout.

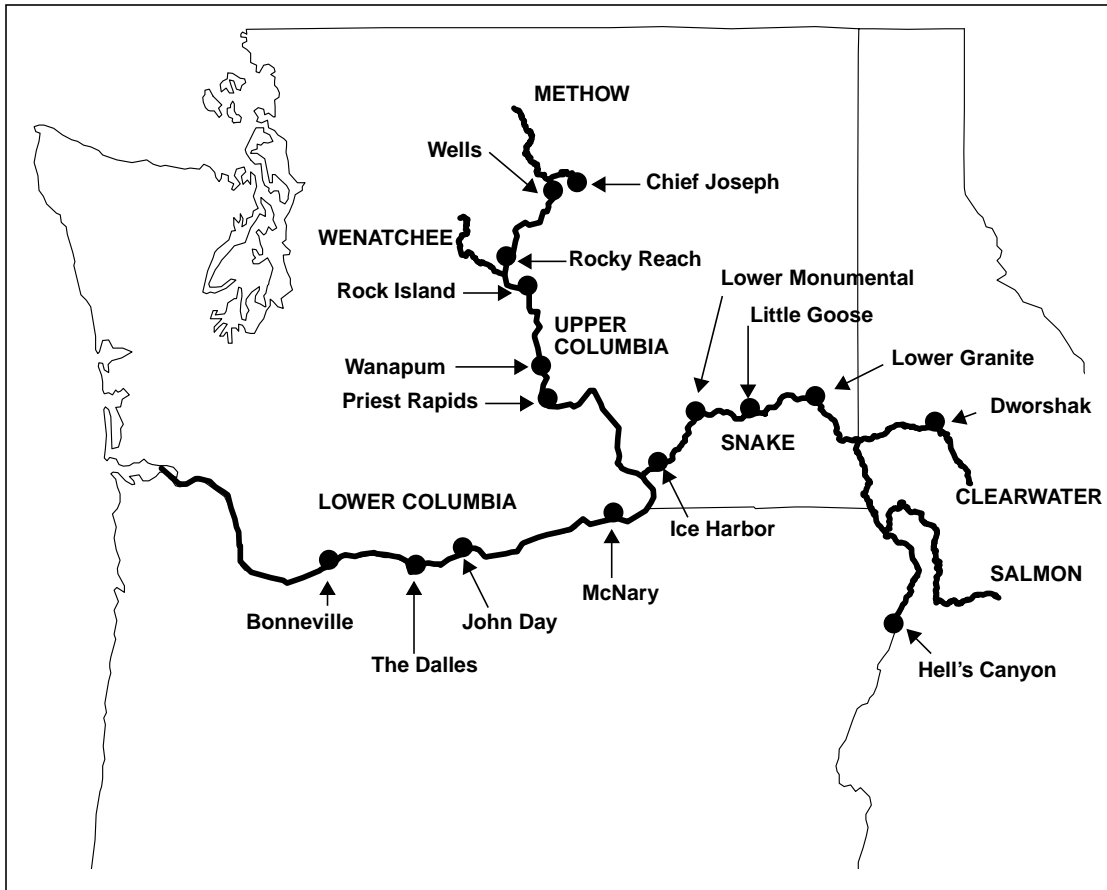


Figure 1.1 A map showing the major features of the Columbia River Basin in Washington, Oregon, and Idaho.

(*O. mykiss*).

Anadromous salmonids spend the first part of their lives in rivers or lakes and then migrate downstream to saltwater as juveniles. After an extended period of growth in saltwater, they return to a freshwater environment to spawn. Because of their migratory nature, they encounter a variety of habitats and thus are exposed to several different sources of mortality. The accumulation of these effects has greatly reduced their numbers in the Columbia River system. Spawning and rearing habitat has been degraded due to development, irrigation, and logging practices. Also, some dams, such as the Grand Coulee, are impassable to fish, and rearing habitat has been entirely lost upstream from the dam. As a result, over fifty percent of spawning habitat has been eliminated above McNary Dam (Raymond, 1988). In the ocean, harvest of adults by sport and commercial fisheries is an additional source of mortality.

The downstream migration of juvenile salmon is a particularly critical stage of the salmon life history (NPPC, 1992), but migratory behavior is not well understood. Some species of salmon migrate for hundreds of miles as juveniles and in doing so incur heavy mortality due to factors such as predation and disease. In addition, during outmigration juvenile salmon undergo smoltification, a series of physiological, behavioral and biochemical changes preparing them for a saltwater habitat (Hoar, 1976). Since arrival to the estuary is coordinated with smoltification (Folmar and Dickhoff, 1980), the timing of outmigration is important to ensure that the smolts reach saltwater when they are physiologically ready.

In the Columbia River system, the downstream migrants are exposed to further hazards due to the presence of dams – some runs must pass nine dams during their migration. In addition to being a direct source of mortality, dams complicate the migration process by creating large reservoirs in which river velocity is significantly reduced (Raymond, 1968),

potentially disrupting the timing of migration. Also, the reservoirs have higher temperatures and less turbidity compared to free flowing rivers, potentially resulting in greater susceptibility to predation and disease (Park, 1969). In light of this, it is not surprising that mitigation efforts have targeted the downstream migration phase as crucial in terms of revitalizing salmon populations in the Columbia River system.

In this thesis, I develop spatial and temporal models of distributions of migrating juvenile salmonids. Model building and testing can be an important component in natural resource management. Models allow for the examination of various long term management scenarios without conducting costly experiments. The predictive ability of models is a useful tool in day to day operations. Also, the process of developing models and applying them to data enhances the understanding of the animal's behavior.

In all cases, the models I develop have practical applications, so comparing the models to data is important. In analyzing data, I have several objectives. First of all, I estimate parameters and construct confidence intervals. Secondly, I assess whether the models are consistent with the data; this involves goodness-of-fit tests. In some cases I evaluate which factors – biotic and abiotic – are important to the models. Finally, I attempt to use the models as predictive tools with independent data.

For the remainder of this chapter, I provide a brief overview of salmon biology and behavior relevant to modeling migrating populations. Chapter 2 reviews the use of models to describe dispersing animal populations. Chapter 3 covers the statistical procedures I follow and discusses the data used in the applications. Chapter 4 presents a model of the travel time of juveniles through a reservoir and includes applications to group releases of migrating chinook salmon and steelhead. Several extensions to the travel time model are presented in chapter 5 – time dependent mortality, delay in migration, a migrational effort component, and time variable parameters. In chapter 6, I develop methods to apply the

travel time model to individuals, and in the process, assess which individual covariates are important to the model. In chapter 7, I develop models of the movement patterns of individuals and apply the models to radio-tracking data. Chapter 8 contains a model of the vertical distribution of fish in the water column in relation to environmental gradients.

All computational algorithms are written in the C programming language (Kernighan and Ritchie, 1978) and run on a Sun Sparcstation 2. Plots were constructed and some of the statistical analyses performed using the S-plus statistical/graphical software package (Becker, et al., 1988).

1.1. Anadromous salmonid biology

overview of anadromous salmonid life history

Although quite variable in their life histories (within and among species), anadromous salmonids share the following traits. Adult fish spawn in freshwater streams or lakes, usually in late summer or fall (Groot and Margolis, 1991). Their large yolky eggs are buried in the substrate, and embryonic development occurs here (Thorpe, 1984). The juveniles emerge from the substrate the following spring as “fry” and are dependent on external food sources upon emerging (Thorpe, 1984). The life histories of the various species diverge at this point, with some species migrating to the estuary at this stage and other species delaying their migration for months or years (Northcote, 1984). After passing through the estuary, the fish carry out most of the growth in the ocean. Depending on the species and stock, the fish spend between one and seven years in the ocean (Groot and Margolis, 1991). Adults then return to their natal streams or lakes (although some straying is common (Quinn, 1984)) and die shortly after spawning.

chinook salmon

Chinook salmon are divided into two “races” (or subspecies, depending on nomenclature), both of which inhabit the Columbia River system. “Ocean-type” chinook

return as adults in the late summer or fall and spawn almost immediately after reaching the natal stream (Healy, 1991). The juveniles migrate as subyearlings, usually several months after emerging as fry, although timing of emigration is quite variable (Reimers and Loeffel, 1967). This group is also referred to as “chinook 0’s” or as fall chinook. Ocean-type chinook are generally found in the southern part of the species’ range. “Stream-type” chinook return as adults in the spring and delay spawning for several months. The juveniles migrate as yearlings after overwintering in the river environment. These fish, also referred to as “chinook 1’s” or as spring chinook, are generally found in the northern part of the species’ range. Although the two types of chinook may occupy the same streams, they appear to be genetically distinct (Carl and Healy, 1984) and show heritable behavioral differences (Taylor and Larkin, 1986; Taylor, 1988). Stream-type juveniles display higher levels of antagonistic behavior and stronger positive current response, consistent with defending territory and extended residence in streams.

sockeye

The life history of sockeye salmon is the most variable of all the Pacific salmon, with a wide variety of adaptations for specialized conditions (Burgner, 1991). In addition to the anadromous form, there is a landlocked form commonly referred to as kokanee. Anadromous sockeye usually spawn in the tributaries of lakes (Groot, 1982). Upon emergence, the fry migrate to a nursery lake where they may spend 1 to 3 years. The sockeye smolts then migrate downstream to the ocean. Ocean residence for sockeye is variable, ranging from 1 to 4 years (Burgner, 1991).

steelhead trout

Steelhead trout (*Oncorhynchus mykiss*) is the same species as rainbow trout, with steelhead a migratory form and rainbows a landlocked form. Steelhead, until recently, were classified as *Salmo gairdneri*, partially reflecting their morphological and behavioral

similarities to Atlantic salmon (*Salmo salar*) (Netboy, 1980). The change of nomenclature is based on the Pacific coast origin of the species and an alignment with Pacific salmon (Light, et al., 1989). The Columbia River Basin is the world's largest producer of steelhead (Netboy, 1980; Light, 1987). Steelhead are generally split into two races: "winter" steelhead return as adults between November and April; and "summer" steelhead return as adults from May to October (Withler, 1966). In the Columbia Basin, winter-run steelhead are found exclusively west of the Cascades, while summer-run steelhead are found in some western tributaries and are the only steelhead found in the Snake and upper Columbia Rivers and their tributaries (Pevin, 1990). Smolts usually migrate in the spring of their second year, but there is variability in the duration of freshwater residence (Withler, 1966). The majority of steelheads spend 2 years in the ocean before returning as adults (Pevin, 1990). Unlike Pacific salmon, steelhead don't always die after spawning (Childerhouse and Trim, 1979). A small percentage return to the ocean after spawning and then return back to freshwater the following year to spawn again.

coho

In Washington and Oregon, coho are found primarily in coastal streams and tributaries of the Lower Columbia (Sandercock, 1991). The freshwater residence of coho is quite variable, and they have the most extended stream residence of Pacific salmon (Taylor and Larkin, 1986). Because few wild populations of coho undergo extensive migrations in the Columbia River or its tributaries, I do not analyze any coho data in this thesis.

smoltification

The initiation of migration is preceded by the parr-smolt transformation (smoltification) (Folmar and Dickhoff 1980), in which the juveniles transform from a stage in their life history adapted for stream inhabitation to a stage adapted for downstream migration and eventually saltwater inhabitation. Smoltification is a series of morphological,

physiological, and behavioral changes. A discussion of smoltification is important for two reasons. First, the morphological, physiological and behavioral changes are all related, and thus understanding how each operates can help elucidate the behavioral changes important to modeling. Also, it is clear that the timing associated with smoltification is critical, and this lends importance to the travel time studies.

Behaviorally, the fish undergo several changes. Prior to smoltification, the fish exhibit positive rheotaxis (Thorpe and Morgan, 1978), and maintain their position in the river or lake. They are also territorial bottom dwellers. Upon smoltification, fish are less prone to hold position against the current, and thus downstream movement becomes initiated. In addition, they become less territorial and more surface oriented.

Morphological changes that occur during smoltification are a silvering in body color and a decrease in weight per unit length (commonly referred to as condition factor) (Wedemeyer, et al. 1980), resulting in a more slender and streamlined fish. Some evidence exists for a threshold size that may be important in the timing of seaward migration (Folmar and Dickhoff, 1980).

Physiologically, several changes occur during smoltification. First, there is heightened hypoosmotic regulatory capability that increases salinity tolerance and preference. Endocrine activity increases, notably in greater levels of thyroxine, and according to Hoar (1965), the endocrine system forms a chemical link between the organism and the environment. The higher hormonal levels may also induce a behavioral response; Godin et al. (1974) demonstrated that artificially increasing thyroxine levels in Atlantic salmon smolts leads to increased migratory behavior. Also, an increase in gill $\text{Na}^+\text{-K}^+$ ATPase activity is typical of fishes existing in saltwater environments. In fact gill $\text{Na}^+\text{-K}^+$ ATPase is often sampled to assess the level of smoltification in juveniles (Zaugg, 1982).

Clearly, smoltification is a complex process, and events are coordinated such that fish are ready to enter saltwater at the appropriate time. Flagg and Smith (1982) determined that juvenile coho with visual signs of smoltification suffered no loss of swimming stamina when transferred from freshwater to seawater, while juveniles without these signs did suffer a loss in swimming stamina. Fish that weren't transferred from fresh water to sea water at the proper time appeared sluggish, potentially increasing their susceptibility to predation. Flagg and Smith (1982) also determined that mortality associated with salt water stress was inversely related to levels of thyroxine and Na^+ , K^+ ATPase, which are indicators of degree of smoltification. Observations also show that some species of salmonids revert back to a freshwater adapted state if they don't reach saltwater within a certain time frame (Hoar, 1976). It appears that a species and stock specific optimal period for reaching saltwater exists that maximizes survival of the fish. Thus, modeling the temporal aspects of migratory behavior can be beneficial in coordinating migrations of hatchery stocks and in determining deleterious effects of delaying the migration of wild stocks.

juvenile salmon migratory behavior

Clearly, many facets of juvenile salmon migratory behavior are not well understood. Behavior patterns are quite variable among species, and in some cases, among stocks. It is possible to generalize some types of behavior across species, but with other types of behavior it is important to note differences. In many cases where a group of workers establishes a behavior pattern for a particular species, another group offers a counter example

In this section, I present some questions pertaining to salmon migratory behavior and results of studies examining these issues. While my focus is on the behavior of steelhead, chinook, sockeye, and coho, I will also present results based on other species of

anadromous salmonids, including Atlantic salmon (*Salmo salar*) and sea trout (*Salmo trutta*).

- What cues the initiation of migration?

A combination of endogenous and exogenous factors cue the initiation of migration. As Groot (1982) stated, “environmental factors interact with endogenous rhythms to modify the organism morphologically, physiologically, and behaviorally to a state of migration readiness, or migration disposition.” The physical and physiological changes mentioned above prepare the fish for migration, but exogenous cues may actually trigger the onset of migration. Several people have demonstrated the importance of photoperiod (Hoar, 1976; Giorgi, et al., 1990). Also, a study by Holtby et al. (1989) indicated that a combination of seasonal timing (perhaps cued by photoperiod) and temperature are important in determining when coho smolts initiate downstream migration. High flows or “freshets” may also induce the juveniles to move downstream.

- Is migration active or passive?

Some dispute exists as to the degree of active migration undertaken by juveniles during downstream migration. Some people argue that active migration would unnecessarily expend energy reserves (Thorpe, 1982) when downstream migration could be achieved by an entirely passive process. Others argue that active migration decreases the time spent migrating and thus minimizes exposure to predators (Neave, 1955). As with other behavioral traits in salmonids, the degree of active migration probably varies among species. Thorpe (1982) speculates that pink, chum and sockeye salmon undergo active migration while coho, chinook and Atlantic salmon partake in passive migration. Many studies are consistent with this speculation. Johnson and Groot (1963) concluded that sockeye smolts migrated actively through the Babine Lake system in British Columbia, and

Groot (1965) observed active migration in sockeye smolts, where the fish migrated at close to their maximum sustained speed. Also, Bax (1982) concluded that chum salmon in the Hood Canal in Washington actively migrated downstream. On the other hand, several radio-tracking studies of Atlantic salmon (Fried, et al. (1978), LaBar et al (1978), and McCleave et al. (1978) in a Maine estuary; Thorpe, et al. (1981), Tytler, et al. (1978) in a Scottish estuary) lend support to passive migration in this species.

Also consistent with passive migration in coho and Atlantic salmon are studies determining that some smolts exhibit a loss of swimming proficiency as compared to fish in the parr stage. Smith (1982), Flagg and Smith (1982) and Glova and McInerney (1977) observed this with coho, and Thorpe and Morgan (1978) determined sustained swimming velocities of Atlantic salmon juveniles decreased substantially during the period of peak downstream migration. It is not clear, though, whether this loss of swimming “proficiency” is due to a physical change or, as Thorpe and Morgan (1978) speculate, “a behavioral refusal to undergo sustained swimming.”

- Do migrating juvenile salmonids have distinct diel patterns?

Hoar (1953, 1956) attributed nocturnal displacement to a loss of visual orientation. Hansen and Jonnson (1985) tested this with Atlantic salmon in the River Imsa, Norway. They trapped significantly more fish during the dark than during the light and concluded that light inhibited displacement. Other studies concluded that Atlantic salmon migrate almost exclusively at night early in the season but lose this tendency as the season progresses (Osterdahl, 1969; Thorpe and Morgan, 1978). Mains and Smith (1964) demonstrated that the majority of ocean-type chinook migration occurs at night in the Columbia and Snake Rivers. There might be less of a tendency for nocturnal migration in stream-type chinook, though (Healy, 1991). Bell (1958) actually observed more migrants during the daylight hours. A study by Meehan and Siniff (1969) in the Taku River in Alaska

demonstrated that chum and coho preferred to migrate at night, while sockeye showed no preference between day and night.

- Do fish school as they migrate?

According to Hoar (1976), sockeye, chum and pink salmon actively school during migration, and the others are strongly territorial, occasionally forming loose aggregations.

- What factors influence migration rate?

Several factors influence downstream migration rate in juvenile salmonids. River velocity is the most obvious factor, and several studies have related migration rate to river velocity or river flow. Berggren and Filardo (1993) demonstrated that river flow is an important factor in predicting migration rates for yearling and sub-yearling chinook and steelhead in the Columbia and Snake Rivers. Bax (1982) correlated downstream migration rate of chum salmon with wind speed in the direction of the migration path, which had an effect on surface currents. Johnson and Groot (1963) determined that migrating sockeye had increased migration rates later in the season. They attributed this to increased “migration drive.” In addition, Washington (1982) provides evidence for a positive relationship between migration rate and fish length with coho smolts.

- What is the spatial distribution of fish in the river?

Bax (1982) determined that juvenile salmonids in the Hood Canal migrate close to the shore early in the season and further offshore later in the season. Mains and Smith (1964) determined that a large proportion of juvenile chinook in the mid-Columbia and Snake Rivers migrated near shore but fish were also found mid-river. In the Hanford reach of the mid-Columbia, Dauble et al. (1989) found that subyearling chinook preferred shallow near-shore locations, and yearling chinook and sockeye smolts preferred deeper mid-channel locations.

2. Overview of models of dispersing animals

2.1. Introduction

In this chapter, I review some models of animal dispersal, focusing on models that I will develop in later chapters.

Models of animal dispersal date back to the early part of this century. Pearson and Blakeman (1908) and Brownlee (1911) are credited with developing the first models of animal dispersal, using random walk models to describe movement patterns. Two landmark works of the middle of the century are Dobzhansky and Wright's (1943), which modeled the dispersal of fruit flies, and Skellam's (1951), which modeled the range expansion of small mammals. Also during this period, Patlak (1953a; 1953b) developed a fairly complex random walk based model of dispersal that was overlooked at the time but has received attention lately. In 1969, two papers marked the beginning of the computer era for dispersal models: Rohlf and Davenport (1969) simulated random walk models to mimic various dispersal behaviors, and Siniff and Jensen (1969) conducted simulations of the movements of foxes and hares in their home ranges. The past two decades have seen many refinements in the models and in methods of applying the models to data.

Models based on the movements of individuals are referred to as "microscopic" models (Aronson, 1985). For these models, the spatial and temporal scales are relatively fine, and more detail can be included in the model. Models based on group dynamics are labeled "macroscopic" models. These models are usually concerned with gross patterns on broader temporal and spatial scales. It is interesting to note that each microscopic model has a corresponding macroscopic model, and *vice versa*. Also, it is not always clear whether a model should be classified as microscopic or macroscopic since there is a gradation

between the two.

2.2. Models of individual movements

random walk models

Simple random walks have formed the basis of several animal movement models. Except in unusual circumstances, however, simple random walks cannot adequately describe the movements of individuals; the random walk represents too much of a simplification. On the other hand, if step size is adequately small and the number of individuals is sufficiently large, the spatial dynamics of a group of random walkers shares many similarities with observed population patterns.

The simple random walk model can be presented as follows. First, assume that an individual moves a distance Δx (in one dimension) during each time interval Δt . Assume that the individual moves to the right with probability α and to the left with probability β , with $\alpha + \beta = 1$. When $\alpha = \beta$ the random walk is termed isotropic, and when $\alpha \neq \beta$ the random walk is anisotropic or biased. After n moves, let n_r be the number of moves to the right and n_l be the number to the left. The position of the individual in units of movement after n steps is

$$m = n_r - n_l. \quad (2.1)$$

The probability of individual occurring at position m after n steps is

$$p(m, n) = \frac{n!}{n_r!n_l!} \alpha^{n_r} \beta^{n_l}; \quad (2.2)$$

that is, $p(m, n)$ follows a binomial distribution. $p(m, n)$ can also be expressed as forward Chapman-Kolmogorov equation (Okubo, 1980):

$$p(m, n) = \alpha \cdot p(m - 1, n - 1) + \beta \cdot p(m + 1, n - 1) . \quad (2.3)$$

The random walk model is easily expanded to two or three spatial dimensions.

Jones (1977) successfully applied a simple random walk on a grid to describe population patterns of cabbage butterflies (*Pieris rapae* L.). An added advantage of random walk models is that behaviors such as taxis, kinesis and density dependence can be easily added to a random walk model, as demonstrated by Rohlf and Davenport (1969).

Several workers have extended the simple random walk model on a regular grid to include movements of various lengths in any direction and correlation in the direction of movements (e.g., Siniff and Jensen, 1969; Skellam, 1973; Kitching and Zalucki, 1982; Kareiva and Shigesada, 1983). In these models, for each movement increment, a length and an angle are drawn from distributions, with the new angle of movement based on the previous angle. Othmer, et al. (1988) provide many modifications to random walk and dispersal models.

Individual movement in continuous time and space

In continuous time and space, the position of an individual can be denoted by $X(t)$, with $X \in R^n$, $n = 1, 2$ or 3 , and $t > 0$. For ease of notation, I will assume $X \in R^1$. The change in position of an individual with respect to time can be described by a stochastic differential equation (SDE) (Gardiner, 1983):

$$\frac{dX}{dt} = r(X, t) + \sigma(X, t) \cdot W(t) . \quad (2.4)$$

$W(t)$ is white noise and has the following properties:

$$\langle W(t) \rangle = 0,$$

$$\langle W(t), W(t + \tau) \rangle = \delta(\tau),$$

where $\delta(t)$ is the Dirac distribution. Ito calculus is assumed. If the parameters r and σ are

constants and $W(t)$ is Gaussian white noise, then $X(t)$ is the Wiener drift process. The Wiener drift process has the following properties (Ross, 1985):

- 1) $X(0) = 0$;
- 2) for $t > 0$, $X(t)$ is normally distributed with mean rt and variance $\sigma^2 t$;
- 3) each disjoint segment of an individual path is independent.

In chapter 7, I apply this process to movement of migrating juvenile salmon.

2.3. Group movements

introduction

The diffusion equation has formed the cornerstone of many models of animal dispersal (Okubo, 1980). While simple passive diffusion is appropriate in some cases, diffusion is often combined with other terms such as population drift or attraction to particular environmental conditions. Also, the simple diffusion equation may be modified to account for factors such as density dependence or variable diffusivity based on environmental conditions.

basic diffusion equation

Ordinary (Fickian) diffusion is a process where the flux J of particles is from high to low concentrations and is proportional to the gradient of concentration. If $p(x,t)$ is concentration (or density), one-dimensional flux is expressed as

$$J = -D \frac{\partial p}{\partial x}, \quad (2.5)$$

with D determining the diffusivity of the particles. Based on equation (2.5), the change in population density through time is

$$\frac{\partial}{\partial t} p(x, t) = D \frac{\partial^2 p}{\partial x^2}. \quad (2.6)$$

In order to solve equation (2.6) for $p(x, t)$, boundary conditions and initial conditions must be specified. The simplest case is to have natural boundaries where X can take on values from $-\infty$ to ∞ , and a point release at $t = 0$ and $X = x_0$. Formally, this is stated as:

$$p(-\infty, t) = p(\infty, t) = 0 ,$$

$$p(x, 0) = \delta(x - x_0) .$$

In this case, the unique $p(x, t)$ that satisfies equation (2.6), assuming $x_0 = 0$ and assuming the parameter D is a constant, is:

$$p(x, t) = \frac{1}{\sqrt{4\pi Dt}} \exp\left(\frac{-x^2}{4Dt}\right) \quad \left(\begin{array}{l} -\infty < x < \infty \\ 0 < t < \infty \end{array} \right) \quad (2.7)$$

(Goel and Richter-Dyn 1974, Gardiner 1983). This solution is a normal distribution with respect to x for fixed t , with mean 0 and variance $2Dt$; note that the variance increases linearly with time.

Both equations (2.6) and (2.7) can be derived from a simple random walk. In the first case, the random walk is expressed as a forward Chapman-Kolmogorov equation with step length Δx and time step Δt . This is then expanded in a Taylor series, higher order terms are ignored, and the diffusion limit is taken, resulting in equation (2.6) (Okubo, 1980). In the second case, the probability of a particle occupying the m th position after n steps, $p(m, n)$, is expressed as a binomial distribution. Using Stirling's formula, $p(m, n)$ is approximated with a normal distribution. The step length and time step are then allowed to become arbitrarily small, and equation (2.7) is obtained (Murray, 1989).

In a classic experiment, Dobzhansky and Wright (1943) released mutant flies

(*Drosophila pseudoobscura*) with orange eyes (to distinguish them from the wild flies) from a point, and then recaptured the individuals along linear transects emanating from the release point. They then compared the observed distribution of flies to equation (2.7). Kareiva (1983) gathered data from mark recapture experiments of 12 species of herbivorous insects, and compared the data to a passive diffusion model. He concluded that in 8 out of 12 cases, a passive diffusion model is consistent with the data.

advection-diffusion

The advection-diffusion equation is appropriate when a population is not only spreading but also “drifting” in a particular direction. This equation can be formulated in one dimension as

$$\frac{\partial p}{\partial t} = -r \frac{\partial p}{\partial x} + D \frac{\partial^2 p}{\partial x^2}, \quad (2.8)$$

where r determines the rate of drifting. With a point release at $x = 0$ and natural boundaries, the solution of equation (2.8) is:

$$p(x, t) = \frac{1}{\sqrt{4\pi Dt}} \exp\left(\frac{-(x - rt)^2}{4Dt}\right). \quad (2.9)$$

For fixed t this is a normal distribution with mean rt and variance $2Dt$. These two equations are derived in a similar manner to the corresponding ordinary diffusion equations but starting with a biased random walk – a random walk where the probability of moving to the right is not equal to the probability of moving to the left.

The advection-diffusion equation has been used most commonly as a model of migration. Wilkinson (1952) used this as a basis of a model of bird migration. Saila and Shappy (1963) present a model migration based on a random walk with a directed movement component and apply the model to migrating adult salmon. They concluded that

very little oriented movement is necessary to achieve the observed migratory patterns. Recently Hiramatsu and Ishida (1989) modified Saita and Shappy's model in terms of the advection-diffusion equation

$$\frac{\partial p}{\partial t} = -r_x \frac{\partial p}{\partial x} + D \left(\frac{\partial^2 p}{\partial x^2} + \frac{\partial^2 p}{\partial y^2} \right), \quad (2.10)$$

where the x axis is aligned in the direction of orientation, and r_x is the drift in that direction. The advection-diffusion equation forms the basis of the travel time models used in chapters 4-6.

spatial heterogeneity

As mentioned in the previous section, environmental heterogeneity can affect the dispersal behavior of animals. There are several ways to incorporate this into a model. One way is to assume that the diffusion coefficient, D , is related to some environmental factor and thus varies spatially.

When there is spatial heterogeneity in the diffusion coefficient, it is important to categorize the response to the heterogeneity as “attractive”, “neutral”, or “repulsive” (Skellam, 1973; Aronson, 1985; Okubo, 1986). In other words, is the diffusiveness of the individual determined by conditions of the current location (repulsive), conditions at the location of the next move (attractive), or an average of both these (neutral)? As shown by Skellam (1973) and Okubo (1986), these distinctions have a drastic effect on the resulting distribution. If we let $D = D(x)$, the following equations describe a repulsive system, a neutral system and an attractive system, respectively:

$$\frac{\partial p}{\partial t} = \frac{\partial^2}{\partial x^2}(Dp) \quad (2.11)$$

$$\frac{\partial p}{\partial t} = \frac{\partial}{\partial x} \left(D \frac{\partial p}{\partial x} \right) \quad (2.12)$$

$$\frac{\partial p}{\partial x} = \frac{\partial}{\partial x} \left(D^2 \frac{\partial}{\partial x} \left(\frac{p}{D} \right) \right). \quad (2.13)$$

In a closed system (i.e., a system with reflecting boundaries), equation (2.11) results in $p(x, t) \rightarrow C/D$, equation (2.12) results in $p(x, t) \rightarrow C$, and equation (2.13) results in $p(x, t) = CD$, where C is a constant determined by the system (Skellam, 1973).

Returning to the site of Dobzhansky and Wright's (1943) original experiment, Dobzhansky et al. (1979) examine the effect of habitat heterogeneity on the dispersal of *Drosophila spp.* They found that a dispersal model with diffusion coefficients related to habitat type was better able to describe observed patterns than one with constant coefficients.

models of chemotaxis

Originally developed to describe the response of cells to a chemical gradient (Keller and Segel, 1971), the chemotaxis model is an alternative way to describe an organism's response to environmental heterogeneity. In chemotaxis, variability in the concentration of a critical chemical produces an advection velocity in the direction of the gradient of concentration. The equation for chemotaxis is of the form:

$$\frac{\partial p}{\partial t} = D \frac{\partial^2 p}{\partial x^2} + \chi \frac{\partial}{\partial x} \left(p \frac{\partial U}{\partial x} \right), \quad (2.14)$$

where U is the concentration of the chemical and χ is the chemotactic coefficient. In ecological applications, $U(x)$ can be viewed as an environmental potential function (Teramoto and Seno, 1988). Equation (2.14) can be rewritten as:

$$\frac{\partial p}{\partial t} = D \frac{\partial^2 p}{\partial x^2} + \chi \frac{\partial}{\partial x} (U' p). \quad (2.15)$$

Thus the effect as the environmental potential is to induce an advective velocity of

magnitude U' . Few studies have actually attempted to apply these models to field data, perhaps because of the difficulty in defining the environmental potential function. In chapter 8, I apply this type of model to the vertical distribution of fish along an environmental gradient.

density dependence

The standard form of the diffusion equation with density dependence is:

$$\frac{\partial u}{\partial t} = D_0 \frac{\partial}{\partial x} \left(D(u) \frac{\partial u}{\partial x} \right) \quad (2.16)$$

(Gurney and Nisbet, 1975; Gurtin and MacCamy, 1977). If $D'(u) > 0$ for $u > 0$, then equation (2.16) models interference among individuals (Alt, 1985). If, on the other hand, $D'(u) < 0$ for $u > 0$, then equation (2.16) models attraction among individuals. Random movement can be included in addition to density dependent movement by formulating the diffusion term as:

$$D(u) = \alpha + \beta(u) \quad (2.17)$$

similar to Shigesada, et al. (1979). Here α is a constant and represents density independent diffusion, and $\beta(u)$ represents density dependent diffusion. When $D(u)$ is of the form $D(u) = (u/u_0)^m$, equation (2.16) is called the porous medium equation (Gurtin and MacCamy, 1977; Murray, 1989), and an analytical solution is available. Note that when $m = 0$, the porous medium equation reduces to simple diffusion. A feature of the porous medium equation is that the population disperses as a front – there is no infinite tail as there is in the simple diffusion equation. This is because $D(u) = 0$ when $u = 0$, as is the case just beyond the dispersing front. Shigesada (1980) applied the porous medium equation with $m = 1$ to dispersing ant lions. Included in her model is a settling phase of the organism.

Density dependent diffusion involving attraction among individuals is more difficult

mathematically. Since the diffusion term is negative, the problem is not well posed (Alt, 1985; Aronson, 1985). A problem is well posed if there is a unique solution that varies continuously with the initial conditions (Haberman, 1987). Slight perturbations result in only slight changes in the unique solution. Because of the compound effect of higher densities attracting more density, spikes of density form, and the position of these spikes is highly sensitive to the initial conditions. This a case, however, where the underlying discrete model is well posed and can be used to simulate density dependence with attraction among individuals.

2.4. Waiting time, Poisson process

We are often interested in the waiting time distribution $f(t)$ of the time to an event or, similarly, the probability of an individual surviving to a particular time. In applications in following chapters, I am interested in the amount of time it takes a fish to pass a dam after it has reached it, and I consider the effect of adding mortality to the travel time model.

Waiting time distributions (or survival curves) are often formulated in terms of a hazard function, $\lambda(t)$, which is the instantaneous failure rate at time t given survival through t . More precisely,

$$\lambda(t) = \lim_{\Delta t \rightarrow 0} \frac{P(t \leq T < t + \Delta t | T \geq t)}{\Delta t} \quad (2.18)$$

(Kalbfleisch and Prentiss, 1980). If we define $\bar{F}(t)$ as $1-F(t)$ (where $F(t)$ is the cumulative distribution function (cdf) of $f(t)$), then

$$\lambda(t) = \frac{f(t)}{\bar{F}(t)} \quad (2.19)$$

(Ross, 1983). The hazard function uniquely determines $F(t)$:

$$F(t) = 1 - \exp\left(-\int_0^t \lambda(u) du\right) . \quad (2.20)$$

Also,

$$f(t) = \lambda(t) \exp\left(-\int_0^t \lambda(u) du\right) . \quad (2.21)$$

The simplest case is when the hazard function is a constant, i.e. $\lambda(t) = \lambda$, and the waiting time probability density function is an exponential distribution

$$f(t) = \lambda e^{-\lambda t} . \quad (2.22)$$

This is equivalent to stating that a Poisson process with rate λ governs the waiting time to the next event (Ross, 1993).

The case where $\lambda(t)$ is not a constant is referred to as a nonhomogeneous Poisson process (Ross, 1993). Define the mean value function as

$$m(t) = \int_0^t \lambda(u) du , \quad (2.23)$$

and it can be shown that

$$\bar{F}(t) = e^{-m(t)} , \quad (2.24)$$

and

$$f(t) = \lambda(t) e^{-m(t)} . \quad (2.25)$$

3. General statistical treatment of spatio-temporal models

3.1. Introduction

Since the statistical approaches I use are common to several applications, I will present a general statistical overview that will be drawn upon in later chapters. In comparing models to data, my primary concern is to estimate parameters and construct confidence intervals around the estimates, determine the goodness-of-fit of the model to the data, and compare alternative models and select the most appropriate one.

3.2. Forms of data

The data used in my analyses come in several forms, and in this section I briefly present the different data types. Data of fish travel times – the time taken for a fish to travel between two points – is obviously temporal in nature, with the spatial component set as the length of the river reach. Travel time data vary depending on whether fish are released as individuals or groups. In group releases, a common mark identifies the fish, and the number of fish, $\{n_t; t = 1, 2, 3, \dots, k\}$, sampled at the downstream collection site during discrete time intervals is observed. Clearly, n_t is integer valued. Each time interval is Δt in duration (usually 1 day), and the final time interval, k , is an interval after the last fish has been

observed. Also, $N = \sum_{t=1}^k n_t$ is the total number of fish. Group covariates – such as date of release and river flow – may be associated with the cohort.

Alternatively, a unique marking may distinguish individuals in a cohort. In this case, the data are of individual travel times, $\{t_i; i = 1, 2, 3, \dots, n\}$, where n is the total number of individuals observed. t_i is positive valued; it can be continuous or discrete. Each individual

may also be characterized by covariates such as river flow, date of release, and fish length.

In radio-tracking data, an individual's position is followed through time. The data are continuous in both time and space and can be denoted as $\{\mathbf{X}(t): t \geq 0\}$. The vector \mathbf{X} can be 1, 2, or 3 dimensional and can take on both positive and negative values. It will be bounded by the system in which the fish are observed. In practice, the position of the individual is noted at successive points in time so that time is discrete, and the positional vector can be denoted as $\{\mathbf{X}_t: t = 0, 1, 2, \dots, n-1\}$, with n the number of observations. Ideally, the time intervals are equal in duration, but this is not always the case. It is often more practical to work with displacements, $\mathbf{Y}_t = \mathbf{X}_t - \mathbf{X}_{t-1}$.

Hydroacoustic instruments observe the distribution of depths of fish in the water column at a fixed location during a period of time. The data are usually discrete, $\{Z_i: i = 1, 2, 3, \dots, n\}$, with Z_i being the number of individuals observed in the i th equally spaced interval of the water column.

3. 3. Forms of the models

In all the models developed below, I start with a probability density function, $f(x, t)$, of individuals through space and time. If the data are continuous in both time and space (e.g., radio-tracking data), then the model can be applied directly to the data in this form. Otherwise, the model needs to be modified to be consistent with the data. For instance, the model can be converted to a spatial distribution, $f(x)$, of individuals at a particular point in time, or a temporal distribution, $g(t)$, at a particular point in space. Also, the data are often discrete – for example the number of fish collected at a dam during a discrete time interval. The model can be converted into a discrete form by integrating. For example:

$$p_i = \int_{x_i}^{x_i + \Delta x} f(x', t_0) dx' \quad (3.1)$$

describes the probability of a fish occurring in the discrete spatial interval $(x, x + \Delta x)$ at time t_0 . If a total of N organisms are observed, then

$$\hat{n}_i = N \cdot p_i \quad (3.2)$$

is the predicted number of individuals occurring in the i th interval. In this form, the \hat{n}_i 's follow a multinomial distribution.

3. 4. Parameter estimation

Consider a vector of random variables, $\mathbf{X} = (X_1, X_2, \dots, X_n)$, representing any of the types of data described above. Assume that \mathbf{X} is drawn from some distribution whose form is known but parameters unknown – $f(x; \theta)$ if \mathbf{X} is continuous, $p(x; \theta)$ if \mathbf{X} is discrete. Parameter estimation is the process of choosing a set of parameters, $\hat{\theta}$, such that the model is as consistent as possible with a vector of observations of the random variables, $\mathbf{x} = (x_1, x_2, \dots, x_n)$. While a wide variety of methods exist for estimating parameters, I have employed two techniques: generalized least squares, and maximum likelihood estimation.

generalized least squares

Least squares parameter estimation is commonly used in regression analyses (Draper and Smith, 1981; Neter, et al. 1985; Seber and Wild, 1989). I have also used it in applications where the model is applied to frequency data. The model takes the form

$$n_i = N \cdot p_i(\mathbf{x}; \hat{\theta}) + \varepsilon_i = \hat{n}_i + \varepsilon_i, \quad (3.3)$$

where n_i is the observed number of individuals in the i th class, N is the total number observed in all classes, p_i is the probability (under the model) of an individual falling in the

i th class, and ε is the error term. Generalized least squares is often used when there are unequal variances among the error terms (Draper and Smith, 1981; Seber and Wild, 1989). With generalized least squares, the following equation is minimized with respect to the parameter vector, $\underline{\theta}$:

$$S(\underline{\theta}; \mathbf{x}) = \sum_{i=1}^k w_i (\hat{n}_i - n_i)^2, \quad (3.4)$$

where k is the number of classes, and w_i is the weight associated with that class. To account for unequal variances, the weighting function $w_i = 1/v_i$ is often used, where v_i is the variance of the i th class.

maximum likelihood

Maximum likelihood estimation proceeds by maximizing the likelihood function, $L(\underline{\theta}; \mathbf{x})$, with respect to the parameters. \mathbf{X} can be either continuous or discrete. The likelihood function is defined as (Mood, et al., 1974; Bickel and Doksum, 1977):

$$L(\underline{\theta}; \mathbf{x}) = \prod_{i=1}^k f(x_i; \underline{\theta}) \quad (3.5)$$

for continuous functions. For discrete models, $p(x_i; \underline{\theta})$ is substituted for $f(x_i; \underline{\theta})$. Maximum likelihood estimation involves selecting the parameter vector, $\hat{\underline{\theta}}$, which is “most likely” to have produced the data. In other words,

$$L(\hat{\underline{\theta}}; \mathbf{x}) = \sup(L(\underline{\theta}; \mathbf{x})) . \quad (3.6)$$

If $L(\underline{\theta}; \mathbf{x})$ is differentiable with respect to the θ_i 's, then it can be maximized by setting

$$\sum_{i=1}^p \frac{\partial L}{\partial \theta_i} = 0, \quad (3.7)$$

where p is the number of parameters being estimated. Otherwise, $L(\theta; \mathbf{x})$ can be maximized numerically.

It is generally easier to work with the log of the likelihood function,

$$l(\theta; \mathbf{x}) = \log L(\theta; \mathbf{x}) = \sum_{i=1}^k \log f(x_i; \theta) . \quad (3.8)$$

With discrete data, based on the multinomial distribution $l(\theta)$ becomes:

$$l(\theta) = c + \sum_{i=1}^k n_i \log \hat{p}_i, \quad (3.9)$$

where c is a combinatorial constant that is unaffected by the choice of parameters.

performance of parameter estimates

In comparing competing parameter estimation methods, the most commonly used criteria for assessing the performance are the bias and the precision of the parameter estimates (Bickel and Doksum, 1977). Bias is defined as $E[\hat{\theta} - \theta^*]$, where θ^* is the true value of the parameter and $\hat{\theta}$ is the estimated value. Obviously, as small a bias as possible is desirable. A common definition of precision is the mean squared error (MSE), given by $E[\hat{\theta} - \theta^*]^2$. MSE is equal to the variance of the parameter estimate plus the bias squared (Bickel and Doksum, 1977), so if the estimate is unbiased, MSE is equal to the variance. In many cases, it is possible to determine these values directly; in cases where this is not possible, simulations can be used. In the last section of this chapter, I discuss simulation procedures.

3. 5. Confidence intervals

Confidence intervals are useful to reveal the variability associated with the parameter

estimates and can be used for statistical inference. In some cases, theoretical confidence intervals based on asymptotic assumptions are available. In other cases, approximate confidence intervals can be constructed using bootstrap methods (Efron, 1982; Efron and Tibshirani, 1986).

I use the following procedure to construct 95 percent bootstrap confidence intervals. For each cohort of size N , the individuals are sampled with replacement N times to produce a new cohort. For each cohort, I then estimate the parameters following the same procedures as with the parameter estimates of the original data. This is repeated 10,000 times, and for each iteration, the parameter estimates are retained. For each parameter, the 10,000 estimates are sorted, and the estimates that fall at the 2.5th and the 97.5th percentiles are used to construct a 95 per cent confidence interval.

3. 6. Goodness-of-fit

Goodness-of-fit tests are used to determine how well a proposed model fits a particular data set. The procedure is to first compute a test statistic based on the deviation of the data from the model (with the parameter estimates) and then compare it to a theoretical or empirical distribution based on the assumption that the model is true. A rough probability of observing the particular data set, given the model is true, can then be determined. If the probability of observing the data is too low, the model is rejected. I should note that I use goodness-of-fit tests to get a rough idea of a model's performance – there is no threshold value below which a model is deemed not to work. In most cases I apply models to a series of data sets, and consistently low p -values is evidence that model is not appropriate. The main purpose of the tests is to assess whether a model is useful in describing observations and hence useful for predictive purposes.

Two types of goodness-of-fit tests have been commonly employed: chi-square type tests and tests based on the empirical distribution function (EDF), although other classes of tests

have been used (D'agostino and Stephens, 1986). Chi-square tests are used when data are grouped into discrete classes, and observed frequencies are compared to expected frequencies based on a model. Although Pearson's X^2 test is the most familiar, other tests fall into this category, such as the G test, Tukey's test and the Rao-Robson test (Moore, 1986). In all cases the test statistic is formulated such that it follows a chi-square distribution, and because of this, these test are usually convenient to use. Tests based on the *EDF* are used most often with continuous data. An empirical density function is constructed by ranking the data, and this is compared to the model's cumulative distribution function (*CDF*). The test statistic is based on the deviation of the *EDF* from the *CDF*, and its distribution is obtained by Monte-Carlo simulations. The most familiar test of this type is the Kolmogorov test (Conover, 1980).

chi-squared goodness-of-fit test

The most commonly used chi-squared test is Pearson's X^2 test (Pearson, 1900), which compares expected frequencies to observed frequencies in discrete cells. If the model is fully specified (i.e., no parameters are estimated from the data), then the cell probabilities can be obtained by integrating over the cell width, w_i :

$$p_i = \int_{w_i} f(x) dx. \quad (3.10)$$

The expected frequency in cell i is then computed as

$$E(n_i) = N \cdot p_i, \quad (3.11)$$

where N is the total sample size. Pearson showed that the test statistic

$$X^2 = \sum_{i=1}^{k+1} \frac{(E(n_i) - n_i)^2}{E(n_i)} \quad (3.12)$$

asymptotically follows a $\chi^2_{(k)}$ distribution

discrete class data

These tests are particularly useful when the data are the form of the frequency of individuals falling into discrete classes. An issue with both these tests is how to lump the classes. If the $E(n_i)$'s are too small, the tests are not valid (Cochran, 1952; Roscoe and Byars, 1971). In all cases, I lump the data such that $E(n_i) > 1.0$ for all i 's.

using chi-squared tests with continuous data

Using chi-squared tests in situations where the data are continuous involves a trade-off: the tests are flexible and easy to use, but because the data must be placed into discrete classes, information is lost and the tests are not as powerful as some alternatives (Moore, 1986). One advantage of using these tests with continuous data, though, is that it is possible to have equiprobable cells, improving the efficiency of the test (Mann and Wald, 1942; Cohen and Sackrowitz, 1975). Mann and Wald (1942) recommended the following equation for choosing the number of cells, k , at significant level α :

$$k = 4 \left(\frac{2N^2}{c(\alpha)^2} \right), \quad (3.13)$$

where $c(\alpha)$ is the $(1-\alpha)$ th quantile of the standard normal distribution. Other people (e.g., Schorr, 1974) have argued that fewer cells than this are optimal, and in light of this, Moore (1986) recommends using a value for k that is between that given by equation (3.13) and half that. I will use equation (3.13) with $\alpha = 0.05$; since equation (3.13) decreases with decreasing α , this practice will cover the range of $\alpha = 0.05$ and lower values.

using chi-squared tests when parameters are estimated in the model

At first glance it appears that chi-squared tests can readily accommodate models that

have parameters estimated from the data. The standard approach is to subtract one degree of freedom for each parameter estimated. As Fisher (1924) showed, however, the type of estimation procedure used affects the outcome of the goodness-of-fit test. The appropriate parameter estimation method to use is the minimum chi-squared criterion. This involves minimizing the X^2 statistic with respect to the parameters and is achieved by solving the following equation:

$$\sum_{i=1}^k \left(\frac{n_i}{p_i(\theta)} \right) \frac{\partial}{\partial \theta_p} p_i(\theta) = 0, p = 1, 2, \dots, r, \quad (3.14)$$

where r is the number of parameters estimated. This method has several drawbacks. First, this equation is difficult to solve – analytical solutions are rarely available, and the response surface is not smooth. Second, chi-square estimation procedure is rarely used, and ideally the parameter estimates used in the goodness-of-fit tests are those obtained from the parameter estimation part of the data analysis. Fortunately, using parameter estimates from other methods (such as maximum likelihood) results in tests that are conservative – i.e., they reject the model too often. Thus there are three choices: 1) use the minimum chi-squared criterion and accept its downfalls, 2) use another estimation method and use a conservative test, or 3) use a test that includes a correction factor, such as the Rao-Robson test (Rao and Robson, 1974).

tests using the empirical density function

When data are continuous and the model is fully specified, tests involving the *EDF* are easy to use and generally more powerful than chi-squared tests. In cases where parameters are estimated from the data, these tests become more difficult to implement, and the theory is not as well developed (Stephens, 1986).

As stated previously, these tests are based on the deviation of the *EDF* from the *CDF*

of the model distribution. The empirical density function is constructed by ranking the observations and then computing

$$F_n(X) = \frac{1}{N} (\# \text{ of observations } \leq x), \quad n = 0, 1, \dots, N. \quad (3.15)$$

This results in a step function that increases $1/N$ in height at each observation. This is compared to the model *CDF*, $F(X)$. The most commonly used statistic is D , first introduced by Kolmogorov (1933):

$$D = \sup_x |F_n(X) - F(X)|, \quad (3.16)$$

which is the largest vertical distance between $F_n(X)$ and $F(X)$. Other statistics have been proposed that involve the squared difference between $F_n(X)$ and $F(X)$ integrated over the entire range of x .

In some cases it is more convenient to work with data after they have been transformed such that

$$Z = F(X), \quad 0 \leq z \leq 1. \quad (3.17)$$

If the model is true Z will be uniformly distributed on $[0,1]$. If $z_{(i)}$ is the i th-ranked transformed data point, then

$$D = \max_i \left\{ \frac{i}{n} - z_{(i)}, z_{(i)} - \frac{(i-1)}{n} \right\}. \quad (3.18)$$

The basic goodness-of-fit test is as follows. We would like to test the hypothesis that a random sample, x_1, x_2, \dots, x_N , came from a fully specified distribution, $F(X)$. In other words,

H_0 : the random sample is from $F(X)$.

H_A : the random sample is not from $F(X)$.

The procedures are followed as outlined above, and the resulting test statistic is compared

to its tabulated distribution. A value falling in the upper extreme of the distribution is evidence against the null hypothesis.

EDF tests with estimated parameters

When parameters are estimated from the data, *EDF* tests become less general. If the parameters are location (e.g., the mean of a normal distribution) and/or scale (e.g., the variance of a normal distribution) parameters, the distribution of the *EDF* statistic is dependent on the family of distribution in question but not on the particular parameter values. This is the case with the normal and exponential distributions, among others, and these distributions of test statistics for many of these families have been tabulated. In cases where a shape parameter is estimated (e.g., Gamma and Inverse Gaussian distributions), the distribution of test statistics is dependent not only on the family of distribution but also on the true parameter values, making the use of these tests quite cumbersome. One way to overcome this is to create the distribution of test statistics with Monte-Carlo simulations as they are needed.

3. 7. Model discrimination, model selection, generalized likelihood ratio test

Several alternative models are often proposed to explain the same data, and objective criteria are needed to choose among models. The alternative models may be nested or non-nested. Nested models are constructed such that a simpler model can be obtained from a more complex model by eliminating one or more parameters from the more complex model. Thus choosing among models reduces to determining the appropriateness of the additional parameters. Non-nested models are not related in this way, and model selection must be based on some other criteria. I will not deal with non-nested models in my thesis.

While adding features to a model is often desirable, the increased complexity comes with a cost. In general, the more parameters contained in a model, the less reliable are

parameter estimates. Criteria to select among models must weigh the trade-off between increased information and decreased reliability. I present three methods, all of which deal with the likelihood function, and because of this, model discrimination is related to parameter estimation. I begin with a discussion of nested models and then show how the three methods choose among models.

Beginning with the simplest case, a null model $f(X; \underline{\theta}_0)$, specified by the parameter vector $\underline{\theta}_0 = (\theta_1, \theta_2, \dots, \theta_k)$, is compared to an alternative model $f(X; \underline{\theta}_A)$, which shares the k parameters of the null model but also contains an additional parameter, θ_{k+1} . In comparing the null to the alternative hypothesis, we are determining the appropriateness of adding the additional parameter to the null model. In other words, we are testing the following hypotheses:

$$H_0: \theta_{k+1} = 0, \text{ versus}$$

$$H_A: \theta_{k+1} \neq 0.$$

This is a two-sided test because the null hypothesis is rejected if θ_{k+1} is determined to be significantly greater or less than 0 (or another pre-determined value). This can be extended to comparisons of models that differ by more than 1 parameter, with the alternative model having parameter space $\underline{\theta}_A = (\theta_1, \theta_2, \dots, \theta_k, \theta_{k+1}, \dots, \theta_{k+r})$.

The likelihood function is based on parameter values and the data. As with parameter estimation, parameters vectors $\hat{\underline{\theta}}_0$ and $\hat{\underline{\theta}}_A$ are chosen to maximize the likelihood function. In other words,

$$L(\hat{\underline{\theta}}_0; \mathbf{x}) = \sup L(\underline{\theta}_0; \mathbf{x})$$

$$L(\hat{\underline{\theta}}_A; \mathbf{x}) = \sup L(\underline{\theta}_A; \mathbf{x}) . \tag{3.19}$$

The three model comparison methods compare these two likelihoods.

generalized likelihood ratio test

The generalized likelihood ratio test (GLRT) (Mood, et al., 1974; Bickel and Doksum, 1977; Hogg and Tannis, 1983), as its name implies, is based on the ratio of the likelihoods.

Define a random variable Λ with realizations, $\lambda(\mathbf{x})$, based on the data, \mathbf{x} :

$$\lambda(\mathbf{x}) = \frac{\sup L(\underline{\theta}_0; \mathbf{x})}{\sup L(\underline{\theta}_A; \mathbf{x})}, \quad (3.20)$$

where L is the likelihood function as in equation (3.8). Note that $0 \leq \lambda \leq 1.0$. This is because the null hypothesis (based on $\underline{\theta}_0$) is nested within the broader hypothesis (based on $\underline{\theta}$), and λ will always be ≤ 1.0 . Also, $\sup L$ will always be ≥ 0 , so $\lambda \geq 0$. In general, $\lambda \ll 1.0$ is grounds for rejecting the null hypothesis.

The likelihood ratio is useful because of the following result (Bickel and Doksum, 1977). First, assume that $\mathbf{x} = x_1, x_2, x_3, \dots, x_n$ is a sample from the probability density function or discrete density function $f(X; \underline{\theta}_A)$ with $\underline{\theta}_A$ a $k+1$ dimensional parameter vector that takes on values unrestricted in R^{k+1} . Also assume that:

- 1) The map $\theta \rightarrow f(x; \theta)$ is smooth in θ for each x ;
- 2) The maximum likelihood estimate $\hat{\theta}$ is consistent (i.e., the estimate $\hat{\theta}$ becomes arbitrarily close to the true value as n gets large).

Then, with λ formulated as above, if $\theta_{k+1} = 0$ (the null hypothesis is true), the asymptotic distribution of $-2 \log \Lambda$ is approximately χ^2 with 1 degree of freedom (Mood, et al., 1974; Bickel and Doksum, 1977). Thus a test of size α is

$$\text{Reject } H_0 \text{ if } -2 \log \Lambda > \chi_{1-\alpha}^2(1),$$

where $\chi^2_{1-\alpha}(1)$ is the $(1-\alpha)$ th quantile of the chi-square distribution with 1 degree of freedom. This test can be extended to the case where the difference between the dimension of the null and alternative models is greater than 1. If the test is formulated as above, and the same assumptions are met, then $-2\log\Lambda$ is approximately χ^2 with r degrees of freedom, where r is the difference in dimension between the two models.

Akaike's information criterion

The other two methods operate under the premise of parsimony – simpler models are favored over more complex ones. The first is called Akaike's information criterion (AIC) (Akaike, 1973). For each alternative model proposed to describe data,

$$AIC_i = 2\log L(\hat{\theta}_i; \mathbf{x}) - 2(k + r_i) , \quad (3.21)$$

where $k + r_i$ is the number of unspecified parameters in the i th model. In a sequence of nested models, the model with the largest AIC_i value is chosen. Compared to the GLRT method, the AIC method assigns proportionately more penalty for models of increasing complexity.

Bayesian information criterion

Both the GLRT and the AIC method have a similar drawback – as the sample size increases there is an increasing tendency to accept the more complex model (Raftery, 1986). The Bayesian information criterion (Schwarz, 1978) takes sample size into account. Although the BIC method was developed from a Bayesian standpoint, the result is insensitive to the prior distribution for adequate sample size. Thus a prior distribution need not be specified (Schwarz, 1978; Raftery, 1986), which simplifies the method. For each model, The BIC is calculated as

$$BIC_i = 2\log L(\hat{\theta}_i; \mathbf{x}) - (k + r_i)\log(n) , \quad (3.22)$$

where n is the sample size. As with the previous method, the model is chosen with the largest BIC. If just two alternative models are being compared, the BIC from the simpler model can be subtracted from the BIC from the more complex model. A positive value indicates that the more complex model should be favored, while a negative value favors the simpler model.

3. 8. Statistical simulations

Simulations are a means to answer some of the questions raised about the statistical procedures outlined in the above sections of this chapter. The general procedures for the statistical simulations is:

- 1) specify the model $f(x;\theta)$ and choose parameter values, θ^* ;
- 2) draw a random sample, (x_1, x_2, \dots, x_n) , of size n from the specified distribution;
- 3) perform the statistical procedure – estimate parameters, compute test statistics;
- 4) repeat steps 2 and 3 many times to generate distributions of parameter estimates and test statistics;
- 5) use these distributions to compute bias or mean squared error (*MSE*) of parameter estimates or to compare the distribution of test statistics to the theoretical distribution.

Simulations can be performed under a variety of conditions, e.g. different sample sizes or parameter values.

After n simulations are run, the bias of a parameter estimate can be formulated as:

$$E(\hat{\theta} - \theta^*) = \frac{1}{n} \sum_{i=1}^n [\hat{\theta}_i - \theta^*] . \quad (3.23)$$

$\hat{\theta}_i$ is the parameter estimate from the i th simulation, and θ^* is the true value of the

parameter. The *MSE* of the parameter estimate can be computed as

$$MSE = \frac{1}{n} \sum_{i=1}^n [\hat{\theta}_i - \theta^*]^2 . \quad (3.24)$$

After a distribution of test statistics is generated, it can be compared directly to the theoretical distribution. In doing so, the consistency of the two distributions can be determined.

3.9. Types of data

In this section I briefly discuss the methods used to mark and track juvenile salmonids and the type of information available from each.

freeze-brand

Freeze branding is an efficient way to mark a large group of fish with the same identification code (Mighell, 1969). A metal branding tool is cooled with liquid nitrogen, and the fish are pressed against the tool. This method does not distinguish among individuals, but release groups can be distinguished. This allows for the determination of release site and release time of recaptured fish. In general, the data acquired from freeze brand fish are the number of fish collected during discrete collection periods.

PIT tag

PIT (passive integrated transponder) tags are used to monitor individual fish. The tag, 12 mm long, is inserted in the fish's body cavity and contains a microchip that is programmed to contain individual fish identification codes (Prentice, et al., 1990). At monitoring sites the tag emits a signal in response to excitation from an interrogation system. The signal is decoded to yield information about instantaneous passage times of individuals. The tags do not seem to adversely affect the fish in terms of survival or

swimming performance (Prentice, et al. 1990).

radio-tracking

Radio-tracking has been used successfully in the past to monitor movements of migrating juvenile salmon. Atlantic salmon (*Salmo salar*) have been radio-tagged and monitored in the northeastern United States (Stasko, 1975), Canada (Brawn, 1982), Norway (Holm, et al., 1982) and Scotland (Tytler, et al., 1978). Several studies have also been performed on juvenile salmonids in the Columbia River Basin (Giorgi et al., 1985; Stuehrenberg et al., 1986). Two qualitatively different types of studies have been performed. In the first type (e.g., Giorgi et al., 1985), individual fish are followed with their position being noted at relatively frequent time increments to create a radio track. This allows one to analyze individual behavior on a relatively fine scale. The other type of study (e.g., Stuehrenberg et al., 1986) involves releasing a group of fish and recording the arrival time of individuals at receivers located at fixed sites downstream. Many more fish can be included in this type of study, with information about the distributions of groups of fish being obtained.

The question of whether internal radio tags affect the migratory behavior of juvenile salmon has been addressed in at least two studies (McCleave and Stred, 1975; Stuehrenberg et al., 1986). Both studies determined that there is no effect of internal radio tags on the swimming stamina of juvenile salmon, although buoyancy may be affected. Also, the latter study made qualitative observations of swimming behavior and concluded that there was no difference in the behavior of fish with dummy tags and control fish.

hydroacoustics

Several studies have employed fixed location hydroacoustic transducers to monitor the abundance of juvenile salmonids (Johnson, et al., 1985; Dawson, et al., 1984b). The

procedure is to attach transducers at the base of a dam and to point it upward through the forebay. The instruments yield an estimate of the density of juvenile salmonids migrating at specific depths (Dawson, et al., 1984a). The equipment cannot distinguish among species.

4. Basic travel time model

4.1. Introduction

The amount of time juveniles spend migrating downstream in rivers has several implications for salmon populations. From a behavioral standpoint, the timing of migration has evolved for individual stocks to take advantage of river currents while avoiding hazards such as predation. Also the migration timing is coordinated with the smoltification process so that the fish reach the saltwater environment when they are physiologically prepared (Folmar and Dickhoff, 1980).

From a management standpoint, understanding and modeling juvenile salmonid travel time is important for several reasons. The ability to predict the arrival times of populations of fish at dams will aid in directing river and dam operations to enhance fish survival. For instance, spilling fish over the top of dams is considered to be a safer passage route than through the turbines. However spilling water for fish passage involves a cost of lost electricity generation, so predicting the abundance of fish in front of dams can help to make this process as efficient as possible. Also, there is the question of whether it is possible to speed up migration rate. Since river currents are thought to be a primary source of downstream movement (Smith, 1982), the reduced river velocity created by dams can potentially greatly increase the travel times of the juveniles. In fact, Raymond (1978) estimated that the construction of dams may have doubled the travel times of some stocks in low flow years. A proposal that is receiving serious consideration is reservoir drawdown. This involves lowering reservoir levels to try to enhance river velocities. Understanding how fish respond to these conditions will be crucial.

In this chapter, I develop a basic travel time model where migration rate is considered

to be constant, and all members of a cohort behave identically. In the next chapter, I incorporate behavioral components into the travel time model, such as travel time related mortality, migrational delay, and diel variation in migration rate. In chapter 6, I allow for population heterogeneity, with the migration rate of individuals being determined by factors such as fish length.

4.2. Development of basic model

overview of modeling downstream migration

Most travel time experiments involve collecting a group of fish, marking them with a tag and then releasing them as a group from a single release point. The fish then migrate downstream and are collected at a downstream collection site, often a dam (see Figure 4.1).

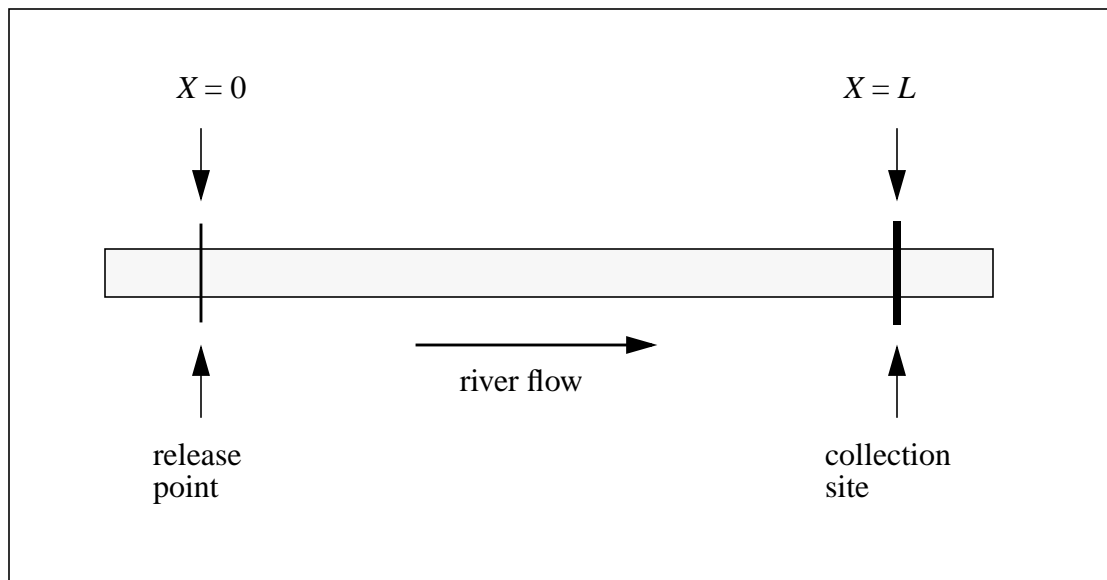


Figure 4.1 A schematic diagram of the travel time problem.

The river is treated as 1-dimensional.

The modeling effort is directed at determining $g(t)$, which is the probability density function for the distribution of arrival times at the downstream collection site. Also of interest is the position of an individual through time. This is denoted by the random variable $X(t)$ with $X \in R^1$ and $t > 0$. X is usually further restricted by the physical domain of the system being studied. With a release point at $X=0$, and a collection site at $X=L$ (as in Figure 4.1), it is assumed that $-\infty < X < L$. Also of interest is $p(x,t)$, which is the density function for an individual occurring at position x at time t . If there are N individuals in a cohort, then $N \cdot p(x,t)$ is the population density. Because individuals leave the river reach

$$\int_X p(x,t) dx \leq 1.0.$$

The travel time of fish through a reach can be thought of in two ways, both of which yield equivalent results. In terms of the process $X(t)$, the travel time T is modeled as the first passage of $X(t)$ from the release point to the collection point. In other words,

$$T = \inf\{t: X(t) < L | X(t_0) = x_0\} \quad (4.1)$$

(Sacerdote, 1988). In terms of the density function $p(x,t)$, the passage of fish through a reach is modeled in terms of the loss of density at an absorbing boundary. In other words, an absorbing boundary is imposed at $X=L$, and thus

$$p(L,t) = 0. \quad (4.2)$$

The theory of boundary crossing has been extensively developed in the mathematical and statistical literature (e.g., Sacerdote, (1988)), where there has been an effort to derive generalizations about a variety of processes crossing different classes of boundaries. A major application in the statistical literature has been the development of sequential analysis (Siegmund, 1985), where rejecting a hypothesis is related to the probability of a

process crossing a boundary. In the biomedical literature, there has been a great deal of activity in applying first passage problems to models of neuronal firing (Lanska, 1988). Boundary crossing models have a lot of potential for ecological applications, where many processes are phenological in nature. There have been a few applications in this area, including applications to the timing of instar development in insects (Kemp, et al., 1989) and population extinction (Dennis, et al., 1991).

In the following section I present some general results for first passage problems. I then focus on the specific case where the parameters are constants. The remainder of the chapter is devoted to statistical methods and applications to data.

assumptions

Several assumptions must be made in order to apply the basic travel time model derived in the following section. In later chapters, I expand the model so that these assumptions are not necessary. The first assumption is that the population of fish is independently, identically distributed. Second, the migration process is time homogeneous – there is no diel or seasonal variation in the migratory behavior. Third, each individual has an equal probability of being sampled at the downstream collection site. This means that survival probabilities are identical among the individuals, and the probability of recapture is also identical.

model development

The travel time model begins with the assumption that the spatial distribution of fish through time is described by an advection-diffusion equation. Several people have suggested using this equation to describe the migration of fish (Saila and Flowers, 1969; DeAngelis and Yeh, 1984; Anderson and Schumaker, 1988; Hiramatsu and Ishida, 1989). Since the available data is of the distribution of fish passing through dams (or collected at

traps) through time, the advection-diffusion equation is used to derive the distribution of fish passing a fixed point through time. In this temporal form, the model can be compared to data to determine the validity of the model and estimate parameters.

The advection-diffusion equation is expressed as:

$$\frac{\partial p}{\partial t} = -r \frac{\partial p}{\partial x} + \frac{\sigma^2}{2} \frac{\partial^2 p}{\partial x^2}. \quad (4.3)$$

The parameter r determines the rate of downstream movement, and σ determines the rate of population spreading. As shown in the Chapter 2, with natural boundaries and a point release at $x_0 = 0$, the unique solution of equation (4.3) is

$$p(x, t) = \frac{1}{\sqrt{2\pi\sigma^2 t}} \exp\left(-\frac{(x - rt)^2}{\sigma^2 t}\right). \quad (4.4)$$

It is not realistic, however, to assume unrestricted boundaries in natural systems. In the case of the Columbia River, dams form delineations, and fish populations are sampled as they pass through dams. To account for this, an absorbing boundary is imposed at the site of a dam. As fish in the population pass a dam, they are “absorbed” from the reservoir and passed through the dam. In terms of the model, we assume that fish are released at $X = 0$ and are collected at $X = L$. The boundary conditions are now

$$p(-\infty, t) = p(L, t) = 0 .$$

Note that there still is a natural boundary upstream from the collection point. This allows fish to move upstream from their point of release. With these boundary conditions and the same initial conditions as above, the solution to equation (4.3) is now:

$$p(x, t) = \frac{1}{\sqrt{2\pi\sigma^2 t}} \left(\exp\left[-\frac{(x-rt)^2}{2\sigma^2 t}\right] - \exp\left[\frac{2Lr}{\sigma^2} - \frac{(x-2L-rt)^2}{2\sigma^2 t}\right] \right) \quad (4.5)$$

(Goel, Richter-Dyn, 1974). Note that this is similar to equation (4.4) but with an added term that accounts for the loss of density at $X = L$. An example of this distribution is presented in Figure 4.2 with $L = 100$. Notice that $p(x, t) = 0$ beyond $X = 100$, and that as t increases the area under $p(x, t)$ decreases corresponding to the “loss of probability” at $X = 100$.

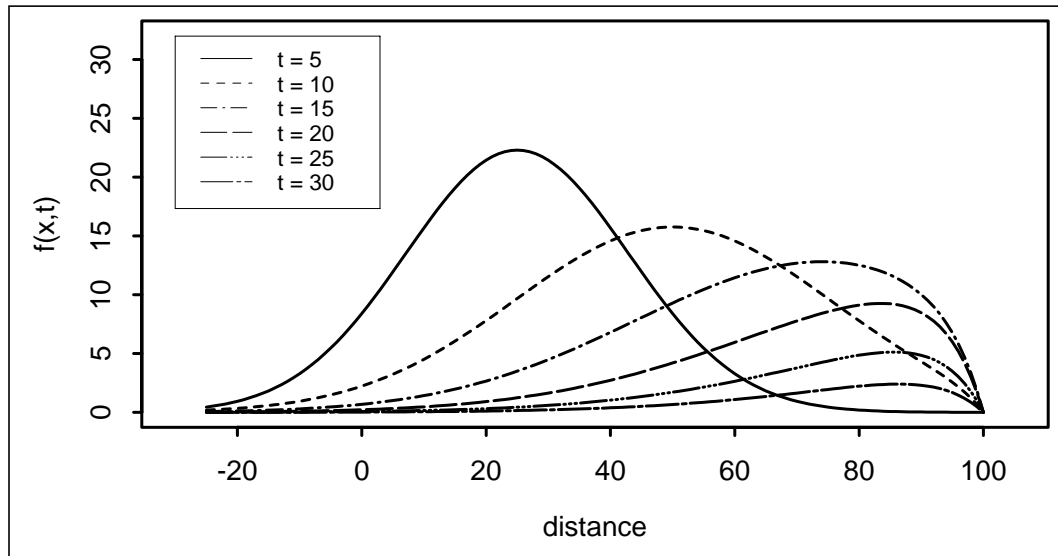


Figure 4.2 Plot of equation (4.5) for various values of t . The parameters r and σ are set at 5 and 8, respectively, and L is set at 100.

Since the loss of density at the absorbing boundary corresponds to fish passage at the dam, we can use equation (4.5) to derive an arrival time distribution. The first step is to determine the probability of remaining in the river, $P(L, t)$, at a given point in time. This is achieved by integrating equation (4.5):

$$\begin{aligned}
P(L, t) &= \int_{-\infty}^L p(x, t) dx \\
&= \left[\Phi\left(\frac{L-rt}{\sigma\sqrt{t}}\right) - \exp\left(\frac{2Lr}{\sigma^2}\right) \Phi\left(\frac{-L-rt}{\sigma\sqrt{t}}\right) \right] .
\end{aligned} \tag{4.6}$$

Φ is the cumulative distribution of the standard normal distribution. To derive a continuous time pdf for the arrival time distribution at $X = L$ for a group of fish released at $X = 0$, equation (4.6) is differentiated to determine the rate of loss of density:

$$\begin{aligned}
g(t) &= -\frac{d}{dt}P(L, t) , \\
&= \frac{L}{\sqrt{2\pi\sigma^2t^3}} \exp\left(\frac{-(L-rt)^2}{2\sigma^2t}\right)
\end{aligned} \tag{4.7}$$

(Cox and Miller, 1965). Plots of this distribution for various values of r and σ are contained in Figure 4.3. With σ and L held constant, as r decreases the mode of the distribution moves to the right, and the distribution flattens out. With r and L held constant, increasing σ has the effect of moving the mode to the left and flattening the distribution. To determine the probability of arrival at $X = L$ during a discrete time interval one integrates equation (4.7):

$$p(t_2, t_1) = \int_{t_1}^{t_2} g(t) dt = -\left[\Phi\left(\frac{L-rt}{\sigma\sqrt{t}}\right) - \exp\left(\frac{2Lr}{\sigma^2}\right) \Phi\left(\frac{-L-rt}{\sigma\sqrt{t}}\right) \right] \Bigg|_{t_1}^{t_2} . \tag{4.8}$$

Further complexity can be added to the model by allowing the parameters r and σ to vary with time in response to such factors as flow conditions and fish maturity.

It is common to reparameterize equation (4.7) with $\mu = L/r$ and $\lambda = L^2/\sigma^2$. This parameterization eliminates reach length, L , from the equation. Equation (4.7) then

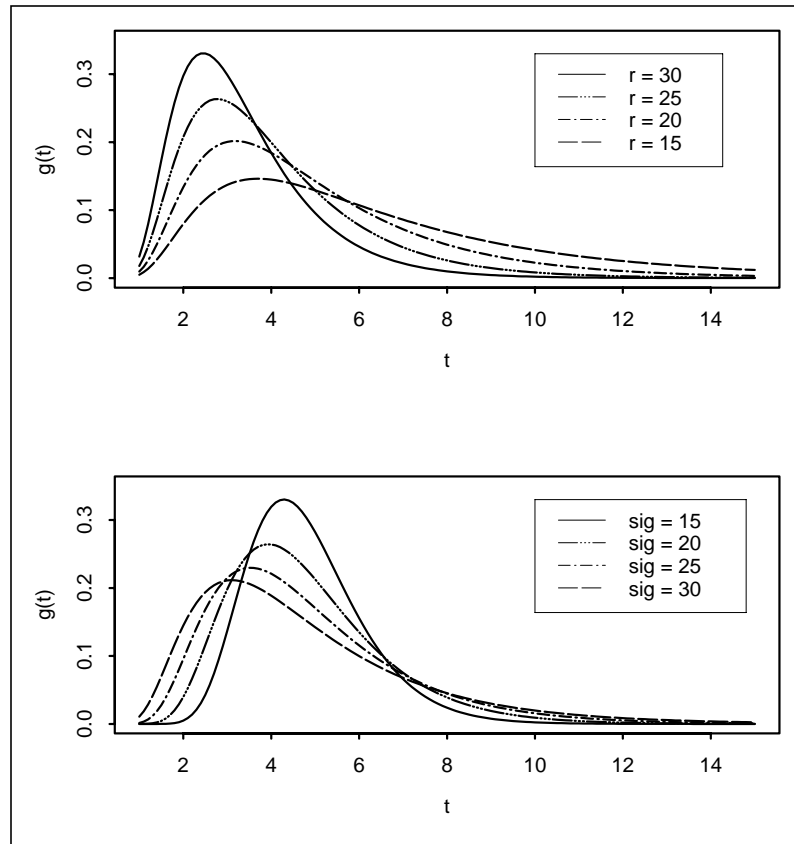


Figure 4.3 Equation (4.7) with various parameter values. In the top figure, σ is set at 25, and r is varied. In the bottom plot, r is set at 25, and σ is varied. In both plots, $L = 120$.

becomes:

$$g(t; \mu, \lambda) = \sqrt{\frac{\lambda}{2\pi t^3}} \exp\left(\frac{-\lambda(t - \mu)^2}{2\mu^2 t}\right) \quad (4.9)$$

in the continuous form, and

$$p(t_2, t_1; \mu, \lambda) = -\left[\Phi\left(\frac{1 - \mu t}{\sqrt{\lambda t}}\right) - \exp\left(\frac{2\mu}{\lambda}\right)\Phi\left(\frac{-1 - \mu t}{\sqrt{\lambda t}}\right)\right] \Bigg|_{t_1}^{t_2} \quad (4.10)$$

in the discrete form. With this parameterization, equation (4.9) has been called the “inverse Gaussian” distribution (Tweedie, 1957a, 1957b; Folks and Chhikara, 1978).

In the appendix to this chapter, I present some useful derivations related to first passage models. In appendix 3.a, I show how to derive first passage distributions with the “method of images,” an intuitive approach that produces useful results. In appendix 3.b, I show how to derive the passage pdf (equation (4.7)) using a Laplace transform method. In appendix 3.c, I develop a numerical approximation for the discrete version of the passage pdf (equation (4.8)) that overcomes the “exponential overflow” problem involved in computing the equation. In appendix 3.d, I demonstrate a method for generating inverse Gaussian variates, a method I use in the simulations in the following section.

4.3. Statistical methods

parameter estimation and confidence intervals

The parameter estimation methods vary depending on whether the data are discrete or continuous. Also, for both cases, alternative methods are available, so I will present alternatives for each.

- continuous case

The maximum likelihood estimators (mles) for the two parameters r and σ were first worked out by Shroödinger (1915). They are:

$$\hat{r} = \frac{L}{\bar{t}} \quad (4.11)$$

$$\hat{\sigma} = L \sqrt{\frac{1}{N} \sum_{i=1}^N \left(\frac{1}{t_i} - \frac{1}{\bar{t}} \right)}, \quad (4.12)$$

where t_i is the observed arrival time of the i th individual, \bar{t} is the average arrival time of the group, and N is the number of individuals in the cohort. The maximum likelihood estimators of these two parameters are independent (Chhikara and Folks, 1989), and much of the statistical inference involving the inverse Gaussian distribution parallels that of the normal distribution. Notice that the mle for r is the average migration rate and the mle for σ involves the difference between the harmonic mean and reciprocal of the arithmetic mean of the travel time. While the mle for r is unbiased, the mle of σ is biased. An (uniform minimum variance) unbiased estimator for σ is

$$\tilde{\sigma} = L \sqrt{\frac{1}{N-1} \sum_{i=1}^N \left(\frac{1}{t_i} - \frac{1}{\bar{t}} \right)} \quad (4.13)$$

(Folks and Chhikara, 1978).

From equations (4.12) and (4.13), the bias of $\hat{\sigma}$ can easily be shown to be

$$bias(\hat{\sigma}) = \sigma \left(\sqrt{\frac{N-1}{N}} - 1 \right). \quad (4.14)$$

Plots of this equation for several values of σ are contained in Figure 4.4. The slopes of these curves are very steep for small sample sizes but flatten out for larger sample sizes.

For the continuous version of the travel time model, theoretical confidence intervals for

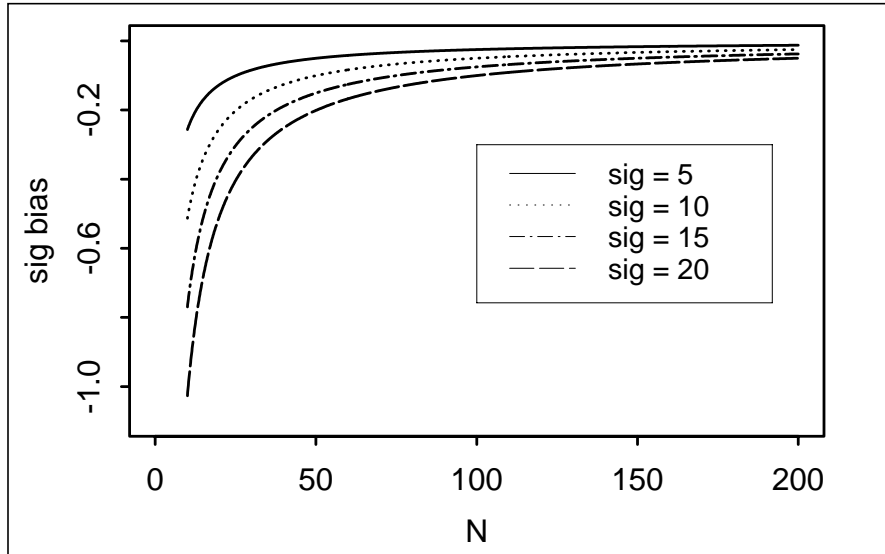


Figure 4.4 Plots of the bias of the parameter estimator $\hat{\sigma}$ versus sample size for several values of σ .

the parameters r and σ are available (Tweedie, 1957a, 1957b; Folks and Chhikara, 1978; Chhikara and Folks, 1989). To construct confidence intervals for r , we begin by noting that the statistic

$$T = \frac{r[\sqrt{N-1}(\hat{t} - L/r)]}{\hat{\sigma}\sqrt{\hat{t}}} \quad (4.15)$$

follows a Student's t distribution with $N-1$ degrees of freedom. Based on this information, we can determine

$$Pr[T > a] = Pr[T < b] = \alpha/2. \quad (4.16)$$

Because Student's t distribution is symmetric, $b = -a$. Thus, a (uniformly most accurate-unbiased) $100(1-\alpha)$ percent confidence interval is

$$\left(\hat{r} \left[1 - \frac{a\hat{\sigma}}{L} \sqrt{\frac{\hat{t}}{n-1}} \right], \hat{r} \left[1 + \frac{a\hat{\sigma}}{L} \sqrt{\frac{\hat{t}}{n-1}} \right] \right), \quad (4.17)$$

if $1 - \frac{a\hat{\sigma}}{L} \sqrt{\frac{\hat{t}}{n-1}} t_{1-\alpha/2} > 0$, and

$$\left(0, \frac{L}{\hat{t}} \left[1 + a \sqrt{\frac{\hat{t}V}{n-1}} \right] \right)$$

otherwise.

For the confidence interval of σ , we first note that

$$\frac{N\hat{\sigma}^2}{\sigma^2} \sim \chi_{n-1}^2 \quad (4.18)$$

(Tweedie (1957a)). Equation (4.18) is then used to determine values a and b such that

$$Pr\left(\frac{N\hat{\sigma}^2}{\sigma^2} > a\right) = Pr\left(\frac{N\hat{\sigma}^2}{\sigma^2} < b\right) = \alpha/2 .$$

A $100(1-\alpha)$ percent confidence interval for σ can then be constructed as:

$$\left(\hat{\sigma} \sqrt{\frac{N}{a}}, \hat{\sigma} \sqrt{\frac{N}{b}} \right). \quad (4.19)$$

Notice that the confidence interval for r is determined by the estimates of r and σ , but the confidence interval for σ is determined only by the estimate of σ . Also, as expected, the confidence intervals of r and σ are dependent on sample size, with the confidence intervals decreasing as N increases.

In Figure 4.5, I use equations (4.17) and (4.19) to construct plots of the length of the 95 percent confidence intervals of r and σ versus sample size for a variety of parameter values.

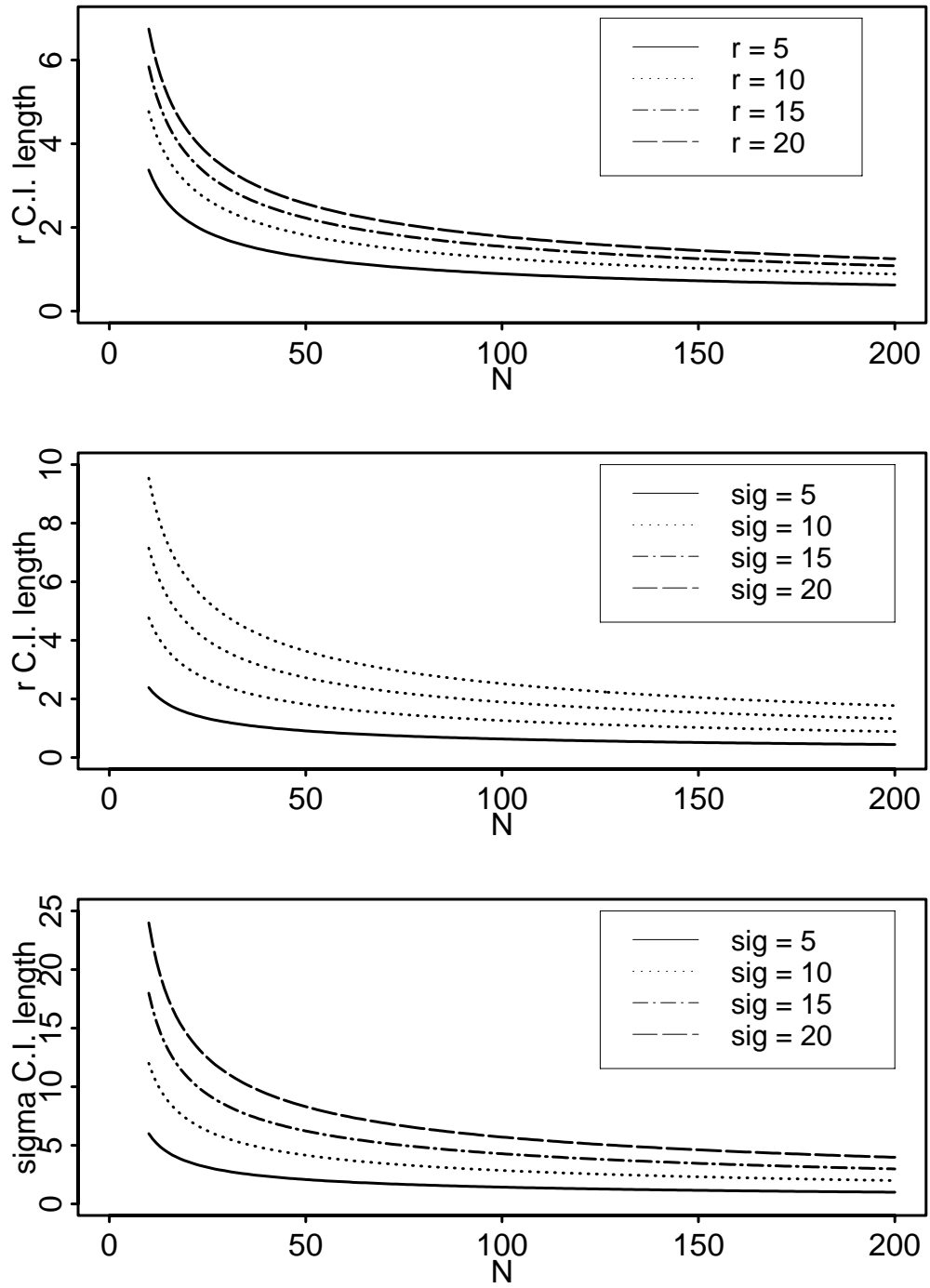


Figure 4.5 Plots of expected 95 percent confidence interval lengths versus sample size for the parameters. In all plots $L = 100$. The first two plots are based on confidence intervals for r , and the last on σ . In the first plot $\sigma = 10.0$, and r is varied. In the last two plots, $r = 10.0$, and σ is varied.

In these plots, I use the expected values of \hat{r} and $\hat{\sigma}$, so the confidence intervals can be thought of as “expected” confidence intervals. In all cases, I set $L = 100$. Since the confidence interval for r is affected by the values of both r and σ , I made two plots. In the first plot, I set $\sigma = 10.0$ and vary r ; in the second plot I set $r = 10.0$ and vary σ . Since the confidence interval of σ is unaffected by r , I made a single plot in which σ is varied. The behavior of the plots is quite similar in all the cases. For small sample sizes, the slope of the curve is steep and negative. By $N = 50$ or so, the curve has substantially flattened. This information is useful in determining appropriate sample sizes for the data analysis.

- discrete case

When data are discrete time observations, closed form solutions of the mles are not available. The mles can be determined, however, by numerically maximizing the likelihood function. With the discrete form of the model (equation (4.8)), the log likelihood function can be formulated based on a multinomial distribution:

$$l(r, \sigma; n_1, n_2, \dots, n_k) = c + \sum_{i=1}^k n_i \log p_i, \quad (4.20)$$

where the index i refers to the time interval, k is the total number of time intervals, n_i is the number of observed individuals in the i th interval, p_i is taken from equation (4.8), and c is a combinatorial constant unaffected by the choice of parameters. To estimate the parameters, I minimize equation (4.20) with respect to the parameters using a downhill simplex technique (Nelder and Mead, 1965; Press et al. 1988).

Another approach for estimating parameters when the data are discrete is generalized least squares or weighted least squares. Based on the multinomial distribution, the variance of the i th class is

$$v_i = Np_i(1 - p_i), \quad (4.21)$$

and to account for unequal variances, the weighting function is $w_i = 1/v_i$. Thus to estimate the parameters, the following equation is minimized with respect to r and σ :

$$S(r, \sigma; n_1, n_2, \dots, n_k) = \sum_{i=1}^k \frac{(Np_i - n_i)^2}{Np_i(1 - p_i)}. \quad (4.22)$$

Later in this chapter I compare these two estimation methods using simulations.

When the data are discrete, parametric confidence intervals are not available. In this case, approximate confidence intervals can be constructed using the bootstrap method as described in chapter 3.

4.4. Simulations

Simulations are often useful in analyzing statistical procedures (Ross, 1990). In many cases, the statistical properties of a distribution can not be or have not been worked out; this is true of the discrete time form of the travel time model and the more complex continuous travel time models developed in later chapters. In these cases, simulations can determine some of the statistical properties. The results of the simulations are useful for choosing among alternative statistical procedures and in determining sample sizes.

A convenient method for generating inverse Gaussian variates has been developed (Michael, et al., 1976) and is quite useful for simulating the basic travel time model, equation (4.7). The details of the procedure are presented in appendix 3d. A general simulation procedure is to generate N individuals in a cohort and then perform statistical procedures such as parameter estimation or a goodness-of-fit test on the cohort. This is the repeated n times to determine properties associated with the parameter estimation method or the appropriateness of the goodness-of-fit test.

continuous case

Since many of the properties associated with the continuous travel time model are available in analytical forms, simulations are not required to determine properties of parameter estimation. A questions remains, however, about the X^2 goodness-of-fit test. This test, used with maximum likelihood parameter estimates, is biased, particularly for small sample sizes (Moore, 1986). It will be helpful to determine the extent of this bias and how it varies with sample size.

Before continuing discussion of the simulation procedure, though, I should note an artifact of using the X^2 test with continuous data. Since the width of the bins (i.e., the values of the e_i 's) is predetermined by sample size, not by the model or particular parameter estimates, the test statistic X^2 takes on discrete values. This is further exacerbated by choosing all the e_i 's to be the same and is particularly noticeable at small sample sizes. Figure 4.6 demonstrates this effect for $N = 20$. In this plot I treat the parameters as known, so the test should be unbiased. The problem that arises is that it is difficult to determine if a test is biased because p -values will also be discrete and will be influenced by where they fall in terms of the discrete jumps. To alleviate this, I develop the following procedure to smooth out the jumps. The first step is to generate n_1 cohorts of size N , and for each cohort determine a test statistic, X^2_i ($i = 1, 2, \dots, n_1$). These test statistics are then ranked to give X^2_r 's ($r = 1, 2, \dots, n_1$). This entire procedure is repeated n_2 times, and an average \bar{X}^2_r for each of the n_1 ranks, \bar{X}^2_r , is calculated. These \bar{X}^2_r 's are continuous and should more closely follow the theoretical distribution. Figure 4.7 demonstrates the output of this procedure for the same sample size and parameter values in Figure 4.6. Notice that the distribution of the test statistic more closely follows the theoretical distribution.

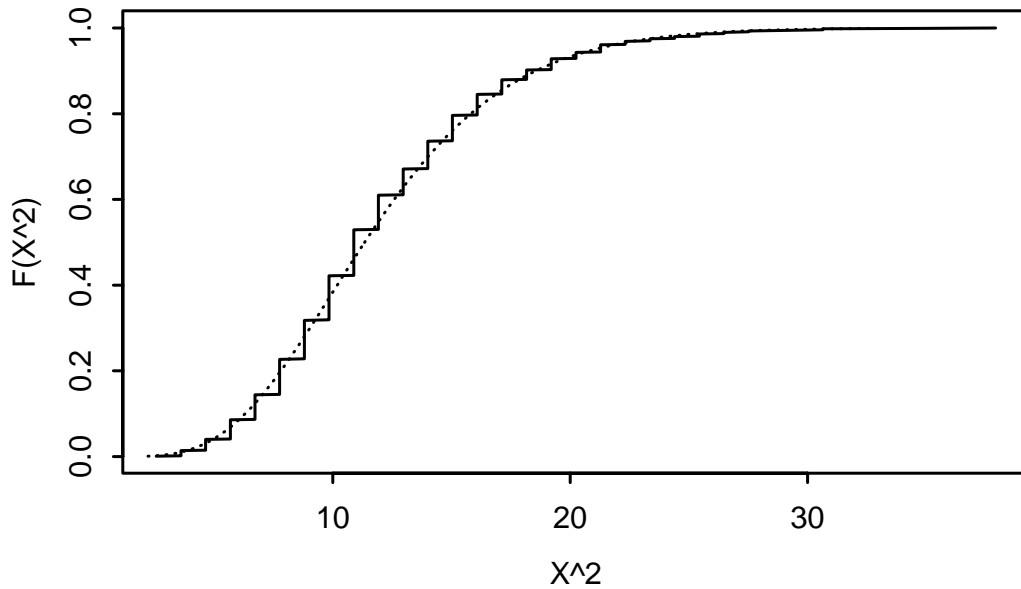


Figure 4.6 A plot of the cumulative distribution of the X^2 statistic versus the X^2 statistic with $L = 100$, $r = 10.0$, $\sigma = 10.0$ and $N = 20$. The dotted line is the theoretical curve. The solid line is based on simulations with $n = 1000$.

To determine if a test is biased, one approach is to begin by choosing an α or several α 's ($0.0 \leq \alpha \leq 1.0$). If the test is unbiased, then the p -values associated with the $(1.0 - \alpha) \cdot n_1$ th ranked \bar{X}^2_r should equal $(1.0 - \alpha)$. If this value is greater than $(1.0 - \alpha)$, the test is considered to be liberal; that is, it does not reject the model enough. If the opposite is true, the model is considered to be conservative.

Figure 4.8 contains the results of simulations of the travel time model. I follow the same procedure as above, except the goodness-of-fit test is performed with estimated parameters. I vary the cohort size from 10 to 200 in increments of 10, with $n_1 = n_2 = 1000$. In the top graph, $\alpha = 0.05$, and $\alpha = 0.10$ in the bottom graph. In both cases, the test appears to be

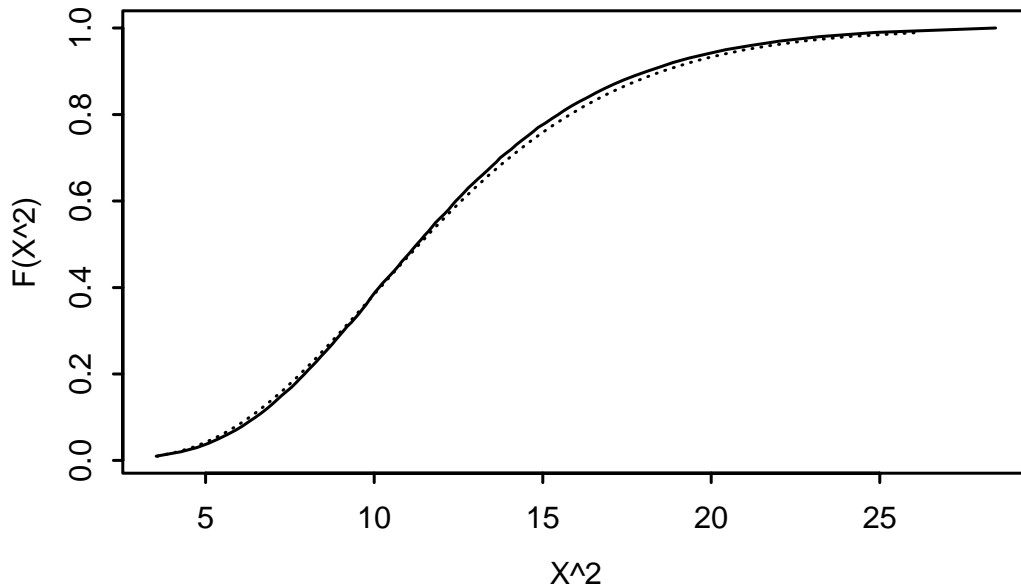


Figure 4.7 Same plot as previous, but with averaged X^2 values from the simulations. For this simulation, $n_1 = 1000$ and $n_2 = 1000$.

unbiased for $N \geq 20$.

discrete data

In this section, I work with the inverse Gaussian distribution (equations (4.9) and (4.10)), the reparameterized version of the basic travel time model. This distribution has two parameters, μ and λ (recall that $\mu = L/r$ and $\lambda = L^2/\sigma^2$), and for these simulations I have chosen $\mu = 10.0$ and $\lambda = 100.0$, roughly corresponding to observed values. The sample size, n , is varied from 25 to 500 in increments of 25. The procedure is as follows. First, create a sample population by selecting n individuals at random from the inverse Gaussian distribution. I use the procedure described by Michael, et al. (1976) to generate variates. These individuals are put into discrete classes (1 day intervals), and model parameters are

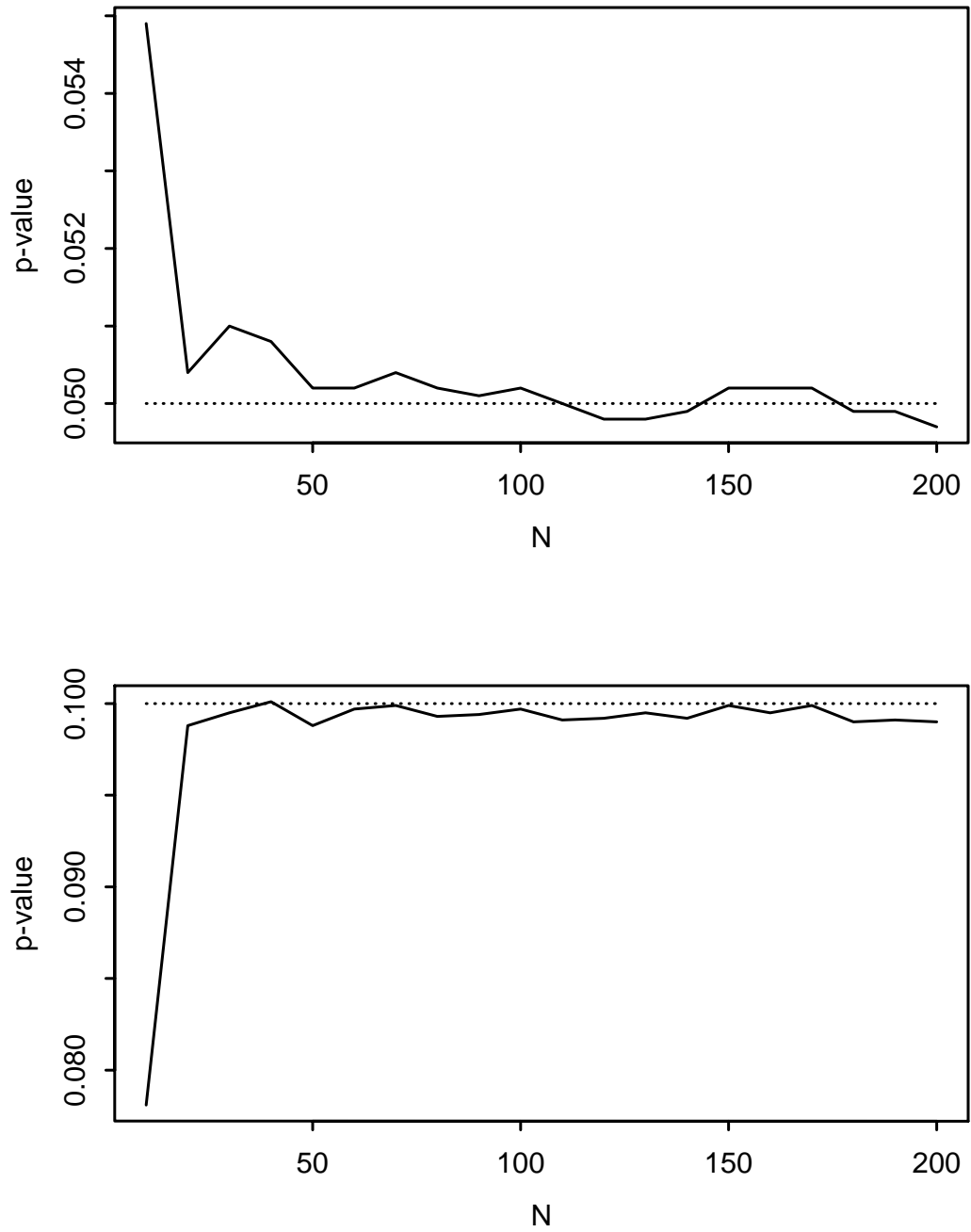


Figure 4.8 Plots of the p -value associated with the $(1.0 - \alpha) \cdot n_1$ th ranked \bar{X}_r^2 value (see text) versus sample size. In the top plot, $\alpha = 0.05$, and in the bottom plot, $\alpha = 0.10$. For both plots, $L = 100$, $r = 10.0$, $\sigma = 10.0$, and $n_1 = n_2 = 1000$.

estimated based on the sample population. This procedure is then repeated 10,000 times so that distributions of parameter estimates can be generated.

parameter estimation

In the simulations, I compare the weighted least squares and the maximum likelihood estimation methods. The two methods appear to be very similar in terms of the mean squared errors (*MSE*) of the parameter estimates (Figure 4.9). In both cases, there is an inverse relationship between *MSE* and sample size, with *MSE* increasing substantially at sample sizes below 100. There does appear to be substantial differences in the bias of the two parameter estimation methods. The weighted least squares method gives biased results for estimates for μ , while the maximum likelihood appears to be unbiased, even at low sample sizes (Figure 4.10). Both methods yield biased estimates of λ for smaller sample sizes. It looks as though the maximum likelihood method is tending toward unbiased estimates as n is gets large, but even at a sample size of 500, the weighted least squares estimates of λ are still substantially biased. Based on these simulations, the maximum likelihood is a more efficient method of parameter estimation. It should be noted, though, that these simulations were performed with particular parameter values. Additional simulations are needed to show that the results are general.

4.5. Application to discrete time data

introduction

As a first example of the application of the travel time model to data, I will apply the model to data of the travel time of fish through a single reservoir. The reservoir is the John Day Pool, the reservoir between McNary and John Day Dams, and the fish observed here are yearling chinook salmon. This data set has several desirable features. First, the fish are traveling through a single relatively homogeneous reach – there are no intervening dams or

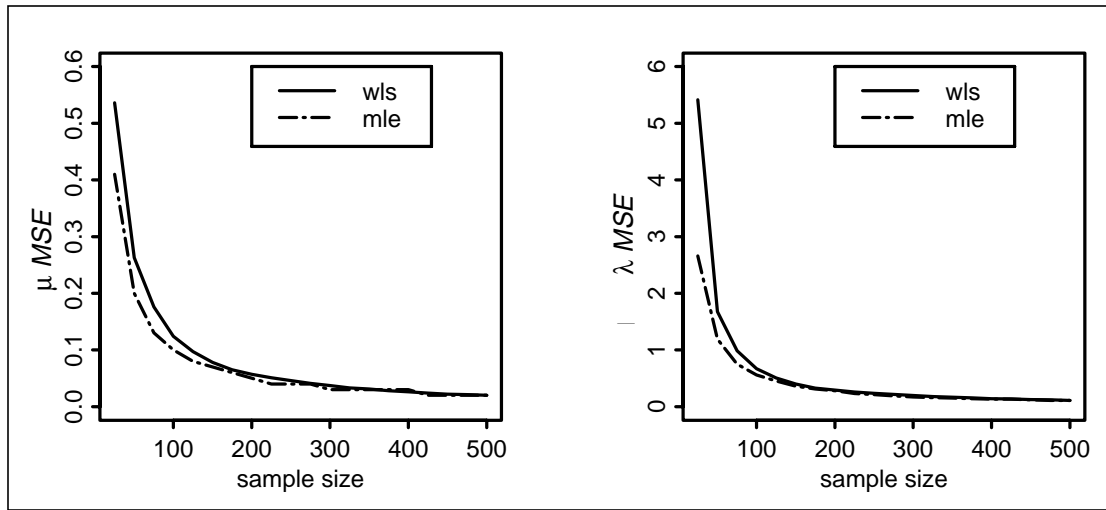


Figure 4.9 Plots of *MSE* versus sample size for the parameters μ and λ for the weighted least squares and maximum likelihood parameter estimation methods.

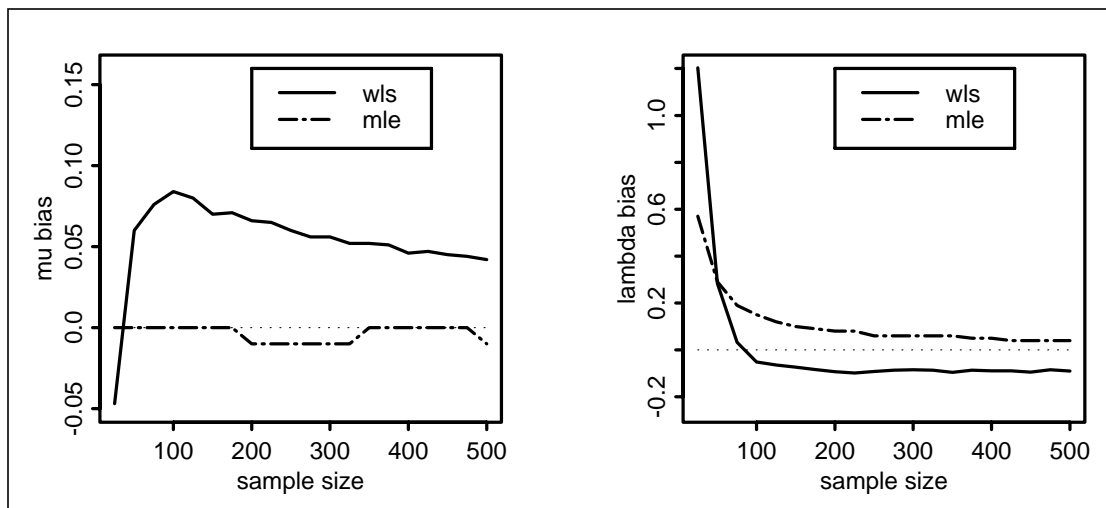


Figure 4.10 Plots of bias versus sample size for the parameters μ and λ for the weighted least squares and maximum likelihood parameter estimation methods.

major tributaries. Also, the study was repeated over four years, and in each year, releases occurred over many days, providing migration characteristics in a variety of conditions. Finally, the fish are active migrants collected from the river. Fish that are raised in hatcheries and then released usually undergo a period of delay before initiating active migration; this adds further complications to the travel time model. Essentially, this data set is a test of whether the simple travel time model can form a basis on to which further complexity can be added as needed.

data

The data consist of yearling chinook salmon collected at McNary Dam, freeze branded with a unique brand (on a daily basis) and then released back into the river below the dam. Approximately 1,000 fish were marked and released per day. Marked fish were sampled as they passed John Day Dam, 122.9 km downstream from the release point. Data were collected over five week periods in 1989, 1990, and 1991; in 1992, six weeks of data were collected. Fish collected and released for 5 days each week (Monday through Friday) were lumped together into weekly cohorts to achieve adequate sample sizes. Cohorts below 20 in sample size were excluded from the analysis. Week 1 of 1990 was excluded because a fire at John Day Dam precluded data collection, and week 5 of 1990 was excluded because the collection facilities were shut down before the groups of this cohort completely passed the dam. A total of sixteen cohorts over the four years were analyzed (Table 4.1). The first two years of the data set have been analyzed statistically by Stevenson and Olson (1991), and they provide a fuller description of the experimental design.

methods

In this application, I apply the discrete time, two parameter, travel time model, equation (4.8), to these data. Parameters are estimated numerically using maximum likelihood based on the multinomial distribution and a downhill simplex fitting routine (Press, et al., 1988).

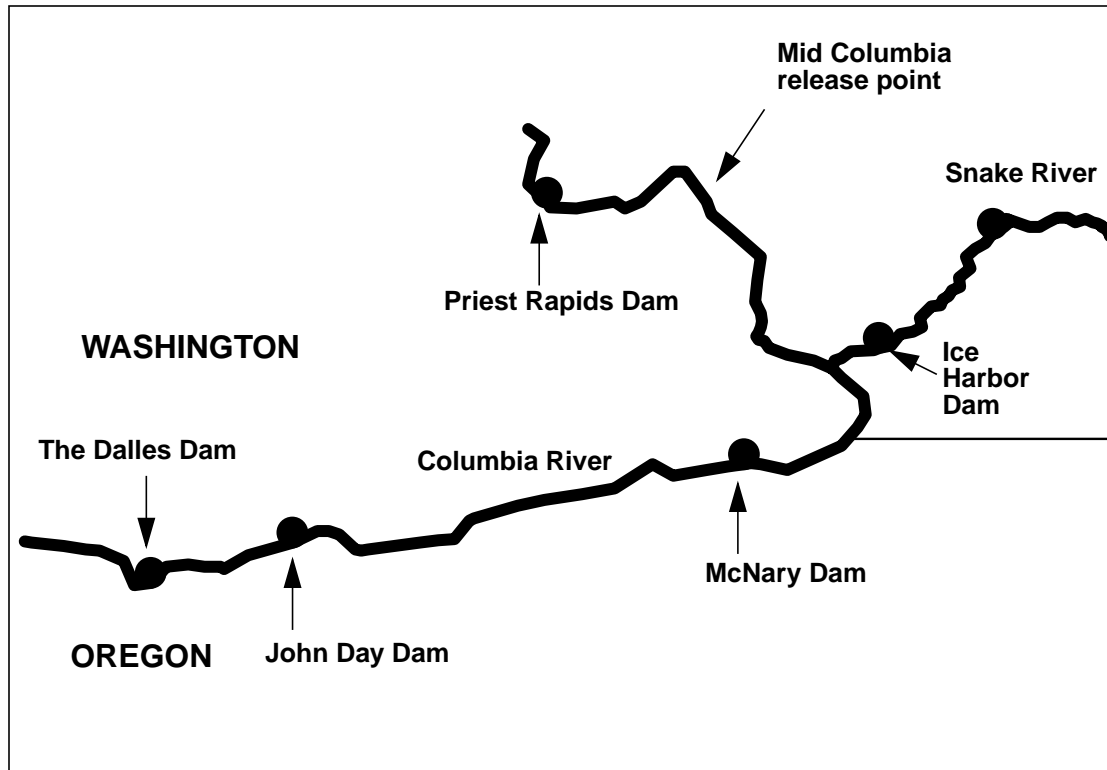


Figure 4.11 A map showing the mid and lower Columbia River release and recapture sites. For the freeze branded chinook, fish were captured, branded, and released at McNary Dam and recaptured at John Day Dam. For the PIT tagged fall chinook analyzed in the next chapter, fish were collected, tagged, and released at the mid-Columbia release point and recaptured at McNary Dam.

Nonparametric 95 per cent confidence intervals are constructed using the bootstrap methods described in chapter 3. Model performance is assessed using Pearson's X^2 statistic.

results

Plots of the data with the best fit model show that the model captures the general behavior of the observed travel time distributions (Figure 4.12). Parameter estimates and

Table 4.1 Descriptive information for the 16 cohorts used in the data analysis. The date of release is for the first release group of the cohort. See text for the procedure used to calculate the average flows for the cohorts.

cohort release information			number sampled	ave. flow (kcfs)
#	year - week	date (Julian date)		
1	1989 - 1	May 01 (121)	27	263.5
2	1989 - 2	May 08 (128)	57	283.2
3	1989 - 3	May 15 (135)	48	258.9
4	1989 - 4	May 22 (142)	32	228.3
5	1990 - 2	April 30 (120)	36	233.9
6	1990 - 3	May 07 (127)	32	231.3
7	1990 - 4	May 14 (134)	24	196.3
8	1991 - 1	April 22 (112)	38	250.0
9	1991 - 2	April 29 (119)	20	236.7
10	1991 - 3	May 06 (126)	24	249.4
11	1992 - 1	April 20 (111)	85	178.3
12	1992 - 2	April 27 (118)	88	195.4
13	1992 - 3	May 04 (125)	88	206.4
14	1992 - 4	May 11 (132)	86	205.2
15	1992 - 5	May 18 (139)	119	202.7
16	1992 - 6	May 25 (146)	80	195.0

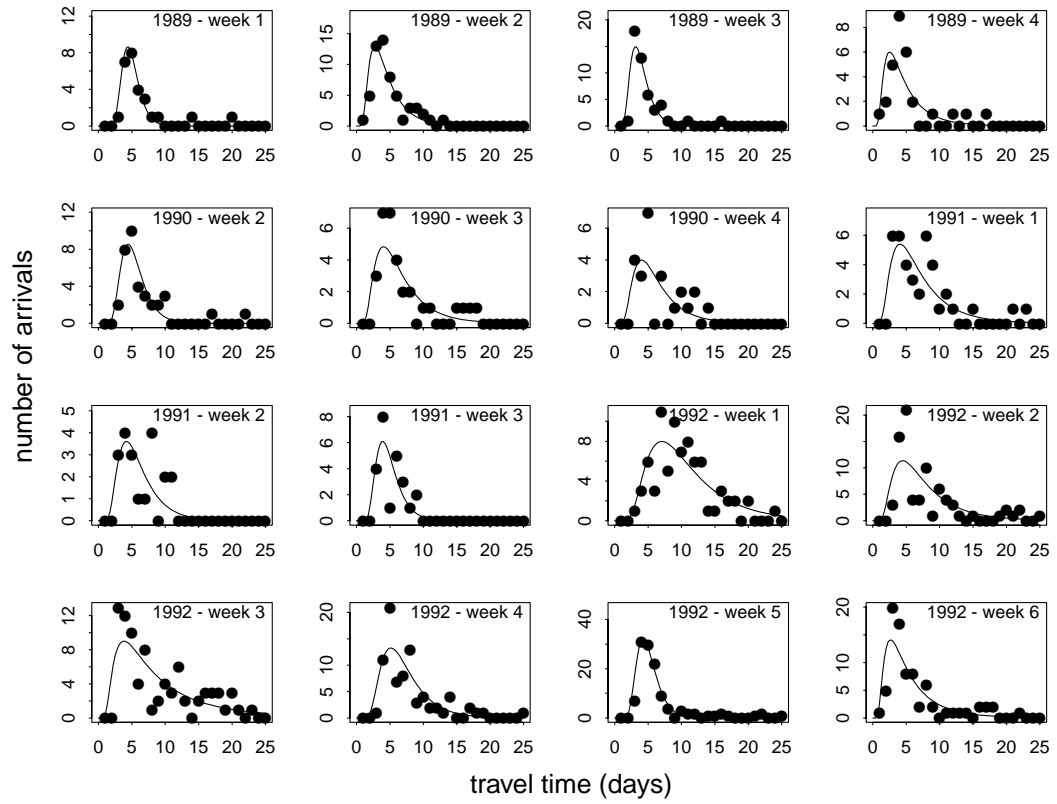


Figure 4.12 Plots of the fitted arrival time model (solid line) versus the data (points) for the sixteen cohorts. The model parameters and results of the goodness-of-fit tests are provided in Table 4.2

confidence intervals are provided in Table 4.2. Estimates of r range from 11.4 to 32.2 km/day, with 95 per cent confidence intervals ranging in width from 4.6 to 17.5 km/day. Estimates of σ ranged from 15.7 to 39.4 km/day^{1/2} with 95 per cent confidence intervals ranging in width from 7.3 to 40.6 km/day^{1/2}. In three cases the model is rejected at the $\alpha = 0.05$ level; for four additional cases, the model is rejected at the $\alpha = 0.10$ level.

discussion

The two parameter arrival time model derived from an advection-diffusion equation works well in describing the downstream movement of actively migrating juvenile salmon under the range of conditions observed in John Day reservoir. In the three out of sixteen cases that the model is rejected (at the $\alpha = 0.05$ level) the data are highly variable, and it is unlikely that any two parameter model would fit.

The difficulty in implementing the model will arise in choosing appropriate parameter values. Table 4.2 reveals variability among cohorts in estimates of r and σ . In the next chapter I will attempt to relate the variability in parameter estimates to observable factors such as river flow and temperature. Variability also arises from sampling error as demonstrated by the broad confidence intervals obtained in the bootstrap analysis. More studies with larger sample sizes would decrease this uncertainty.

4.6. Application to continuous data

In this section, I apply the basic travel time model (equation (4.7)) to continuous data. I analyze data representing several groups (steelhead, spring and fall chinook) from a variety of release points over several years. All the fish in this analysis were collected in a river, marked with a PIT tag, released and then recaptured at a downstream collection site.

Table 4.2 Parameter estimates, confidence intervals and goodness-of-fit results for the sixteen cohorts. The units for r are km/day, and the units for σ are km/day^{1/2}. For the goodness-of-fit test results, df refers to the degrees of freedom. The model is rejected for small p -values, e.g., $p > \alpha$, with α often chosen as 0.05.

cohort		parameter estimation		goodness-of-fit		
#	year - week	\hat{r} (95% C.I.)	$\hat{\sigma}$ (95% C.I.)	χ^2	df	p
1	1989 - 1	25.5 (18.3,28.8)	15.7 (10.9,26.8)	1.87	3	0.600
2	1989 - 2	28.1 (24.2,32.8)	35.1 (26.6,42.7)	4.97	6	0.548
3	1989 - 3	32.2 (26.6,37.5)	25.1 (18.7,31.3)	6.20	3	0.112
4	1989 - 4	26.3 (20.6,38.1)	39.4 (11.7,52.3)	8.63	4	0.071
5	1990 - 2	23.2 (16.8, 26.5)	19.7 (15.4,28.7)	5.47	6	0.486
6	1990 - 3	19.3 (15.6,29.5)	28.4 (13.9,32.4)	4.99	5	0.417
7	1990 - 4	20.2 (16.5,25.9)	27.5 (20.4,32.1)	9.22	4	0.056
8	1991 - 1	17.8 (14.6,23.5)	29.3 (21.6,34.2)	6.54	7	0.479
9	1991 - 2	21.0 (17.4, 26.2)	25.4 (18.6,30.2)	3.59	4	0.464
10	1991 - 3	25.9 (22.3,30.4)	22.1 (16.9,26.0)	5.01	3	0.171
11	1992 - 1	11.4 (9.8,13.8)	20.7 (15.3,23.9)	14.16	15	0.514
12	1992 - 2	16.2 (11.0, 22.4)	28.0 (20.2, 33.7)	51.21	16	0.000
13	1992 - 3	12.5 (10.7,15.3)	34.2 (30.3, 37.6)	25.28	17	0.089
14	1992 - 4	17.6 (13.0, 20.3)	22.1 (18.2,28.1)	31.52	12	0.002
15	1992 - 5	24.9 (20.8,27.5)	18.8 (14.2,25.2)	42.61	10	0.000
16	1992 - 6	22.3 (18.8,30.9)	39.6 (28.7,45.4)	16.61	10	0.084

data

To avoid confusion, I have adopted the following terminology in referring to the PIT tag data.

- *individual* – each individual fish has a unique code, and thus individual travel times can be distinguished.
- *release group* – a group of individuals that was tagged and released from the same point at the same time; all the fish in a release group have the same release identification code in the PIT tag database.
- *cohort* – one to several release groups lumped together to achieve an adequate sample size; cohorts are the unit of analysis for the travel time studies.
- *cohort set* – a group of cohorts that are composed of fish with similar characteristics and released from the same point over several years.

Based on the results of the simulations and the plots of the confidence intervals and bias, I use a target cohort sample size of 50 fish (that is, the number of fish observed at the downstream collection site), with a minimum sample size of 40. Release groups are lumped together (if necessary) from up to 3 consecutive days of release to achieve these sample sizes. Once a cohort reaches 50 fish, I do not add any further release groups to it. If a minimum sample size of 40 could not be obtained from release groups over a three day period, these groups are excluded from the analysis.

I use several criteria to decide which cohort sets to include in the analysis in this and later chapters in addition to the sample size criteria mentioned above. The ideal cohort set has:

- releases over several years and a number of cohorts per year;
- stocks of known origin (hatchery versus wild) and preferably wild;
- migration routes along relative homogeneous river reaches with no intervening dams.

All of the cohort sets did not meet all of these, and I included sets that expanded the scope of the study.

In Appendix 1, I provide the release group identification numbers for all the PIT tag data used in this and subsequent chapters. This appendix also shows how I lumped release groups to form cohorts.

I chose 3 cohort sets to analyze in this section. The first two are fish that were captured, tagged, and released at the Snake River trap and recaptured at Lower Granite Dam, also on the Snake river (Figure 4.13). The reach length is 52 kilometers. One of the cohort sets

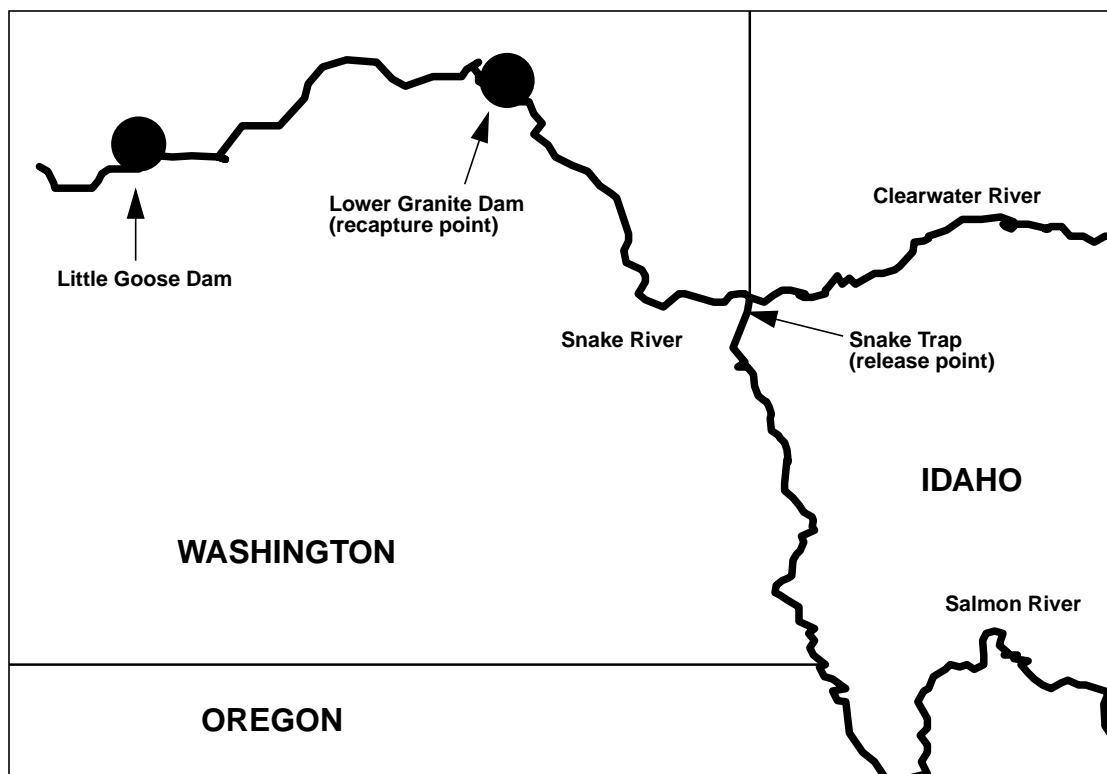


Figure 4.13 Map showing the release and recapture sites for the Snake River chinook and steelhead.

consists of chinook salmon of unknown origin (hatchery versus wild), often referred to as “run-of-the-river” fish. Although the run type (spring or yearling versus fall or subyearling) of these fish is not determined, it is likely that the vast majority of these fish are spring chinooks based on the distribution of lengths (most fish longer than 110 millimeters) and the timing of migration (early spring). Also, I excluded groups released after May 15 because after this date average fish length and migration rate began declining, indicating a possible presence of fall chinook. I refer to these fish as “spring” chinook, but acknowledge that a small percentage of the fish may actually be fall chinook. This is consistent with other treatments of this group of fish (e.g., Fish Passage Center, 1991). Groups were released from early March through mid May. 101 cohorts were analyzed over the 5 year period 1989-1993. Beginning in 1992, hatchery stocks were distinguished at release time, and wild stocks were distinguished in 1992 and 1993. I lump these groups together, though, to be consistent with earlier years.

The other Snake River cohort set is composed of wild steelhead. 101 cohorts of steelhead were analyzed over the same 5 year period. Groups were released from early April through early June.

The third set of fish included in this analysis are wild, fall chinook captured, tagged, and released in the Hanford reach of the mid-Columbia River (see Figure 4.11). Releases occurred during the three years 1991-1993 in early to mid June. They were recaptured at McNary Dam, which is 121 kilometers downstream.

data analysis

The basic travel time model (equation (4.7)) is applied to each cohort. Maximum likelihood estimates (equations (4.11) and (4.12)) are calculated for r and σ , with 95 percent confidence intervals (based on equations (4.17) and (4.19)) constructed around these

estimates. Also, X^2 goodness-of-fit test for continuous data (as described in Chapter 3) is performed for each cohort. The computer code used to perform these algorithms is provided in appendix 3.

results

Table 4.4 - Table 4.6 (in the appendix of this chapter) contains parameter estimates, confidence intervals, and the results of the goodness-of-fit tests for each cohort. Since there is a large amount of information in these tables, I have condensed the results into summary statistics and plots.

It is clear from Table 4.4 - Table 4.6 that there is a great deal of variability in the parameter estimates within cohort sets. In particular, it appears that r increases through the season in some cases. I will analyze this variability in greater detail in the following chapters. In this chapter, I will present the means and standard errors of the cohorts for each of the cohort sets for qualitative comparisons (Table 4.3).

From Table 4.3 it can be seen that the Snake River steelhead migrate at a substantially greater rate (approximately twice as fast) than the Snake River chinook, while the Snake River chinook migrate at a greater rate than the mid-Columbia fall chinook. The comparison between the Snake River steelhead and chinook is particularly relevant because they migrated in the same river reach during the same time period. The estimates of σ were slightly higher for the steelhead than the spring chinook and fall chinook, which were similar to each other.

One way to graphically demonstrate the results of a number of goodness-of-fit tests is to plot the cumulative distribution of the p -values. If the model and data are in perfect accordance, the p -values will be distributed uniformly on (0,1) and should roughly fall on a straight line through the origin and the point (1.0, 1.0). Departures between the model and

Table 4.3 Summary statistics of the parameter estimates averaged on a yearly basis for each of the three cohort sets.

year	number of cohorts	mean value (standard error)	
		r	σ
Snake River spring chinook			
1989	38	5.79 (1.41)	8.44 (2.00)
1990	13	6.71 (2.78)	8.86 (3.64)
1991	17	4.85 (1.82)	6.38 (2.36)
1992	6	4.50 (2.87)	7.04 (4.50)
1993	27	8.23 (2.37)	7.81 (2.22)
Snake River steelhead			
1989	16	18.11 (6.68)	15.57 (5.73)
1990	27	12.97 (3.66)	10.66 (3.01)
1991	20	14.67 (4.84)	11.02 (3.62)
1992	18	10.86 (3.78)	10.36 (3.62)
1993	20	16.80 (5.50)	13.66 (4.48)
mid Columbia fall chinook			
1991	2	3.33 (4.71)	9.62 (13.65)
1992	5	3.58 (2.53)	6.93 (4.91)
1993	6	3.79 (2.40)	7.50 (4.76)

the data can be qualitatively assessed by inspecting this plot.

Figure 4.14 is a plot of the goodness-of-fit test results for the Snake River chinook. While none of the years fall on the 45 degree line, some of the years have quite favorable results. The cohorts from 1989 perform the best overall, with cohorts from 1990, 1991, and

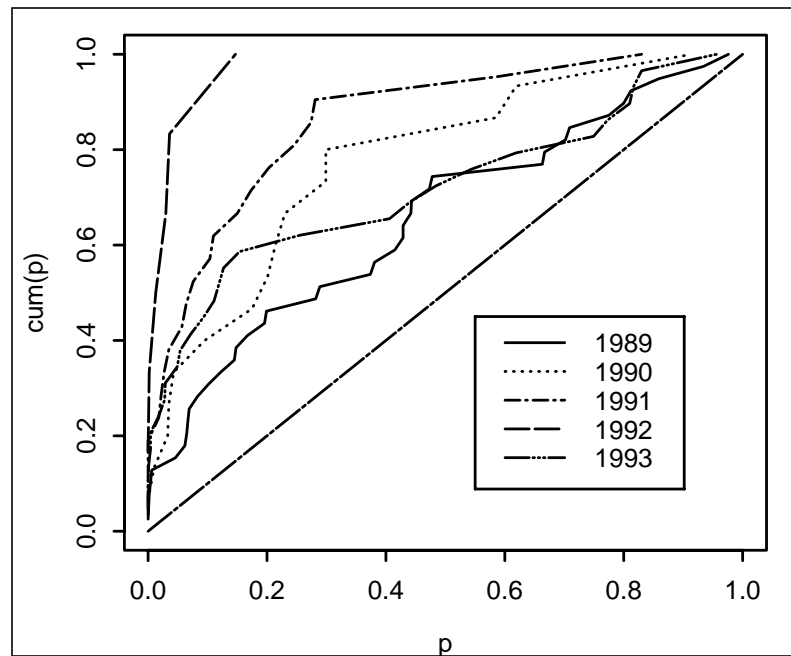


Figure 4.14 Cumulative plots of the goodness-of-fit p -values for the Snake River chinook.

1993 also having the vast majority of p -values above 0.01. The cohorts from 1992 performed poorly relative to the others. 1992 was an extremely low flow year, and this may have affected the behavior of the fish.

The results of the goodness-of-fit tests for the Snake River steelhead (Figure 4.15) are not as favorable as with the chinook. In all years, at least 50 percent of the cohorts have p -values less than 0.01. The results from the mid Columbia fall chinook are also not favorable, with 8 out of 13 cohorts having p -values less than 0.001. This indicates that the model is not fully capturing the behavior of these two groups of fish.

Figure 4.16 contains plots of cumulative distribution functions from the fitted models

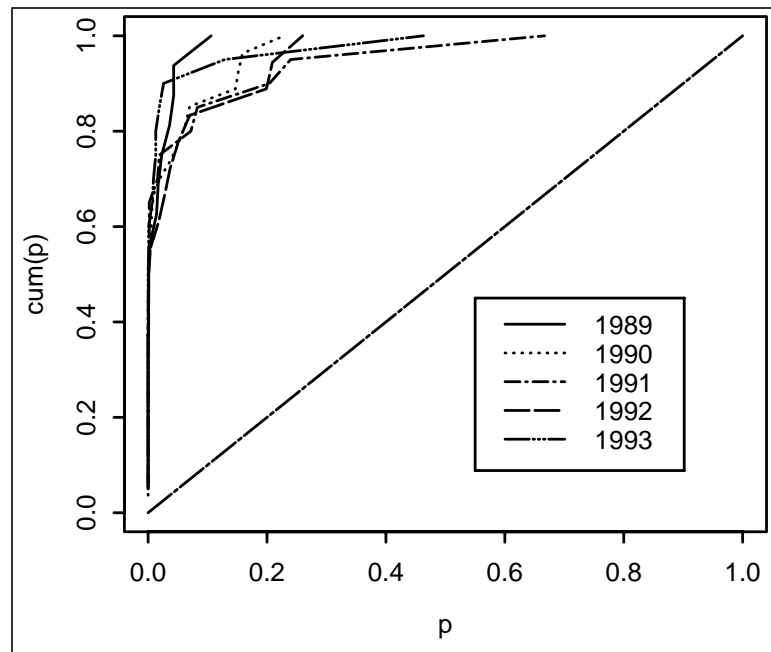


Figure 4.15 Cumulative plots of the goodness-of-fit p -values for the Snake River steelhead.

for the Snake River chinook. The data are included in these plots. These example plots are from cohorts with a variety of p -values to demonstrate the range of model performance. It is clear from these plots that the model does well in describing the data. Even in the case where $p = 0.001$, there is not a wide departure between the model and the data. Figure 4.17 and Figure 4.18 contain similar plots for the steelhead and fall chinook. In these plots, cohorts with p -values below 0.001 were chosen to examine why the model failed. In the case of the steelhead, approximately 75 percent of the fish arrived during a very short period, with the remaining fish trickling in over a more extended period. The model could not capture this behavior. In the case of the fall chinook, it appears that most of the fish delayed migration (or migrated extremely slowly) for over 20 days and then started arriving at the dam. Again, the model could not capture this behavior.

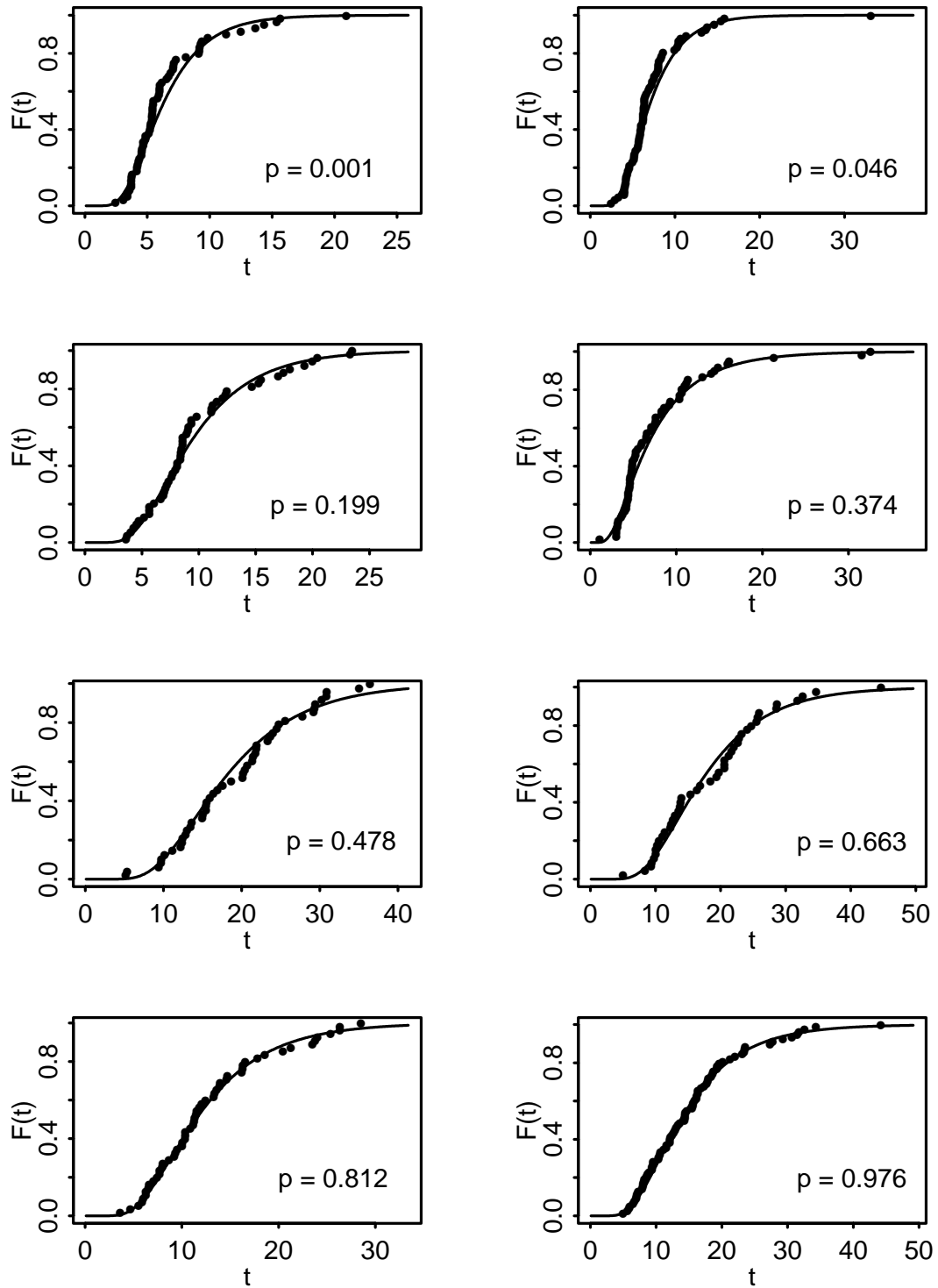


Figure 4.16 Plots of the cumulative travel times for the Snake River chinook. The solid line is the best fit model, and the points are the data. The p -value is from the goodness-of-fit test.

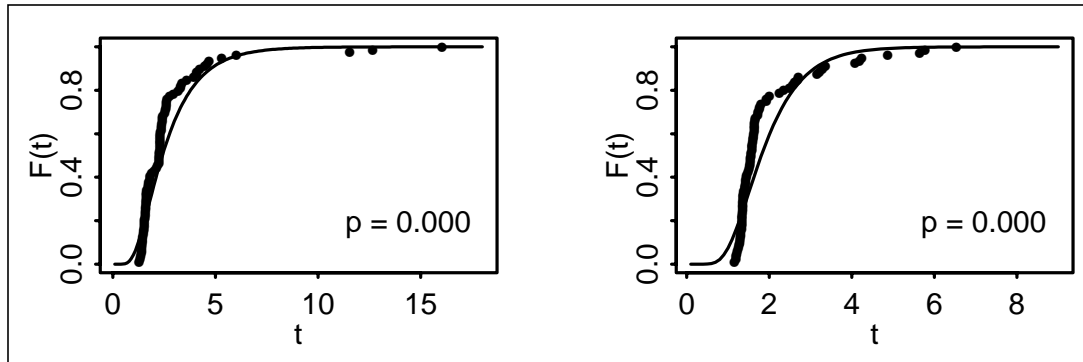


Figure 4.17 Plots of the cumulative travel times for the Snake River steelhead. The solid line is the best fit model, and the points are the data. The p -value is from the goodness-of-fit test.

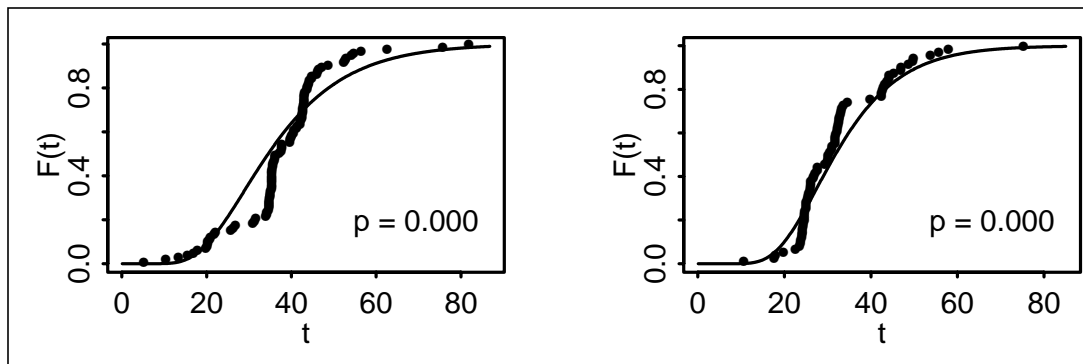


Figure 4.18 Plots of the cumulative travel times for the mid-Columbia fall chinook. The solid line is the best fit model, and the points are the data. The p -value is from the goodness-of-fit test.

discussion

The two parameter, continuous time, travel time model is effective at describing the arrival time distributions of the Snake River spring chinook. For the vast majority of cohorts, the model would not be rejected based on the goodness-of-fit tests. Also, even when the model has low p -values from the goodness-of-fit test, the plots show that there may still be good correspondence between the model and data. As with the lower Columbia chinook analyzed in the previous section, the cohorts from 1992 did not perform as well as those from the other years, which may be due to the extremely low flows that year.

The model does not work as well for the fall chinook and steelhead. The model is probably too simple for these groups; additional components are needed to capture the more complex behavior of these fish.

Besides positive goodness-of-fit results (at least for the spring chinook), the model has other desirable features. It is easy to apply to data, with parameter estimates and confidence intervals easily computed. The two parameters are intuitive and are biologically meaningful: r is the average downstream migration rate, and σ is the rate of population spreading. Also, since both the parameters are rates, they can be compared among cohorts even when the river reaches are different lengths.

4.7. Appendices

appendix 4.a

The method of images is an intuitively appealing approach to boundary crossing problems. It involves the placement of a source term on one side of a boundary and a sink term on the other side (Daniels, 1982). The sink term has the effect of drawing off density from the source term as it reaches the boundary. The approach produces some nice generalities about boundary crossing problems.

With natural boundary conditions, it was shown previously in this chapter that the solution to the advection-diffusion equation with constant coefficients,

$$\frac{\partial f}{\partial t} = -r \frac{\partial f}{\partial x} + \frac{\sigma^2}{2} \frac{\partial^2 f}{\partial x^2}, \text{ is}$$

$$f(x, t) = \frac{1}{\sqrt{2\pi\sigma^2 t}} \exp\left(-\frac{(x-rt)^2}{2\sigma^2 t}\right) \quad (4.23)$$

with initial conditions $f(x, 0) = \delta(x)$. An absorbing boundary at $x = L$ can be achieved by placing a sink term with weight κ at $x = 2L$ (Daniels, 1982). $f(x, t)$ can then be expressed as

$$p(x, t) = \frac{1}{\sqrt{2\pi\sigma^2 t}} \left(\exp\left(-\frac{(x-rt)^2}{2\sigma^2 t}\right) - \kappa \cdot \exp\left(-\frac{(x-2L-rt)^2}{2\sigma^2 t}\right) \right). \quad (4.24)$$

Since $f(x, t)$ vanishes at $x = L$, κ can be solved for by setting $f(L, t) = 0$ in equation (4.24). $\kappa = 2Lr/\sigma^2$ is obtained by completing the square in the second term.

appendix 4.b

In this appendix, I will discuss a method involving Laplace transforms for determining first passage distributions (Riccardia, 1977). I will develop the general approach and then show it can be used in the case of the Wiener drift process with a simple boundary to produce equation (4.7). I have based the derivation on several references: Darling and Siegert (1953), Prabhu (1965), Riccardia (1977), and Chhikara and Folks (1989).

This method takes advantage of the following theorem (due to Siegert (1951)). First, let $X(t)$ be a homogeneous Markov process with continuous sample paths. Define $f(x, t|x_0, t_0)$ as the conditional probability density function for $X(t) = x$ given that $X(t_0) = x_0$. Also, define $g(t, L|t_0, x_0)$ as the probability density function for the time T

when X first reaches the state L , $L > x_0$. The random variable T can be expressed as:

$$T = \inf\{t | X(t) \geq L\} . \quad (4.25)$$

Also, let f^* denote the Laplace transform of f . In other words,

$$f^*(x|x_0, \lambda) = \int_0^\infty e^{-\lambda t} f(x, t|x_0, t_0) dt . \quad (4.26)$$

Similarly, let g^* be the Laplace transform of g .

The following theorem Siegert (1951) is useful in determining g from f and L .

Theorem 4.1

If $x_0 < L < x$, then

$$g^*(L|x_0, \lambda) = \frac{f^*(x|x_0, \lambda)}{f^*(x|L, \lambda)} . \quad (4.27)$$

proof:

The proof follows by considering paths that lie at $x > L$ at time t . Paths that are beyond L at time t must have first reached L at some time s with $s < t$. Thus, we can write the conditional probability distribution for x in terms of possible paths from x_0 to x :

$$f(x, t|x_0, t_0) = \int_0^t g(t, L|t_0, x_0) f(x, t|L, t-s) ds . \quad (4.28)$$

Applying the convolution theorem for Laplace transforms to equation (4.28) yields:

$$f^*(x|x_0, \lambda) = \frac{g^*(L|x_0, \lambda)}{f^*(x|L, \lambda)} . \quad (4.29)$$

Rearranging terms results in equation (4.27).

This theorem is useful in cases where the Laplace transform is known for f . The Laplace

transform for g can then be determined from equation (4.27). If the inverse Laplace transform is known for g^* , then g can be obtained. In many cases, this is not practical. In some cases, such as the Wiener process and Weiner process with drift, the pertinent Laplace transforms and inverse Laplace transforms are known, and equation (4.27) can be used to determine the first passage distributions.

In the case of the Wiener Process with drift,

$$f^*(x|x_0, \lambda) = \int_0^\infty \frac{1}{\sqrt{2\pi\sigma^2 t}} \exp\left(-\frac{(x-x_0-rt)^2}{\sigma^2 t}\right) e^{-\lambda t} dt . \quad (4.30)$$

After combining the exponents, completing the square, and rearranging terms, we end up with:

$$f^*(x|x_0, \lambda) = \frac{1}{x-x_0} \exp\left(-\frac{x-x_0}{\sigma^2}(\sqrt{r^2-2\sigma^2\lambda}-r)\right) \cdot \int_0^\infty t \frac{x-x_0}{\sqrt{2\pi\sigma^2 t^3}} \exp\left(-\frac{(x-x_0-rt)^2}{\sigma^2 t}\right) dt . \quad (4.31)$$

Integrating (4.31) by parts yields:

$$f^*(x|x_0, \lambda) = \frac{1}{\sqrt{r^2-2\sigma^2\lambda}} \exp\left(\frac{x-x_0}{\sigma^2}(\sqrt{r^2-2\sigma^2\lambda}-r)\right) . \quad (4.32)$$

Substituting L for x_0 in equation (4.32) and plugging this into equation (4.27) yields:

$$g^*(L|x_0, \lambda) = \exp\left(\frac{x_0-L}{\sigma^2}(\sqrt{r^2-2\sigma^2\lambda}-r)\right) . \quad (4.33)$$

Making use of the fact that $L^{-1}(\exp(-a\sqrt{p})) = \frac{a}{2\sqrt{\pi}}t^{-3/2}e^{-a^2/4t}$ (Haberman, 1987), we

arrive at:

$$g(t|L) = \frac{1}{\sigma\sqrt{2\pi t^3}} \exp\left(\frac{-(L-rt)^2}{2\sigma^2 t}\right). \quad (4.34)$$

An alternative approach for determining the Laplace transform of the arrival time distribution is as follows. This approach begins by considering equation (4.5), the probability density for $X(t) = x$ given that the process hasn't reached the barrier by time t . This can be written as $p(x, t|x_0, t_0)$ for $x < L$, $t < T$ (recall from above that T is defined as the time of absorption at the boundary). Also define

$$P(x, t|x_0, t_0) = \int_{-\infty}^x p(y, t|x_0, t_0) dy, \quad (4.35)$$

and note that $P(L, t|x_0, t_0) = \text{prob}(T \geq t)$. P satisfies the backward Chapman-Kolmogorov equation (Cox and Miller, 1965); in other words, P satisfies

$$\frac{\partial P}{\partial t} = r \frac{\partial P}{\partial x_0} + \frac{\sigma^2}{2} \frac{\partial^2 P}{\partial x_0^2}. \quad (4.36)$$

Also, P can be related to the arrival time distribution by the relation

$$g(t|L, x_0) = -\frac{d}{dt} P(L, t|x_0, t_0). \quad (4.37)$$

Plugging equation (4.37) into equation (4.36) and taking the Laplace transform of both sides yields

$$\lambda g^* = r \frac{d}{dx_0} g^* + \frac{\sigma^2}{2} \frac{d^2}{dx_0^2} g^*. \quad (4.38)$$

This is a second order linear ordinary differential equation and can be solved directly. The general form of the solution is

$$g^* = Ae^{x_0\alpha_1} + Be^{x_0\alpha_2}. \quad (4.39)$$

α_1 and α_2 are the roots of the characteristic equation $\frac{1}{2}\alpha^2 + r\alpha = \lambda$. Thus

$$\alpha_1, \alpha_2 = \frac{-r \pm \sqrt{r^2 + 2\lambda\sigma^2}}{\sigma^2},$$

and α_1 is positive (and real) and α_2 is negative. The particular solution can be obtained from the following information. First, g^* is bounded for $\lambda > 0$:

$$g^*(t|\lambda) = \int_0^\infty e^{-\lambda t} g(t) dt \leq \int_0^\infty g(t) dt \leq 1. \quad (4.40)$$

Thus the coefficient $B = 0$, or else the second term of the general solution would become unbounded as $x_0 \rightarrow -\infty$. The coefficient A can be determined by noting that when $x_0 = L$, absorption is immediate, and $g^*(t|\lambda) = 1$. This yields $A = e^{-L}$, and

$$g^* = \exp\left((x_0 - L) \frac{-r + \sqrt{r^2 + 2\lambda\sigma^2}}{\sigma^2}\right). \quad (4.41)$$

This is the same as equation (4.33) and is inverted in the same manner to give $g(t)$.

appendix 4.c

In computing equation (4.8) an exponential overflow problem can be encountered. This equation involves multiplying an exponential that is large (sometimes larger than the machine can handle) by a standard normal probability that is very small. Dennis et al. (1991) present a method for combining these two terms in a numerical approximation for

equation (4.8). Since I use this approximation extensively in computations, I will present the details.

The cumulative distribution function for the inverse Gaussian is

$$G(t;r, \sigma, L) = 1 - \left[\Phi\left(\frac{L - rt}{\sigma\sqrt{t}}\right) - \exp\left(\frac{2Lr}{\sigma^2}\right)\Phi\left(\frac{-L - rt}{\sigma\sqrt{t}}\right) \right] , \quad (4.42)$$

where Φ is the cdf of the standard normal distribution. Problems may arise in evaluating the above equation because the second term involves multiplying a large number, $\exp(\bullet)$, by a very small number, $\Phi(\bullet)$. For certain combinations of r , σ , L and t either of these numbers may be beyond the precision of the computer used. Dennis, et al. (1991) present a method that circumvents this problem by combining the two components of the second term. The following has been modified from their approach.

First, making use of the relation $\Phi(x) = 1 - \Phi(-x)$, rewrite equation (4.42) as

$$G(t) = \Phi(y) + \exp\left(\frac{2Lr}{\sigma^2}\right)\Phi(-z) , \quad (4.43)$$

with

$$y = \frac{rt - L}{\sigma\sqrt{t}}$$

$$z = \frac{rt + L}{\sigma\sqrt{t}}.$$

Now denote the pdf of the standard normal distribution as ϕ . It is easy to show that

$$\phi(y) = \exp\left(\frac{2Lr}{\sigma^2}\right)\phi(z) , \quad (4.44)$$

and thus

$$\Phi(y) = \exp\left(\frac{2Lr}{\sigma^2}\right)\Phi(z) . \quad (4.45)$$

It follows that

$$\begin{aligned} \exp\left(\frac{2Lr}{\sigma^2}\right)\Phi(-z) &= \exp\left(\frac{2Lr}{\sigma^2}\right)[1 - \Phi(z)] \\ &= \frac{\phi(y)}{\phi(z)}[1 - \Phi(z)] . \end{aligned} \quad (4.46)$$

This can be evaluated using the following approximations for Φ (Abramowitz and Stegun, 1965). If $x < 4$,

$$\Phi(x) \approx 1 - \phi(x)[d_1q_y + d_2q_y^2 + \dots + d_5q_y^5] , \quad (4.47)$$

where $q_y = 1/(1+d_0)$, $d_0 = 0.2316419$, $d_1 = 0.319381530$, $d_2 = -0.356563782$, $d_3 = 1.781477937$, $d_4 = -1.821255978$, and $d_5 = 1.330274429$. For $x \geq 4$

$$\Phi(x) \approx 1 - \frac{\phi(x)}{x} \left[1 - \frac{1}{x^2} + \dots + \frac{(-1)^s 1 \cdot 3 \cdot \dots \cdot (2s-1)}{x^{2s}} \right] \quad s = 1, \dots, 7. \quad (4.48)$$

Therefore, for $z < 4$, using equations (4.46) and (4.47),

$$\exp\left(\frac{2Lr}{\sigma^2}\right)\Phi(-z) \approx \phi(y)[d_1q_z + d_2q_z^2 + \dots + d_5q_z^5] . \quad (4.49)$$

And for $z \geq 4$, using equations (4.46) and (4.48),

$$\exp\left(\frac{2Lr}{\sigma^2}\right)\Phi(-z) \approx \frac{\phi(y)}{z} \left[1 - \frac{1}{z^2} + \dots + \frac{(-1)^s 1 \cdot 3 \cdot \dots \cdot (2s-1)}{z^{2s}} \right] . \quad (4.50)$$

The code to evaluate $G(t)$ using the above procedure is contained in Appendix 3.

appendix 4.d

Several of the simulations I perform require the generation of inverse Gaussian random variates. A standard procedure for generating random variates, x , from a probability density function, $f(x)$, is to use the inverse of the cumulative distribution function, $F(x)$. The procedure involves generating a uniform random variate on the range (0,1) and using the transformation $x = F^{-1}(x)$ to generate the random variate. To perform this a closed form solution of F^{-1} is required, but this is not known for the inverse Gaussian distribution.

Another approach utilizes a known relationship $v = g(x)$, with the random variate, v , coming from an easily generated distribution. This procedure becomes a bit more complicated when there is more than one root, x_i , for a given observation, v_0 , and it must be determined how to choose one of the roots.

Michael, et al. (1976) present a procedure for generating inverse Gaussian random variates using a transformation that yields two roots. One of the roots is selected with an assigned probability. The inverse Gaussian can be written as

$$f(x; \mu, \lambda) = \sqrt{\frac{\lambda}{2\pi x^3}} \exp\left[-\frac{\lambda(x - \mu)^2}{2\mu^2 x}\right], \quad x > 0, \mu > 0, \lambda > 0. \quad (4.51)$$

The parameter $\mu = L/r$, and $\lambda = L^2/\sigma^2$. With the transformation

$$V = g(X) = \frac{\lambda(x - \mu)^2}{\mu^2 x}, \quad (4.52)$$

V is distributed as χ^2 with one degree of freedom. The χ^2 variates, v , are easily generated as squares of standard normal random variates. For a particular observation, v_0 , equation (4.52) has two roots:

$$x_1 = \mu + \frac{\mu^2 v_0}{2\lambda} - \frac{\mu}{2\lambda} \sqrt{4\mu\lambda v_0 - \mu^2 v_0^2}$$

$$x_2 = \mu^2 / x_1. \quad (4.53)$$

Michael, et al. (1976) show that the root x_j should be chosen with probability

$$p_1(v_0) = \frac{\mu}{\mu + x_1}. \quad (4.54)$$

Thus a general procedure for generating inverse Gaussian random variates is as follows. First, generate a random variate from a standard normal distribution and square it to generate an observation from $\chi^2_{(1)}$, v_0 . Next, use equation (4.53) to calculate the roots x_1 and x_2 . Finally, perform a Bernoulli trial with equation (4.54) to select the appropriate root. The computer code to perform this procedure is provided in Appendix 3.

appendix 4.e

The results of the application of the two parameter travel time model (equation (4.7)) to continuous PIT tag data are contained in Table 4.4 through Table 4.6.

Table 4.4 Results of the application of the two parameter, travel time model to Snake River, spring chinook PIT tag data. The cohort number corresponds to the numbers in Appendix 1. The methods for estimating parameters, constructing confidence intervals, and conducting goodness-of-fit tests are provided in chapter 4.6.

<i>species: chinook run type: unknown rearing type: unknown release site: Snaketrap</i>							
group #	# of fish	release date	parameter est. (95% confidence int.)		goodness-of-fit		
			r (km/day)	σ (km/day ^{1/2})	X^2	df	p
1989							
1	48	03/24/89	2.69 (2.33, 3.06)	5.46 (4.60, 6.91)	13.63	14	0.478
2	61	03/27/89	2.94 (2.62, 3.26)	5.22 (4.46, 6.40)	16.56	16	0.415
3	57	03/28/89	2.74 (2.40, 3.07)	5.42 (4.62, 6.71)	15.32	15	0.429
4	55	03/29/89	2.85 (2.56, 3.13)	4.42 (3.76, 5.50)	23.87	15	0.067
5	45	03/30/89	2.79 (2.39, 3.19)	5.69 (4.76, 7.27)	11.29	14	0.663
6	57	03/31/89	2.77 (2.33, 3.22)	7.25 (6.18, 8.98)	22.26	15	0.101
7	54	04/01/89	3.25 (2.81, 3.70)	6.48 (5.50, 8.08)	24.00	15	0.065
8	57	04/02/89	3.04 (2.59, 3.50)	7.04 (6.00, 8.72)	24.16	15	0.062
9	47	04/03/89	2.95 (2.49, 3.41)	6.57 (5.52, 8.34)	30.77	14	0.006
10	52	04/04/89	3.31 (2.89, 3.72)	5.87 (4.96, 7.35)	10.31	15	0.800
11	78	04/05/89	3.36 (2.97, 3.76)	6.80 (5.91, 8.12)	8.15	18	0.976
12	77	04/07/89	3.70 (3.34, 4.05)	5.84 (5.07, 6.98)	13.27	18	0.775
13	54	04/09/89	3.30 (2.88, 3.71)	6.02 (5.11, 7.50)	9.33	15	0.859
14	43	04/10/89	3.16 (2.58, 3.74)	7.58 (6.32, 9.74)	15.42	13	0.282
15	55	04/11/89	4.04 (3.49, 4.60)	7.29 (6.19, 9.06)	10.13	15	0.812
16	48	04/12/89	4.93 (4.31, 5.56)	6.95 (5.85, 8.80)	10.79	14	0.702
17	53	04/13/89	5.14 (4.44, 5.85)	8.07 (6.84, 10.08)	19.34	15	0.199
18	66	04/14/89	5.81 (5.19, 6.43)	7.50 (6.45, 9.12)	22.48	17	0.167
19	51	04/15/89	5.09 (4.39, 5.80)	7.94 (6.71, 9.97)	20.65	15	0.148
20	68	04/16/89	7.24 (6.33, 8.15)	9.99 (8.61, 12.12)	25.53	17	0.083
21	64	04/17/89	7.49 (6.52, 8.46)	10.13 (8.70, 12.37)	22.69	16	0.122
22	66	04/18/89	8.01 (6.90, 9.11)	11.40 (9.81, 13.87)	39.45	17	0.002
23	63	04/19/89	8.64 (7.41, 9.87)	11.89 (10.20, 14.54)	15.71	16	0.473
24	59	04/20/89	8.97 (7.66, 10.27)	11.94 (10.19, 14.71)	18.61	16	0.289
25	62	04/21/89	9.16 (7.87, 10.45)	12.01 (10.29, 14.71)	25.03	16	0.069
26	60	04/22/89	7.80 (6.86, 8.75)	9.34 (7.98, 11.49)	38.17	16	0.001
27	69	04/23/89	8.15 (7.34, 8.97)	8.51 (7.34, 10.30)	21.72	17	0.196
28	61	04/24/89	6.51 (5.38, 7.64)	12.40 (10.61, 15.22)	17.18	16	0.374
29	70	04/25/89	6.84 (6.09, 7.60)	8.68 (7.49, 10.49)	14.00	17	0.667
30	66	04/26/89	7.47 (6.74, 8.20)	7.79 (6.70, 9.47)	13.39	17	0.709
31	66	04/27/89	6.93 (6.13, 7.73)	8.85 (7.62, 10.77)	27.94	17	0.046
32	71	04/28/89	8.57 (7.71, 9.43)	8.88 (7.68, 10.71)	17.17	17	0.443
33	41	04/30/89	10.26 (9.07, 11.44)	8.34 (6.93, 10.81)	13.24	13	0.429
34	64	05/09/89	11.53 (9.74, 13.31)	15.05 (12.92, 18.38)	35.16	16	0.004
35	62	05/10/89	7.75 (6.61, 8.89)	11.54 (9.88, 14.14)	17.06	16	0.381

Table 4.4 (Continued) Results of the application of the two parameter, travel time model to Snake River, spring chinook PIT tag data. The cohort number corresponds to the numbers in Appendix 1. The methods for estimating parameters, constructing confidence intervals, and conducting goodness-of-fit tests are provided in chapter 4.6.

<i>species: chinook run type: unknown rearing type: unknown release site: Snaketrap</i>							
group #	# of fish	release date	parameter est. (95% confidence int.)		goodness-of-fit		
			r (km/day)	σ (km/day ^{1/2})	X^2	df	p
36	64	05/11/89	7.55 (6.46, 8.64)	11.35 (9.74, 13.85)	16.16	16	0.442
37	61	05/12/89	6.95 (5.98, 7.91)	10.24 (8.76, 12.57)	8.46	16	0.934
38	84	05/13/89	6.29 (5.62, 6.96)	8.83 (7.71, 10.47)	25.48	19	0.145
1990							
1	59	04/09/90	5.30 (4.67, 5.94)	7.55 (6.44, 9.30)	27.63	16	0.035
2	60	04/17/90	8.50 (7.70, 9.30)	7.61 (6.50, 9.36)	20.43	16	0.201
3	52	04/17/90	8.13 (7.12, 9.14)	9.11 (7.71, 11.40)	43.54	15	0.000
4	54	04/19/90	8.85 (7.92, 9.77)	8.14 (6.91, 10.14)	17.33	15	0.299
5	59	04/20/90	6.34 (5.28, 7.40)	11.55 (9.86, 14.24)	23.76	16	0.095
6	59	04/21/90	6.27 (5.38, 7.17)	9.83 (8.39, 12.12)	32.14	16	0.010
7	66	04/22/90	6.21 (5.31, 7.11)	10.51 (9.04, 12.79)	21.27	17	0.214
8	62	04/23/90	5.55 (4.74, 6.37)	9.72 (8.33, 11.91)	26.87	16	0.043
9	70	04/24/90	5.16 (4.42, 5.89)	9.78 (8.44, 11.81)	15.14	17	0.585
10	80	04/25/90	4.54 (3.95, 5.13)	8.88 (7.74, 10.59)	23.43	18	0.175
11	52	04/27/90	6.29 (5.70, 6.88)	6.03 (5.10, 7.55)	8.23	15	0.914
12	41	04/30/90	5.75 (5.00, 6.50)	7.06 (5.87, 9.14)	10.90	13	0.619
13	54	05/07/90	10.34 (9.18, 11.51)	9.47 (8.04, 11.81)	17.33	15	0.299
1991							
1	55	04/08/91	2.94 (2.63, 3.25)	4.83 (4.10, 6.01)	24.53	15	0.057
2	42	04/09/91	3.28 (2.95, 3.61)	4.11 (3.42, 5.30)	18.19	13	0.150
3	63	04/10/91	3.38 (3.07, 3.69)	4.72 (4.05, 5.77)	48.89	16	0.000
4	84	04/12/91	3.59 (3.31, 3.87)	4.82 (4.21, 5.71)	27.05	19	0.104
5	69	04/15/91	3.05 (2.74, 3.36)	5.33 (4.60, 6.46)	20.57	17	0.246
6	66	04/17/91	4.04 (3.61, 4.46)	6.16 (5.30, 7.49)	50.97	17	0.000
7	47	04/18/91	4.39 (3.92, 4.86)	5.44 (4.57, 6.91)	24.98	14	0.035
8	55	04/19/91	3.62 (3.18, 4.06)	6.08 (5.16, 7.56)	44.16	15	0.000
9	65	04/22/91	4.89 (4.25, 5.53)	8.34 (7.17, 10.16)	30.00	16	0.018
10	62	04/23/91	5.11 (4.46, 5.76)	8.06 (6.90, 9.87)	18.90	16	0.274
11	90	04/25/91	6.63 (5.70, 7.57)	12.43 (10.90, 14.65)	17.07	19	0.585
12	63	04/26/91	6.29 (5.59, 6.98)	7.91 (6.78, 9.67)	21.14	16	0.173
13	81	04/27/91	5.49 (5.01, 5.97)	6.69 (5.83, 7.97)	31.26	18	0.027
14	53	04/29/91	5.62 (5.07, 6.17)	6.00 (5.09, 7.50)	23.42	15	0.076
15	51	04/30/91	6.09 (5.28, 6.91)	8.35 (7.05, 10.48)	19.24	15	0.203
16	63	05/10/91	9.92 (8.68, 11.15)	11.14 (9.56, 13.63)	65.17	16	0.000
17	53	05/11/91	10.33 (9.52, 11.15)	6.59 (5.59, 8.23)	9.83	15	0.830
1992							
1	50	04/07/92	3.94 (3.49, 4.38)	5.61 (4.74, 7.07)	25.48	14	0.030
2	57	04/08/92	3.73 (3.26, 4.20)	6.53 (5.56, 8.08)	29.84	15	0.013

Table 4.4 (Continued) Results of the application of the two parameter, travel time model to Snake River, spring chinook PIT tag data. The cohort number corresponds to the numbers in Appendix 1. The methods for estimating parameters, constructing confidence intervals, and conducting goodness-of-fit tests are provided in chapter 4.6.

<i>species: chinook run type: unknown rearing type: unknown release site: Snaketrap</i>							
group #	# of fish	release date	parameter est. (95% confidence int.)		goodness-of-fit		
			r (km/day)	σ (km/day ^{1/2})	X^2	df	p
3	84	04/14/92	3.95 (3.55, 4.34)	6.57 (5.74, 7.79)	63.71	19	0.000
4	52	04/20/92	4.59 (3.98, 5.20)	7.35 (6.22, 9.20)	20.69	15	0.147
5	45	04/23/92	5.45 (4.84, 6.06)	6.21 (5.20, 7.93)	24.89	14	0.036
6	46	05/01/92	5.36 (4.40, 6.32)	9.96 (8.35, 12.68)	33.83	14	0.002
1993							
1	47	04/09/93	3.65 (3.13, 4.17)	6.57 (5.52, 8.34)	20.64	14	0.111
2	71	04/10/93	3.76 (3.43, 4.09)	5.14 (4.44, 6.20)	17.73	17	0.406
3	60	04/11/93	3.57 (3.21, 3.92)	5.22 (4.46, 6.42)	11.57	16	0.773
4	59	04/12/93	3.48 (3.12, 3.84)	5.31 (4.53, 6.54)	14.75	16	0.543
5	44	04/13/93	3.61 (3.27, 3.95)	4.20 (3.51, 5.38)	9.32	14	0.810
6	46	04/15/93	4.38 (3.95, 4.81)	4.91 (4.12, 6.25)	10.17	14	0.749
7	59	04/18/93	5.59 (5.00, 6.17)	6.75 (5.77, 8.32)	19.25	16	0.256
8	43	04/21/93	5.48 (4.83, 6.12)	6.40 (5.34, 8.23)	19.14	13	0.119
9	47	04/22/93	6.27 (5.52, 7.02)	7.25 (6.09, 9.21)	14.13	14	0.440
10	82	04/23/93	7.14 (6.61, 7.68)	6.52 (5.69, 7.76)	9.17	18	0.956
11	47	04/25/93	7.47 (6.68, 8.27)	7.10 (5.96, 9.01)	21.36	14	0.093
12	51	04/26/93	8.37 (7.59, 9.15)	6.84 (5.78, 8.59)	10.06	15	0.816
13	64	04/27/93	8.09 (7.39, 8.79)	7.07 (6.07, 8.63)	15.56	16	0.484
14	43	04/28/93	8.29 (7.37, 9.21)	7.42 (6.19, 9.54)	22.12	13	0.054
15	58	04/29/93	9.71 (8.77, 10.64)	8.16 (6.96, 10.08)	35.03	16	0.004
16	60	04/30/93	10.34 (9.34, 11.35)	8.67 (7.41, 10.66)	24.87	16	0.072
17	53	05/01/93	10.83 (10.08, 11.58)	5.91 (5.01, 7.38)	9.83	15	0.830
18	57	05/02/93	11.41 (10.48, 12.33)	7.41 (6.31, 9.17)	28.58	15	0.018
19	56	05/03/93	13.55 (12.45, 14.64)	7.94 (6.76, 9.85)	12.79	15	0.619
20	98	05/04/93	12.97 (11.73, 14.20)	12.31 (10.85, 14.40)	56.90	20	0.000
21	69	05/05/93	11.08 (9.96, 12.20)	10.02 (8.64, 12.13)	29.84	17	0.028
22	72	05/06/93	10.65 (9.57, 11.73)	10.10 (8.74, 12.17)	29.67	17	0.029
23	79	05/07/93	9.16 (8.16, 10.16)	10.54 (9.18, 12.58)	24.94	18	0.127
24	67	05/08/93	9.20 (8.33, 10.06)	8.36 (7.20, 10.16)	22.85	17	0.154
25	96	05/09/93	9.67 (9.03, 10.30)	7.24 (6.37, 8.48)	40.56	20	0.004
26	84	05/11/93	12.21 (11.01, 13.41)	11.35 (9.91, 13.46)	30.19	19	0.049
27	74	05/13/93	12.40 (10.55, 14.24)	16.21 (14.05, 19.47)	65.05	18	0.000

Table 4.5 Results of the application of the two parameter, travel time model to mid-Columbia, fall chinook, PIT tag data. The cohort number corresponds to the numbers in Appendix 1. The methods for estimating the parameters, constructing confidence intervals, and conducting goodness-of-fit tests are provided in chapter 4.6.

<i>species: chinook</i> <i>run type: fall</i> <i>rearing type: wild</i> <i>release site: Mid Columbia</i>							
group #	# of fish	release date	parameter est. (95% confidence int.)		goodness-of-fit		
			r (km/day)	σ (km/day ^{1/2})	X^2	df	p
1991							
1	154	06/07/91	3.35 (3.07, 3.64)	10.75 (9.70, 12.15)	147.82	25	0.000
2	97	06/07/91	3.30 (3.02, 3.59)	8.49 (7.48, 9.94)	120.43	20	0.000
1992							
1	75	06/03/92	3.57 (3.26, 3.87)	7.74 (6.72, 9.29)	53.52	18	0.000
2	73	06/03/92	3.53 (3.27, 3.79)	6.53 (5.65, 7.86)	56.04	17	0.000
3	68	06/04/92	3.77 (3.47, 4.06)	6.78 (5.85, 8.22)	105.53	17	0.000
4	63	06/04/92	3.28 (3.02, 3.54)	6.24 (5.35, 7.63)	39.84	16	0.001
5	60	06/04/92	3.75 (3.41, 4.09)	7.37 (6.30, 9.06)	54.00	16	0.000
1993							
1	61	06/07/93	4.26 (3.84, 4.67)	8.57 (7.33, 10.52)	35.25	16	0.004
2	81	06/08/93	3.62 (3.30, 3.94)	8.30 (7.24, 9.89)	35.93	18	0.007
3	115	06/08/93	3.78 (3.55, 4.01)	7.12 (6.33, 8.21)	43.04	22	0.005
4	75	06/09/93	3.76 (3.49, 4.02)	6.47 (5.61, 7.76)	49.04	18	0.000
5	118	06/09/93	3.74 (3.47, 4.01)	8.34 (7.42, 9.60)	70.14	22	0.000
6	120	06/15/93	3.61 (3.41, 3.80)	6.24 (5.56, 7.17)	40.83	22	0.009

Table 4.6 Results of the application of the two parameter, travel time model to Snake River, steelhead PIT tag data. The cohort number corresponds to the numbers in Appendix 1. The methods for estimating the parameters, constructing confidence intervals, and conducting goodness-of-fit tests are provided in chapter 4.6.

<i>species: steelhead</i> <i>rearing type: wild</i> <i>release site: Snake Trap</i>							
group #	# of fish	release date	parameter est. (95% confidence int.)		goodness-of-fit		
			r (km/day)	σ (km/day ^{1/2})	X^2	df	p
1989							
1	64	04/16/89	12.99 (11.10, 14.88)	15.01 (12.88, 18.32)	26.84	16	0.043
2	43	04/19/89	17.83 (15.06, 20.61)	15.23 (12.71, 19.59)	31.05	13	0.003
3	66	04/20/89	16.93 (14.30, 19.56)	18.62 (16.01, 22.64)	50.97	17	0.000
4	45	04/22/89	16.04 (12.23, 19.85)	22.59 (18.92, 28.86)	24.89	14	0.036
5	64	04/23/89	20.07 (18.06, 22.08)	12.83 (11.01, 15.66)	23.28	16	0.106
6	63	04/25/89	18.77 (17.10, 20.45)	10.98 (9.42, 13.43)	38.63	16	0.001

Table 4.6 (Continued) Results of the application of the two parameter, travel time model to Snake River, steelhead PIT tag data. The cohort number corresponds to the numbers in Appendix 1. The methods for estimating the parameters, constructing confidence intervals, and conducting goodness-of-fit tests are provided in chapter 4.6.

<i>species: steelhead</i>			<i>rearing type: wild</i>		<i>release site: Snake Trap</i>		
group #	# of fish	release date	parameter est. (95% confidence int.)		goodness-of-fit		
			r (km/day)	σ (km/day ^{1/2})	X^2	df	p
7	49	04/27/89	14.29 (12.29, 16.30)	13.15 (11.08, 16.60)	42.94	14	0.000
8	48	04/30/89	14.53 (12.53, 16.53)	12.88 (10.83, 16.30)	26.37	14	0.023
9	63	05/02/89	16.06 (13.91, 18.22)	15.29 (13.11, 18.70)	30.79	16	0.014
10	79	05/04/89	18.71 (16.37, 21.05)	17.30 (15.05, 20.65)	88.73	18	0.000
11	79	05/06/89	21.78 (19.71, 23.84)	14.15 (12.32, 16.89)	32.91	18	0.017
12	117	05/07/89	23.81 (22.08, 25.54)	13.91 (12.38, 16.03)	82.79	22	0.000
13	80	05/09/89	26.36 (23.83, 28.88)	15.86 (13.81, 18.90)	82.23	18	0.000
14	87	05/10/89	20.51 (17.95, 23.06)	19.00 (16.64, 22.47)	103.92	19	0.000
15	62	05/11/89	18.06 (15.54, 20.57)	16.68 (14.29, 20.43)	26.87	16	0.043
16	47	05/13/89	13.09 (10.76, 15.42)	15.65 (13.14, 19.87)	38.00	14	0.001
1990							
1	61	04/17/90	13.68 (12.36, 15.00)	9.95 (8.51, 12.21)	34.00	16	0.005
2	51	04/19/90	13.53 (12.30, 14.77)	8.53 (7.21, 10.71)	24.88	15	0.052
3	69	04/21/90	14.90 (13.53, 16.26)	10.54 (9.09, 12.76)	52.45	17	0.000
4	72	04/22/90	16.81 (15.41, 18.22)	10.43 (9.02, 12.56)	28.56	17	0.039
5	52	04/23/90	14.77 (13.14, 16.41)	10.90 (9.23, 13.65)	20.69	15	0.147
6	111	04/24/90	12.98 (12.24, 13.72)	7.88 (6.99, 9.12)	85.11	21	0.000
7	86	04/25/90	12.04 (11.30, 12.79)	7.17 (6.27, 8.48)	60.84	19	0.000
8	95	04/26/90	12.01 (11.20, 12.82)	8.26 (7.27, 9.69)	51.96	20	0.000
9	66	04/28/90	11.07 (10.14, 12.00)	8.14 (7.00, 9.90)	53.39	17	0.000
10	55	04/29/90	11.04 (10.17, 11.91)	6.91 (5.87, 8.59)	32.38	15	0.006
11	50	04/30/90	10.31 (9.28, 11.35)	8.11 (6.84, 10.21)	29.56	14	0.009
12	76	05/01/90	10.79 (9.79, 11.78)	9.49 (8.24, 11.37)	59.95	18	0.000
13	72	05/03/90	12.00 (10.87, 13.12)	9.90 (8.56, 11.92)	44.67	17	0.000
14	53	05/05/90	12.04 (10.54, 13.54)	11.22 (9.51, 14.02)	28.17	15	0.021
15	80	05/06/90	12.91 (11.46, 14.35)	12.95 (11.28, 15.43)	69.10	18	0.000
16	146	05/07/90	11.90 (10.96, 12.85)	12.04 (10.84, 13.65)	102.18	24	0.000
17	87	05/08/90	12.94 (11.74, 14.14)	11.21 (9.81, 13.25)	48.79	19	0.000
18	55	05/09/90	13.26 (11.10, 15.42)	15.69 (13.33, 19.50)	38.27	15	0.001
19	52	05/10/90	10.03 (8.03, 12.03)	16.18 (13.69, 20.26)	73.31	15	0.000
20	68	05/12/90	8.97 (7.55, 10.39)	14.00 (12.07, 16.97)	26.71	17	0.063
21	50	05/14/90	8.14 (7.11, 9.16)	9.04 (7.63, 11.39)	19.36	14	0.152
22	44	05/15/90	8.85 (7.85, 9.85)	7.90 (6.60, 10.13)	22.45	14	0.070
23	61	05/17/90	9.05 (8.16, 9.94)	8.24 (7.05, 10.11)	21.54	16	0.159
24	60	05/25/90	14.40 (13.26, 15.54)	8.31 (7.11, 10.22)	19.80	16	0.229
25	57	05/28/90	20.04 (17.88, 22.20)	13.01 (11.09, 16.11)	33.63	15	0.004
26	62	05/30/90	23.56 (20.36, 26.76)	18.56 (15.90, 22.74)	59.97	16	0.000
27	58	06/01/90	18.16 (16.09, 20.24)	13.24 (11.29, 16.35)	40.28	16	0.001

Table 4.6 (Continued) Results of the application of the two parameter, travel time model to Snake River, steelhead PIT tag data. The cohort number corresponds to the numbers in Appendix 1. The methods for estimating the parameters, constructing confidence intervals, and conducting goodness-of-fit tests are provided in chapter 4.6.

<i>species: steelhead</i>			<i>rearing type: wild</i>		<i>release site: Snake Trap</i>		
group #	# of fish	release date	parameter est. (95% confidence int.)		goodness-of-fit		
			r (km/day)	σ (km/day ^{1/2})	X^2	df	p
1991							
1	57	04/26/91	8.74 (7.59, 9.90)	10.51 (8.95, 13.01)	12.16	15	0.667
2	50	04/27/91	10.38 (9.46, 11.30)	7.19 (6.07, 9.05)	17.32	14	0.240
3	49	04/28/91	9.10 (7.91, 10.28)	9.76 (8.23, 12.33)	60.98	14	0.000
4	60	04/29/91	8.86 (7.70, 10.01)	10.75 (9.19, 13.22)	24.87	16	0.072
5	54	05/05/91	11.93 (10.91, 12.96)	7.79 (6.61, 9.70)	35.33	15	0.002
6	68	05/08/91	13.80 (12.56, 15.03)	9.83 (8.47, 11.92)	40.24	17	0.001
7	359	05/10/91	12.54 (12.07, 13.01)	9.18 (8.56, 9.92)	262.94	36	0.000
8	188	05/11/91	15.14 (13.98, 16.31)	14.92 (13.59, 16.65)	53.60	27	0.002
9	113	05/12/91	13.97 (13.05, 14.88)	9.47 (8.41, 10.94)	136.98	21	0.000
10	126	05/12/91	14.94 (13.92, 15.96)	10.76 (9.61, 12.33)	162.48	23	0.000
11	59	05/13/91	14.64 (13.27, 16.02)	9.85 (8.41, 12.14)	37.29	16	0.002
12	84	05/14/91	14.27 (13.22, 15.32)	9.16 (8.00, 10.87)	66.86	19	0.000
13	56	05/15/91	13.13 (11.85, 14.41)	9.45 (8.04, 11.72)	23.07	15	0.083
14	85	05/17/91	17.52 (16.24, 18.80)	10.16 (8.88, 12.04)	69.00	19	0.000
15	152	05/18/91	21.18 (19.80, 22.56)	13.44 (12.12, 15.20)	123.95	25	0.000
16	339	05/19/91	21.68 (20.65, 22.71)	14.93 (13.90, 16.17)	330.99	35	0.000
17	51	05/20/91	19.80 (17.55, 22.04)	12.83 (10.84, 16.10)	28.41	15	0.019
18	58	05/23/91	17.14 (14.70, 19.57)	16.01 (13.65, 19.77)	40.93	16	0.001
19	55	05/25/91	18.47 (16.14, 20.80)	14.33 (12.17, 17.81)	29.11	15	0.016
20	56	05/26/91	16.24 (14.70, 17.77)	10.17 (8.65, 12.61)	19.21	15	0.204
1992							
1	61	04/18/92	8.33 (7.48, 9.18)	8.22 (7.03, 10.09)	28.39	16	0.028
2	58	04/21/92	8.60 (7.65, 9.54)	8.76 (7.47, 10.82)	40.93	16	0.001
3	64	04/22/92	8.94 (8.31, 9.57)	6.07 (5.21, 7.41)	26.25	16	0.051
4	67	04/25/92	10.23 (9.53, 10.92)	6.41 (5.52, 7.79)	41.36	17	0.001
5	64	04/28/92	12.51 (11.34, 13.68)	9.49 (8.14, 11.58)	27.44	16	0.037
6	72	04/30/92	13.69 (11.72, 15.66)	16.22 (14.04, 19.55)	56.33	17	0.000
7	180	05/01/92	12.59 (12.02, 13.17)	7.89 (7.17, 8.82)	201.00	27	0.000
8	154	05/02/92	14.51 (13.65, 15.38)	10.24 (9.24, 11.57)	132.55	25	0.000
9	69	05/03/92	12.99 (11.68, 14.31)	10.85 (9.36, 13.14)	40.86	17	0.001
10	44	05/04/92	12.79 (11.46, 14.13)	8.76 (7.32, 11.23)	22.45	14	0.070
11	44	05/05/92	15.02 (13.34, 16.70)	10.18 (8.51, 13.05)	31.73	14	0.004
12	54	05/06/92	13.59 (12.49, 14.68)	7.79 (6.61, 9.71)	19.33	15	0.199
13	40	05/07/92	12.34 (10.79, 13.88)	9.77 (8.10, 12.70)	16.80	13	0.209
14	61	05/08/92	6.85 (5.36, 8.34)	15.92 (13.62, 19.54)	42.10	16	0.000
15	88	05/09/92	10.46 (9.31, 11.61)	12.02 (10.53, 14.20)	22.50	19	0.260
16	90	05/10/92	7.43 (6.62, 8.25)	10.26 (9.00, 12.09)	115.82	19	0.000

Table 4.6 (Continued) Results of the application of the two parameter, travel time model to Snake River, steelhead PIT tag data. The cohort number corresponds to the numbers in Appendix 1. The methods for estimating the parameters, constructing confidence intervals, and conducting goodness-of-fit tests are provided in chapter 4.6.

<i>species: steelhead</i>			<i>rearing type: wild</i>		<i>release site: Snake Trap</i>		
group #	# of fish	release date	parameter est. (95% confidence int.)		goodness-of-fit		
			r (km/day)	σ (km/day ^{1/2})	X^2	df	p
17	60	05/11/92	7.15 (5.97, 8.34)	12.26 (10.48, 15.08)	58.43	16	0.000
18	42	05/12/92	7.39 (5.57, 9.22)	15.34 (12.78, 19.80)	25.81	13	0.018
1993							
1	38	04/20/93	11.04 (9.40, 12.67)	10.63 (8.78, 13.94)	26.84	13	0.013
2	51	04/24/93	10.97 (9.17, 12.76)	13.77 (11.64, 17.29)	28.41	15	0.019
3	62	04/26/93	14.29 (12.96, 15.61)	9.85 (8.44, 12.07)	63.03	16	0.000
4	50	04/28/93	13.16 (11.58, 14.74)	10.94 (9.23, 13.77)	36.36	14	0.001
5	57	04/29/93	14.65 (13.07, 16.22)	11.08 (9.44, 13.71)	31.11	15	0.009
6	50	04/30/93	14.52 (12.65, 16.39)	12.32 (10.39, 15.50)	20.04	14	0.129
7	87	05/01/93	16.58 (15.34, 17.82)	10.27 (8.99, 12.15)	35.14	19	0.013
8	85	05/02/93	15.45 (14.07, 16.83)	11.66 (10.20, 13.82)	92.81	19	0.000
9	72	05/03/93	17.98 (15.93, 20.02)	14.70 (12.71, 17.71)	46.33	17	0.000
10	217	05/04/93	19.14 (18.06, 20.23)	13.37 (12.25, 14.80)	181.01	29	0.000
11	97	05/05/93	18.46 (16.42, 20.50)	16.91 (14.89, 19.79)	130.39	20	0.000
12	253	05/05/93	16.74 (15.52, 17.96)	17.37 (16.01, 19.07)	222.33	31	0.000
13	59	05/06/93	18.08 (15.17, 20.99)	18.76 (16.02, 23.12)	69.49	16	0.000
14	236	05/07/93	19.80 (18.55, 21.05)	15.76 (14.49, 17.37)	182.93	30	0.000
15	93	05/08/93	15.67 (13.96, 17.39)	15.07 (13.24, 17.71)	47.23	20	0.001
16	40	05/09/93	15.89 (13.70, 18.08)	12.22 (10.14, 15.90)	12.80	13	0.463
17	66	05/10/93	17.47 (15.91, 19.03)	10.87 (9.35, 13.22)	34.61	17	0.007
18	85	05/11/93	19.19 (17.42, 20.96)	13.42 (11.73, 15.90)	32.76	19	0.026
19	84	05/13/93	24.79 (22.02, 27.57)	18.39 (16.07, 21.82)	60.05	19	0.000
20	61	05/13/93	22.13 (19.46, 24.81)	15.85 (13.57, 19.46)	56.43	16	0.000

5. Extensions of the travel time model

5.1. Introduction

In the previous chapter, I developed the basic two parameter travel time model (equations (4.7) and (4.8)) and applied it to several data sets. In some cases it worked quite well, in others not so well. In general, though, the model has desirable properties and can form the basis of models that include more complex behavior.

In this chapter I expand the model to make it more realistic. In section 5.2 mortality is no longer considered to be equal within the cohorts but is dependent upon the amount of time spent in the river. In section 5.3 I incorporate migrational delay into the model. In the last section of this chapter, section 5.e, I explore factors related to migration rate and attempt to use these factors to predict model parameters. In addition, in chapter 6 I allow for population heterogeneity and attempt to determine how various factors affect migratory behavior.

I use some of the travel time data from the previous chapter to test for the appropriateness of the added features. Since I do not want to use the same data in several treatments (to avoid multiple comparisons), I have divided the Snake River trap chinook and steelhead data into treatment groups. To randomly place the cohorts into 5 treatment groups, I used the following procedure. I started by dividing the cohorts in a year into blocks of 5 or 6 in a chronological sequence; the blocks with 6 members were randomly assigned so that all the extra cohorts didn't come at the end of the season. From each of these blocks, 5 cohorts were randomly assigned to each of the treatment groups. This ensured that cohorts were randomly assigned to the treatment groups and that the yearly chronological sequence of cohorts was represented in each treatment group. For the mid-

Columbia fall chinook, I assigned cohorts into two treatment groups because of the smaller number of cohorts.

5.2. Time dependent mortality

Previously, I assumed equal survival probabilities among the individuals in a cohort of fish during the migration period. With this assumption, mortality will decrease the numbers of the cohort but will not affect the shape of the arrival time distribution. If, on the other hand, mortality is related to the amount of time spent in the river, then it will affect the shape of the arrival time distribution, with slower fish being more susceptible to mortality.

If the reservoir mortality rate is $\alpha(t)$, then as shown in equation (2.24), the probability of surviving through time t is

$$Pr[T > t] = e^{-\int_0^t \alpha(s) ds} . \quad (5.1)$$

This mortality can be incorporated into the migration model as follows:

$$\frac{\partial p}{\partial t} = -r \frac{\partial p}{\partial t} + \frac{\sigma^2}{2} \frac{\partial^2 p}{\partial x^2} - \alpha(t)p . \quad (5.2)$$

Solutions of equation (5.2) have the form

$$p(x, t) \cdot e^{-\int_0^t \alpha(t) dt} . \quad (5.3)$$

Referring to this density as $p_m(x, t)$ and using equation (4.5) for $p(x, t)$, we have:

$$p_m(x, t) = \frac{1}{\sqrt{2\pi\sigma^2 t}} \left(\exp\left(-\frac{(x-rt)^2}{2\sigma^2 t}\right) - \exp\left(\frac{2Ar}{\sigma^2} - \frac{(x-2A-rt)^2}{2\sigma^2 t}\right) \right) \cdot e^{-\int_0^t \alpha(s) ds} . \quad (5.4)$$

Carrying out the same procedure as before, that is, integrating from $-\infty$ to A with respect to x and differentiating with respect to t , we end up with:

$$g_L(t) = g(t) \cdot e^{-\int_0^t \alpha(s) ds} + \left[\Phi\left(\frac{L-rt}{\sigma\sqrt{t}}\right) - \exp\left(\frac{2Lr}{\sigma^2}\right) \Phi\left(\frac{-L-rt}{\sigma\sqrt{t}}\right) \right] \cdot \alpha(t) e^{-\int_0^t \alpha(s) ds} \quad , \quad (5.5)$$

where $g_L(t)$ represents the loss from the reservoir (due to both dam passage and mortality) and $g(t)$ is equation (4.7), the basic arrival time distribution. The first term in the right side of equation (5.5) is loss due to fish leaving the reservoir, and the second term is loss due to mortality. This makes intuitive sense because $g(t)$ is the pdf for dam passage in the absence of mortality, and $e^{-\int_0^t \alpha(s) ds}$ represents the probability of surviving through time t . In the second part of equation (5.5), the term in brackets represents the fish remaining in the reservoir, and $\alpha(t) e^{-\int_0^t \alpha(s) ds}$ is the survival probability density function. To obtain a probability density function, $g_m(t)$, for the arrival time given time dependent in-river mortality, the passage portion of equation (5.5) must be normalized:

$$g_m(t) = \frac{g(t) e^{-\int_0^t \alpha(s) ds}}{\int_0^\infty g(\tau) e^{-\int_0^\tau \alpha(s) ds} d\tau} \quad . \quad (5.6)$$

The simplest case is when α is constant, and Figure 5.1 contains plots of equation (5.6) for various values of constant α . Note that as α increases, the mode of the distribution shifts to the left, and the right tail becomes thinner. An α of 0.02 corresponds roughly to 18 per cent mortality after 10 days. At this and higher levels of mortality, including mortality has little effect on the shape of the arrival time distribution.

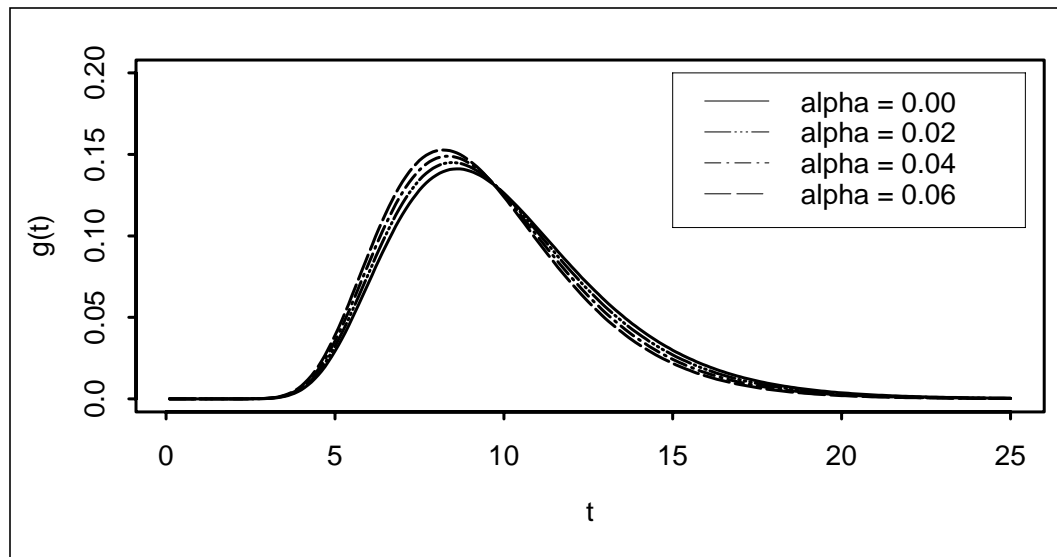


Figure 5.1 Plots of equation (5.6) for various values of α . Both r and σ are set at 10.0; L is set at 100.

The model discrimination methods described in chapter 3 can determine the ability of the model to detect travel time dependent mortality. In this case, the null model is the basic arrival time distribution, equation (4.7). The alternative model is the arrival distribution described by equation (5.6). I should emphasize that this will test for the ability of the model to detect travel time dependent mortality in the river. Accepting the null hypothesis does not necessarily mean the effect does not exist.

results

The results of the data analysis for the Snake River trap chinook and steelhead are contained in Table 5.1 and Table 5.2. Each line in the table represents the results from a single cohort. The cohorts are identified by year and cohort number, so these results can be directly compared to those found in Table 4.4 and Table 4.6 (basic travel time model

Table 5.1 Results from the application of the travel time dependent mortality model to Snake River chinook PIT tag data. Each row is a cohort. A negative value for BIC lends support to the null model. See text for further details of the analysis.

cohort	# of fish	parameter estimates			likelihoods			
		r	σ	α	l_0	l_A	ratio	BIC
1989								
1	48	2.55	5.46	0.012	-166.88	-166.88	0.00	-3.87
7	54	2.96	6.48	0.022	-180.04	-180.04	0.00	-3.99
13	54	3.09	6.02	0.018	-176.02	-176.02	0.00	-3.99
18	66	5.70	7.49	0.011	-174.07	-174.07	-0.00	-4.19
24	59	8.85	11.94	0.008	-139.46	-139.46	-0.00	-4.08
32	71	8.38	7.30	0.015	-159.62	-157.80	3.64	-0.62
37	61	6.70	10.25	0.016	-159.96	-159.96	-0.00	-4.11
1990								
1	59	5.10	7.55	0.019	-162.63	-162.63	-0.00	-4.08
9	70	4.93	9.78	0.012	-207.84	-207.84	0.00	-4.25
12	41	5.64	7.06	0.013	-106.59	-106.59	0.00	-3.71
1991								
5	69	2.91	5.33	0.014	-225.63	-225.63	0.00	-4.23
8	55	3.49	6.08	0.012	-172.85	-172.85	0.00	-4.01
17	53	10.32	6.59	0.003	-91.08	-91.08	0.00	-3.97
1992								
6	46	5.08	9.96	0.015	-133.54	-133.54	0.00	-3.83
1993								
1	47	3.51	6.57	0.011	-149.96	-149.96	0.00	-3.85
8	43	5.42	6.40	0.007	-111.69	-111.69	0.00	-3.76
16	60	10.25	8.67	0.013	-116.58	-116.58	0.00	-4.09
17	53	11.11	4.93	0.031	-82.08	-81.05	2.07	-1.90
24	67	9.10	8.36	0.003	-139.99	-139.65	0.68	-3.53

Table 5.2 Results from the application of the travel time dependent mortality model to Snake River steelhead PIT tag data. Each row is a cohort. A negative value for BIC lends support to the null model. See text for further details of the analysis.

cohort	# of fish	parameter estimates			likelihoods			
		r	σ	α	l_0	l_A	ratio	BIC
1989								
3	66	16.83	18.61	0.0052	-117.72	-117.72	-0.00	-4.19
6	63	17.75	12.71	0.0000	-108.89	-104.11	9.57	5.42
13	80	26.33	15.85	0.0034	-87.89	-87.89	0.00	-4.38
1990								
5	52	14.77	10.91	0.0000	-85.12	-85.12	-0.00	-3.95
10	55	11.35	5.61	0.0581	-91.19	-87.94	6.49	2.49
14	53	13.27	8.32	0.0187	-100.79	-91.91	17.75	13.78
21	50	7.64	9.05	0.0483	-115.68	-115.68	-0.00	-3.91
25	57	20.04	13.01	0.0000	-75.97	-75.97	0.00	-4.04
1991								
1	57	8.27	10.51	0.0370	-131.50	-131.50	-0.00	-4.04
9	113	13.87	9.47	0.0145	-179.38	-179.38	0.00	-4.73
12	84	14.17	9.16	0.0167	-128.96	-128.96	0.00	-4.43
18	58	17.14	16.01	0.0000	-97.93	-97.93	-0.00	-4.06
1992								
3	64	8.73	6.08	0.0505	-118.79	-118.79	-0.00	-4.16
7	180	13.23	6.12	0.0050	-278.24	-262.08	32.32	27.12
18	42	7.23	15.34	0.0050	-112.78	-112.78	0.00	-3.74
1993								
5	57	14.65	11.08	0.0000	-93.72	-93.72	0.00	-4.04
10	217	19.58	12.67	0.0000	-305.57	-301.26	8.64	3.26
15	93	15.67	15.07	0.0000	-164.82	-164.82	-0.00	-4.53
19	84	24.75	18.39	0.0032	-108.48	-108.48	-0.00	-4.43

results) and release information can be found in Appendix I. These tables also contain parameter estimates for the travel time model with mortality, likelihoods for the null and alternative models, and the likelihood ratios and BIC values. The BIC value in these tables is the difference between the BIC values for the alternative and null models. A negative value lends support to the null model, and positive one lends support to the alternative model.

Little support exists for including travel time dependent mortality in the model for the Snake River chinook (Table 5.1). 16 out of the 19 cohorts had likelihood ratios less than 0.01, and for none of the cohorts would the null model be rejected based on a likelihood ratio test or based on the BIC values. This is not to say that travel time dependent mortality is not occurring for these groups, but this model cannot detect it with these data. Other types of data are necessary to observe this effect. On a positive note, the fact that this type of mortality seems to have little effect on the arrival time distribution makes modeling arrival times less complex.

The results from the steelhead cohorts are a bit perplexing. As with the chinook, the majority of cohorts (14 out of 19) had likelihood ratios less than 0.01. But the remaining 5 cohorts all had fairly large ratios, and for all these cohorts the null hypothesis would be rejected based on a likelihood ratio test or BIC values. The estimates of the mortality term, α , for these groups is quite variable, ranging from less than 0.0001 to 0.058. This leads me to believe that these results are spurious – the added term allows for a better fit of the model to the data but not in a biologically meaningful way.

5.3. Delay in migration

introduction

In the previous chapter, I assumed that fish migrate at a constant rate during the entire

migration period. In some cases, however, fish may delay their migration. In this section, I examine two types of delay – delay in front of a dam before passage and delay before the fish initiate downstream migration. In both these cases, the delay may be substantial, and incorporating a delay term in the travel time model may be worthwhile.

There is some evidence that fish delay their passage as they encounter a dam. Dams produce turbulence and a significant amount of noise that may deter fish from passing. Also dam passing often involves extreme changes in pressure, which the fish resist. First, I examine the dam delay process by analyzing some chinook radio-tracking data at John Day and Lower Granite Dams. I then incorporate the delay model into the basic travel time model and apply this to PIT tag data.

Sometimes fish are tagged and released before they are ready to initiate migration. This may be the case when hatchery fish are released before they are fully smolted or when wild fish are collected in their rearing habitat, tagged, and then released back in the river. The mid-Columbia fall chinook examined in the previous chapter may be an example of the latter case. These fish were beach seined, and most of the fish were less than 75 mm in length, probably too small to initiate migration. For these fish I incorporate a migratory delay term into the travel time model.

formulation of the model

If the delay probability density function is $d(t)$, and $d(t)$ is independent of the arrival distribution, then we can express the passage distribution incorporating delay as a convolution integral (Mood, et al. 1974):

$$g_D(t) = \int_0^t d(t - \tau)g(\tau)d\tau . \quad (5.7)$$

$g(t)$ is the arrival distribution without delay (equation (4.7)) and $g_D(t)$ is the arrival

distribution with delay included. Note that it does not matter whether the delay occurs before or after the migratory period; the general equation remains the same.

Although the waiting time process is likely to be complex, a reasonable simplification is a waiting time process with instantaneous passage rate $\alpha(t)$. This yields a delay pdf of

$$d(t) = \alpha(t)e^{-\int_0^t \alpha(s)ds} . \quad (5.8)$$

Assuming a constant α equation (5.7) becomes

$$g_D(t) = \int_0^t \alpha e^{-\alpha \cdot (t-\tau)} g(\tau) d\tau , \quad (5.9)$$

and the average delay is $1/\alpha$. Figure 5.2 represents the components of equation (5.9) graphically. The delay term (top plot) and reservoir travel time term (middle plot) are both incorporated into the arrival time with delay equation (bottom plot). Assuming the basic travel time distribution (equation (4.7)) for $g(t)$, plots of equation (5.9) are presented in Figure 5.3 for several values of constant α . As average delay increases (i.e., as α decreases), the mode of the distribution shifts to the right, and the curve flattens out.

application of the delay model to radio-tracking data

It is clear from Figure 5.3 that delay at a dam can produce substantial effects on fish arrival distributions. With most arrival time data, where fish are sampled as they pass a dam, separating river travel time from dam delay is difficult. Fortunately there is some data available where dam delay can be observed directly. These data are from radio tag studies where groups of fish are released upstream from a dam. The time when an individual first reaches the forebay in front of the dam is recorded as well as when the fish passes through the dam. The difference between these two times is dam delay. A distribution of these times is obtained from a group of individuals released at the same time.

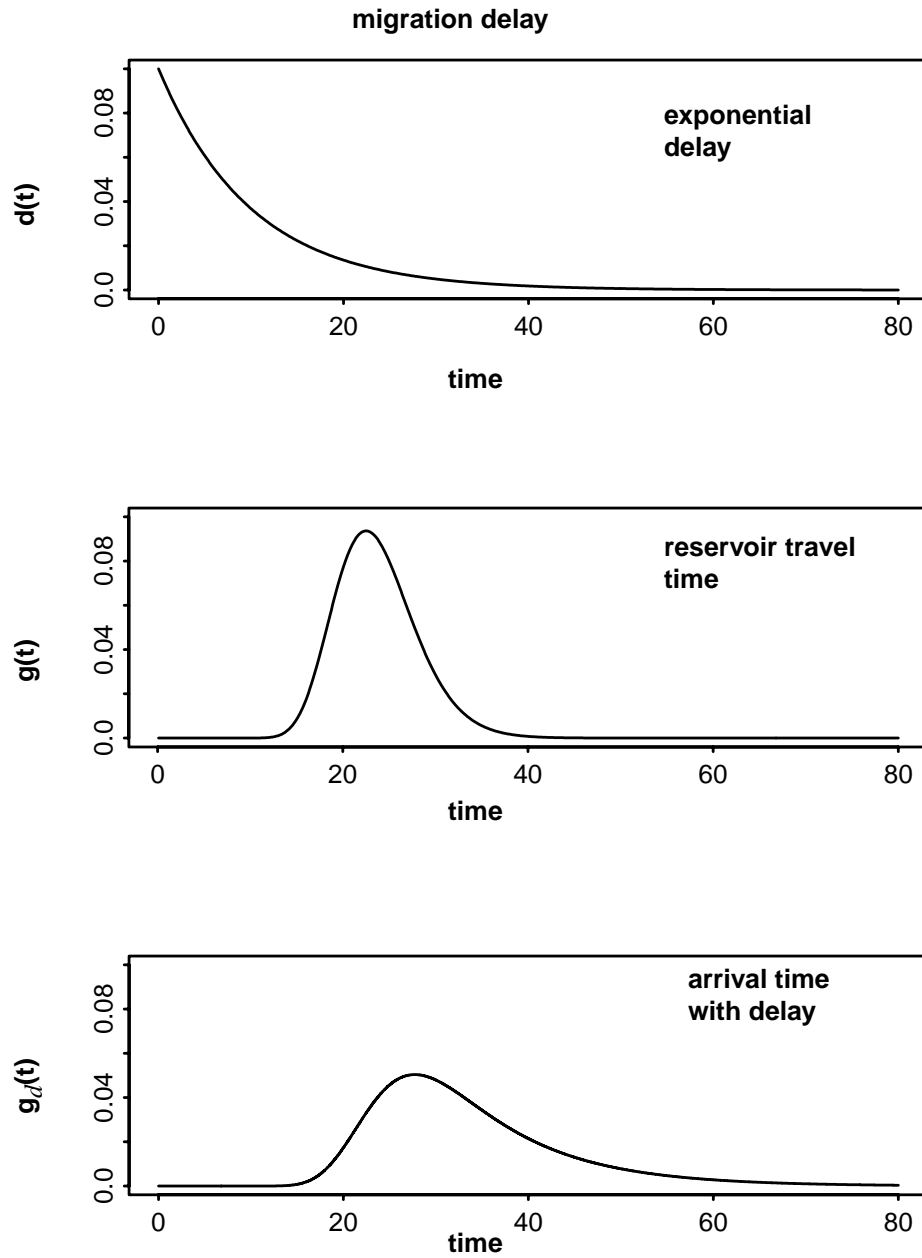


Figure 5.2 A graphical representation of the arrival time distribution with a delay term added. The top graph is exponential delay with constant α . The middle graph is the two parameter travel time model (equation (4.7)). The bottom graph represents equation (5.9), the arrival time distribution with the delay term incorporated.

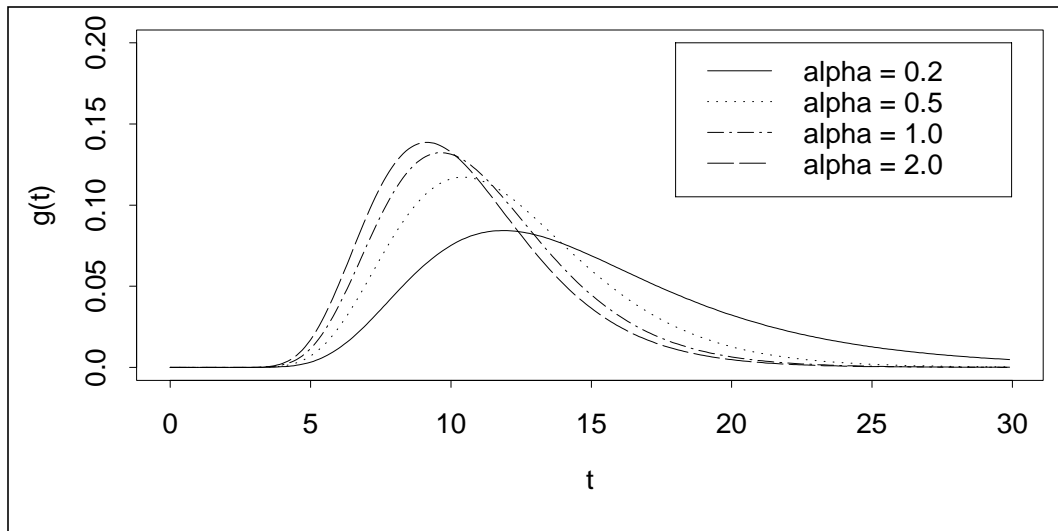


Figure 5.3 Plots of equation (5.9) for various values of α . Both r and σ are set at 10.0; L is set at 100.

Applying delay models to independent data sets has several advantages. Since delay is being observed directly, more accurate parameter estimates can be obtained. These parameter estimates can then either be applied directly to the travel time model with delay (equation (5.7)), or the parameter estimates can be compared to those obtained by applying equation (5.7) to travel time data. Also, these data will allow for a more direct assessment of model performance and for comparison among alternative models.

I will examine three alternative models for delay. The first is a simple model where delay is determined by a constant passage rate. The second model introduces diel behavior with separate passage rates for daytime and nighttime periods. The third model separates the fish into two types: those who pass quickly and those who pass more slowly.

Two radio-tag studies have been performed on juvenile salmonids in the Columbia

River system: one at John Day Dam in 1984 (Giorgi et al., 1985) and the other at Lower Granite Dam in 1985 (Stuehrenberg et al., 1986). In these studies fish were fitted with miniature radio-tags and released upstream from the dam. Several receivers were situated at the dam and were able to detect when they first arrived at the front of the dam and when they passed the dam. The difference between these two times is the delay.

In the John Day study, fish were released on 4 days. On the first three days (May 1, May 10, and May 14), 28 fish were released; half were released in the morning and half were released in the afternoon. On the fourth release day, only 11 fish were released, and I did not include these fish in the analysis. The fish were collected from the John Day Dam and released 6.3 km. upstream from the dam. In the Lower Granite study, 4 groups of approximately 100 fish were released 4.8 km. upstream from the dam. These fish were collected at the bypass facilities of Lower Granite and McNary Dams. The first group was not analyzed because of technical difficulties encountered at the dam. The last three groups were released on April 17, April 24 and May 1.

Stuehrenberg et al., (1986) also performed behavioral test to determine the impact of the tags on the fish. They determined that the radio-tags did not significantly affect either swimming velocity or mortality but that the tags may affect the buoyancy of the fish. Because of this problem, these data are not ideal. They are, however, the only data where dam delay is directly observed. For this reason I have chosen to analyze these data to obtain rough parameter estimates and some qualitative results. In addition, the methodology I present will be applicable in the future if better data become available.

To analyze the data I use the following procedure. First I estimate the parameters using maximum likelihood. If numerical solutions are required, I use the downhill simplex method (Nelder and Mead, 1965; Press, et al., 1988). Also, log likelihoods are computed for comparisons among models within a data set. In addition, I perform an X^2 goodness-of-

fit test, following the procedure for continuous data outlined in chapter 3.

The first model is the waiting time model with constant α . The pdf for delay is

$$d(t) = \alpha e^{-\alpha t} . \quad (5.10)$$

The maximum likelihood estimate for α is

$$\hat{\alpha} = N / \sum_{i=1}^N t_i = \frac{1}{\bar{t}} , \quad (5.11)$$

where N is the number of fish in the cohort, t_i is the waiting time of the i th individual and \bar{t} is the average waiting time for the group.

The second model includes a different passage rate for daytime and nighttime, α_d and α_n respectively. The delay pdf for passage during the day is

$$d(t) = \alpha_d e^{-[\alpha_d t_d + \alpha_n t_n]} . \quad (5.12)$$

In this notation t_d is the time spent waiting during the day, and t_n is time spent waiting during the night period. The pdf for passage occurring during the night period is the same as equation (5.12) but with α_n substituted for α_d in front of the exponential term on the right side. Note that since individual fish arrive at the dam at different times of the day, each fish will have a different waiting time pdf. The mle's of the two parameters α_n and α_d are determined numerically.

A third model is a double exponential model. The model essentially divides the population into two groups: those that pass the dam quickly and those that pass more slowly. The model is expressed as

$$d(t) = wt \cdot \alpha_f e^{-\alpha_f t} + (1.0 - wt) \cdot \alpha_s e^{-\alpha_s t} . \quad (5.13)$$

α_f corresponds to the fast passage rate, α_s is the slow passage rate, and wt assigns a weight to the two types of passage, with $0 \leq wt \leq 1.0$. Again, the mle's of the parameters are determined numerically, and a log likelihood is computed.

results

The parameter estimates, likelihoods and goodness-of-fit results for the Lower Granite data are contained in table Table 5.3, and for the John Day data in Table 5.4. In these tables,

Table 5.3 Delay model results from the Lower Granite data. For the simple model, $\alpha_1 = \alpha$. For the diel delay model, $\alpha_1 = \alpha_n$, and $\alpha_2 = \alpha_d$. For the double exponential model, $\alpha_1 = \alpha_f$ and $\alpha_2 = \alpha_s$. Based on BIC values, the “best” model has the largest value.

model	α_1	α_2	wt	lik	ratio	BIC _i	X^2	p
Release data: April 17; n = 61								
simple	1.13			-247.19		-498.50	105.64	<0.001
diel	1.42	0.91		-245.70	3.00	-499.61	106.26	<0.001
2 exp	66.87	0.85	0.26	-224.14	46.10	-460.62	32.13	0.010
Release date: April 24; n = 65								
simple	3.48			-190.45		-385.08	123.54	<0.001
diel	6.29	1.33		-173.83	33.24	-356.02	100.15	<0.001
2 exp	113.70	2.07	0.41	-151.30	78.31	-315.12	14.22	0.58
Release date: May 1; n = 70								
simple	2.91			-217.68		-439.61	272.86	<0.001
diel	7.01	0.70		-181.43	72.51	-371.35	152.86	<0.001
2 exp	70.65	1.21	0.59	-148.06	139.24	-308.87	27.71	0.048

$\alpha_1 = \alpha$ for the simple model, $\alpha_1 = \alpha_n$ and $\alpha_2 = \alpha_d$ for the diel-delay model, and $\alpha_1 = \alpha_f$ and $\alpha_2 = \alpha_s$ for the double-exponential model. The BIC values reported are those for the

Table 5.4 Delay model results from the John Day data. For the simple model, $\alpha_1 = \alpha$. For the diel delay model, $\alpha_1 = \alpha_n$, and $\alpha_2 = \alpha_d$. For the double exponential model, $\alpha_1 = \alpha_f$ and $\alpha_2 = \alpha_s$. Based on BIC values, the “best” model has the largest value.

model	α_1	α_2	wt	lik	ratio	BIC_i	X^2	p
Release data: May 1; n = 19								
simple	6.53			-43.74		-90.42	30.89	< 0.001
diel	8.78	5.07		-43.03	1.42	-91.94	30.89	< 0.001
2 exp	71.67	2.59	0.63	-30.93	25.62	-70.69	4.37	0.89
Release date: May 10; n = 25								
simple	13.38			-39.60		-82.42	25.44	0.008
diel	29.86	4.18		-29.39	20.43	-65.21	24.40	0.007
2 exp	101.59	7.87	0.45	-33.98	11.24	-77.62	12.96	0.23
Release date: May 14; n = 23								
simple	13.51			-36.22		-75.58	27.30	0.004
diel	38.61	4.04		-23.34	25.76	-52.95	19.39	0.036
2 exp	473.63	9.88	0.27	-29.25	13.93	-67.91	17.13	0.072

individual models (not comparisons between models as in the last application). According to this criterion, the most desirable model is the one with the largest BIC value.

Figures 5.4 and 5.5 contain plots of the fitted models versus the data. In these plots, the percentiles of the data are plotted against the percentiles predicted by the model. A straight line through the origin and the point (1.0, 1.0) would signify an exact correspondence between the two. The columns of plots represent the three models, and the rows represent the three data sets.

For the Lower Granite data, the average waiting time ($1/\alpha$) is approximately 20 hours for the first group and approximately 8 hours for the second and third groups. In all three

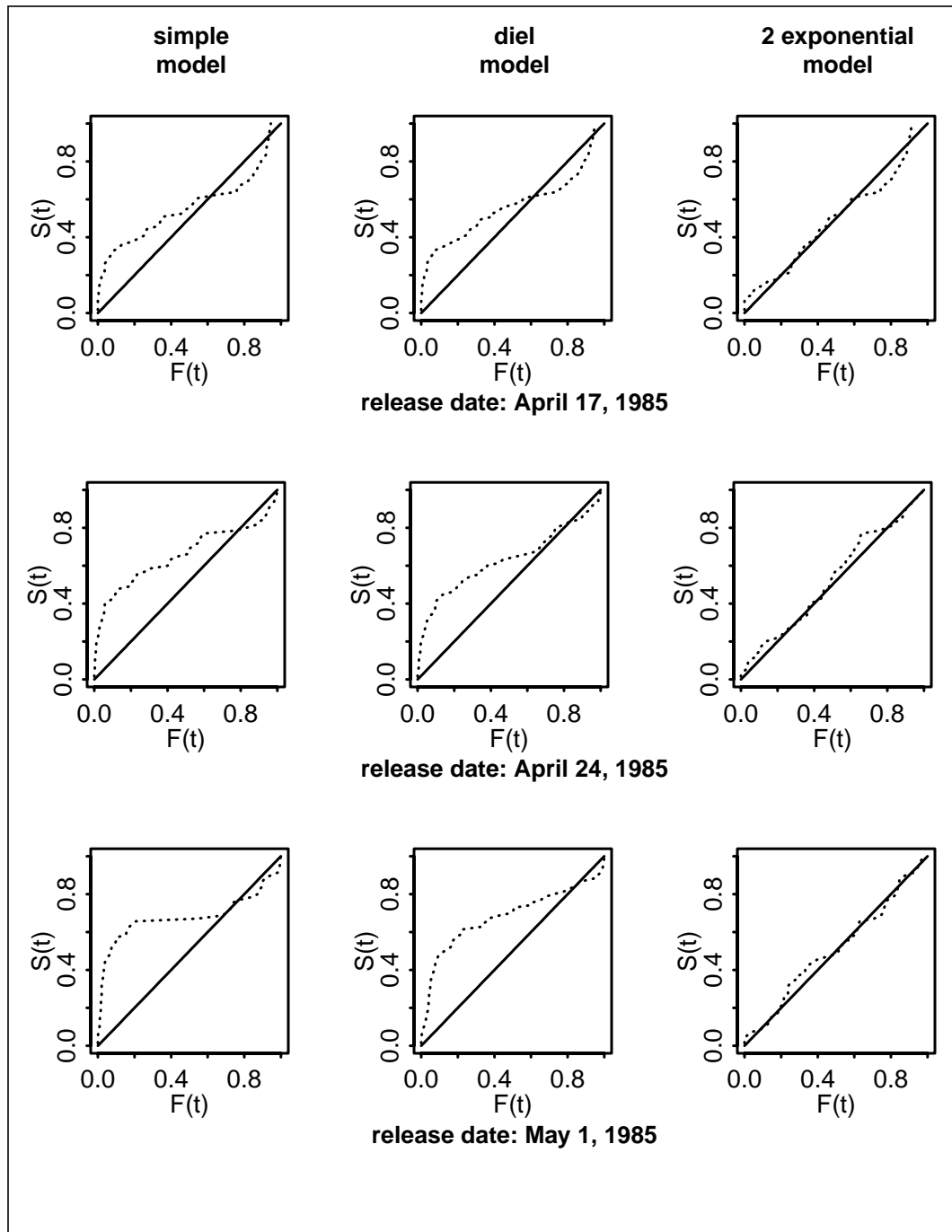


Figure 5.4 Plots of the percentiles of the data versus percentiles of the delay models for the Lower Granite radio-tracking data. The solid line represents perfect correspondence between the model and data.

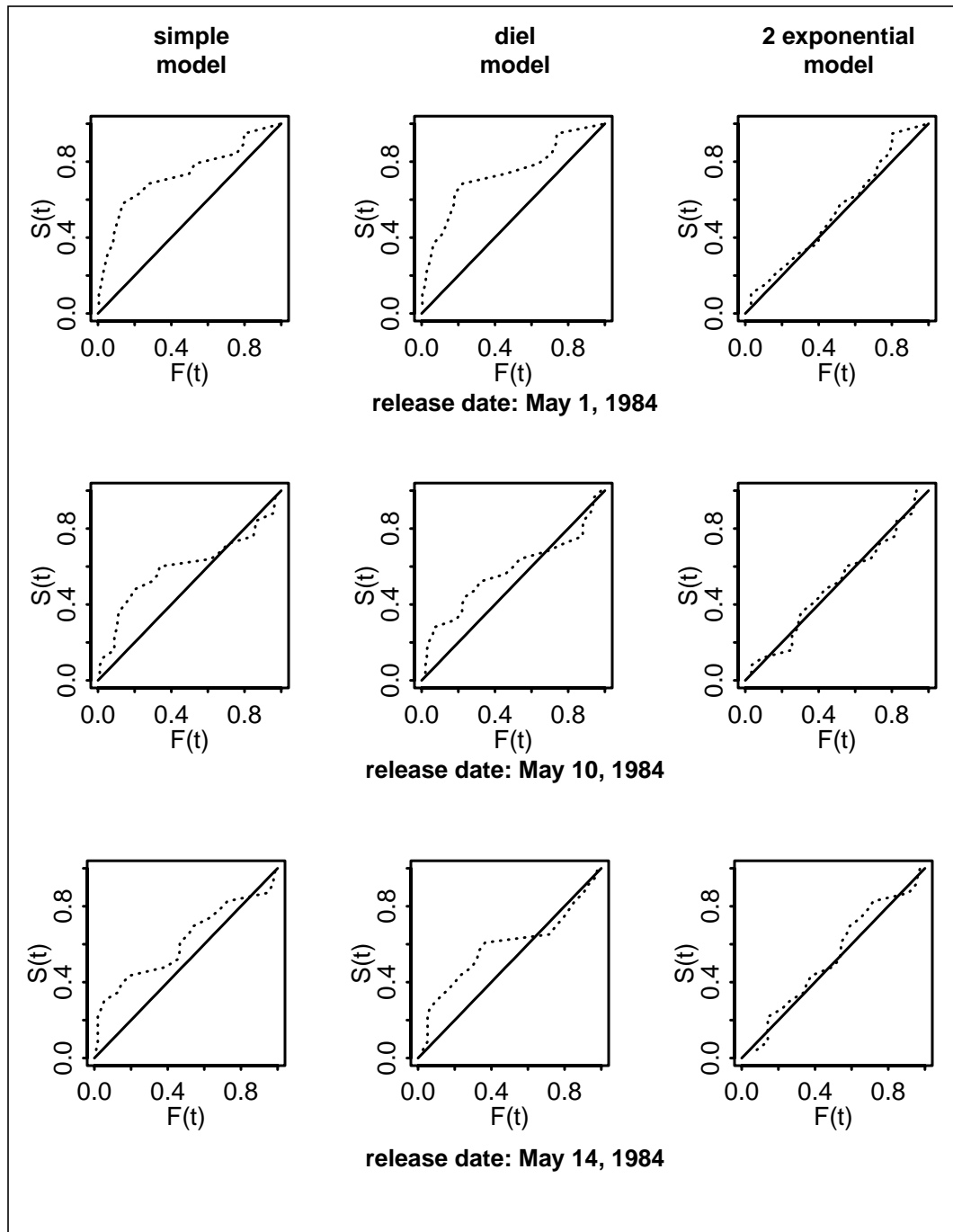


Figure 5.5 Plots of the percentiles of the data versus percentiles of the delay models for the John Day radio-tracking data. The solid line represents perfect correspondence between the model and data.

cases, the plots (Figure 5.4) show that the simple waiting time model cannot adequately describe the data. The model under predicts early fish passage and overpredicts late fish passage. The results of the goodness-of-fit tests (all p -values below 0.001) confirm this.

Comparing the likelihood ratios and BIC values from second model to the first show that this model is a marked improvement in the last two data sets, but the first model would be selected for the first data set. In all three cases, the fish are more inclined to pass during the nighttime hours, with a tenfold difference between nighttime and daytime passage rates in the last data set. These results are consistent with diel behavior and a tendency toward nighttime passage. However, the plots show that this model still does not adequately describe the data and suffers from the same shortcomings as the first model.

The third model was partly motivated by the shortcomings of the first two. Based on likelihood ratios and BIC values, this model is a substantial improvement over the first two. Also, the plots show that this model does a reasonable job of describing the data. Among the three data sets, the estimates of α_f and α_s are roughly of the same order of magnitude, with α_f fifty to one hundred times larger than α_s . For example, in the first group of fish, average waiting time for the fast fish is on the order of 20 minutes, while the slow group waits for more than a day, on average, before passing the dam. There is a noticeable difference among the three data sets in the estimates of the parameter wt (the proportion of fish in the fast group), which increases with release date, ranging from 0.257 in the earliest release to 0.594 in the latest release. This is consistent with the fish being more eager to migrate later in the season.

For the John Day data, the average waiting time is under 4 hours for the first group and under 2 hours for the last two groups. As with the Lower Granite data, the simple model cannot adequately describe the data based on the plots (Figure 5.5). Based on BIC values, the diel delay model would be selected over the simple model in 2 out of 3 cases, but the

plots indicate that this model is inadequate for the John Day data. The double exponential model is a clear improvement over the simple model, based on the BIC values. Also, the plots and the goodness-of-fit results indicate that this model represents the data well.

Some general conclusions from this analysis are the following. Fish passed John Day more rapidly than they passed Lower Granite, and fish passed more rapidly later in the season at both dams. The simple waiting time model could not adequately describe the data. The diel passage model is an improvement but still did not adequately describe the data. The double exponential model did an excellent job of describing the data.

application to travel time data

In this section, I apply the travel time/delay model equation (5.9) to pit tag data. In this application, I use treatment groups from the Snake River spring chinook and steelhead and the mid-Columbia fall chinook. The cohorts are identified by year and cohort number, so these results can be directly compared to those found in Table 4.4 through Table 4.6 (basic travel time model results) and release information can be found in Appendix I. For each cohort, I numerically calculate maximum likelihood estimates of r , σ and α . I also report the likelihoods for the travel time/delay model and the null model, which is the basic travel time model (equation (4.7)). I also report the ratios of these likelihoods and the BIC values. The BIC value reported is the difference between the value for time/delay model and the null model. A negative value lends support to the null model.

For the spring chinook, all but one of the cohorts had slightly higher likelihoods for the model with the delay component (Table 5.5). For none of the cohorts, though, would the delay model be selected over the basic travel time model based on BIC criterion. Also, the maximum likelihood estimates of α varied substantially ranging from $\alpha = .202$ (corresponding to an average waiting time of ~ 5 days) to $\alpha = 6.81$ (average waiting time under 4 hours). On the other hand, many of the α 's were in the 3-4 range, which is

Table 5.5 Results from the application of the travel time/delay model to Snake River, spring chinook, PIT tag data. Each row is a cohort. A negative BIC value lends support to the null model. See text for further details of the analysis.

cohort	# of fish	parameter estimates			likelihoods			
		r	σ	α	l_0	l_A	ratio	BIC
1989								
3	57	3.70	6.68	0.202	-196.66	-195.56	2.19	-1.86
10	52	4.48	7.18	0.243	-168.49	-168.00	0.96	-2.99
15	55	6.58	9.02	0.202	-171.46	-171.46	0.00	-4.01
17	53	5.32	8.53	3.012	-151.52	-151.48	0.09	-3.88
26	60	8.21	10.12	3.011	-143.13	-142.85	0.55	-3.54
33	41	12.90	9.50	0.963	-79.23	-79.22	0.03	-3.69
34	64	12.39	17.07	3.171	-138.73	-138.15	1.16	-3.00
1990								
3	52	8.56	9.86	3.123	-119.82	-119.48	0.70	-3.25
8	62	5.88	10.74	1.921	-177.67	-177.34	0.65	-3.47
10	80	4.79	9.73	1.670	-246.49	-246.30	0.38	-4.00
1991								
4	84	3.80	5.19	1.265	-248.59	-248.53	0.11	-4.33
10	62	5.27	8.48	3.303	-177.90	-177.89	0.04	-4.09
16	63	10.32	11.91	4.889	-137.90	-137.63	0.54	-3.60
1992								
2	57	3.91	7.03	1.581	-178.31	-178.01	0.61	-3.44
1993								
4	59	4.43	6.22	0.311	-182.60	-181.88	1.43	-2.65
9	47	6.45	7.59	4.305	-117.86	-117.83	0.06	-3.79
15	58	10.49	7.32	6.797	-114.68	-113.49	2.38	-1.68
21	69	11.68	10.82	4.158	-135.66	-135.57	0.19	-4.04
26	84	12.96	12.41	4.074	-160.80	-160.35	0.90	-3.53

consistent with the results from the radio-tracking data.

I was not able to successfully apply the more complex models (diel delay and double exponential delay) to these data. There are probably too many parameters to be fit.

The results from the steelhead are somewhat perplexing. On the one hand, for 13 out of 19 cohorts, we would select the model with the delay component based on the BIC criterion (Table 5.6). The parameter estimates, however, have a great deal of variability with some unrealistically high values for r and unrealistically low values for σ . I would be very hesitant to use these results. The added component seems to make up for some of the deficiency of the null model for this data but in a biologically unrealistic and inconsistent manner.

The results for the fall chinook are contained in Table 5.7. The results appear to be positive – 5 out of the 6 cohorts had positive BIC values, some of which were quite high. Also there is a fair degree of consistency among parameter estimates, which is desirable. Most of the values of α are close to 0.1, resulting in an average waiting time of 10 days. The 1992 results are not as positive as the 1991 and 1993 results. 1992 was an extremely low flow year, and the behavior of the fish may have been affected by this.

Figure 5.6 contains plots of the cumulative of the best fit model compared to the cumulative travel times for the six cohorts. The plots of the cohorts from 1991 and 1992 (the first three plots) indicate some inconsistency between the model and data. The plots of the 1993 cohorts, on the other hand, show a great deal of consistency between the model and data. Clearly more years of data will help to elucidate these differences.

5.4. Predicting model parameters and travel times

The application of the two parameter, travel time model (equations (4.7) and (4.8)) to brand and PIT tag data in the previous chapter revealed quite a bit of variability in

Table 5.6 Results from the application of the travel time/delay model to Snake River steelhead PIT tag data. Each row is a cohort. A negative BIC value lends support to the null model. See text for further details of the analysis

cohort	# of fish	parameter estimates			likelihoods			
		r	σ	α	l_0	l_A	ratio	BIC
1989								
4	45	44.49	3.93	0.869	-83.59	-75.15	16.88	13.08
6	63	29.93	4.48	0.968	-81.60	-75.04	13.11	8.97
11	79	41.33	0.10	0.885	-101.52	-88.74	25.57	21.20
1990								
2	51	20.43	5.25	0.771	-79.07	-77.15	3.84	-0.09
7	86	17.14	3.01	0.779	-134.72	-124.82	19.80	15.34
15	80	23.72	1.94	0.712	-152.68	-133.65	38.06	33.67
18	55	14.58	18.35	2.822	-109.54	-108.75	1.60	-2.41
24	60	23.45	0.20	0.761	-86.53	-80.06	12.93	8.83
1991								
3	49	9.61	10.63	3.297	-107.54	-107.10	0.88	-3.01
6	68	21.22	6.62	0.758	-111.19	-106.90	8.58	4.36
14	85	24.91	4.13	1.318	-112.02	-94.14	35.76	31.31
16	339	23.70	14.98	8.373	-445.62	-440.32	10.60	4.77
1992								
6	72	26.24	7.99	0.911	-131.02	-110.83	40.39	36.11
9	69	22.26	0.69	0.600	-123.11	-105.97	34.28	30.04
13	40	12.85	10.38	5.954	-71.46	-71.28	0.35	-3.34
1993								
2	51	11.80	15.63	2.954	-110.26	-109.50	1.52	-2.41
9	72	18.92	15.95	6.944	-113.12	-112.68	0.89	-3.39
11	97	36.90	0.82	0.711	-156.05	-131.73	48.63	44.06
20	61	41.29	2.40	0.917	-81.87	-69.57	24.61	20.50

Table 5.7 Results from the application of the travel time dependent mortality model to mid-Columbia fall chinook PIT tag data. Each row is a cohort. A negative BIC value lends support to the null model. See text for further details of the analysis

cohort	# of fish	parameter estimates			likelihoods			
		r	σ	α	l_0	l_A	ratio	BIC
1991								
1	154	4.60	11.95	0.098	-655.93	-642.39	27.07	22.03
1992								
2	73	4.76	6.23	0.113	-272.21	-271.75	0.91	-3.38
3	68	4.14	5.74	0.306	-250.37	-244.51	11.72	7.50
19933								
2	81	5.65	3.83	0.081	-316.33	-309.19	14.27	9.88
4	75	5.74	1.90	0.090	-272.00	-264.44	15.13	10.82
5	118	5.36	3.39	0.100	-446.97	-426.93	40.08	35.31

parameter estimates among cohorts (see Table 4.2, Table 4.4, Table 4.5, and Table 4.6). In order to use the model in a predictive mode, parameter values must be selected *a priori*. Thus it would be desirable to relate some of this variability to external factors, making parameter selection more efficient. In this section, I relate parameter estimates from the travel time model to the factors date of release and average river flow in regression models. I apply the regression models to two data sets. The first is the Snake River trap run-of-the-river chinook that have been analyzed previously. The second group are run-of-the-river spring chinook that were captured and released at the Clearwater River trap and recaptured at Lower Granite Dam, 61 kilometers downstream. Both of these groups were tagged each year from 1989-1993. The parameter estimates and covariates associated with the cohorts for these two groups are provided in Appendix 2 in Table A2.1 and Table A2.2. After an

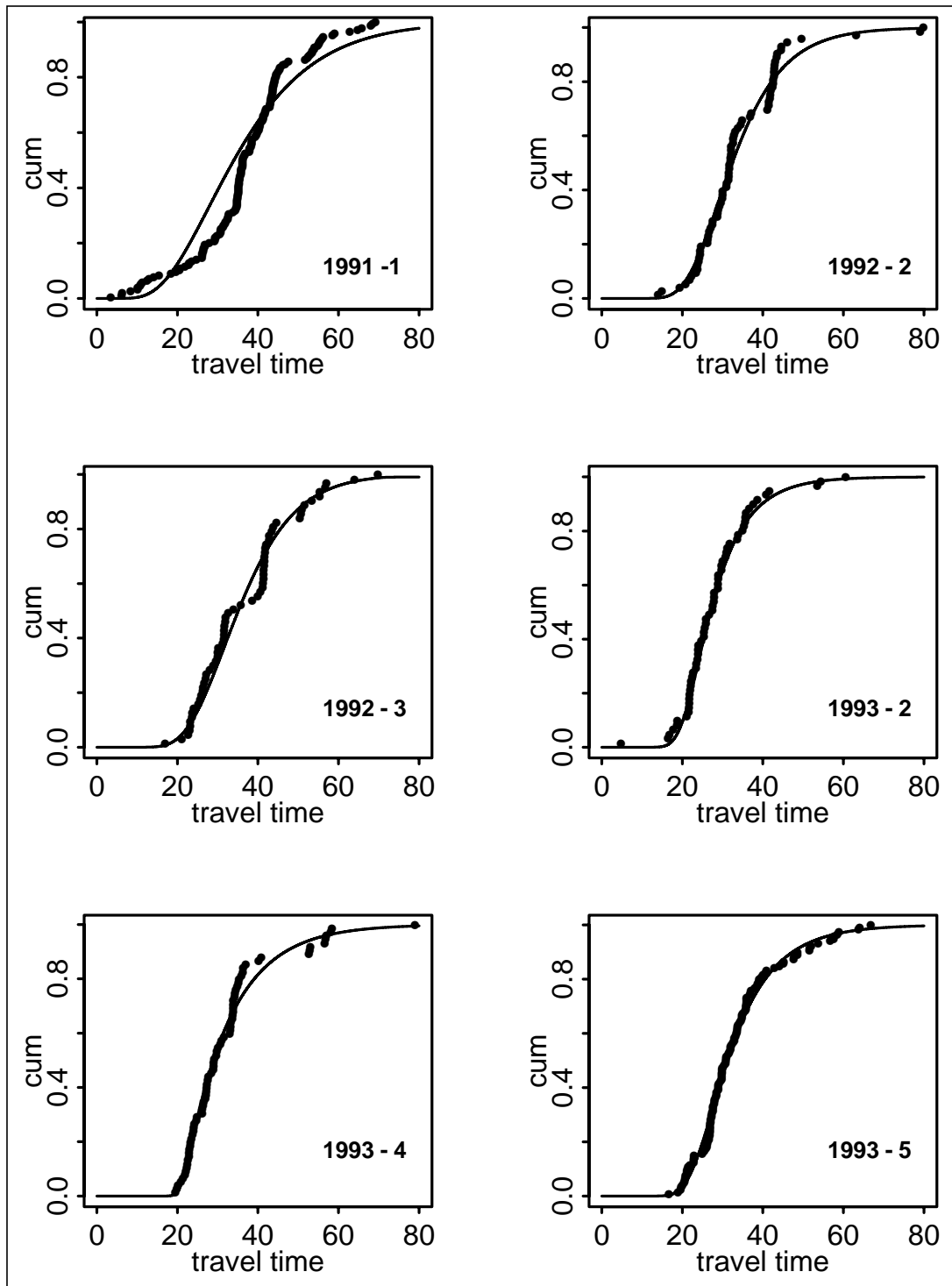


Figure 5.6 Plots of the cumulative travel times for the mid-Columbia Fall chinook. The solid line represents model predictions, and the points are the data.

initial analysis of these data, I use the results of the regressions to predict arrival times. This involves fitting the regression equations to four years of data and then applying the resulting regression coefficients to a fifth year.

My procedure for applying the regression models is as follows. First, using migration rate (r) as a response variable, I construct a sequence of regression equations. The first four are a sequence that increases in complexity; the last two result from dropping a coefficient from the most complex of the first four equations. I then apply these regression equations to the estimated migration rates on a yearly basis. For both of the data sets, there is variability in the number of cohorts for each year, and I chose to analyze years that have at least 20 cohorts. For the Snake River groups, 1989 and 1993 have 20 or more cohorts; for the Clearwater Trap groups, 1991 and 1992 have 20 or more cohorts.

regression equations for migration rate

Migration rate (r) will be predicted using the following six regression models:

model 1) The null model assumes that r is unaffected by the two factors and has average value β_0 :

$$r_i = \beta_0 + \varepsilon_i. \quad (5.14)$$

Variation about the average rate is expressed by ε_i .

model 2) This model assumes a linear relationship between migration rate and flow:

$$r_i = \beta_0 + \beta_1 F_i + \varepsilon_i. \quad (5.15)$$

River velocity is assumed to be proportional to river flow. The intercept term (β_0) is a combination of directed movement independent of flow and a potential non-zero intercept from the river velocity/river flow relationship.

model 3) The linear flow and date model assumes that fish migrate more actively later in the season, by migrating in the higher flow regions of the river and/or by spending a greater proportion of the day in the river flow versus holding up along the shore. The model assumes a linear increase in migration tendency with date as expressed by the coefficient β_2 :

$$r_i = \beta_0 + (\beta_1 + \beta_2 D_i) F_i + \varepsilon_i. \quad (5.16)$$

model 4) A more realistic model of migration tendency would have fish migrating at a minimum rate early in the season and reach a maximum rate later in the season. Although a number of models can produce this behavior, I have chosen to use

$$r(t) = r_{min} + r_{max} \left[\frac{1}{1 + \exp(-\alpha(t - T_0))} \right]. \quad (5.17)$$

The term in the brackets is the *CDF* of the logistic distribution. Early in the season fish migrate at a rate of r_{min} , and later migrate at a threshold rate of $r_{min} + r_{max}$. T_0 determines when the migrate changes from low to high, and α determines the rate of this change. A sample plot of equation (5.17) is provided in figure 5.7. Thus, the regression equation can be formulated as a regression model

$$r_i = \beta_0 + \beta_1 F_i + \beta_2 F_i \left[\frac{1}{1 + \exp(-\alpha(t - T_0))} \right] + \varepsilon_i. \quad (5.18)$$

model 5) This model eliminates β_1 from model 4:

$$r_i = \beta_0 + \beta_2 F_i \left[\frac{1}{1 + \exp(-\alpha(t - T_0))} \right] + \varepsilon_i. \quad (5.19)$$

model 6) This model is created by removing β_0 from model 4:

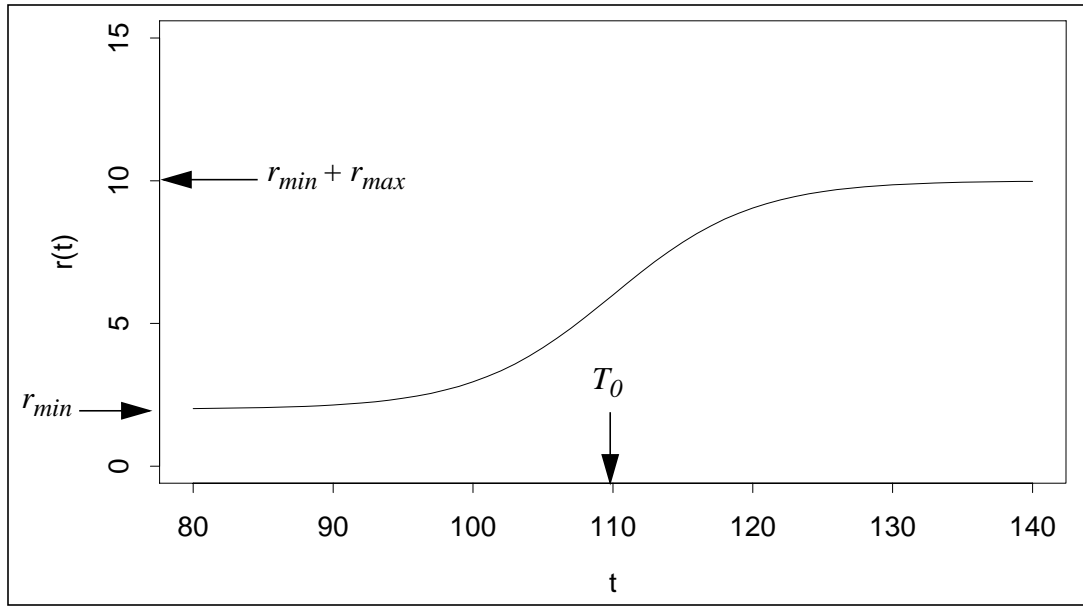


Figure 5.7 A plot of equation (5.17) with $r_{min} = 2.0$, $r_{max} = 8.$, $\alpha = 0.2$, and $T_0 = 110$.

$$r_i = \beta_1 F_i + \beta_2 F_i \left[\frac{1}{1 + \exp(-\alpha(t - T_0))} \right] + \varepsilon_i \quad (5.20)$$

regression equations for σ

To predict values of σ I used the following two models.

model 1) The null hypothesis assumes that σ is a constant plus error:

$$\sigma_i = \beta_0 + \varepsilon_i \quad (5.21)$$

model 2) This assumes that the “rate of spreading” is linearly related to migration rate.

In this formulation, I use \tilde{r} determined from the previous regressions, which is based solely on river flow and date of release. The equation is:

$$\sigma_i = \beta_0 + \beta_1 \tilde{r}_i + \varepsilon_i. \quad (5.22)$$

I will select one of the six regression equations to determine \tilde{r} in this equation.

Least-squares regression was used to fit each of the six models for r and two models for σ to the data from individual years. For all regressions, the parameter estimates and standard errors, deviance, and coefficient of multiple determination are reported. Since the residuals are not necessarily normally distributed, I will not conduct F -tests for levels of significance.

results of the regression analyses

The results of this regression analysis for migration rate of the Snake River chinook are contained in Table 5.8 and for the Clearwater Trap chinook in Table 5.9. These results show that some of the variability in migration rate can be related to the factors river flow and date of release. For all 4 years of data analyzed, the multiple R^2 values are greater than .736 for model 3 through 6. The linear equation (model 3) works well; in three of the four cases, its R^2 values are close to those of the nonlinear models. Although model 4 yields consistently high R^2 values, the standard errors are high, diminishing its predictive capabilities, and in one case (Clearwater trap, 1992) the regression results are unrealistic. Model 5 offers an improvement over model 4. The R^2 values are the same as or close to those of model 4, and the standard errors are small. Model 6 does not work as well as model 5, and in one case (Snake trap, 1993), it yields unrealistic results. Models 3 and 5 are the best candidates for predicting migration rates. The advantage of model 3 is that it has one fewer parameter, but the threshold time relationship contained in model 5 might be more realistic and can more reasonably handle dates outside those observed in this analysis. A plot of regression model 5 for r is contained in Figure 5.8. Note that if Julian date is held constant, there is a linear relationship between r and date. Also, if flow is held constant, the nonlinear relationship

Table 5.8 Regression results for the Snake River spring chinook. For models 4, 5, and 6 $\beta_1 = r_{min}$ and $\beta_2 = r_{max}$.

model	parameter estimates (standard error)					resid. ss	mult. R^2
	β_0	β_1	β_2	α	T_0		
1989 n = 23							
model 1	6.90 (0.46)					109.30	
model 2	-13.69 (4.39)	0.22 (0.046)				53.17	0.514
model 3	-5.51 (2.60)	-0.085 (0.048)	0.0020(0.00027)			14.50	0.867
model 4	-4.86 (2.94)	0.052 (0.16)	0.11 (0.15)	0.11 (0.12)	101.6 (21.0)	10.95	0.900
model 5	-4.49 (2.29)		0.16 (0.029)	0.089 (0.030)	95.0 (4.1)	10.99	0.900
model 6		-4.07(8342.00)	4.23(8346.00)	0.015 (1.26)	-143.6 (152400.0)	26.84	0.754
1993 n = 25							
model 1	7.91 (0.62)					231.10	
model 2	-3.50 (1.89)	0.14 (0.023)				86.95	0.624
model 3	11.26 (5.10)	-0.56 (0.23)	0.0044 (0.0014)			61.08	0.736
model 4	21.80 (14.54)	-0.28 (0.23)	0.18 (0.10)	0.34 (0.11)	116.3 (1.9)	23.08	0.900
model 5	3.89 (0.55)		0.069 (0.0071)	0.50 (0.29)	112.3 (1.5)	33.60	0.855
model 6		0.057 (0.011)	0.052 (0.012)	0.58 (0.69)	110.3 (2.4)	44.09	0.809

Table 5.9 Regression results for the Clearwater Trap spring chinook. For models 4, 5, and 6 $\beta_1 = r_{min}$, and $\beta_2 = r_{max}$.

model	parameter estimates (standard error)					resid. ss	mult. R^2
	β_0	β_1	β_2	α	T_0		
1991 n = 25							
model 1	3.92 (0.32)					60.54	
model 2	-8.06 (1.37)	0.19 (0.021)				13.83	0.772
model 3	6.49 (2.01)	-0.30 (0.064)	0.0024 (0.00031)			3.70	0.939
model 4	3.55 (4.81)	-0.026 (0.11)	0.078 (0.065)	0.14 (0.15)	112.2 (1.8)	3.28	0.946
model 5	2.26 (0.30)		0.065 (0.0067)	0.18 (0.048)	112.0 (1.3)	3.32	0.945
model 6		0.042 (0.0037)	0.048 (0.0054)	0.25 (0.077)	111.5 (1.1)	3.55	0.941
1992 n=35							
model 1	4.14 (0.32)					120.00	
model 2	1.02 (1.16)	0.067 0.024				97.31	0.189
model 3	5.21 (0.46)	-0.28 (0.023)	0.0023 (0.00014)			10.34	0.914
model 4	4.02 (3.54)	-2.15 (600.95)	2.33 (601.00)	0.0080 (0.41)	-200.9 (50000.3)	10.64	0.911
model 5	2.84 (0.20)		0.13 (0.027)	0.10 (0.03)	131.7 (5.6)	10.64	0.911
model 6		0.072 (0.0031)	0.096 (0.011)	0.26 (0.12)	133.8 (3.6)	15.21	0.873

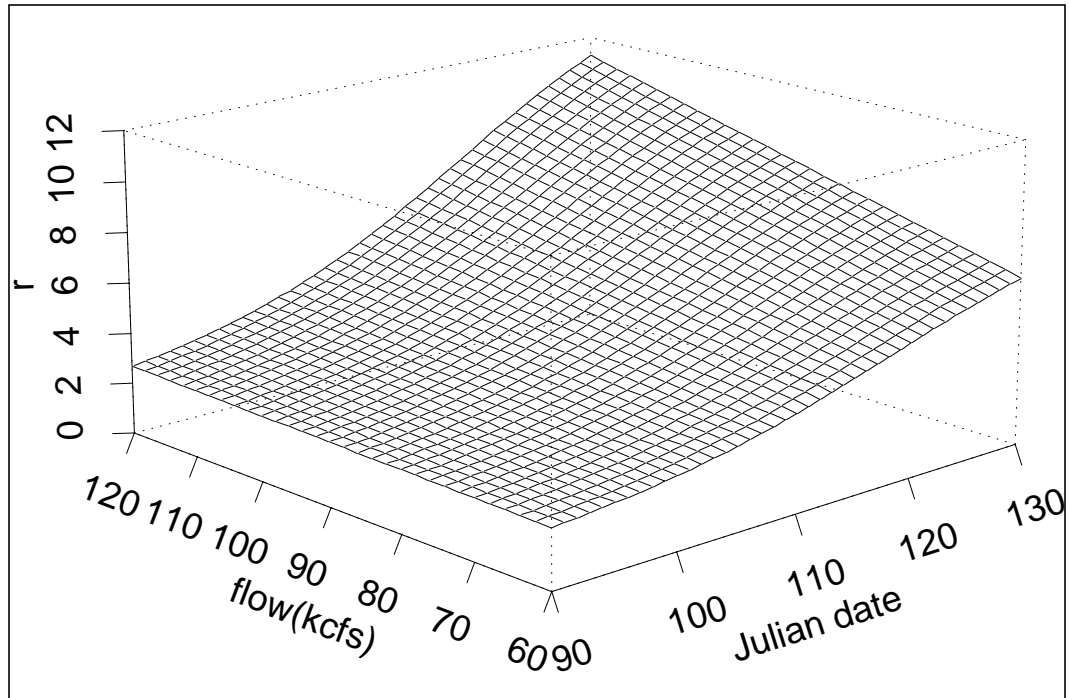


Figure 5.8 A plot of regression model 5 for r (equation (5.19)). For this plot, $\beta_0 = 2.0$, $\beta_2 = \alpha = 0.1$, and $T_0 = 118$.

between r and date is apparent.

Based on the results of the previous regressions, I used model 5 to determine \tilde{r} for the σ regressions. The results of these regressions are contained in Table 5.9. In all four cases

Table 5.10 Regression results using estimates of σ as the response variable.

model	parameter estimates (stand. error)		resid. ss	mult. R^2
	β_0	β_1		
Snake trap 1989				
model 1	9.23 (0.48)		115.60	
model 2	3.03 (0.95)	0.90 (0.13)	36.12	0.688
Snake trap 1993				
model 1	7.33 (0.38)		87.75	
model 2	3.29 (0.75)	0.51 (0.089)	36.06	0.589
Clearwater trap 1991				
model 1	6.27 (0.35)		73.38	
model 2	2.67 (0.58)	0.92 (0.14)	25.16	0.657
Clearwater trap 1992				
model 1	7.17 (0.51)		307.00	
model 2	0.80 (0.52)	1.54 (0.12)	47.70	0.845

there is a positive linear relationship between σ and \tilde{r} ($R^2 = .589 - .845$).

predicting travel times

The goal of the regression analysis is to determine model parameters based on predicting factors. These in turn will be used to predict the arrival distribution of fish at a

downstream site based on the passage distribution at an upstream site. In this section, I demonstrate this procedure by using the results from regressions to try to predict the arrival times of the 1993 Snake trap chinook cohorts and the 1992 Clearwater trap chinook (since the 1993 sample size is small) at Lower Granite Dam. In this analysis, I apply the two parameter travel time model with parameters predicted for each cohort to determine predicted arrival time distributions at Lower Granite Dam. I then pool together the predicted arrival distributions for the cohorts to yield an arrival distribution for all the fish through the year. This distribution is compared to the data and the sum of the squared deviations is reported.

For comparison purposes, I use three approaches to determine model parameters. In the first approach, I pool together the cohorts from the four other years, apply regression model 5 for r and model 2 for σ , and determine regression coefficients for these data. The regression coefficients along with the covariates date of release and river flow are then used to determine model parameters for the fifth year's cohorts. This approach uses independent data from four years to predict arrival time distributions for the fifth and is the standard method for using the travel time model predictively.

In the second approach, instead of using independent data to determine regression coefficients, I use the "in-year" regression coefficients to predict model parameters. In other words, I take the regression coefficients from the 1993 analysis (reported in Table 5.8) and use the 1993 covariates to determine model parameters for the 1993 cohorts. Again, I use model 5 for r and model 2 for σ . This is a bit circular but represents the best that these regression equations can do if we have perfect knowledge of the regression coefficients.

The third approach uses the maximum likelihood estimates (mle's) of the model parameters for each of the cohorts. This represents the best that travel the model can do to predict arrival times if we have perfect knowledge of the individual cohorts.

The regression results for the four years pooled data are contained in Table 5.11. These

Table 5.11 Results from the application of regression model 5 for r and model 2 for σ to the Snake trap and Clearwater trap spring chinook four year composite data.

model	parameter estimates (standard error)					resid. ss	mult. R^2
	β_0		β_2	α	T_0		
Snake trap chinook 1989-1992							
model 5 for r	1.53 (0.69)		0.099 (0.019)	0.099 (0.036)	105.8 (3.9)	81.20	0.681
model 2 for σ	2.50 (0.31)	0.95 (0.12)				145.90	0.519
Clearwater trap chinook 1989-1991, 1993							
model 5 for r	2.61 (0.39)		0.14 (0.030)	0.096 (0.028)	129.3 (4.8)	61.97	0.840
model 2 for σ	6.04 (0.54)	0.21 (0.11)				222.6	0.060

are the coefficients to be applied to the fifth year's data with the first method outlined above. Even with the pooled data, the regressions for r are reasonable ($R^2 = .681$ and $.840$). For σ , the Clearwater trap regressions had a very low R^2 value, indicating that this model offers little improvement over the null model of constant σ .

Plots of the predicted arrival distributions and the actual observations are shown in Figure 5.9 (Snake trap) and Figure 5.9 (Clearwater trap). For the Snake trap spring chinook, the predicted arrival distribution based on independent data (top plot) captures the general shape of the data but misses some of the details. The predicted arrival distribution based on the "in-year" regression (middle plot) reduces the sum-of-squares by 18 per cent and begins to capture some of the bimodality of the data. The predicted curve based on the mle's is sharply two-peaked (bottom plot) and confers an additional 46 per cent reduction in the

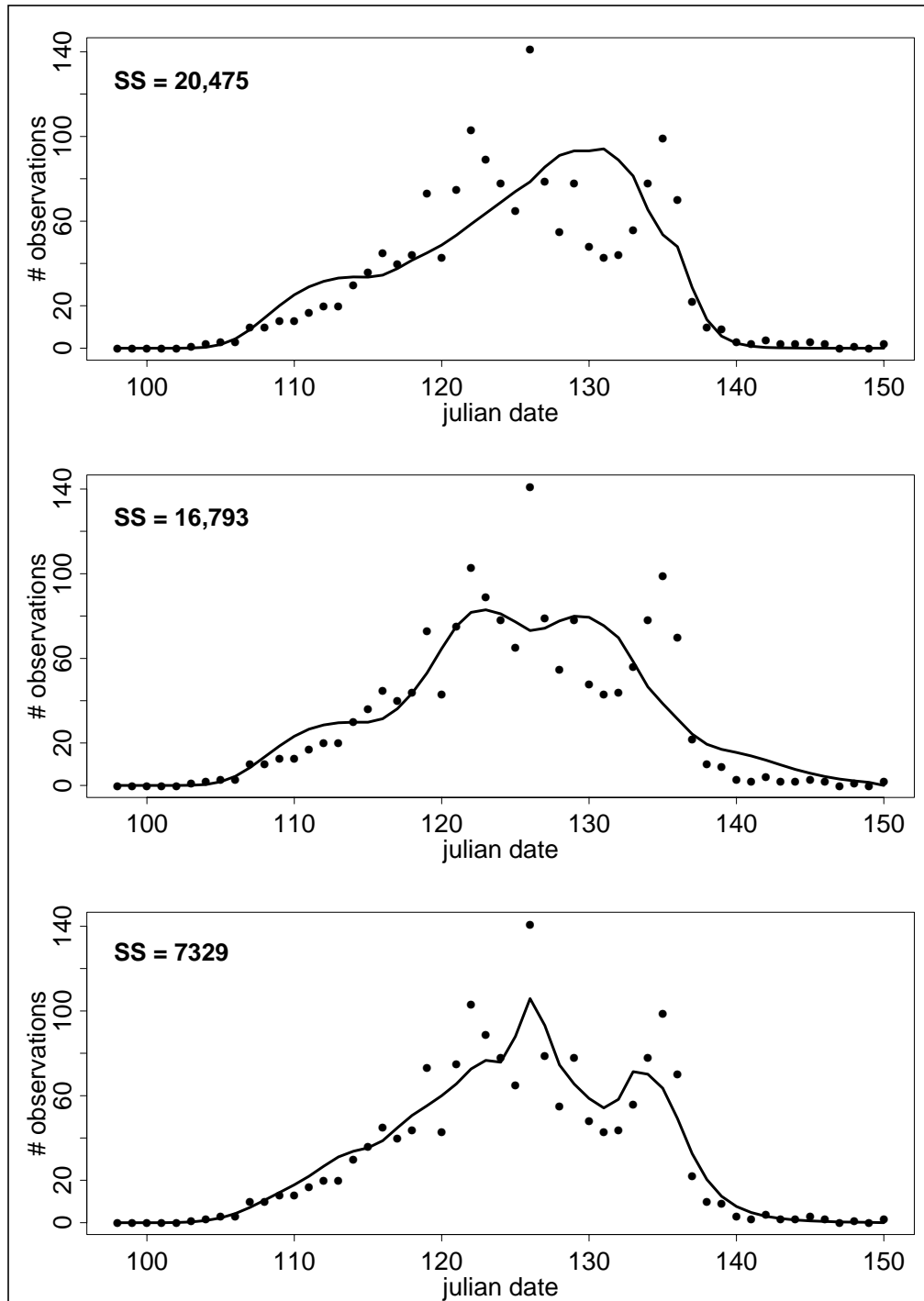


Figure 5.9 Plots of predicted arrival times (solid line) and observed arrival times (points) for the Snake River trap chinook. In the top plot, the predicted curve is based on independent data. In the middle plot, the predicted curve is based on an "in-year" regression to determine travel time parameters. In the bottom plot, the predicted curve is obtained after estimating travel time parameters for each cohort. Also, the sum of the squared deviations between model and data is reported for each plot.

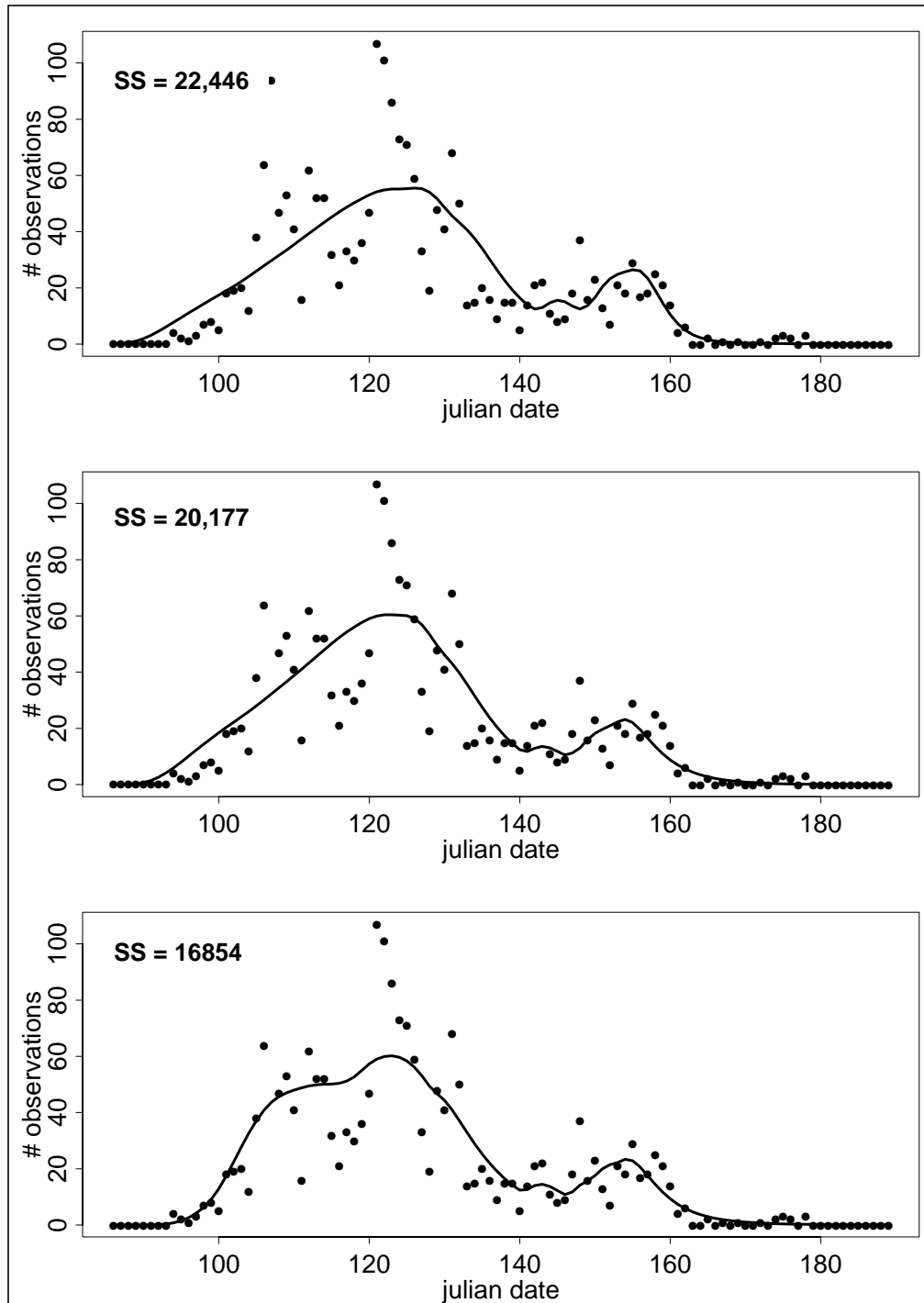


Figure 5.10 Plots of predicted arrival times (solid line) and observed arrival times (points) for the Clearwater trap chinook. In the top plot, the predicted curve is based on independent data. In the middle plot, the predicted curve is based on an “in-year” regression to determine travel time parameters. In the bottom plot, the predicted curve is obtained after estimating travel time parameters for each cohort. Also, the sum of the squared deviations between model and data is reported for each plot.

sum-of-squares, a substantial improvement over the previous two. It is interesting to note that while the “in-year” regression for migration rate had an R^2 of .855 and .589 for σ , using the actual mle’s reduced the sum-of-squares of the arrival distribution by over 50 per cent (that is, comparing the middle and bottom plots).

For the Clearwater trap fish (Figure 5.9), the “in-year” regression based arrival distribution reduces the sum-of-squares by 10 per cent, and the mle based distribution by an additional 15 per cent over the arrival distribution based on independent data. In this case, the arrival distribution based on independent data performs well when compared to the “in-year” arrival distribution.

For both these two data sets, the arrival distribution based on independent data captures the general shape of the observations. While comparisons to the plots based on “in-year” regressions and on mle’s indicate that improvements could be made, these improvements may not necessarily enhance the utility of the model. The types of management actions based on these plots (such as increased spill or augmented flows) would probably not be tuned to fine scale variability but would be based on the gross features captured by the top plots.

6. Travel time model with individual covariates

6.1. Introduction

The models developed in the preceding chapters have all assumed that cohorts of fish released at the same time have identical behavior, an assumption that makes the models more tractable. In reality, the cohorts are probably heterogeneous, and variability may exist in characteristics that affect individuals' behavior and ultimately their travel time. In this chapter, I develop procedures for incorporating individual variability into the travel time model. Individuals can be distinguished by biotic and abiotic factors, and relating variability in travel times to variability in individual covariates will enhance the predictive capabilities of the models.

The biotic trait that I incorporate into the model is fish length. The lengths of all PIT tagged fish are measured at the time of release, and the effects of this covariate can be determined for single release groups. The abiotic factors I examine at the individual level are average river flow, dates of release, and river temperature. Since fish released at the same time encounter similar levels of these factors, series of releases from the same point are required to examine the effects of these covariates.

In the next section of this chapter, I develop the models that include individual covariates and statistical procedures to analyze them. In the following sections, I apply the technique to several data sets. I first apply the model with only the length covariate, since this covariate is commonly available and varies within single release groups. This model is applied to several releases of spring and fall chinook and steelhead. I then expand the model to incorporate date of release, river flow, and river temperature and apply this to a series of releases of fall chinook in the Snake River in the years 1991-1993 and sockeye released in

the mid-Columbia in the years 1992 and 1993.

6.2. Development of model and statistical technique

I assume that each fish has an arrival distribution based on equation (4.7), but its migration rate (determined by the parameter r) is uniquely determined based on a covariate vector \mathbf{X}_i . In other words, the arrival distribution of the i th individual is $g_i(t; \underline{\theta}, \mathbf{X}_i)$, determined by the parameter vector $\underline{\theta}$, which is common to the group, and the covariate vector \mathbf{X}_i , which is unique to the individual. The parameter vector is defined as

$$\underline{\theta} = (\beta_0, \beta_1, \beta_2, \dots, \beta_p, \sigma), \quad (6.1)$$

and in the simplest case, r_i is determined by a multiple linear function of the covariates and β 's:

$$r_i = \beta_0 + \beta_1 X_{i1} + \beta_2 X_{i2} + \dots + \beta_p X_{ip}. \quad (6.2)$$

Alternatively, the covariates and β 's may be incorporated in mechanistic functions motivated by salmon biology.

If t_i is the observed arrival time of the i th individual, the likelihood function is:

$$L(\underline{\theta}, \mathbf{X}_i) = \prod_{i=1}^n g_i(t_i; \mathbf{X}_i, \underline{\theta}). \quad (6.3)$$

The parameters can be determined by maximizing the log likelihood function,

$$l(\underline{\theta}) = \log L(\underline{\theta}) = \sum_{i=1}^n \log g_i(t_i; \mathbf{X}_i, \underline{\theta}), \quad (6.4)$$

with respect to $\underline{\theta}$. This is performed numerically using the downhill simplex method (Nelder and Mead, 1965; Press, et al., 1988).

To analyze the importance of each covariate, I construct a sequence of nested models beginning with the simplest model that contains only the intercept term to the fullest model with all the covariates. The covariates are added one at a time. For each alternative model, parameters are estimated, and likelihoods are computed. The importance of each additional covariate (in the form that it is included in the model) is assessed by comparing the likelihoods and BIC values of alternative models.

6.3. Applications with length covariate

The importance of fish length to migration rate has been analyzed in several studies (Brett, Hollands, and Alderdice, 1958; Washington, 1982). Longer fish are generally more mature (in terms of age and smoltification) and are expected to migrate at a faster rate than shorter fish. As a first application of the procedure, I compare the null hypothesis that r_i is constant within a cohort to the alternative hypothesis that r_i is linearly related to fish length. In other words,

$$H_0: r_i = \beta_0$$

$$H_A: r_i = \beta_0 + \beta_1 \cdot length_i.$$

For each cohort, likelihoods, l_0 and l_A , are computed for the null and alternative hypotheses respectively. Comparing these two likelihoods yields an assessment of the performance of the two models relative to each other. With a likelihood ratio test, the null hypothesis is rejected at the 0.05 level if the ratio is greater than $\chi^2_{1(0.05)} = 3.84$. Using Akaike's information criterion (AIC) the null model is rejected if the ratio is greater than 2.0. Using the Bayesian information criterion (BIC), the null model is rejected if the BIC for the length model (BIC_l) is greater than the BIC for the null model (BIC_0), and I report the value $BIC_l - BIC_0$. I will use these values as a rough measures of the relative

performance of the two models.

Three sets of cohorts are analyzed in this section. The first two sets are Snake River spring chinook and steelhead analyzed in previous chapters. The third set is the mid-Columbia fall chinook.

results

The results of the analysis of the 3 data sets are contained in Table 6.1 - Table 6.5. These tables provide averages and standard deviations of length for each release group. Also contained in the tables are parameter estimates for the length model as well as log likelihoods for the null and alternative models, the ratios between the two, and the BIC values.

There is some support for the length model in the Snake River chinook cohorts (Table 6.1 and Table 6.2). Nine out of the 18 cohorts had likelihood ratios greater than 2.0, which is the AIC value at which the null hypothesis is rejected, but the null model is only rejected for five out of 18 cases based on the BIC values. The parameter estimate results are somewhat contrary to what I expected, however. In 14 out of 18 cohorts, $\hat{\beta}_1$ is negative, indicating that the model predicts increasing migration rate for decreasing fish lengths. This is also true for 8 out of the 9 cohorts that had likelihood ratios greater than 2.0.

The results for the steelhead (Table 6.3 and Table 6.4) are similar to the Snake River chinook results. Five out of the 19 cohorts had likelihood ratios greater than 2.0, and three out of 19 has positive BIC values, supporting the null model in most cases. Also, eight out of 19 had negative values for $\hat{\beta}_1$.

Although the length covariate appears to have some importance in the travel time model for these two groups, it would be difficult to implement the length model based on these

Table 6.1 Results from the application of the individual covariate travel time model with length covariate to cohorts of Snake River “run-of-the-river” chinook. Note that a negative BIC value lends support to the null model (that is, the model without the length covariate).

cohort #	# of fish	length		parameter estimates			likelihoods			
		mean	s.d.	β_0	β_1	σ	l_0	l_A	ratio	BIC
1989										
1	55	128.25	9.28	3.61	-0.006	4.42	-177.51	-177.44	0.15	-3.86
2	57	128.18	10.51	4.99	-0.015	7.02	-199.30	-199.07	0.46	-3.58
3	43	128.21	12.47	10.42	-0.056	7.26	-148.90	-147.10	3.60	-0.16
4	64	134.77	12.06	15.49	-0.059	9.97	-159.53	-158.50	2.06	-2.10
5	69	126.26	18.92	12.81	-0.036	8.34	-156.14	-154.79	2.70	-1.53
6	66	124.61	18.06	9.53	-0.016	7.75	-152.75	-152.46	0.59	-3.60
7	64	115.88	17.39	4.16	0.030	11.26	-164.28	-163.75	1.04	-3.12
1990										
1	54	115.07	13.02	16.86	-0.069	7.83	-114.29	-112.20	4.17	0.18
2	66	118.95	14.24	15.49	-0.077	10.07	-182.78	-179.99	5.58	1.39
3	52	117.13	15.14	9.54	-0.028	5.90	-122.53	-121.38	2.29	-1.66

Table 6.2 Results from the application of the individual covariate travel time model with length covariate to cohorts of Snake River “run-of-the-river” chinook. Note that a negative BIC value lends support to the null model (that is, the model without the length covariate).

cohort #	# of fish	length		parameter estimates			likelihoods			
		mean	s.d.	β_0	β_I	σ	l_0	l_A	ratio	BIC
1991										
1	55	124.22	12.06	4.00	-0.009	4.82	-178.31	-178.14	0.33	-3.67
2	66	128.32	9.84	9.03	-0.039	6.02	-197.19	-195.71	2.97	-1.22
3	51	127.88	10.16	5.61	0.004	8.35	-135.23	-135.22	0.01	-3.92
1992										
1	50	130.00	9.32	8.14	-0.032	5.51	-147.50	-146.59	1.82	-2.10
1993										
1	60	127.08	10.77	1.67	0.015	5.18	-182.64	-182.25	0.79	-3.31
2	46	123.72	11.22	10.29	-0.047	4.54	-124.04	-120.45	7.18	3.35
3	64	120.33	13.07	3.21	0.041	6.92	-135.87	-134.53	2.68	-1.48
4	57	122.02	10.87	12.48	-0.009	7.41	-95.49	-95.47	0.04	-4.00
5	74	121.14	18.26	-4.94	0.148	15.13	-154.11	-148.98	10.27	5.97

Table 6.3 Results from the application of the individual covariate travel time model with length covariate to cohorts of Snake River steelhead. Note that a negative BIC value lends support to the null model (that is, the model without the length covariate).

cohort #	# of fish	length		parameter estimates			likelihoods			
		mean	s.d.	β_0	β_I	σ	l_0	l_A	ratio	BIC
1989										
1	64	185.89	29.98	27.94	-0.042	12.62	-84.61	-83.51	2.20	-1.96
2	79	182.48	20.62	8.13	0.058	17.19	-126.17	-125.68	0.97	-3.40
3	47	168.94	17.28	18.66	-0.019	11.69	-90.22	-90.16	0.11	-3.74
1990										
1	61	182.57	23.54	15.63	-0.011	9.93	-101.38	-101.30	0.17	-3.94
2	95	176.74	14.80	0.67	0.067	6.84	-158.91	-154.53	8.76	4.21
3	146	171.97	16.02	8.33	0.021	12.01	-287.36	-287.11	0.50	-4.49
4	68	173.94	16.79	6.42	0.015	13.98	-168.08	-168.02	0.11	-4.10
5	61	169.43	17.40	11.38	-0.014	8.22	-128.11	-127.93	0.35	-3.76

Table 6.4 Results from the application of the individual covariate travel time model with length covariate to cohorts of Snake River steelhead. Note that a negative BIC value lends support to the null model (that is, the model without the length covariate).

cohort #	# of fish	length		parameter estimates			likelihoods			
		mean	s.d.	β_0	β_1	σ	l_0	l_A	ratio	BIC
1991										
1	50	181.12	16.12	6.17	0.023	7.15	-89.39	-89.07	0.64	-3.27
2	126	178.67	15.29	24.78	-0.055	10.62	-201.54	-199.96	3.15	-1.69
3	56	173.95	16.23	13.99	-0.005	9.45	-94.36	-94.35	0.02	-4.01
4	51	165.82	17.33	11.55	0.050	12.75	-68.50	-68.23	0.54	-3.39
1992										
1	67	181.40	17.63	8.21	0.011	6.40	-114.00	-113.84	0.31	-3.89
2	154	176.60	17.70	17.05	-0.014	10.23	-245.01	-244.83	0.36	-4.68
3	90	171.41	14.71	15.14	-0.038	7.34	-214.97	-213.39	3.15	-1.35
1993										
1	50	178.28	21.30	7.47	0.032	10.85	-88.79	-88.35	0.88	-3.03
2	87	177.00	20.10	-3.21	0.114	9.44	-123.06	-115.73	14.66	10.19
3	59	173.93	19.03	-13.20	0.183	17.88	-100.69	-97.86	5.66	1.59
4	40	175.38	16.32	10.32	0.032	12.18	-64.90	-64.77	0.26	-3.43

data because of the variability in parameter estimates. More information will be required to understand why the relationship between migration rate and fish length is sometimes positive and sometimes negative.

The results for the mid-Columbia fall chinook (Table 6.5) strongly support the inclusion of the length covariate in the travel time model. All the BIC values are positive, with 4 out of 5 values greater than 10.0. Also there is consistency in the values of $\hat{\beta}_0$ and $\hat{\beta}_1$, with most estimates of β_0 in the 3.0 - 5.0 range and most estimates of β_1 in the 0.10 to 0.14 range. Thus, including length information in the travel time model for these fish would be quite useful.

6.4. Multiple covariate model

In this section I will extend the individual covariate model to include several covariates. This approach is useful when fish are released over an extended period of time so that there is not only variability in population traits but also in river conditions. It is also useful when sample sizes for individual release groups are small, and cohorts of adequate sample size cannot be formed from fish released over a short period of time. I apply this model to two groups: fall chinook tagged in the Snake River above Lower Granite Dam during the years 1991-1993, and wild sockeye tagged at Rock Island dam on the mid-Columbia during the years 1992 and 1993 and recaptured at McNary Dam.

In addition to the length covariate, I also incorporate the covariates date of release, river temperature at release, and average river flow during the individual's migration period. For this analysis I add the covariates one at a time in sequential linear models. I chose to do this for the sake of simplicity, but the covariates could be incorporated in nonlinear models based on salmon behavior. Since the covariates are being added one at a time, the importance of adding the new covariate to the previous model is observed. I add the

Table 6.5 Results from the application of the individual covariate travel time model with length covariate to cohorts of mid Columbia fall chinook. Note that a negative BIC value lends support to the null model (that is, the model without the length covariate).

cohort #	# of fish	length		parameter estimates			likelihoods			
		mean	s.d.	β_0	β_1	σ	l_0	l_A	ratio	BIC
1991										
2	97	63.32	4.38	-0.60	0.062	6.86	-393.05	-390.38	5.33	0.76
1992										
1	75	71.37	7.16	-5.11	0.125	5.58	-288.71	-264.16	49.11	44.79
4	63	69.00	7.21	-3.64	0.102	4.60	-239.05	-219.76	38.57	34.43
1993										
1	61	66.80	6.49	-5.36	0.145	3.99	-222.15	-195.54	53.21	49.10
3	115	66.20	5.46	-4.96	0.134	5.92	-425.60	-404.48	42.24	37.50

covariates as a multiple linear model in the following nested sequence:

$$H_0: r_i = \beta_0$$

$$H_1: r_i = \beta_0 + \beta_1 \cdot X_{1i}$$

$$H_2: r_i = \beta_0 + \beta_1 \cdot X_{1i} + \beta_2 \cdot X_{2i}$$

$$H_3: r_i = \beta_0 + \beta_1 \cdot X_{1i} + \beta_2 \cdot X_{2i} + \beta_3 \cdot X_{3i}$$

$$H_4: r_i = \beta_0 + \beta_1 \cdot X_{1i} + \beta_2 \cdot X_{2i} + \beta_3 \cdot X_{3i} + \beta_4 \cdot X_{4i}$$

where

X_1 = fish length (in mm),

X_2 = average river flow during the migration period (kcfs),

X_3 = Julian date of release, and

X_4 = river temperature (degrees centigrade) at time of release.

Other sequences could also have been used.

I apply this sequence of models to each year of data from both data sets. I estimate parameters (β 's and σ) and report likelihoods for each model. The effect of added covariates can be assessed by computing likelihood ratios between successive models and by comparing BIC values. Note that in this case, I report BIC values for the individual models, so that any of the two models can be compared directly, with the simpler model (that is, the one with fewer parameters) being rejected if it has a lower BIC value.

results

The results for the Snake River fall chinook are contained in Table 6.6. The covariate date of release is extremely important in all three years, with likelihood ratio values ranging from 22.86 to 104.28 larger than the next smaller model nested within (i.e., comparing the model with length flow and date to the one with length and flow). On the other hand, the temperature covariate is never important, with likelihood ratio values ranging from 0.0 to 0.79 larger than those of the model nested within. Length and flow both appear to be important covariates, but the results are not as strong as with the date covariate, particularly in the 1992 data. For all three years, it appears that the best model is the one with length, flow, and date (model 3).

The results for the sockeye are contained in Table 6.6. The length covariate appears to be the most important with large increases in the likelihoods relative to the null model. Flow is also important, with large increases in the likelihoods associated with adding this covariate to the model. Also, date appears to be an important covariate but not as important as the previous two. In both years, temperature had little effect on the model. The order of inclusion may have some importance on the relative importance of the covariates, but it appears that the best model should incorporate length, flow, and date, as with the fall chinook.

log likelihood versus log sigma

An interesting result is observed by plotting log likelihood versus log sigma for the 5 alternative models in each of the three years (Figure 6.1). In each year the relationship between these two variables is almost perfectly linear. The inverse relationship indicates that some of the variability in arrival times that was attributed to random movement in the null model is actually the result of population heterogeneity. Thus the more relevant information about the individuals available, the more precise the predictions about arrival

Table 6.6 Results of the application of the individual covariate model to Snake River fall chinook. Note that the BIC values are reported for each of the hypotheses. When two hypotheses are compared, the simpler model is not rejected if it has a larger BIC value than the more complex model.

hypothesis	parameter estimates						likelihoods		
	β_0 (int.)	β_1 (len.)	β_2 (flow)	β_3 (date)	β_4 (temp)	σ	lik.	ratio	BIC _i
1991 n = 32									
0	1.41					4.91	-142.04		-291.01
1	-1.56	0.044				4.18	-136.90	10.27	-284.20
2	-3.41	0.050	0.028			3.74	-133.31	17.45	-280.48
3	-17.07	-0.019	0.072	0.099		2.61	-121.88	40.31	-261.09
4	-16.79	-0.018	0.072	0.097	-0.0137	2.61	-121.86	40.34	-264.51
1992 n = 40									
0	3.03					11.27	-164.59		-336.56
1	-2.25	0.069				10.58	-162.07	5.05	-335.20
2	-5.66	0.074	0.074			10.20	-160.61	7.96	-335.98
3	-43.91	0.004	0.343	0.234		5.95	-139.04	51.10	-296.52
4	-42.78	0.010	0.331	0.215	0.1082	5.89	-138.65	51.89	-299.43
1993 n = 251									
0	1.42					6.89	-1174.27		-2359.59
1	-1.07	0.034				6.05	-1156.74	35.07	-2330.06
2	-3.39	0.043	0.023			4.90	-1119.92	108.70	-2217.74
3	-15.43	0.014	0.053	0.076		3.73	-1067.78	212.98	-2163.19
4	-15.43	0.014	0.053	0.075	0.0002	3.73	-1067.78	212.98	-2168.71

Table 6.7 Results of the application of the individual covariate model to mid-Columbia sockeye. Note that the BIC values are reported for each of the hypotheses. When two hypotheses are compared, the simpler model is not rejected if it has a larger BIC value than the more complex model.

hypothesis	parameter estimates						likelihoods		
	β_0 (int.)	β_1 (len.)	β_2 (flow)	β_3 (date)	β_4 (temp)	σ	lik.	ratio	BIC _i
1992 n = 148									
0	16.37					35.11	-495.68		-1001.35
1	-14.50	0.265				29.63	-470.42	50.53	-955.83
2	-46.60	0.292	0.504			26.58	-454.35	82.67	-928.69
3	-63.34	0.266	0.459	0.192		25.95	-451.00	89.37	-926.99
4	-63.62	0.267	0.461	0.193	0.0015	25.99	-451.00	89.37	-931.98
1993 n = 521									
0	21.24					40.83	-1627.24		-3266.99
1	-33.85	0.612				31.24	-1499.07	256.35	-3016.91
2	-34.55	0.497	0.099			30.59	-1477.03	300.43	-2979.08
3	-22.91	0.609	0.142	-0.213		30.07	-1470.02	314.45	-2971.31
4	-23.15	0.610	0.143	-0.212	0.0002	30.17	-1470.00	314.47	-2977.54

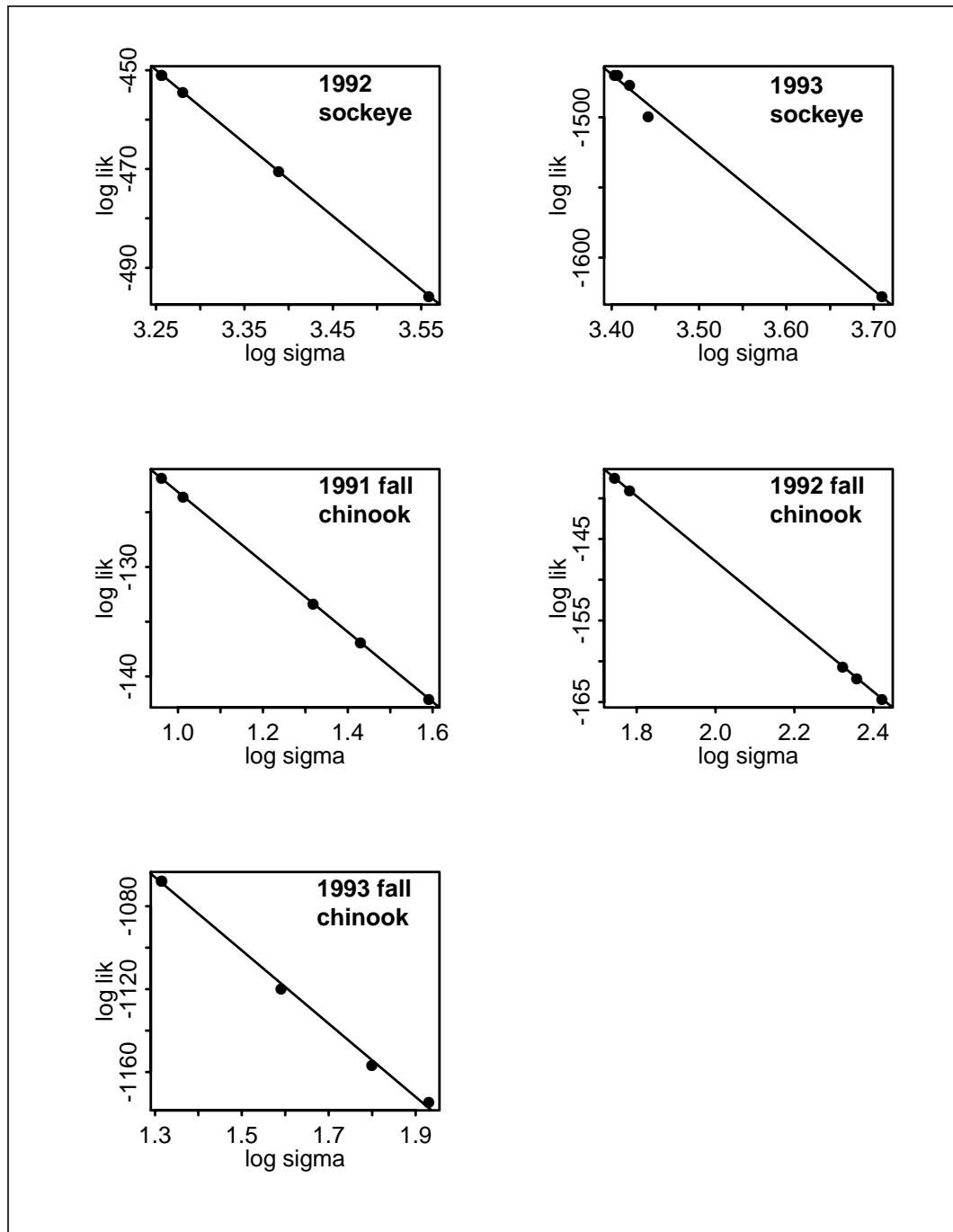


Figure 6.1 Plots of log likelihood versus $\log \sigma$ for the 5 alternative models.

times will be. This analysis found that the covariates fish length, river flow, and date of release are important; other covariates may also be determined to be important, further increasing the precision.

7. Movements of individuals

7.1. Introduction and motivation

In constructing models of the dispersal of organisms, one of the basic choices is whether to focus on individuals or populations. This choice is often dictated by the objective of the model. For instance, models of the spread of populations on the time scale of generations needn't be concerned with individual movements. On the other hand, most population dispersal models do make assumptions about the movements of individuals, and, particularly if the model operates on relatively short time scales, it is often informative to determine the validity of the assumptions. Analyzing data of individual movements is a means of doing this.

One of the assumptions of the travel time model described previously (equations (4.7) and (4.8)) is that the movements of individuals follow a Wiener drift process. A restrictive property of this process is that disjoint movement increments are independent, no matter how fine the time scale. Clearly this property is limiting in describing the movement of animals. In the short term, an animal moving at a particular velocity will likely continue at that velocity. In the longer term, however, independent increments may be realistic.

Analyzing group release travel time data, as I have done in previous chapters, cannot confirm the Wiener drift process assumption. With this type of data, information about individual movements is lost, and several different movement processes could produce similar arrival distributions. To overcome these limitations, I analyze the movements of juvenile salmonids observed in radio-tracking experiments. I compare these data to two models: the Wiener process and a model based on the Ornstein-Uhlenbeck process. This latter model has the following two properties: 1) In the short term, disjoint increments are

correlated; and 2) as the time increment gets large, the process becomes indistinguishable from the Wiener process. In addition, the models are nested; as the correlation parameter in the O-U based model gets large, the behavior of the two models approaches each other.

In analyzing the radio-tracking data, I will address the following questions: 1) Is the distribution of movements consistent with the models, and if so, which model is more appropriate; and 2) is the correlation among movements important at the time scale of the data.

7.2. Models

Wiener process

The Wiener process (or Brownian motion) is the continuous analog to the standard random walk (Ross, 1985). The Wiener process with drift can be derived from a biased random walk, a random walk in which the probabilities of moving to the right and to the left are not equal (but are constant). The process $X(t)$ is said to be the Wiener drift process if it has the following properties (Ross, 1985):

- 1) $X(0) = 0$;
- 2) for $t > 0$, $X(t)$ is normally distributed with mean rt and variance $\sigma^2 t$;
- 3) each disjoint segment of an individual path is independent.

As stated above, the major drawback of this process for modeling movements of organisms is property 3.

telegrapher's equation

A natural extension of this model that incorporates correlation among movements is based on a correlated random walk. The correlated random walk is presented as follows. Let X_t be a discrete time, discrete space process with $x \in \text{integers}$ and $t = 0, 1, 2, \dots$. The

transition probabilities of X are defined as follows:

$$\begin{aligned} p &= Pr(\text{particle moves one unit in the same direction as the previous movement}) \\ q &= Pr(\text{particle moves one unit in the opposite direction of the last step}) \\ p + q &= 1. \end{aligned} \tag{7.1}$$

The standard initial conditions are that $x_0 = 0$, and for the first step, the probability of moving to the right = the probability of moving to the left = $1/2$.

Following the approach of Goldstein (1951), it is possible to derive a limiting continuous distribution based on this process called the telegrapher's equation:

$$\frac{\partial^2}{\partial t^2} p(x, t) + 2\lambda \frac{\partial}{\partial t} p(x, t) = \gamma^2 \frac{\partial^2}{\partial x^2} p(x, t). \tag{7.2}$$

The same result can be obtained by beginning with the continuous (in time and space) analog to the correlated random walk. In this process, a particle moves in one direction with a constant speed γ until it reverses direction and then moves in the opposite direction with the same speed. The direction reversing process is governed by a Poisson process with parameter λ .

The first two moments of the displacement process defined by the telegraph equation are easily obtained and are quite tractable:

$$E(X) = 0 \tag{7.3}$$

$$Var(X) = \gamma^2 \left[\frac{t}{\lambda} - \frac{1}{2\lambda^2} (1 - e^{-2\lambda t}) \right]. \tag{7.4}$$

For small t

$$Var(X) \approx \gamma^2 t^2 \tag{7.5}$$

which is characteristic of wave equations. Also when t is large

$$\text{Var}(X) \approx \frac{\gamma^2}{\lambda} t \quad (7.6)$$

which is similar to that of the Wiener process with diffusion coefficient $D = \gamma^2/2\lambda$.

Equation (7.2) can be solved for $p(x,t)$ with initial conditions $p(x,0) = 0$ and $\partial p/\partial x(x,0) = 0$

$$p(x,t) = \frac{e^{-\lambda t}}{2} \left[\delta(x - \gamma t) + \delta(x + \gamma t) + \frac{\lambda}{\gamma} \left(I_0(\Lambda) + \frac{\lambda t}{\Lambda} I_1(\Lambda) \right) \right] \quad (7.7)$$

$$\Lambda = \lambda \sqrt{t^2 - x^2/\gamma^2} \quad , \quad (7.8)$$

where I_0 and I_1 are modified Bessel functions and δ is the Dirac distribution. Unfortunately, the pdf derived from this equation is rather complex and is probably not practical as a model of animal movement at the level of the individual, although it has been applied to population patterns (Holmes, 1993).

O-U based model

An alternative model of correlated movement is based on the Ornstein-Uhlenbeck (O-U) process (Uhlenbeck and Ornstein, 1930). The O-U process was first presented as an alternative model for Brownian motion and was developed to describe the velocities of particles. The model operates under the assumption that as a particle travels with greater velocity, it is increasingly likely to contact another particle and meet resistance. Thus, there is a tendency for particles to be brought back to zero velocity, and with the O-U process, the strength of this tendency is linearly related to the magnitude of the velocity. There is correlation between movements occurring over short periods of time and a tendency to return to zero velocity. This type of process resembles, in some cases, the movement

patterns of animals on a short time scale. From this velocity based model, the distribution of displacements can be obtained, which is compatible with individual movement data.

To begin, let $X(t)$ be the position of a particle at time t . Define $V(t)$ as the velocity at time t . Since the O-U process applies to particles with zero mean velocity, the mean must be subtracted off. Denote

$$U(t) = V(t) - \bar{V} . \quad (7.9)$$

If $U(t)$ follows an Ornstein-Uhlenbeck process, then:

$$\frac{\partial}{\partial t} p(u, t) = \frac{\partial}{\partial u}(\beta u p) + \frac{\sigma^2}{2} \frac{\partial^2 p}{\partial u^2} . \quad (7.10)$$

The parameter σ characterizes the spread of the particles, and the parameter β characterizes the propensity of the particle to return to its mean velocity. The conditional distribution $p(u, t | u_0, s)$, $t > s$, is a Gaussian distribution with

$$E(U(t)) = u_0 \exp(-\beta t) \quad (7.11)$$

$$\text{Var}(U(t)) = \frac{\sigma^2}{2\beta} [1 - \exp(-2\beta t)] . \quad (7.12)$$

In contrast to the Wiener process, the variance of the O-U process stabilizes as t gets large.

The displacements predicted by the process can be obtained by integrating:

$$Y(T_i) = X(t_i) - X(t_{i-1}) = \int_{t_{i-1}}^{t_i} U(s) ds . \quad (7.13)$$

Here T_i is defined as the time interval $t_i - t_{i-1}$. This integration is considered a stochastic integration because $U(s)$ is a stochastic process (Cox and Miller, 1965). As reported by Doob (1942) Y has a Gaussian distribution with

$$E(Y) = 0 \quad (7.14)$$

$$Var(Y) = \frac{2\sigma^2}{\beta^2}[\beta T - 1 + e^{-\beta T}] . \quad (7.15)$$

Interestingly, the mean and variance are the same as those of the telegrapher's equation.

Also,

$$Cov(Y_i, Y_{i+1}) = \frac{\sigma^2}{\beta^2}[1 - e^{-\beta T_i} - e^{-\beta T_{i+1}} + e^{-\beta(T_i + T_{i+1})}] . \quad (7.16)$$

Thus the joint distribution of Y_i and Y_{i+1} is a bivariate normal with mean and variance given in equations (7.14) and (7.15) and with correlation coefficient

$$\begin{aligned} \rho(Y_i, Y_{i+1}) &= \frac{Cov(Y_i, Y_{i+1})}{Var(Y_i)Var(Y_{i+1})} \\ &= \frac{[1 - e^{-\beta T_i} - e^{-\beta T_{i+1}} + e^{-\beta(T_i + T_{i+1})}]}{2[\beta T - 1 + e^{-\beta T_i}]^{1/2}[\beta T - 1 + e^{-\beta T_{i+1}}]^{1/2}} . \end{aligned} \quad (7.17)$$

An important feature of this equation is that as the time scale gets larger, the correlation decays. Also, the correlation coefficient depends only on β and not on σ , and Figure 7.1 shows that there is an inverse relationship between β and $\rho(Y_i, Y_{i+1})$. In addition, as $\beta \rightarrow \infty$ (with σ/β a constant), the variance approaches a linear relationship with time, and the covariance goes to 0. The process then becomes indistinguishable from the Wiener process.

If the time increments are equal, the data can be analyzed with standard time series analysis. If the data have unequal time increments, as with many radio-tracking studies, the analysis is not as simple. The equations describing the Wiener drift process and the O-U

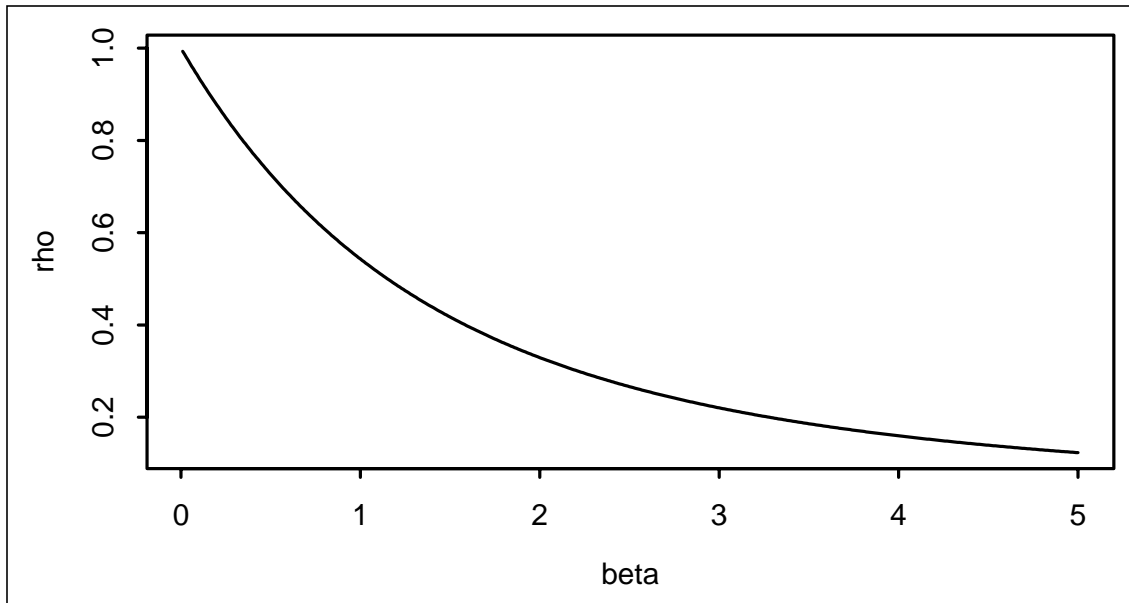


Figure 7.1 The relationship between the parameters ρ and β based on equation (7.17). The time increment is $T_i = T_{i+1} = 1.0$.

displacement process do not require equal time increments, though, and thus can form the basis of the analysis of unequal time increment data.

7.3. Statistical analysis

The data are a series of observations of an individual with the position $X(t_i)$ noted at time t_i , $i = 0, 1, 2, \dots, n$. The data are converted to a two dimensional vector (y_i, T_i) , where $y_i = x_i - x_{i-1}$ is the i th displacement and $T_i = t_i - t_{i-1}$ is the time duration of the displacement.

The first question I address is do the y_i 's agree with property (2) of the Wiener process. In other words, do the y_i 's have the distribution $N(rT_i, \sigma^2 T_i)$. To test this, I use Liliefors's

test for normality (Conover, 1980). This is a Kolmogorov-Smirnoff type of test specific to a population of normal variables with unknown mean and variance. The first step is to estimate the parameters r and σ , which are then used to determine mean and variance. I use maximum likelihood to estimate the parameters. The likelihood function is

$$L(r, \sigma; Y) = \prod_{i=1}^n f_W(y_i, T_i; r, \sigma). \quad (7.18)$$

The maximum likelihood estimator (mle) for r is:

$$\hat{r} = \frac{\sum y_i}{\sum T_i}, \quad (7.19)$$

which is just the average downstream velocity of the individual. To estimate σ , I plug \hat{r} into the likelihood function and maximize $\log(L)$ with respect to σ numerically, using a downhill simplex method (Press, et al. 1988).

The statistic of Lilliefors's test measures the deviation of the observations from a cumulative normal distribution. This statistic is compared to a lookup table to determine the approximate probability. Normality is rejected for small p -values.

The third property of the Wiener process is independent increments. If normality is rejected, then the increments can be transformed to standard normal variables as follows:

$$Z_i = \frac{(Y_i - \hat{r}T_i)}{\hat{\sigma}\sqrt{T_i}}. \quad (7.20)$$

The property of independence of successive increments can be tested for by determining whether the Z_i 's are uncorrelated. (In general, showing that two random variables are uncorrelated does not demonstrate independence; in the case of normal random variable, however, it does). The correlation between successive movements can be determined by

computing the correlation coefficient

$$\rho(Z_i, Z_{i+1}) = \frac{1}{n-1} \sum_{i=1}^{n-1} Z_i \cdot Z_{i+1}, \quad (7.21)$$

where n is the number of movement increments observed. To test the null hypothesis of no (or negative) correlation among successive Z_i 's versus the alternative hypothesis of positive correlation, the test statistic

$$t_\rho = \rho \sqrt{\frac{n-2}{1-\rho^2}} \quad (7.22)$$

is compared to a t distribution with $n-2$ degrees of freedom (Sokal and Rohlf, 1981). The null hypothesis is rejected for small p -values.

To estimate the parameters for the O-U based model, I follow a similar procedure. I first subtract off the average (time scaled) displacement from the observations. This is identical to the first step above and can be expressed as

$$Y'_i = Y_i - \hat{r}t. \quad (7.23)$$

The transformed variable Y' has mean displacement of 0. The likelihood function is

$$L(\sigma, \beta; Y') = \prod_{i=1}^{n-1} f_{OU}(Y'_i, Y'_{i+1}; \sigma, \beta), \quad (7.24)$$

where f_{OU} is a bivariate normal distribution with parameters defined in equations (7.14), (7.15), and (7.16). Again, the parameters σ and β are estimated by maximizing the log of (7.24) numerically with respect to the parameters.

The importance of the parameter β , which determines correlation in the O-U based model, can be assessed by computing the log likelihood ratios and BIC values. I report the difference between the BIC values for the O-U based model and Wiener drift model. The

null model (Wiener drift model) is rejected for positive BIC values.

7.4. Application to radio-tracking data

data

The study site is the John Day reservoir on the Columbia River in front of the John Day Dam (Giorgi, et al. 1986). At this site, the river is relatively straight and is approximately a kilometer wide. The study was conducted during the Summer of 1983. Individual fish were collected at the John Day Dam, radio tagged, and released 6.3 kilometers upstream from the dam. Two boats followed the individuals with the fish's position being noted by hand held receivers at approximately 20 minute intervals. The individuals were followed for up to eight hours with radio tracks up to six kilometers long. 17 chinook and 8 steelhead were released and followed. Many of the individuals had tracks that were too short for adequate analysis. I chose to analyze the tracks of the three chinook and two steelhead that had at least 19 "fixes" and track durations of at least six hours. Since the primary interest in these data is the downstream movement of the individuals, I ignored the horizontal movements of the fish and converted the data to downstream displacements. Figure 7.2 contains plots of downstream displacement versus time for the five individuals.

results

The results of the data analysis are contained in Table 7.1. For two out of three of the chinook and one out of two steelhead, normality is not rejected based on Lilliefors's test. For both of these chinook, though, zero or negative correlation is rejected at the $\alpha = 0.05$ level. For the steelhead (steelhead 170), zero or negative correlation is not rejected, and thus the two properties of the Wiener process are not rejected for this individual.

For the three chinook, the O-U displacement model is supported over the Wiener drift model based on BIC values. For the two steelhead, the opposite is true, and the simple

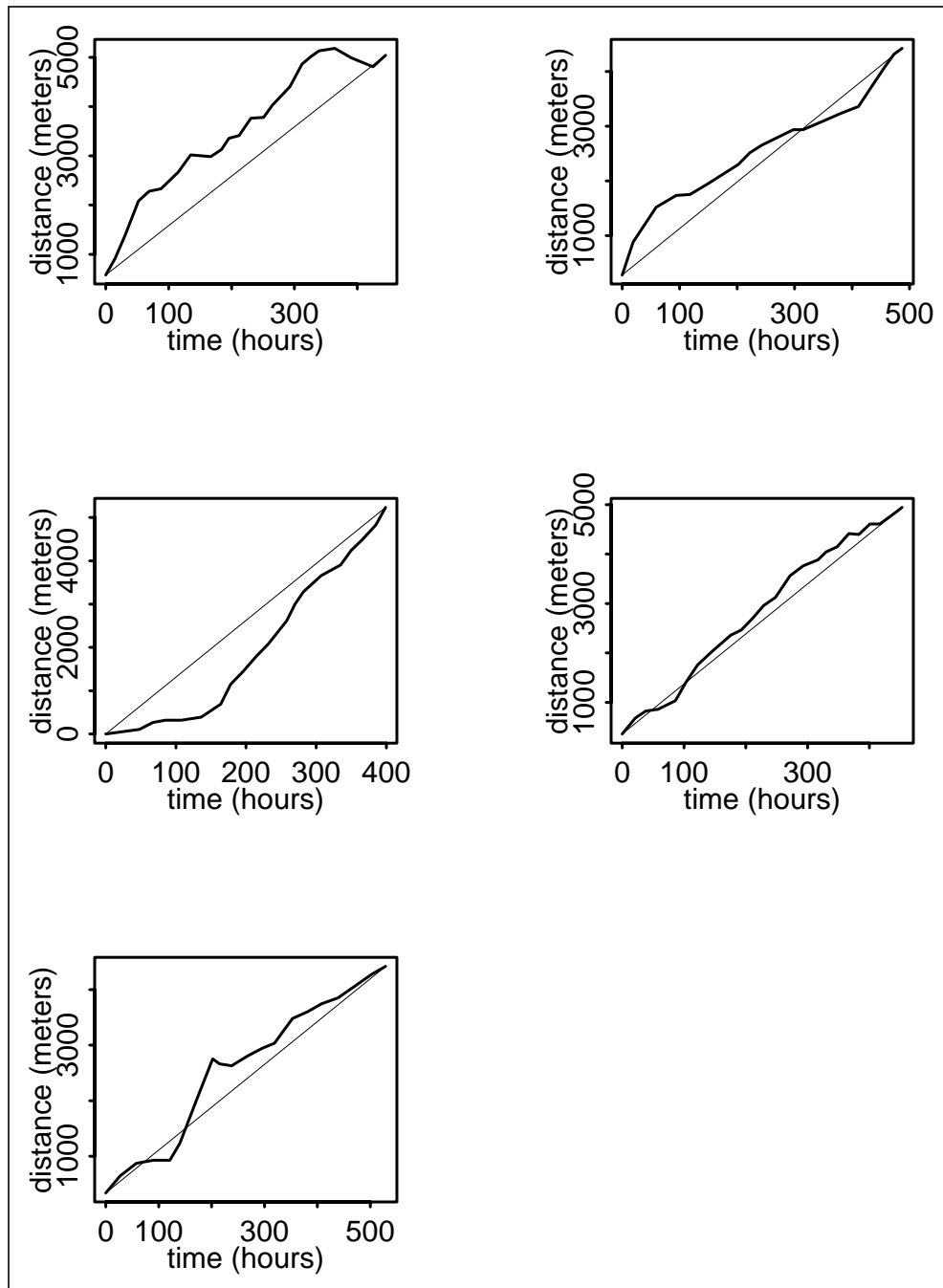


Figure 7.2 Plots of downstream displacement versus time for the radio tagged, individual chinook and steelhead. The slope of the straight line represents the average downstream displacement rate.

Table 7.1 Results from the radio tracking data analysis. The test on the correlation coefficient is only conducted for the individuals where normality is not rejected based on Liliefors's test. For Liliefors's test, normality is rejected for low p -values (typically $p < .05$). Based on the BIC value, the null model (the Wiener drift model) is rejected for positive values. Other details of the analysis are contained in the text.

track information			Wiener process					O-U based model		likelihoods	
Individual	# of fixes	length (min.)	parameters		Liliefors's	correlation		$\hat{\sigma}$	$\hat{\beta}$	ratio	BIC
			\hat{r}	$\hat{\sigma}$	T	$\hat{\rho}$	p				
chinook 627	24	445	9.59	68.07	0.145 ^b	0.40	0.032	19.37	0.080	4.847	1.78
chinook 633	19	487	7.57	35.00	0.208 ^e	0.61		7.64	0.064	7.630	4.80
chinook 876	21	399	13.58	58.91	0.175 ^c	0.60	0.003	15.94	0.058	5.794	2.85
steelhead 170	24	453	9.87	34.55	0.136 ^a	-0.026	0.547	266.74	119.06	0.000	-3.09
steelhead 667	20	529	7.52	57.19	0.281 ^f	0.34		18.20	0.157	0.650	-2.24

Wiener drift model is supported.

With only 5 fish analyzed, it is not possible to determine whether either of the models is “appropriate”. For the chinook, the Wiener drift model appears to be inadequate, with the results of the correlation test and the likelihood ratio comparisons indicating that some type of correlation structure is required to accurately model the data. More analysis is required to determine if the O-U displacement model is consistent with the chinook’s behavior, though. For the steelhead, one of the fish’s behavior is consistent with the Wiener process, as the normality and independence properties are not rejected. Again, more fish will need to be analyzed to make conclusive statements.

It should be emphasized that the results are dependent on time scale. In this case, the average time increment is approximately 20 minutes. At a shorter time scale, correlation may be important for the steelhead, and at a longer time scale, the correlation may cease to be important for the chinook.

discussion

Although I have not encountered any studies that have applied the O-U process to the movements of individuals, it appears to have promise. The conditional distribution of the displacement of an individual given the last time period’s displacement is easily formulated. Also, the theory can accommodate unequal time intervals.

There are two features of the O-U process that are consistent with the behavior of migrating juvenile salmon. The first feature of the O-U process is that if a particle is moving with a certain velocity, there is a tendency to remain at that velocity in the short run. This feature is very appropriate for dispersing organisms. Another feature of the O-U process is that there is a tendency to bring particles back to their mean velocity – the further a particle’s velocity is from the mean velocity, the greater the tendency. This is also a

desirable property. Migrating juvenile salmon appear to undergo a relatively passive migration process (Smith, 1982), expending little energy as they are carried downstream with the current. There are reasons, however, for individuals to move out of this “low energy” state (e.g. predator avoidance, feeding behavior) and actively move in either the upstream or downstream direction. Because of the swimming energetics of juvenile salmon, the fish cannot maintain this energy expenditure for an extended period of time before they must return to the “low energy” state and replenish their oxygen debt (Brett, 1965). This is reminiscent of the O-U process.

While it is improbable that migrating salmon are strict adherents to the O-U process, there does seem to be some value in applying the model. On the time scale of days and kilometers, the Wiener process with drift is a useful model of migrating juveniles and is being used to predict their arrival times at dams (chapter 4). Looking at migratory process on the time scale of hours and meters is a valuable exercise because it can lend validity to the migration model at the longer time scales.

8. Vertical distribution models

8.1. Introduction

Modeling the distribution of organisms in heterogeneous environments is a difficult problem that has received considerable attention (see Levin (1976) and Okubo (1980) for reviews). The difficulty lies in formulating a model, measuring the proper environmental conditions, and determining the organism's response to the environment. In natural populations, the problem is even more difficult because the environment is often patchy and observed distributions of animals are usually the result of a variety of behaviors, some of which are independent of environmental conditions.

Several types of models have been formulated to describe distributions of populations in response to environmental stimuli. Clark and Levy (1988) use dynamic programming to model the vertical distribution of sockeye salmon in Lake Babine, British Columbia. In their model the vertical position of an individual is determined by a trade-off between feeding and predator avoidance. Another approach is to model dispersal as a diffusion process with the diffusion parameter a function of some environmental stimulus (Skellam, 1973; Okubo, 1986). Dobzhansky, et al. (1979) used this approach to model the dispersal of fruit flies in a heterogeneous habitat. The chemotaxis model originally developed by Keller and Segel (1971) has received many applications to cellular systems. In this model, a component of organism movement is based on random dispersal, and a component is based on movements dictated by some environmental gradient. There have been few applications of this model to "higher" organisms, possibly because of the difficulty in modeling the organism's response to the gradient. Kareiva and Odell (1987) present one of the few examples, with the distribution of predators (lady bugs) influenced by a gradient of

prey (aphids) density.

In this chapter, I apply a chemotaxis type model to the vertical distribution of juvenile salmonids entering the forebay of a dam. The distribution of fish entering the forebay has direct consequences on their passage route through the dam. The main downstream passage routes through dams are the spillway, the turbines, and the fish bypass system; each of these routes has a different mortality rate. The vertical position of a fish is particularly important in determining whether it will pass through the bypass system (higher in the water column) or the turbines (lower in the water column); obviously the bypass system is a more favorable route.

The vertical distribution of fish in the water column can be observed with hydroacoustics (Dawson, et al., 1984a, 1984b). Figure 8.1 shows data for both daytime and nighttime distributions of juvenile salmonids entering the forebay of Lower Monumental Dam in April and May, 1985 (Johnson, et al., 1985). Each plot represents composite distributions over a 5 day period. Some observations from these data are: 1) clear differences exist between daytime and nighttime distributions, indicating that environmental cues may be important; 2) there appears to be consistency in the distributions through time, indicating that there are potential trends to be modeled; and 3) the distributions have quite a bit of spread, indicating that a random dispersal element may be important. One drawback of this type of data is that different stocks or species cannot be distinguished. There appear to be two types of fish in the daytime data – one residing lower in the water column and one residing higher in the column that becomes more prevalent later in the season. The two main groups of juvenile salmonids passing Lower Monumental Dam during this time of year are steelhead and spring chinook. A study by Smith (1974) in the forebay of Lower Monumental Dam showed that during the daytime, steelhead tend to be surface oriented, and chinook tend to migrate lower in the water column. In some cases,

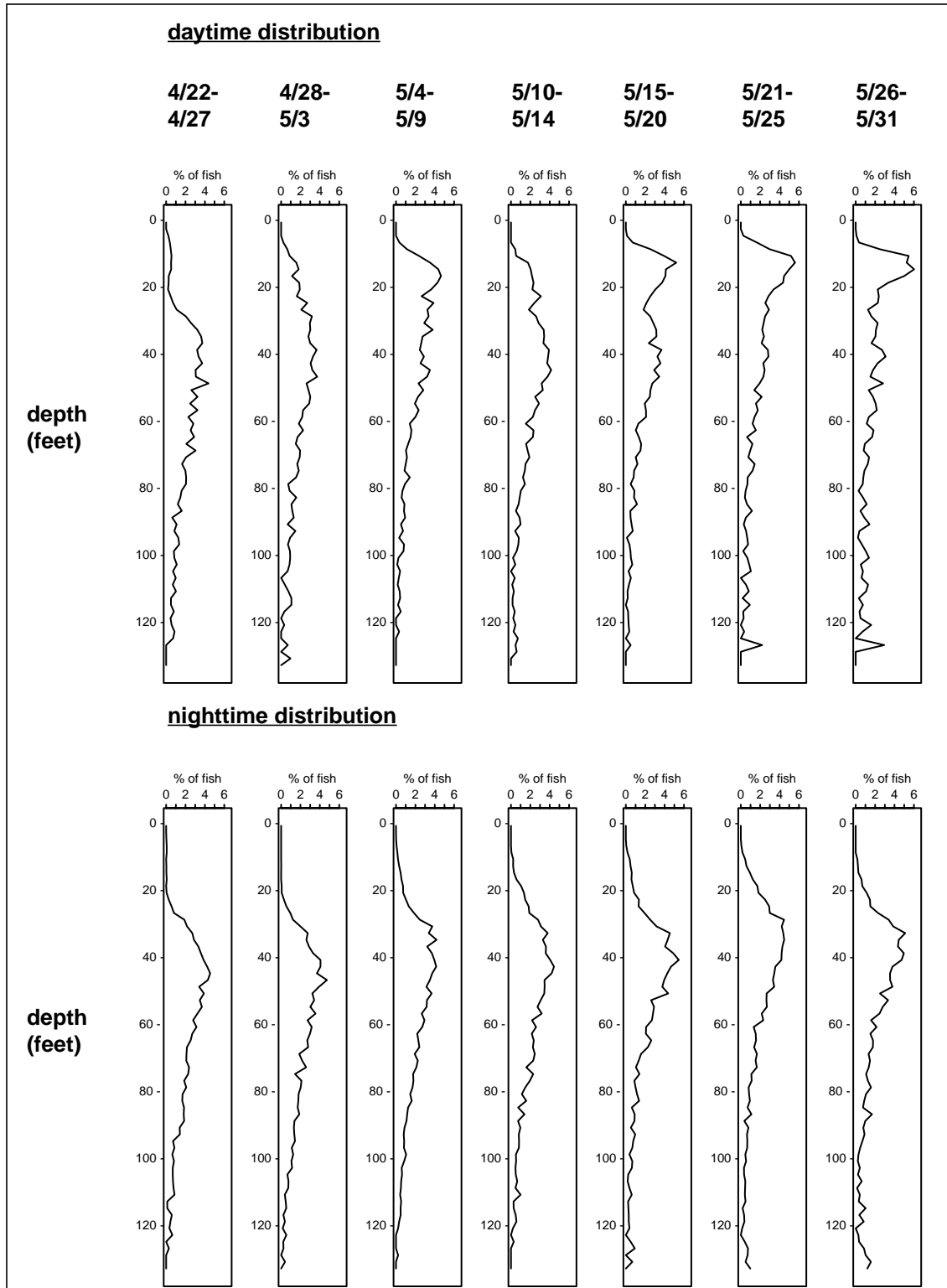


Figure 8.1 Plots of the vertical distribution of juvenile salmonids in the forebay of Lower Monumental Dam. The fish are lumped into two feet intervals. The top plots are for daytime distributions, and the bottom plots are for nighttime distributions.

it will be possible to compare hydroacoustic data to dam passage counts that distinguish among species.

Two gradients that may be affecting the vertical distributions are light and pressure. Both of these gradients are measurable and are somewhat smooth, making the system amenable to modeling.

8.2. The model

The population dynamics of a group of organisms can be expressed as:

$$\frac{\partial}{\partial t}n(\mathbf{x}, t) = -\text{div}J(\mathbf{x}, t) \quad (8.1)$$

where $n(\mathbf{x}, t)$ is the population density and $J(\mathbf{x}, t)$ is the flux. Note that the spatial component, \mathbf{x} , can be multi-dimensional. If we consider simple diffusion along an environmental gradient, the population flux can be expressed as

$$J(\mathbf{x}, t) = -\nabla\lambda n(\mathbf{x}, t) - n(\mathbf{x}, t)\nabla U(\mathbf{x}) \quad (8.2)$$

where $U(\mathbf{x})$ is the environmental potential function (Teramoto and Seno, 1988). In the one dimensional case, equation (8.2) can be written as

$$\frac{\partial n}{\partial t} = \lambda \frac{\partial^2 n}{\partial x^2} + \frac{\partial}{\partial x}n\left(\frac{\partial U}{\partial x}\right). \quad (8.3)$$

The first term on the right side is the diffusion term, with λ determining the magnitude of the diffusion relative to the second term. The second term introduces an advection that is dictated by the gradient of the environmental potential function. Next assume that the fish reach some stationary distribution during the daytime and nighttime periods. To find a steady-state solution, set

$$J(x, t) = 0, \quad (8.4)$$

or equivalently,

$$\lambda \frac{\partial n}{\partial x} + n \frac{\partial U}{\partial x} = 0. \quad (8.5)$$

At the steady-state there is no longer time dependence, so we can rewrite equation (8.5) in terms of ordinary differential equations:

$$\lambda \frac{dn}{dx} + n \frac{dU}{dx} = 0. \quad (8.6)$$

Assuming that $U(x)$ is provided, we can solve for n :

$$n(x) = c \cdot e^{-\frac{1}{\lambda}U(x)} \quad (8.7)$$

where c is a constant of integration.

The problem comes in determining $U(x)$. First assume that there is some measurable environmental stimulus $E(x)$, and that $U(x)$ is a function of this; that is:

$$U(x) = f(E(x)) . \quad (8.8)$$

I also assume that there is a desirable level of the stimulus, E^* , and the advective term of the chemotaxis equation is toward this desirable level:

$$U(x) = f(|E^* - E(x)|) . \quad (8.9)$$

8.3. Example – light gradient

An equation for the decay of light in a water column is

$$I(z) = I_0 e^{-\alpha z}, \quad (8.10)$$

where z is depth, I_0 is the light intensity at the surface, and α is the decay coefficient. This function is plotted in Figure 8.2. Now assume that there is a desirable light level, I^* . The

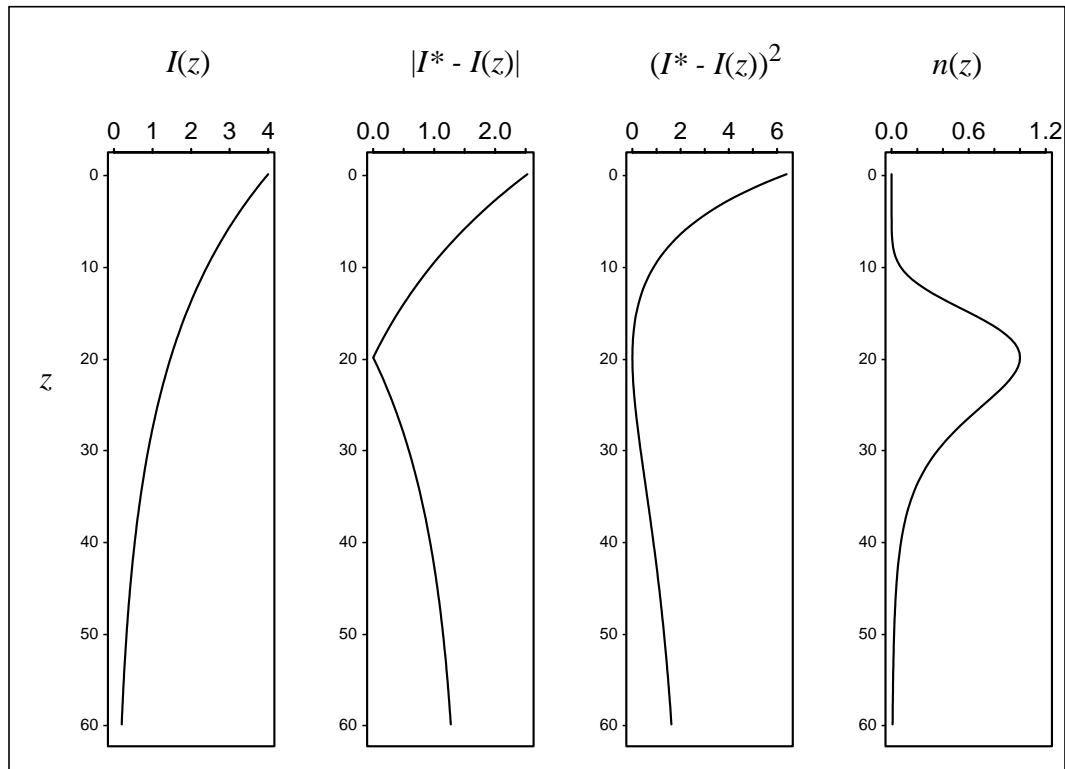


Figure 8.2 Plots of the important components of equations (8.10) - (8.13). For these plots, I used the following values: $I_0 = 4.0$; $\alpha = 0.05$; $I^* = 1.47$; $\lambda = 3.0$; $\chi = 1.0$.

environmental potential function can then be expressed as:

$$U(z) = f(|I^* - I(z)|) . \quad (8.11)$$

As stated above, the difficulty lies in finding the appropriate function f . A plot of $|I^* - I(z)|$ versus z (Figure 8.2) reveals an abrupt change in the slope of the curve at I^* . This carries through to modeled distribution of fish, $n(z)$, and this abrupt change in distribution is not observed in the data. A simple modification that produces a smooth curve is

$$f(|I^* - I(z)|) = \chi \cdot (I^* - I(z))^2 . \quad (8.12)$$

This is plotted in Figure 8.2. In this equation I introduce a constant χ that determines the intensity of the chemotactic response and is often termed the chemotactic coefficient. The steady state distribution of organisms along a light gradient is then

$$n(z) = c \cdot \exp\left(-\frac{\chi}{\lambda}(I^* - I(z))^2\right), \quad (8.13)$$

which is also plotted in Figure 8.2.

The squared term in equation (8.12) might be justified because the light gradient experienced by the fish is not simple. As a fish looks upwards or downwards, it is not experiencing the local gradient but an integration of light levels above or below based on its “line of sight” (Pitcher, 1986); this has the effect of intensifying the gradient. Obviously direct studies would be necessary to justify this term (or some other form), but in the mean time, it produces a tractable model that is consistent with the data.

8.4. Application to data

As an example, I apply the light gradient based vertical distribution model (equation (8.13)) to the daytime distribution of the fish at Lower Monumental Dam (top plots of Figure 8.1). I assume that two distinct types of fish passed the dam, so I introduce a weighting factor, w , to separate the two groups. Also, I assume that each group has distinct values for λ , χ , and I^* . The parameters describing light intensity, α and I_0 , are common to the two groups. Thus, the equation describing the vertical distribution of fish approaching the dam is

$$\begin{aligned} n(z) = & w \cdot c_1 \cdot \exp\left(-\frac{\chi_1}{\lambda_1}(I_1^* - I(z))^2\right) \\ & + (1 - w) \cdot c_2 \cdot \exp\left(-\frac{\chi_2}{\lambda_2}(I_2^* - I(z))^2\right). \end{aligned} \quad (8.14)$$

The data are reported as the number of fish observed in 2 feet intervals (total depth - 133 ft). To accommodate the discrete form of the data, equation (8.14) must be integrated:

$$n_i = N \int_{z_i}^{z_{i+1}} n(z) dz. \quad (8.15)$$

N is the total number of fish observed, and n_i is the number of fish observed in the i th vertical interval. I evaluated this integral numerically using Romberg integration (Press, et al. 1988).

To fit the model to the data, I use the following procedure. First, since the preferred depth, z^* (corresponding to the preferred light intensity, I^*), is the mode of the distribution, I select values of z^* for the two groups based on the two local maxima of fish frequencies from the data. Also, I do not have information about the light intensity, which would have to be measured directly, or decay rate, which depends on factors such as turbidity. Since initial light intensity, I_0 , can be factored out from the inner term of the exponential, and since the two parameters χ and λ occur as a ratio, I define a new parameter, ζ , which is defined as

$$\zeta = I_0^2 \cdot \frac{\chi}{\lambda}. \quad (8.16)$$

This parameter is the ratio of chemotactic movement to diffusive movement scaled by initial light intensity. Thus, I need to estimate 4 parameters: ζ_1 , ζ_2 , α , and w . I estimate these parameters with the maximum likelihood method based on a multinomial distribution (see Chapter 3). The maximum likelihood is determined numerically with the downhill simplex method (Press, et al., 1988).

I first apply the model to the composite data from the seven periods (April 22 - May 31) and estimated the parameters. I then use all these parameter estimates except w and apply the model to the weekly data. To fit these data, I only vary w , the weighting function that

distinguishes between the groups of fish.

results

Table 8.1 contains values of the parameter estimates, and Figure 8.3. contains a plot of

Table 8.1 Parameter estimates for equation (8.14) applied to daytime hydroacoustic data from Lower Monumental Dam for the composite data.

z^*_1	z^*_2	ζ_1	ζ_2	α	w	lik.
13.0	39.0	118.30	18.46	0.022	0.146	3.940

the model versus the data for the composite data. The correspondence between the data and the fitted model is excellent. Table 8.1 shows that the two groups have quite different preferred depths, 14 feet versus 40 feet, with approximately 15 per cent of the fish in the first group. Also, there is a large difference between the estimates of ζ for the two groups. This indicates that relative to each other, the second group undergoes a great deal more random movement, and the first group's position is more dictated by the light intensity.

For the weekly data, the estimates of w and likelihoods are contained in Table 8.2 and plots of the model versus the data are in Figure 8.3. For all but the first week, the model and data are quite consistent. The values of w can be compared to observed passage timing of steelhead and yearling chinook on the Snake River (Fish Passage Center, 1987). Steelhead passage was shifted 10-15 days later than yearling chinook passage, which is consistent with an increasing portion of the higher swimming fish as the season progressed.

These results indicate that vertical distributions are quite constant through the season. Also, hydroacoustic data may be useful in distinguishing among species of salmonids.

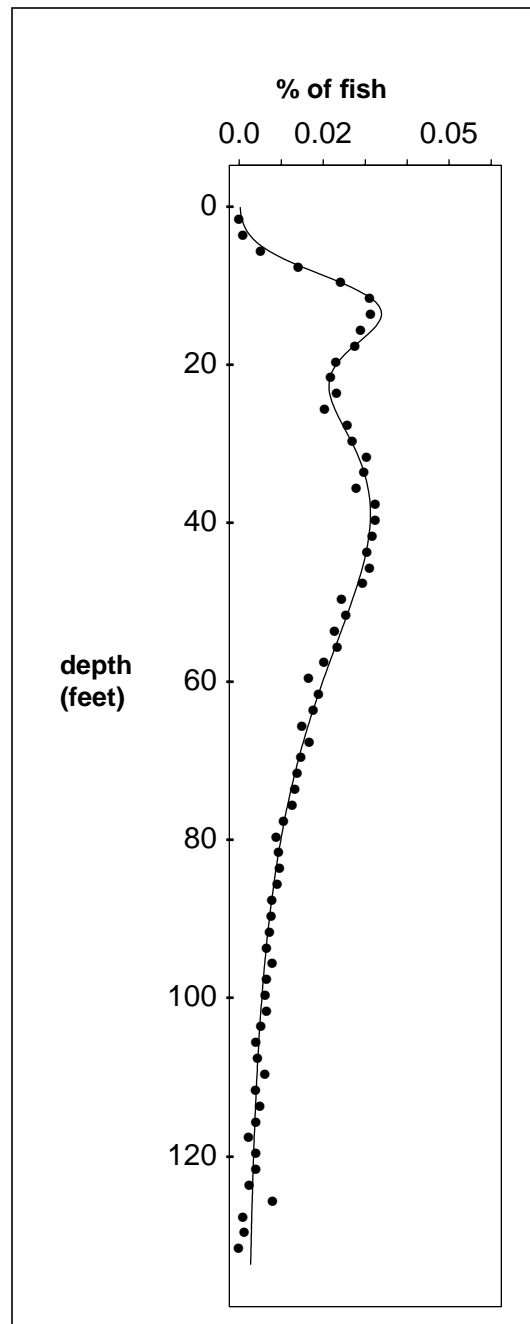


Figure 8.3 The vertical distribution model (equation (8.14)) with the parameters contained in Table 8.1 compared to the composite daytime distribution of juvenile salmonids at Lower Monumental Dam (points).

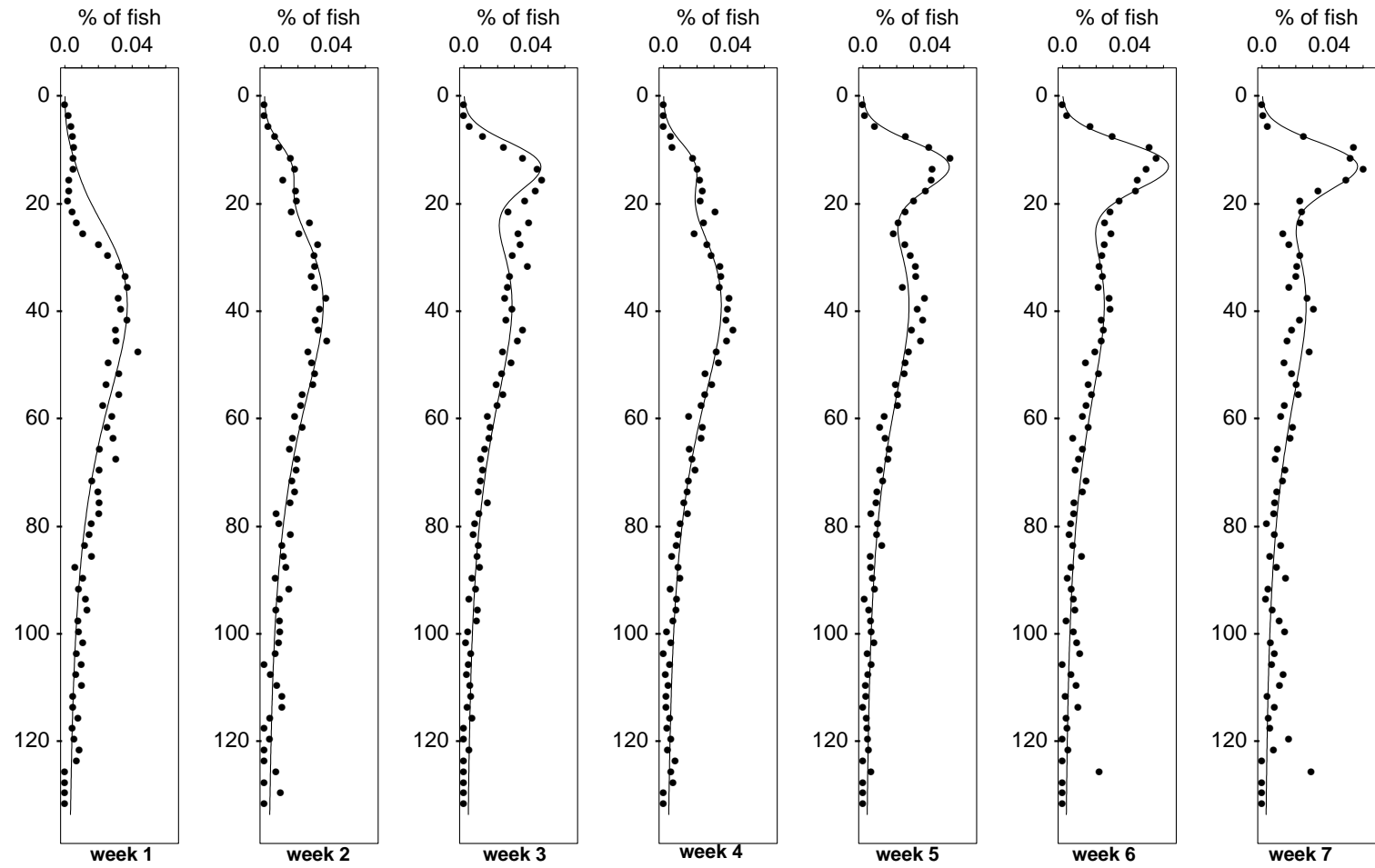
Table 8.2 Estimates of the weekly proportion of the two groups of salmonids at Lower Monumental Dam and likelihoods based on equation (8.14).

week #	w	lik.
1	0.99	3.959
2	0.93	3.961
3	0.76	3.824
4	0.92	3.869
5	0.73	3.822
6	0.66	3.886
7	0.70	3.981

8.5. Discussion

This chapter contains a preliminary presentation of a vertical distribution model and an initial application to data. The model, with a few simple assumptions, is remarkably consistent with data from Lower Monumental Dam. In order to apply the model, more studies are required. Ideally, the reaction of juvenile salmonids to a light gradient will be better understood to strengthen the model. Also, it would be beneficial to conduct controlled experiments where the physical features are characterized leaving just the behavioral parameter to be estimated.

Figure 8.4 The vertical distribution model (equation (8.14)) with the parameters contained in Table 8.1 (but with the parameter w obtained from Table 8.2) compared to the daytime distribution of juvenile salmonids at Lower Monumental Dam (points) on a weekly basis.



9. Summary

9.1. Overview

This thesis contains models that describe spatial and temporal distributions of migrating juvenile salmonids and applications of the models to data. In developing and applying these models, I had several objectives. The first objective was to present models that may be of practical use as management tools. Understanding population dynamics and determining which behavioral factors are important in shaping these dynamics is crucial in the efforts to restore salmonid populations in the Columbia River system. The second objective was to develop statistical methods to compare the models to data. These methods are required to estimate parameters, assess whether the models are consistent with observations, and to determine which features should be included or excluded. The third objective was to provide examples of the data analysis methods to illustrate the type of information that can be obtained. Also, this will initiate the assessment process for these models and provide parameter estimates for future applications.

9.2. Summary by chapter

The first chapter introduces some of the problems afflicting salmonid populations in the Columbia River system and discusses how modeling efforts can contribute to alleviating some of the problems. It also presents an overview of salmonid life history and a brief review of juvenile salmonid behavior.

Chapter 2 discusses models of dispersing animals. Models based on an advection-diffusion equation are applicable to migrating populations. The advection term determines the directed movement of the population, and the diffusion term describes the spreading of the population. The diffusion term can be modified to reflect features such as spatial

heterogeneity and density dependence. Waiting time models, which determine the time until an event, also capture certain features of dispersing populations such as survival and migrational delay.

The third chapter contains the statistical methods used in comparing models to data. The primary parameter estimation method I use is maximum likelihood, which can be employed analytically or numerically. Goodness-of-fit methods differ depending on whether the data are continuous or discrete and whether parameters are being estimated. I use goodness-of-fit tests based on the chi-square distribution and on the empirical density function. It is often useful to discriminate among alternative models of varying complexity. I present several methods to do this, all based on comparing likelihoods.

The fourth chapter develops a two parameter model of the travel time of fish through a reservoir based on an advection-diffusion equation. One parameter determines the downstream migration rate and one determines the rate of population spread. The model accommodates discrete or continuous time data, and I apply it to several data sets of both types. The model successfully describes travel time distributions of run-of-the-river spring chinook, but describing steelhead and fall chinook is more problematic.

The fifth chapter expands the travel time model to incorporate more complex behavior. Travel time dependent mortality is modelled with a constant hazard rate. This type of mortality does not have much effect on the shape of the travel time distribution, and the data analysis bears this out. Next, a delay term based on a Poisson process is incorporated into the travel time model. Migrational delay can occur as fish hold up before passing a dam or before migration is initiated. Several radio-tracking studies confirm that dam delay occurs for chinook, but this delay is not detectable for Snake River run-of-the-river spring chinook travel time data. The delay term improves the model for Snake River steelhead (based on likelihood ratios), but the results are inconsistent and probably not biologically relevant.

For mid-Columbia fall chinook, a delay term, interpreted as a delay before the initiation of migration, substantially improves the travel time model. Finally, I present a hierarchical sequence of models to describe the variation in migration rates for similar groups of fish migrating in a river reach. These regression models are based on date of release and average river flow. A four parameter model, with linear flow relationship and a nonlinear time relationship, worked best with several groups of run-of-the-river spring chinook. The results from the regressions were used to predict travel times for an independent data set.

In chapter 6, I allow for population heterogeneity, with migration rates of individuals related to the factors fish length, date of release, river flow, and river temperature. For the run-of-the-river spring chinook and steelhead, fish length is not an important factor, but it is important for mid-Columbia fall chinook. When several factors are applied sequentially for Snake River fall chinook and mid-Columbia sockeye, date of release, fish length, and average river flow are all important in determining migration rate, while river temperature is not.

In chapter 7, downstream migration is considered in terms of individual movements. I examine two models, one based on the Wiener process that has independent increments and one based on the Ornstein-Uhlenbeck process that incorporates correlation among movements. The models are compared to radio-tracking data, and correlation is determined to be important at the observed time scale (approximately 20 minutes) for the chinook but not for the steelhead.

The vertical distribution of fish in a water column is described in terms of a chemotaxis-type model in chapter 8. In this model, an individual's position is determined by random movement and reaction to an environmental gradient. I apply the model with a light intensity gradient to hydroacoustic data from the forebay of Lower Monumental Dam on the Snake River. The correspondence between the model and data is excellent.

9.3. Recommendations for salmon population management

The objective of this thesis is to present models of salmon populations that can be used for management purposes. To this effect, some of the models have been incorporated into the Columbia River Salmon Passage¹ model (Anderson, et al., 1993), a system model that describes the downstream migration of juvenile salmonids. In this section, I discuss my results in this context and make some recommendations.

The two parameter travel time model (equations (4.7) and (4.8)) is particularly effective for describing arrival distributions of run-of-the-river, yearling chinook, for which abundant data exists. The model accommodates both discrete and continuous data and is easily applied. In continuous form, $g(t)$, the probability density function for the arrival times of fish at the downstream collection site, is expressed as

$$g(t) = \frac{L}{\sqrt{2\pi\sigma^2 t^3}} \exp\left(\frac{-(L - rt)^2}{2\sigma^2 t}\right), \quad (9.1)$$

where L is the length of the river reach. The parameters are intuitive and biologically meaningful: r is the downstream migration rate, and σ describes the rate of spreading of the population. The model, in its simplest form, does not work as well for steelhead and fall chinook. Although the model captures the important features of steelhead arrival time distributions, more modeling efforts are needed to understand the departure of observed steelhead travel time distributions from model-predicted distributions.

The travel time model is improved for fall chinook by incorporating a delay term, which corresponds to a delay in the initiation of migration. In its simplest form, this is modeled as

1. The Columbia River Salmon Passage model is being developed at the University of Washington at the Center for Quantitative Studies in Fisheries, Forestry, and Wildlife and the Fisheries Research Institute. Information about the model can be obtained from Dr. James J. Anderson, Fisheries Research Institute.

an exponential waiting time process. More complexity can be added by relating the instantaneous departure rate, α , to time (for example, the fish are more likely to initiate migration as the season progresses) and covariates, \mathbf{X} , particularly fish length. The delay model is then expressed as

$$d(t) = \alpha(t, \mathbf{X}) e^{-\int_0^t \alpha(\tau, \mathbf{X}) d\tau} . \quad (9.2)$$

This equation is easy to evaluate if the form of $\alpha(t, \mathbf{X})$ is not complex.

The delay in front of a dam before fish passage is an important component of downstream migration. I developed three alternative models to describe this delay process and applied the models to radio tag data, where exact times of arrival to the forebay and dam passage are observed. These data show that dam delay can be substantial; one group of chinook delayed for an average of 20 hours at Lower Granite Dam. The model that works best to describe these data splits the fish in two groups: those that pass quickly with rate α_f , and those that pass slowly with rate α_s . This model works substantially better than one with daytime and nighttime passage rates. Unfortunately, dam delay is difficult to detect with travel time data and is difficult to observe directly. More work is necessary to determine the extent of dam delay and how it varies from dam to dam.

Utilizing the travel time model in a predictive manner involves selecting model parameters *a priori*. I related the observed variation in parameter estimates to the factors date of release and average river flow in regression equations. I tested several alternative equations and determined that the following set worked the best to predict values of r and σ :

$$\tilde{r}_i = \beta_0 + \beta_2 F_i \left[\frac{1}{1 + \exp(-\alpha(t - T_0))} \right] \quad (9.3)$$

and

$$\tilde{\sigma}_i = \beta_0 + \beta_1 \tilde{r}_i. \quad (9.4)$$

In the first equation, migration rate is linearly related to flow, F_i , and the term in the brackets represents a nonlinear relationship with date of release, where migration rate begins at a lower rate early in the season and increases to an upper level as the season progresses. The second regression equation linearly relates σ , the rate of population spread, to migration rate. These two regression equations were applied to four groups of run-of-the-river chinook (composed primarily of yearling chinook of both wild and hatchery origins). The regression equation for r had R^2 values ranging from .855 to .945, and the regression equation for σ had R^2 values ranging .589 to .845. These regression equations can be used to determine model parameters based on date of release and river flow. The travel time model can then be implemented to predict the downstream arrival distributions.

When information on the variability of individuals within a cohort was included in the travel time model, fish length was determined to be an important factor for mid-Columbia subyearling chinook but not for Snake River yearling chinook and steelhead. Also, for sequential releases of Snake River subyearling chinook and Columbia River sockeye, I determined that fish length, date of release, and average river flow are important factors at the level of the individual, but river temperature is not. River temperature may be important, though, in determining the timing of runs on a year to year basis. The importance of fish length in the fall chinook may be partly due to its relation to the onset of migration, and incorporating fish length into the delay term can account for this.

The vertical distribution model can benefit future modeling applications. The position of fish in the water column as they approach the dam is related to their passage route through the dam – spillway, fish bypass system, or turbines. Since each pathway has a different associated mortality, utilizing a vertical distribution model to predict passage routes will be useful in ascribing total passage mortality. The modeling demonstrated that

observed vertical distributions are predictable and that different species have different distributions. Future experimental work in this area will help to identify underlying mechanisms of the vertical distribution process.

Overall conclusions are as follows. First, simple models based on diffusion equations are quite tractable mathematically and capture many of the features of the distributions of migrating juvenile salmonids. Statistical techniques, primarily based on likelihood functions, are readily applied to these models to estimate parameters, assess model goodness-of-fit, and to compare among alternative models. This combination of modeling and statistics is a powerful method in establishing models as predictive tools for management purposes.

References

- Abramowitz, M., and I. A. Stegun. 1965. Handbook of Mathematical Functions. Dover, New York.
- Alt, W. 1985. Models for mutual attraction and aggregation of motile individuals. Lecture Notes in Biomathematics 57: 33-38.
- Akaike, H. 1973. Information theory and an extensions of the maximum likelihood principle. Proceedings of the Second International Symposium on Information Theory.
- Anderson, J.J., D. Askren, T. Frever, J. Hayes, A. Lockhart, M. McCann, P. Pulliam, R. Zabel. 1993. Columbia River Salmon Passage Model User's Manual. Center for Quantitative Studies in Fisheries, Forestry, and Wildlife, University of Washington, Seattle.
- Anderson, J.J., and N. Schumaker. 1988. A model to predict smolt migration rate. Proceedings of the 1988 Workshop on Chinook and Coho. Bellingham, Washington.
- Aronson, D.G. 1985. The role of diffusion in population biology: Skellam revisited. Lecture Notes in Biomathematics 57: 2-6.
- Bax, N. J. 1982. Seasonal and annual variations in the movement of juvenile chum salmon through Hood Canal, Washington. Salmon and Trout Migratory Behavior Symposium (E.L. Brannon, and E.O. Salo, eds.). Contribution 793, School of Fisheries, University of Washington, Seattle.
- Becker, R. A., J. M. Chambers, and A. R. Wilks. 1988. The New S Language. Wadsworth and Brooks/Cole Advanced Books and Software. Pacific Grove, California.
- Bell, R. 1958. Time, size, and estimated numbers of seaward migrants of chinook salmon and steelhead trout in the Brownlee-Oxbow section of the middle Snake River. State of Idaho Department of Fish and Game, Boise, Idaho. 36 pp.
- Berggren, T.J., and M.J. Filardo. 1993. An analysis of variables influencing the migration of juvenile salmonids in the Columbia River basin. N. Amer. J. Fish. Manag. 13: 48-63.

- Bickel, P.J., and K.A. Doksum. 1977. *Mathematical Statistics*. Holden-Day, Inc. Oakland, California.
- Brawn, V.M. 1982. Behavior of Atlantic Salmon (*Salmo salar*) during Suspended Migration in an Estuary, Sheet Harbour, Nova Scotia, Observed Visually and by Ultrasonic Tracking. *Can. J. Fish. Aquat. Sci.* 39: 248-256.
- Brett, J.R. 1965. The swimming energetics of salmon. *Sci. Am.* 213: 80-85.
- Brett, J.R., M. Hollands, and D.F. Alderdice. 1958. The effect of temperature on the cruising speed of young sockeye and coho salmon. *Journal of the Fisheries Research Board of Canada* 15: 587-605.
- Brownlee, J. 1911. The mathematical theory of random migration and epidemic distribution. *Proce. Roy. Soc. Edinburgh* 31: 262-289.
- Burgner, R. L. 1991. Life history of sockeye salmon. In: *Pacific Salmon Life Histories* (C. Groot and L. Margolis, editors). University of British Columbia Press, Vancouver, British Columbia.
- Carl, L. M., and M. C. Healey. 1984. Differences in enzyme frequency and body morphology among three life history types of chinook salmon (*Oncorhynchus tshawytscha*) in the Nanaimo River, British Columbia. *Can. J. Fish. Aquat. Sci.* 41: 1070-1077.
- Chapman, D. W. 1986. Salmon and steelhead abundance in the Columbia River in the nineteenth century. *Trans. Amer. Fish. Soc.* 115: 662-670.
- Clark, C.W., and D.A. Levy. 1988. Diel vertical migrations by juvenile sockeye salmon. *Amer. Nat.* 131: 271-290.
- Chhikara, R.S., and J.L. Folks. 1989. *The Inverse Gaussian Distribution*. Marcel-Dekker, Inc., New York.
- Childerhose, R. J. and M. Trim. 1979. *Pacific Salmon and Steelhead Trout*. Douglas and McIntyre, Ltd., Vancouver, British Columbia.
- Cochran, W.G. 1952. The χ^2 test of goodness of fit. *Annals of Mathematical Statistics* 23: 315-345.
- Cohen, A. and H. B. Sackrowitz. 1975. Unbiasedness of the chi-square, likelihood ratio, and other goodness of fit tests for the equal cell case. *American Statist.* 4 :959-964.

- Conover, W.J. 1980. Practical Nonparametric Statistics, 2nd edition. John Wiley and Sons, New York.
- Cox, D.R., and H.D. Miller. 1965. The Theory of Stochastic Processes. Chapman and Hall, New York.
- D'agostino, R.B., and M. A. Stephens (eds.). 1986. Goodness-Of-Fit Techniques. Marcel Dekker, Inc. New York.
- Daniels, H. E. 1982. Sequential tests constructed from images. The Annals of Statistics 10: 394-400.
- Darling, D. A., and A. J. F. Siegert. 1953. The first passage problem for a continuous Markov process. Ann. Math. Statist. 24: 624-639.
- Dauble, D.D., T.L. Page, and R. W. Hanf, Jr. 1989. Spatial distribution of juvenile salmon in the Hanford Reach, Columbia River. Fishery Bulletin 87: 775-790.
- Dawson, J., L. Johnson, W.A. Karp, and G.A. Raemhild. 1984a. Fixed-location hydroacoustics for quantitative fisheries. Biosonics, Inc., Seattle.
- Dawson, J. A. Murphy, P. Neelson, P. Tappa, and C. VanZee. 1984b. Hydroacoustic assessment of downstream migrating salmon and steelhead at Wanapum and Priest Rapids Dams in 1983. Biosonics, Inc., Seattle WA.
- DeAngelis, D.L., and G.T. Yeh. 1984. An introduction to modeling migratory behavior in fishes. In: Mechanisms of Migration in Fishes, ed. by J.D. McCleave, G.P. Arnold, J.J. Dodson, and W.H. Neill, pp. 445-469. New York: Plenum Press.
- Dennis, B., P.L. Munholland, and J.M. Scott. 1991. Estimation of growth and extinction parameters for endangered species. Ecological Monographs 61: 115-143.
- Dobzhansky, Th., J.R. Powell, C.E. Taylor, and M. Andregg. 1979. Ecological variables affecting the dispersal behavior of *Drosophila pseudoobscura* and its relatives. *Am. Nat.* 114: 325-334.
- Dobzhansky, T., and S. Wright. 1943. Genetics of natural populations X. Dispersion rates in *Drosophila pseudoobscura*. *Genetics* 28: 304-340.
- Doob, J.L. 1942. The Brownian movement and stochastic equations. *Annals of Mathematics* 43: 351-369.
- Draper, N. R., and H. Smith. 1981. Applied Regression Analysis. John Wiley and Sons,

New York.

- Efron, B. 1982. The Jackknife, the Bootstrap and Other Resampling Plans. CBMS-NSF Regional Conference Series in Applied Mathematics 38. Society for Industrial and Applied Mathematics, Philadelphia.
- Efron, B., and R. Tibshirani. 1986. Bootstrap methods for standard errors, confidence intervals, and other measures of statistical accuracy. *Statistical Science* 1: 54-77.
- Fish Passage Center. 1987. Migrational Characteristics of Columbia Basin Salmon and Steelhead Trout; Smolt Monitoring Program Annual Report 1986, Volume I. Report to the Bonneville Power Administration, Portland, Oregon. Project number 86-60.
- Fish Passage Center. 1991. Annual Report. Report to the Bonneville Power Administration, Portland, Oregon. Project number 87-127.
- Fisher, R. A. 1924. The conditions under which χ^2 measures the discrepancy between observations and hypothesis. *J. Royal Statist. Soc.* 87: 442-450.
- Flagg, T.A., and L.S. Smith. 1982. Changes in swimming behavior and stamina during the smolting of Coho salmon. Salmon and Trout Migratory Behavior Symposium (E.L. Brannon, and E.O. Salo, eds.). Contribution 793, School of Fisheries, University of Washington, Seattle.
- Folks, J.L., and R.S. Chhikara. 1978. The inverse Gaussian distribution and its statistical applications -- a review. *J. Royal Statistical Society B.* 40: 263-289.
- Folmar, C.F., and W.W. Dickhoff. 1980. The parr-smolt transformation (smoltification) and seawater adaptation in salmonids. *Aquaculture* 21: 1-37.
- Fried, S. M., J. D. McCleave, and G. W. Le Bar. 1978. Seaward migration of hatchery reared Atlantic salmon, *Salmo salar*, smolts in the Penobscot River estuary, Maine: riverine movements. *J. Fish. Res. Bd. Can.* 35: 76-87.
- Gardiner, C.W. 1983. Handbook of Stochastic Processes for Physics, Chemistry and the Natural Sciences. Springer-Verlag, Berlin.
- Giorgi, A.E., Stuehrenberg, L.C., Miller, D.R., and Sims, C.W. 1985. Smolt Passage Behavior and Flow-Net Relationship in the Forebay of John Day Dam. Bonneville Power Administration, Contract No. DE-A179-84BP39644.
- Giorgi, A. E., G. E. Swan, W. D. Zaugg and S. McCutcheon 1990. Biological manipulation

of migration rate: the use of advanced photoperiod to accelerate smoltification in yearling chinook salmon. Annual Report of Research Financed by Bonneville Power Administration (Agreement DE-A179-88-BP50301) and Coastal Zone and Estuarine Studies Division. Northwest Alaska Fisheries Center, National Marine Fisheries Center, National Oceanic and Atmospheric Administration.

- Glova, G. J., and J. E. McInerney. 1977. Critical swimming speeds of coho salmon (*Oncorhynchus kisutch*) fry to smolt stages in relation to salinity and temperature. J. Fish. Res. Bd. Can. 34: 151-154.
- Godin, J. G., P. A. Dill, and D. E. Drury. 1974. Effects of thyroid hormones on behavior of yearling Atlantic salmon (*Salmo salar*). J. Fish. Res. Bd. Can. 31: 1787-1790.
- Goel, N.S., and Richter-Dyn, N. 1974. Stochastic Models in Biology. Academic Press, New York.
- Goldstein, S. 1951. On diffusion by discontinuous movements, and on the telegraph equation. Quart. J. Mech. and Appl. Math. 4: 129-156.
- Groot, C. 1965. On the orientation of young sockeye salmon (*Oncorhynchus nerka*) during their seaward migration out of lakes. Behav. suppl. 14: 1-198.
- Groot, C. 1982. Modifications on a theme - a perspective on migratory behavior of Pacific salmon. Salmon and Trout Migratory Behavior Symposium (E.L. Brannon, and E.O. Salo, eds.). Contribution 793, School of Fisheries, University of Washington, Seattle.
- Groot, C. and L. Margolis. 1991. Pacific Salmon Life Histories. University of British Columbia Press, Vancouver, British Columbia.
- Gurney, W.S.C., and R.M. Nisbet. 1975. The regulation of inhomogeneous populations. J. Theor. Biol. 52: 441-457.
- Gurtin, M.E., and R.C. MacCamy. 1977. On the diffusion of biological populations. Math. Biosciences 33: 35-49.
- Haberman, R. 1987. Elementary Applied Differential Equations. Prentice-Hall, Inc., Englewood Cliffs, New Jersey.
- Hansen, L.P., and B. Jonnson. 1985. Downstream migration of hatchery-reared smolts of the Atlantic salmon (*Salmo salar* L.) in the River Imsa, Norway. Aquaculture 45: 237-248.

- Healy, M. C. 1991. Life history of chinook salmon. In: Pacific Salmon Life Histories (C. Groot and L. Margolis, editors). University of British Columbia Press, Vancouver, British Columbia.
- Hiramatsu, K.; Ishida, Y. 1989. Random movement and orientation in pink salmon (*Oncorhynchus gorbuscha*) migrations. *Can. J. Fish. Aquat. Sci.* 46:1062-1066.
- Hoar, W.S. 1953. Control and timing of fish migration. *Biol. Rev.* 28: 437-452.
- Hoar, William S. 1956. The behavior of migrating pink and chum salmon fry. *J. Fish. Res. Bd. Canada* 13(3):309-325.
- Hoar, W. S. 1965. The endocrine system as a chemical link between the organism and its environment. *Trans. Roy. Soc. Canada* 3 (ser. 4): 175-200.
- Hoar, W.S. 1976. Smolt transformation: evolution, behavior, and physiology. *J. Fish. Res. Board Can.* 33: 1234-1252.
- Hogg, R.V, and E.A. Tanis. 1983. *Probability and Statistical Inference*, 2nd edition. Macmillan Publishing Co., Inc. New York.
- Holm, M., I. Huse, E. Waatevik, K. B. Doving and J. Aure. 1982. Behavior of Atlantic salmon smolts during seaward migration. I: Preliminary report on ultrasonic tracking in a Norwegian fjord system.
- Holms, E. E. 1993. Are diffusion models too simple? A comparison with telegraph models of invasion. *American Naturalist* 142: 779-795.
- Holtby, L. B., T. E. McMahaon, and J. C. Scrivener. 1989. Stream temperature and inter-annual variability in the emigration timing of coho salmon (*Oncorhynchus kisutch*) smolts and fry and chum salmon (*O. keta*) fry from Carnation Creek, British Columbia. *Can. J. Fish. Aquat. Sci.* 46: 1396-1405.
- Johnson, W. E., and C. Groot. 1963. Observations on the migration of young sockeye salmon (*Oncorhynchus nerka*) through a large, complex lake system. *J. Fish. Res. Bd. Can.* 20: 919-937.
- Johnson, L., A. Murphy, and C. Rawlinson. 1985. Hydroacoustic Assessment of Downstream Migrating Salmonids at Lower Monumental Dam in Spring 1985. Prepared for the Bonneville Power Administration, contract number DE-A C79-85 BP23174.

- Jones, R.E. 1977. Movement patterns and egg distribution in cabbage butterflies. *J. Anim. Ecol.* 46: 195-212.
- Kalbfleisch, J. D., and R. L. Prentiss. 1980. *The Statistical Analysis of Failure Time Data*. John Wiley and Sons. New York.
- Kareiva, P.M. 1983. Local movement in herbivorous insects; applying a passive diffusion model to mark-recapture field experiments. *Oecologia* 57:322-327.
- Kareiva, P., and G. Odell. 1987. Swarms of predators exhibit "preytaxis" if individual predators use area-restricted search. *Am. Nat.* 130: 233-270.
- Kareiva, P., and N. Shigesada. 1983. Analyzing insect movement as a correlated random walk. *Oecologia* 56: 234-238.
- Keller, E.F., and L.A. Segel. 1971. Model for chemotaxis. *J. Theor. Biol.* 30: 225-234.
- Kemp, W.P., B. Dennis, and P. L. Munholland. 1989. In: *Estimation and analysis of insect populations* (L. McDonald, B. Manly, J. Lockwood, and J. Logan, editors). *Lecture Notes in Statistics* 55: 118-127.
- Kernighan, B. W., and D. M. Ritchie. 1978. *The C Programming Language*. Prentice-Hall, Inc. Englewood Cliffs, New Jersey.
- Kitching, R.L., and M.P. Zalucki. 1982. Component analysis and modelling of the movement process: analysis of simple tracks. *Res. Popul. Ecol.* 24: 224-238.
- Kolmogorov, A. N. 1933. Sulla determinazione empirica di una legge di distribuziane. *Giorna. Ist. Attuari.* 4: 83-91.
- LaBar, G.W., J.D. McCleave and S.M. Fried. 1978. Seaward migration of hatchery-reared Atlantic salmon (*Salmo salar*) smolts in the Penobscot River estuary, Maine: open-water movements.
- Lanska, V. 1988. Statistical inference for stochastic neuronal models. In: *Biomathematics and Related Computational Problems*, ed. L.M. Ricciardi. Dordrecht: Kluwer Academic Publishers.
- Levin, S.A. 1976. Population dynamic models in heterogenous environments. *Ann. Rev. Ecol. Syst.* 7: 287-310.
- Light, J. T. 1987. Coastwide abundance of North American steelhead trout. (Document submitted to annual meeting of the International North Pacific Fisheries

- Commission.) FRI-UW-8710. Fisheries Research Institute, University of Washington, Seattle.
- Light, J. T., C. K. Harris and R. L. Burgner. 1989. Ocean distribution and migration of steelhead (*Oncorhynchus mykiss*, formerl *Salmo gairdneri*). (Document submitted to the International North Pacific Fisheries Commission.) FRI-UW-8912. Fisheries Research Institute, University of Washington, Seattle.
- McCleave, J.D., and Stred, K.A. 1975. Effect of dummy telemetry transmitters on stamina of Atlantic salmon (*Salmo salar*) smolts. J. Fish. Res. Bd. Canada 32:559-563.
- Mains, E.M., and J.M. Smith. 1964. The distribution, size, time, and current preferences of seaward migrant chinook salmon in the Columbia and Snake Rivers. Fisheries Research Papers, Washington Department of Fisheries, 2(3): 5-43.
- Mann, H. B., and A. Wald. 1942. On the choice of the number of class intervals in the application of the chi-square test. Ann. Math. Stat. 13:306-317.
- Meehan, W. R., and D. B. Siniff. 1962. A study of the downstream migrations of anadromous fishes in the Taku River, Alaska. Trans. Amer. Fish. Soc. 91: 399-407.
- Michael, J. R., W.R. Schucany, and R.W. Haas. 1976. Generating random variates using transformations with multiple roots. The American Statistician 30: 88-90.
- Mighell, James L. 1969. Rapid cold-branding of salmon and trout with liquid nitrogen. J. Fish. Res. Bd. Canada. 26: 2763-2769.
- Mood, A.M., F.A. Graybill, and D.C. Boes. 1974. Introduction to the Theory of Statistics, 3rd edition. McGraw-Hill, New York.
- Moore, D. S. 1986. Tests of the chi-squared type. In: Goodness-Of-Fit Techniques (R. B. D'agostino and M. A. Stephens, editors). Marcel Dekker, Inc. New York.
- Murray, J.D. 1989. Mathematical Biology. Springer-Verlag, New York.
- Neave, F. 1955. Notes on the seaward migration of pink and chum salmon fry. Journal of the Fisheries Research Board of Canada 12: 369-374.
- Nelder, J. A. and R. Mead. 1965. A simplex method for function minimization. Computer Journal 7: 308-313.
- Netboy, A. 1980. The Columbia River Salmon and Steelhead Trout – Their Fight for Survival. University of Washington Press, Seattle, WA.

- Neter, J., Wasserman, W., and M. H. Kutner. 1985. *Applied Linear Statistical Models*, second edition. Irwin. Homewood, Illinois.
- Northcote, T.G. 1984. Mechanisms of fish migration in rivers. In: *Mechanisms of Migrations in Fishes* (McCleave, J.D., G.P. Arnold, J.J. Dodson, W.H. Neill, editors). Plenum Press, New York.
- NPPC (Northwest Power Planning Council). 1992. *Strategy for Salmon*. Northwest Power Planning Council, Portland, Oregon.
- Okubo, A. 1980. *Diffusion and Ecological Problems: Mathematical Models*. Springer-Verlag, New York.
- Okubo, A. 1986. Dynamical aspects of animal grouping: swarms, schools, flocks, and herds. *Adv. Biophys.* 22: 1-94.
- Osterdahl, L. 1969. The smolt run of a small Swedish river. In *Salmon and Trout in Streams* (T. G. Northcote, ed.) pp. 205-215. H. R. MacMillan lectures in fisheries. University of British Columbia.
- Othmer, H.G., S.R. Dunbar, and W. Alt. 1988. Models of dispersal in biological systems. *J. Math. Biology* 26: 263-298.
- Park, D. L. 1969. Seasonal changes in downstream migration of age-group 0 chinook salmon in the upper Columbia River. *Trans. Amer. Fish. Soc.* 98: 315-317.
- Patlak, C.S. 1953a. Random walk with persistence and bias. *Bull. Math. Biophys.* 15: 311-338.
- Patlak, C.S. 1953b. A mathematical contribution to the study of the orientation of organisms. *Bull. Math. Biophys.* 15: 431-476.
- Pearson, K. 1900. On the criterion that a given system of deviations from the probable in the case of a correlated system of variables is such that it can reasonably supposed to have arisen from random sampling. *Phil. Mag., Series 5*, 50: 157.
- Pearson, K., and J. Blakeman. 1908. A mathematical theory of random migration. *Mathematical contributions to the theory of evolution XV*, Drapers Company Research Memoirs: Biometric Series. Cambridge University Press, London.
- Pevin, C. M. 1990. *The Life History of Naturally Produced Steelhead Trout in the Columbia Basin*. M.S. Thesis, University of Washington, Seattle.

- Pitcher, T. J. 1986. *The Behavior of Teleost Fishes*. Johns Hopkins University Press, Baltimore, Maryland.
- Prabhu, N.U. 1965. *Stochastic Processes*. The Macmillan Company, New York.
- Prentice, E. F., T. A. Flagg, and C. S. McCutcheon. 1990. Feasibility of using implantable passive integrated transponder (PIT) tags in salmonids. *American Fisheries Society Symposium* 7:317-322.
- Press, W.H., B.P. Flannery, S.A. Teukolsky and W.T. Vetterling. 1988. *Numerical Recipes in C*. Cambridge University Press. Cambridge.
- Quinn, T.P. 1984. Homing and straying in Pacific salmon. In: *Mechanisms of Migrations in Fishes* (McCleave, J.D., G.P. Arnold, J.J. Dodson, W.H. Neill, editors). Plenum Press, New York.
- Raftery, A. E. 1986. Choosing models for cross-classification. *American Sociological Review* 51: 145-146.
- Rao, K. C. and D. S. Robson. 1974. A chi-square statistic for goodness-of-fit within the exponential family. *Comm. Statist.* 3: 1139-1153.
- Raymond, H.L., 1968. Migration rates of yearling chinook salmon in relation to flows and impoundments in the Columbia and Snake Rivers. *Trans. Am. Fish. Soc.* 97: 356-359.
- Raymond, H.L., 1979. Effects of dams and impoundments on migrations of juvenile chinook salmon and steelhead from the Snake River, 1966 to 1975. *Trans. Am. Fis. Soc.* 108: 505-529.
- Raymond, H. L. 1988. Effects of hydroelectric development and fisheries enhancement on spring and summer chinook salmon and steelhead in the Columbia River Basin. *North American J. Fisheries Management* 8: 1-24.
- Reimers, P. E., and R. E. Loeffel. 1967. The length of residence of juvenile fall chinook salmon in selected Columbia River tributaries. *Res. Briefs Fish Comm. Oreg.* 13: 5-19.
- Ricciardi, M.L. 1977. *Diffusion Processes and Related Topics in Biology*. Lecture Notes in Mathematics 14, Springer-Verlag, New York.
- Rohlf, F. J., and D. Davenport. 1969. Simulation of simple models of animal behavior with

- a digital computer. *J. Theoret. Biol.* 23: 400-424.
- Roscoe, J.T., and J.A. Byars. 1971. Sample size restraints commonly imposed on the use of chi-square statistic. *Journal of the American Statistical Association* 66: 755-759.
- Ross, S. M. 1983. *Stochastic Processes*. John Wiley and Sons, New York.
- Ross, S. M. 1985. *Introduction to Probability Models*, 3rd edition. Academic Press, Orlando, Florida.
- Ross, S. M. 1990. *A Course in Simulation*. Macmillan Publishing Company, New York. 202 pp.
- Ross, S. M. 1993. *Introduction to Probability Models*, 5th edition. Academic Press, San Diego California.
- Sacerdote, L. 1988. Some remarks on first-passage time problems. In: *Biomathematics and Related Computational Problems* (L.M. Ricciardi, ed.), pp. 567-579. Kluwer Academic Publishers.
- Saila, S.B., and J.M. Flowers. 1969. Toward a generalized model of fish migrations. *Trans. Amer. Fish. Soc.* 98: 582-588.
- Saila, S.B., and R. A. Shappy. 1963. Random movement and orientation in salmon migration. *J. Cons. Int. Explor. Mer.* 28:153-166.
- Sandercock, F. K. 1991. Life history of coho salmon. In: *Pacific Salmon Life Histories* (C. Groot and L. Margolis, editors). University of British Columbia Press, Vancouver, British Columbia.
- Schrödinger, E. 1915. Zur Theorie der Fall- und Steigversuche an Teilchen mit Brownscher Bewegung. *Physikalische Zeitschrift* 16: 289-295.
- Schwarz, G. 1978. Estimating the dimension of a model. *Annals of Statistics* 6:461-464.
- Schorr, B. 1974. On the choice of the class intervals in the application of the chi-square test. *Math. Operations Forsch. u. Statist.* 5: 357-377.
- Seber, G. A. F., and C. J. Wild. 1989. *Nonlinear regression*. John Wiley and Sons. New York.
- Shigesada, N. 1980. Spatial distribution of dispersing animals. *J. Math. Biol.* 9: 85-96.
- Shigesada, N., K. Kawasaki, and E. Teramoto. 1979. Spatial segregation of interacting

- species. *J. Theor. Biol.* 79: 83-99.
- Siebert, A. J. F. 1951. on the first passage time probability problem. *Phys. Rev.* 81: 617-623.
- Siegmund, D. 1985. *Sequential Analysis: Tests and Confidence Intervals*. Springer-Verlag, New York. 272 pp.
- Siniff, D.B., and C.R. Jensen. 1969. A simulation model of animal movement patterns. *Adv. in Ecol. Res.* 6: 185-219.
- Skellam, J.G. 1951. Random dispersal in theoretical populations. *Biometrika* 38:196-218.
- Skellam, J.G. 1973. The formulation and interpretation of mathematical models of diffusory processes in population biology. In: *The Mathematical Theory of the Dynamics of Biological Populations* (M.S. Bartlett and R.W. Hiorns, eds.), pp. 63-85. New York: Academic Press.
- Smith, J. R. 1974. Distribution of seaward-migrating chinook salmon and steelhead trout in the Snake River above Lower Monumental Dam. *Marine Fisheries Review* 36: 42-45.
- Smith, L.S. 1982. Decreased swimming performance as a necessary component of the smolt migration in salmon migration in the Columbia River. *Aquaculture* 28: 153-161.
- Sokal, R.R., and F.J. Rohlf. 1981. *Biometry*. W. H. Freeman and Company, New York.
- Stasko, A.B. 1975. Progress of migrating Atlantic salmon (*Salmo salar*) along an estuary, observed by radio-tracking. *J. Fish Biol.* 7:329-338.
- Stephens, M. A. 1986. Tests based on EDF statistics. In: *Goodness-of-fit Techniques* (R. A. D'agostino and M.A. Stephens, editors). Marcel Dekker, Inc. New York.
- Stevenson, J. and D. Olsen. 1991. Yearling chinook salmon travel time and flow regime relationships in the John Day Pool, 1989 and 1990. Report to the Pacific Northwest Utilities Conference Committee, Portland, Oregon.
- Stuehrenberg, L.C., Giorgi, A.E., Sims, C.W., Ramonda-Powell, J., and Wilson J. 1986. Juvenile Radio-Tag: Lower Granite Dam. Report to the Bonneville Power Administration, Project No. 85-35.
- Taylor, E. B. 1988. Adaptive variation in rheotactic and agonistic behavior in newly

- emerged fry of chinook salmon, *Oncorhynchus tshawytscha*, from ocean- and stream-type populations. Ca. J. Fish. Aquat. Sci. 45: 237-243.
- Taylor, E. B., and P. A. Larkin. 1986. Current response and agonistic behavior in newly emerged fry of chinook salmon, *Oncorhynchus tshawytscha*, from ocean- and stream-type populations. Ca. J. Fish. Aquat. Sci. 43: 565-573.
- Teramoto, E., and H. Seno. 1988. Modeling of biological aggregation patterns. In: Biomathematics and Related Computational Problems, ed. L.M. Ricciardi. Dordrecht: Kluwer Academic Publishers.
- Thorpe, J.E. 1982. Migration in salmonids with special reference to juvenile movements in freshwater. Salmon and Trout Migratory Behavior Symposium (E.L. Brannon, and E.O. Salo, eds.). Contribution 793, School of Fisheries, University of Washington, Seattle.
- Thorpe, J.E. 1984. Downstream movements of juvenile salmon: a forward speculative view. In: Mechanisms of Migrations in Fishes (McCleave, J.D., G.P. Arnold, J.J. Dodson, W.H. Neill, editors). Plenum Press, New York.
- Thorpe, J.E., and R. I. G. Morgan. 1978. Periodicity in Atlantic salmon *Salmo salar* L. smolt migration. J. Fish Biol. 12: 541-548.
- Thorpe, J.E., L.G. Ross, G. Struthers and W. Watts. 1981. Tracking Atlantic salmon smolts, *Salmo salar* L., through Loch Voil, Scotland. J. Fish. Biol. 19: 519-537.
- Tweedie, M. C. K. 1957a. Statistical properties of inverse Gaussian distributions I. Ann. Math. Statist. 28: 362-377.
- Tweedie, M.C.K. 1957b. Statistical properties of inverse Gaussian distributions II. Ann. Math. Statist. 28: 696-705.
- Tytler, P., J. E. Thorpe, and W. M. Shearer. 1978. Ultrasonic tracking of the movements of atlantic salmon smolts (*Salmo salar* L) in the estuaries of two Scottish rivers. J. Fish Biol. 12: 575-586.
- Uhlenbeck, G.E., and L.S. Ornstein. 1930. On the theory of Brownian motion. Physical Review 36: 823-841.
- Washington, P.M. 1982. The influence of the size of juvenile coho salmon (*Oncorhynchus kisutch*) on seaward migration and survival. Salmon and Trout Migratory Behavior Symposium. E.L. Brannon, and E.O. Salo, eds. Contribution 793, School of

Fisheries, University of Washington, Seattle.

- Wedemeyer, G. A., R. L. Saunders and W. C. Clarke. 1980. Environmental factors affecting smoltification and early marine survival of anadromous salmonids. *Marine Fisheries review* 42: 1-14.
- Wilkinson, D.H. 1952. The random elements in bird "navigation". *J. Exp. Biol.* 29: 532-560.
- Withler, I. L. 1966. Variability in life history characteristics of steelhead trout (*Salmo gairdneri*) along the Pacific coast of North America. *J. Fish. Research Board Canada* 23: 365-392.
- Zaug, W. S. 1982. Relationships between smolt indices and migration in controlled and natural environments. *Salmon and Trout Migratory Behavior Symposium* (E.L. Brannon, and E.O. Salo, eds.). Contribution 793, School of Fisheries, University of Washington, Seattle.

Appendix 1. PIT tag¹ release groups

Table A1.1 PIT tag release group information. The table includes release group information, release group identification code, number of individuals observed at Lower Granite Dam (GRJ), and the cohort number assigned to the group.

<i>species: chinook run type: unknown</i> <i>rearing type: unknown release site: Snake trap</i>			
Release Group	Release Date	# obs'd at GRJ	cohort #
1989			
EWB89083.SNK	03/24/89	48	1
EWB89086.SNK	03/27/89	61	2
EWB89087.SNK	03/28/89	57	3
EWB89088.SNK	03/29/89	55	4
EWB89089.SNK	03/30/89	45	5
EWB89090.SNK	03/31/89	57	6
EWB89091.SNK	04/01/89	54	7
EWB89092.SNK	04/02/89	57	8
EWB89093.SNK	04/03/89	47	9
EWB89094.SNK	04/04/89	52	10
EWB89095.SNK	04/05/89	45	11
EWB89096.SNK	04/06/89	33	
EWB89097.SNK	04/07/89	43	12
EWB89098.SNK	04/08/89	34	
EWB89099.SNK	04/09/89	54	13
EWB89100.SNK	04/10/89	43	14
EWB89101.SNK	04/11/89	55	15
EWB89102.SNK	04/12/89	48	16
EWB89103.SNK	04/13/89	53	17
EWB89104.SNK	04/14/89	66	18
EWB89105.SNK	04/15/89	51	19
EWB89106.SNK	04/16/89	68	20
EWB89107.SNK	04/17/89	64	21
EWB89108.SNK	04/18/89	66	22
EWB89109.SNK	04/19/89	63	23
EWB89110.SNK	04/20/89	59	24
EWB89111.SNK	04/21/89	62	25
EWB89112.SNK	04/22/89	60	26

Table A1.1 (Continued) PIT tag release group information. The table includes release group information, release group identification code, number of individuals observed at Lower Granite Dam (GRJ), and the cohort number assigned to the group.

<i>species: chinook run type: unknown</i> <i>rearing type: unknown release site: Snake trap</i>			
Release Group	Release Date	# obs'd at GRJ	cohort #
1990			
EWB89113.SNK	04/23/89	69	27
EWB89114.SNK	04/24/89	61	28
EWB89115.SNK	04/25/89	70	29
EWB89116.SNK	04/26/89	66	30
EWB89117.SNK	04/27/89	66	31
EWB89118.SNK	04/28/89	37	32
EWB89119.SNK	04/29/89	34	
EWB89120.SNK	04/30/89	15	
EWB89121.SNK	05/01/89	18	33
EWB89122.SNK	05/02/89	8	
EWB89129.SNK	05/09/89	64	34
EWB89130.SNK	05/10/89	62	35
EWB89131.SNK	05/11/89	65	36
EWB89132.SNK	05/12/89	61	37
EWB89133.SNK	05/13/89	84	38
1990			
EWB90099.SNK	04/09/90	37	1
EWB90100.SNK	04/10/90	22	
EWB90107.PS	04/17/90	60	2
EWB90107.SNK	04/17/90	13	3
EWB90108.SNK	04/18/90	39	
EWB90109.SNK	04/19/90	54	4
EWB90110.SNK	04/20/90	59	5
EWB90111.SNK	04/21/90	59	6
EWB90112.SNK	04/22/90	66	7

1. These data were obtained from the Fish Passage Center, Portland, Oregon.

Table A1.1 (Continued) PIT tag release group information. The table includes release group information, release group identification code, number of individuals observed at Lower Granite Dam (GRJ), and the cohort number assigned to the group.

<i>species: chinook run type: unkown</i>			
<i>rearing type: unkown release site: Snake trap</i>			
Release Group	Release Date	# obs'd at GRJ	cohort #
EWB90113.SNK	04/23/90	62	8
EWB90114.SNK	04/24/90	70	9
EWB90115.SNK	04/25/90	36	10
EWB90116.SNK	04/26/90	44	10
EWB90117.SNK	04/27/90	16	11
EWB90118.SNK	04/28/90	12	11
EWB90119.SNK	04/29/90	24	11
EWB90120.SNK	04/30/90	14	12
EWB90121.SNK	05/01/90	22	12
EWB90122.SNK	05/02/90	5	12
EWB90127.SNK	05/07/90	14	13
EWB90128.SNK	05/08/90	18	13
EWB90129.SNK	05/09/90	22	13
1991			
EWB91098.PS	04/08/91	36	1
EWB91098.SNK	04/08/91	19	1
EWB91099.SNK	04/09/91	42	2
EWB91100.SNK	04/10/91	63	3
EWB91102.FSN	04/12/91	21	4
EWB91102.PS	04/12/91	41	4
EWB91102.SNK	04/12/91	22	4
EWB91105.PS	04/15/91	69	5
EWB91107.PS	04/17/91	66	6
EWB91108.PS	04/18/91	47	7
EWB91109.PS	04/19/91	55	8
EWB91112.PS	04/22/91	65	9
EWB91113.PS	04/23/91	62	10
EWB91115.PS	04/25/91	54	11
EWB91115.SNK	04/25/91	36	11
EWB91116.SNK	04/26/91	63	12
EWB91117.SNK	04/27/91	81	13
EWB91119.PS	04/29/91	32	14
EWB91119.SNK	04/29/91	21	14

Table A1.1 (Continued) PIT tag release group information. The table includes release group information, release group identification code, number of individuals observed at Lower Granite Dam (GRJ), and the cohort number assigned to the group.

<i>species: chinook run type: unkown</i>			
<i>rearing type: unkown release site: Snake trap</i>			
Release Group	Release Date	# obs'd at GRJ	cohort #
EWB91120.PS	04/30/91	39	15
EWB91120.SNK	04/30/91	7	15
EWB91121.SNK	05/01/91	5	15
EWB91130.SNK	05/10/91	63	16
EWB91131.SNK	05/11/91	28	17
EWB91132.SNK	05/12/91	11	17
EWB91133.SN0	05/12/91	14	17
1992			
EWB92098.PS	04/07/92	26	1
EWB92099.PS	04/08/92	28	2
EWB92105.FSN	04/14/92	6	3
EWB92105.SNK	04/14/92	31	3
EWB92111.SNK	04/20/92	6	4
EWB92112.SNK	04/21/92	17	4
EWB92113.SNK	04/22/92	15	4
EWB92114.SNK	04/23/92	16	5
EWB92115.SNK	04/24/92	6	5
EWB92116.SNK	04/25/92	7	5
EWB92122.SNK	05/01/92	15	6
EWB92123.SNK	05/02/92	19	6

Table A1.2 PIT tag release group information. The table includes release group information, release group identification code, number of individuals observed at Lower Granite Dam (GRJ), and the cohort number assigned to the group.

<i>species: chinook</i> <i>rearing type: wild</i>		<i>run type: unkown</i> <i>release site: Snaketrap</i>	
Release Group	Release Date	# obs'd at GRJ	group #
1993			
EWB93099.SNK	04/09/93	3	1
EWB93100.SNK	04/10/93	26	2
EWB93101.SNK	04/11/93	11	3
EWB93102.SNK	04/12/93	14	4
EWB93103.SNK	04/13/93	12	5
EWB93104.SNK	04/14/93	4	6
EWB93105.SNK	04/15/93	8	
EWB93106.SNK	04/16/93	3	
EWB93107.SNK	04/17/93	2	7
EWB93108.SNK	04/18/93	3	
EWB93109.SNK	04/19/93	3	
EWB93110.SNK	04/20/93	6	8
EWB93111.SNK	04/21/93	4	9
EWB93112.SNK	04/22/93	8	10
EWB93113.SNK	04/23/93	5	11
EWB93114.SNK	04/24/93	4	
EWB93115.SNK	04/25/93	6	12
EWB93116.SNK	04/26/93	4	13
EWB93117.SNK	04/27/93	19	14
EWB93118.SNK	04/28/93	6	15
EWB93119.SNK	04/29/93	13	16
EWB93120.SNK	04/30/93	10	17
EWB93121.SNK	05/01/93	7	18
EWB93122.SNK	05/02/93	9	19
EWB93123.SNK	05/03/93	11	20
EWB93124.SNK	05/04/93	29	21
EWB93125.SNK	05/05/93	33	22
EWB93126.SNK	05/06/93	30	23
EWB93127.SNK	05/07/93	30	24
EWB93128.SNK	05/08/93	28	

Table A1.2 (Continued) PIT tag release group information. The table includes release group information, release group identification code, number of individuals observed at Lower Granite Dam (GRJ), and the cohort number assigned to the group.

<i>species: chinook</i> <i>rearing type: wild</i>		<i>run type: unkown</i> <i>release site: Snaketrap</i>	
Release Group	Release Date	# obs'd at GRJ	group #
EWB93129.SNK	05/09/93	12	25
EWB93130.SNK	05/10/93	23	
EWB93131.SNK	05/11/93	15	26
EWB93132.SNK	05/12/93	16	
EWB93133.SN2	05/13/93	1	27
EWB93133.SNK	05/13/93	16	
EWB93134.SNK	05/14/93	11	

Table A1.3 PIT tag release group information. The table includes release group information, release group identification code, number of individuals observed at Lower Granite Dam (GRJ), and the cohort number assigned to the group.

<i>species: chinook</i> <i>rearing type: hatchery</i>		<i>run type: unk.</i> <i>release site: snake trap</i>	
Release Group	Release Date	# obs'd at GRJ	group #
1992			
EWB92098.PS	04/07/92	24	1
EWB92099.PS	04/08/92	29	2
EWB92105.FSN	04/14/92	14	3
EWB92105.SNK	04/14/92	33	
EWB92111.SNK	04/20/92	4	4
EWB92112.SNK	04/21/92	7	
EWB92113.SNK	04/22/92	3	
EWB92114.SNK	04/23/92	6	5
EWB92115.SNK	04/24/92	4	
EWB92116.SNK	04/25/92	6	

Table A1.3 (Continued) PIT tag release group information. The table includes release group information, release group identification code, number of individuals observed at Lower Granite Dam (GRJ), and the cohort number assigned to the group.

<i>species: chinook</i> <i>run type: unk.</i> <i>rearing type: hatchery release site: snake trap</i>			
Release Group	Release Date	# obs'd at GRJ	group #
EWB92122.SNK	05/01/92	7	6
EWB92123.SNK	05/02/92	5	
1993			
EWB93099.SNK	04/09/93	44	1
EWB93100.SNK	04/10/93	45	2
EWB93101.SNK	04/11/93	49	3
EWB93102.SNK	04/12/93	45	4
EWB93103.SNK	04/13/93	19	5
EWB93104.SNK	04/14/93	9	
EWB93105.SNK	04/15/93	16	6
EWB93106.SNK	04/16/93	8	
EWB93107.SNK	04/17/93	9	
EWB93108.SNK	04/18/93	7	7
EWB93109.SNK	04/19/93	17	
EWB93110.SNK	04/20/93	23	
EWB93111.SNK	04/21/93	39	8
EWB93112.SNK	04/22/93	39	9
EWB93113.SNK	04/23/93	30	10
EWB93114.SNK	04/24/93	43	
EWB93115.SNK	04/25/93	41	11
EWB93116.SNK	04/26/93	47	12
EWB93117.SNK	04/27/93	45	13
EWB93118.SNK	04/28/93	37	14
EWB93119.SNK	04/29/93	45	15
EWB93120.SNK	04/30/93	50	16
EWB93121.SNK	05/01/93	46	17
EWB93122.SNK	05/02/93	48	18
EWB93123.SNK	05/03/93	45	19
EWB93124.SNK	05/04/93	69	20
EWB93125.SNK	05/05/93	36	21
EWB93126.SNK	05/06/93	42	22
EWB93127.SNK	05/07/93	49	23
EWB93128.SNK	05/08/93	39	24

Table A1.3 (Continued) PIT tag release group information. The table includes release group information, release group identification code, number of individuals observed at Lower Granite Dam (GRJ), and the cohort number assigned to the group.

<i>species: chinook</i> <i>run type: unk.</i> <i>rearing type: hatchery release site: snake trap</i>			
Release Group	Release Date	# obs'd at GRJ	group #
EWB93129.SNK	05/09/93	27	25
EWB93130.SNK	05/10/93	34	
EWB93131.SNK	05/11/93	21	26
EWB93132.SNK	05/12/93	32	
EWB93133.SNK	05/13/93	30	27
EWB93134.SNK	05/14/93	16	

Table A1.4 PIT tag release group information. The table includes release group information, release group identification code, number of individuals observed at Lower Granite Dam (GRJ), and the cohort number assigned to the group.

<i>species: chinook</i> <i>run type: unk.</i> <i>rearing type: unk.</i> <i>release site: Clearw. trap</i>			
Release Group	Release Date	# obs'd at GRJ	group #
1989			
EWB89088.CLW	03/29/89	47	1
EWB89089.CLW	03/30/89	33	
EWB89090.CLW	03/31/89	51	2
EWB89091.CLW	04/01/89	39	3
EWB89092.CLW	04/02/89	40	
EWB89093.CLW	04/03/89	51	4
EWB89094.CLW	04/04/89	48	5
EWB89095.CLW	04/05/89	43	
EWB89096.CLW	04/06/89	33	6
EWB89097.CLW	04/07/89	42	

Table A1.4 (Continued) PIT tag release group information. The table includes release group information, release group identification code, number of individuals observed at Lower Granite Dam (GRJ), and the cohort number assigned to the group.

<i>species: chinook</i>		<i>run type: unk.</i>	
<i>rearing type: unk.</i>		<i>release site: Clearw. trap</i>	
Release Group	Release Date	# obs'd at GRJ	group #
EWB89102.CLW	04/12/89	23	7
EWB89103.CLW	04/13/89	37	
EWB89105.CLW	04/15/89	28	8
EWB89106.CLW	04/16/89	35	
EWB89143.CLW	05/23/89	10	9
EWB89144.CLW	05/24/89	39	
EWB89145.CLW	05/25/89	51	10
EWB89150.CLW	05/30/89	62	11
1990			
EWB90089.CLW	03/30/90	46	1
EWB90090.CLW	03/31/90	51	2
EWB90091.CLW	04/01/90	40	3
EWB90092.CLW	04/02/90	42	
EWB90093.CLW	04/03/90	46	4
EWB90094.CLW	04/04/90	45	
EWB90095.CLW	04/05/90	44	5
EWB90096.CLW	04/06/90	37	
EWB90097.CLW	04/09/90	40	6
EWB90098.CLW	04/08/90	48	
EWB90099.CLW	04/09/90	47	7
EWB90100.CLW	04/10/90	43	
EWB90101.CLW	04/11/90	42	8
EWB90102.CLW	04/12/90	45	
EWB90103.CLW	04/13/90	48	9
EWB90104.CLW	04/14/90	43	
EWB90105.CLW	04/15/90	58	10
EWB90106.CLW	04/16/90	55	11
EWB90107.CLW	04/17/90	29	12
EWB90108.CLW	04/18/90	29	
EWB90122.CLW	05/02/90	23	13
EWB90123.CLW	05/03/90	28	
EWB90137.CLW	05/17/90	30	14
EWB90138.CLW	05/18/90	41	

Table A1.4 (Continued) PIT tag release group information. The table includes release group information, release group identification code, number of individuals observed at Lower Granite Dam (GRJ), and the cohort number assigned to the group.

<i>species: chinook</i>		<i>run type: unk.</i>	
<i>rearing type: unk.</i>		<i>release site: Clearw. trap</i>	
Release Group	Release Date	# obs'd at GRJ	group #
EWB90139.CLW	05/19/90	36	15
EWB90140.CLW	05/20/90	35	
EWB90141.CLW	05/21/90	58	16
EWB90142.CLW	05/22/90	37	17
EWB90143.CLW	05/23/90	46	
EWB90144.CLW	05/24/90	61	18
1991			
EWB91093.CLW	04/03/91	39	1
EWB91094.CLW	04/04/91	43	
EWB91095.CLW	04/05/91	52	2
EWB91096.CLW	04/06/91	54	3
EWB91097.CLW	04/07/91	58	4
EWB91098.CLW	04/08/91	64	5
EWB91099.CLW	04/09/91	50	6
EWB91100.CLW	04/10/91	57	7
EWB91101.CLW	04/11/91	62	8
EWB91101.FCL	04/11/91	15	9
EWB91102.CLW	04/12/91	47	
EWB91102.FCL	04/12/91	14	10
EWB91103.CLW	04/13/91	46	
EWB91104.CLW	04/14/91	30	11
EWB91105.CLW	04/15/91	30	
EWB91106.CLW	04/16/91	58	12
EWB91107.CLW	04/17/91	51	13
EWB91108.CLW	04/18/91	50	14
EWB91109.CLW	04/19/91	60	15
EWB91110.CLW	04/20/91	47	16
EWB91111.CLW	04/21/91	51	17
EWB91112.CLW	04/22/91	56	18
EWB91113.CLW	04/23/91	47	19
EWB91114.CLW	04/24/91	57	20
EWB91115.CLW	04/25/91	59	21
EWB91116.CLW	04/26/91	64	22

Table A1.4 (Continued) PIT tag release group information. The table includes release group information, release group identification code, number of individuals observed at Lower Granite Dam (GRJ), and the cohort number assigned to the group.

<i>species: chinook</i>			
<i>rearing type: unk.</i>		<i>run type: unk.</i>	
<i>release site: Clearw. trap</i>			
Release Group	Release Date	# obs'd at GRJ	group #
EWB91128.CLW	05/08/91	22	23
EWB91129.CLW	05/09/91	44	
EWB91130.CLW	05/10/91	73	24
EWB91131.CLW	05/11/91	69	25
1992			
EWB92082.CLW	03/22/92	3	1
EWB92083.CLW	03/23/92	3	2
EWB92084.CLW	03/24/92	3	3
EWB92085.CLW	03/25/92	6	4
EWB92086.CLW	03/26/92	8	
EWB92087.CLW	03/27/92	7	5
EWB92088.CLW	03/28/92	5	
EWB92089.CLW	03/29/92	7	6
EWB92090.CLW	03/30/92	7	
EWB92091.CLW	03/31/92	8	7
EWB92092.CLW	04/01/92	12	
EWB92093.CLW	04/02/92	14	8
EWB92094.CLW	04/03/92	19	
EWB92095.CLW	04/04/92	25	9
EWB92096.CLW	04/05/92	22	10
EWB92097.CLW	04/06/92	16	11
EWB92098.CLW	04/07/92	17	12
EWB92099.CLW	04/08/92	8	13
EWB92100.CLW	04/09/92	23	
EWB92101.CLW	04/10/92	11	14
EWB92102.CLW	04/11/92	3	15
EWB92103.CLW	04/12/92	3	16
EWB92104.CLW	04/13/92	2	17
EWB92104.UFW	04/13/92	1	
EWB92105.CLW	04/14/92	1	18
EWB92105.FCL	04/14/92	1	19
EWB92106.CLW	04/15/92	5	
EWB92107.CLW	04/16/92	40	20
EWB92108.CLW	04/17/92	5	21

Table A1.4 (Continued) PIT tag release group information. The table includes release group information, release group identification code, number of individuals observed at Lower Granite Dam (GRJ), and the cohort number assigned to the group.

<i>species: chinook</i>			
<i>rearing type: unk.</i>		<i>run type: unk.</i>	
<i>release site: Clearw. trap</i>			
Release Group	Release Date	# obs'd at GRJ	group #
EWB92109.CLW	04/18/92	14	22
EWB92110.CLW	04/19/92	10	
EWB92111.CLW	04/20/92	5	23
EWB92112.CLW	04/21/92	2	
EWB92113.CLW	04/22/92	8	24
EWB92114.CLW	04/23/92	26	25
EWB92115.CLW	04/24/92	15	26
EWB92116.CLW	04/25/92	10	
EWB92118.CLW	04/27/92	4	27
EWB92119.CLW	04/28/92	1	
EWB92120.CLW	04/29/92	2	28
EWB92121.CLW	04/30/92	7	29
EWB92127.CLW	05/06/92	15	30
EWB92139.CLW	05/18/92	6	31
EWB92140.CLW	05/19/92	6	
EWB92141.CLW	05/20/92	8	
EWB92145.CLW	05/24/92	7	32
EWB92146.CLW	05/25/92	4	
EWB92147.CLW	05/26/92	7	33
EWB92148.CLW	05/27/92	5	
EWB92149.CLW	05/28/92	6	34
EWB92150.CLW	05/29/92	3	
EWB92151.CLW	05/30/92	6	35
EWB92152.CLW	05/31/92	3	

Table A1.5 PIT tag release group information. The table includes release group information, release group identification code, number of individuals observed at Lower Granite Dam (GRJ), and the cohort number assigned to the group.

<i>species: chinook</i>		<i>run type: unknown</i>	
<i>rearing type: wild</i>		<i>release site: Clearw. trap</i>	
Release Group	Release Date	# obsd at GRJ	group #
1993			
EWB93100.CLW	04/10/93	13	1
EWB93101.CLW	04/11/93	4	2
EWB93102.CLW	04/12/93	3	
EWB93106.CLW	04/16/93	6	3
EWB93110.CLW	04/20/93	14	4
EWB93111.CLW	04/21/93	3	
EWB93112.CLW	04/22/93	6	5
EWB93113.CLW	04/23/93	1	
EWB93114.CLW	04/24/93	1	6
EWB93115.CLW	04/25/93	7	
EWB93116.CLW	04/26/93	12	7
EWB93117.CLW	04/27/93	4	
EWB93120.CLW	04/30/93	4	
EWB93121.CLW	05/01/93	12	8
EWB93122.CLW	05/02/93	4	

Table A1.6 PIT tag release group information. The table includes release group information, release group identification code, number of individuals observed at Lower Granite Dam (GRJ), and the cohort number assigned to the group.

<i>species: chinook</i>		<i>run type: unknown</i>	
<i>rearing type: hatchery</i>		<i>release site: Clearw. trap</i>	
Release Group	Release Date	# obs'd at GRJ	group #
1992			
EWB92082.CLW	03/22/92	53	1
EWB92083.CLW	03/23/92	49	2
EWB92084.CLW	03/24/92	45	3
EWB92085.CLW	03/25/92	32	4
EWB92086.CLW	03/26/92	18	
EWB92087.CLW	03/27/92	21	5
EWB92088.CLW	03/28/92	19	
EWB92089.CLW	03/29/92	33	6
EWB92090.CLW	03/30/92	26	
EWB92091.CLW	03/31/92	25	7
EWB92092.CLW	04/01/92	19	
EWB92093.CLW	04/02/92	20	8
EWB92094.CLW	04/03/92	33	
EWB92095.CLW	04/04/92	35	9
EWB92096.CLW	04/05/92	35	10
EWB92097.CLW	04/06/92	34	11
EWB92098.CLW	04/07/92	36	12
EWB92099.CLW	04/08/92	41	13
EWB92100.CLW	04/09/92	18	
EWB92101.CLW	04/10/92	47	14
EWB92102.CLW	04/11/92	49	15
EWB92103.CLW	04/12/92	47	16
EWB92104.CLW	04/13/92	37	17
EWB92104.UFW	04/13/92	13	
EWB92105.CLW	04/14/92	58	18
EWB92105.FCL	04/14/92	11	19
EWB92106.CLW	04/15/92	40	
EWB92107.CLW	04/16/92	5	20
EWB92108.CLW	04/17/92	46	21
EWB92109.CLW	04/18/92	35	22
EWB92110.CLW	04/19/92	38	

Table A1.6 (Continued) PIT tag release group information. The table includes release group information, release group identification code, number of individuals observed at Lower Granite Dam (GRJ), and the cohort number assigned to the group.

<i>species: chinook run type: unknown</i>			
<i>rearing type: hatchery release site: Clearw. trap</i>			
Release Group	Release Date	# obs'd at GRJ	group #
EWB92111.CLW	04/20/92	41	23
EWB92112.CLW	04/21/92	41	
EWB92113.CLW	04/22/92	48	24
EWB92114.CLW	04/23/92	30	25
EWB92115.CLW	04/24/92	25	26
EWB92116.CLW	04/25/92	9	
EWB92118.CLW	04/27/92	5	27
EWB92119.CLW	04/28/92	46	
EWB92120.CLW	04/29/92	40	28
EWB92121.CLW	04/30/92	49	29
EWB92127.CLW	05/06/92	35	30
EWB92139.CLW	05/18/92	7	
EWB92140.CLW	05/19/92	16	31
EWB92141.CLW	05/20/92	15	
EWB92145.CLW	05/25/92	25	32
EWB92146.CLW	05/25/92	12	
EWB92147.CLW	05/26/92	27	33
EWB92148.CLW	05/27/92	21	
EWB92149.CLW	05/28/92	32	34
EWB92150.CLW	05/29/92	16	
EWB92151.CLW	05/30/92	36	35
EWB92152.CLW	05/31/92	11	
1993			
EWB93100.CLW	04/10/93	43	1
EWB93101.CLW	04/11/93	35	2
EWB93102.CLW	04/12/93	25	
EWB93106.CLW	04/16/93	44	3
EWB93110.CLW	04/20/93	36	4
EWB93111.CLW	04/21/93	33	
EWB93112.CLW	04/22/93	29	5
EWB93113.CLW	04/23/93	31	
EWB93114.CLW	04/24/93	34	6
EWB93115.CLW	04/25/93	20	

Table A1.6 (Continued) PIT tag release group information. The table includes release group information, release group identification code, number of individuals observed at Lower Granite Dam (GRJ), and the cohort number assigned to the group.

<i>species: chinook run type: unknown</i>			
<i>rearing type: hatchery release site: Clearw. trap</i>			
Release Group	Release Date	# obs'd at GRJ	group #
EWB93116.CLW	04/26/93	34	7
EWB93117.CLW	04/27/93	24	
EWB93120.CLW	04/30/93	23	
EWB93121.CLW	05/01/93	18	8
EWB93122.CLW	05/02/93	10	

Table A1.7 PIT tag release group information. The table includes release group information, release group identification code, number of individuals observed at McNary Dam (MCJ), and the cohort number assigned to the group.

<i>species: chinook run type: fall</i>			
<i>rearing type: wild release site: Mid Colum.</i>			
Release Group	Release Date	# obs'd at MCJ	group #
1991			
LRB91157.CO2	06/07/91	154	1
LRB91158.CO1	06/07/91	97	2
1992			
LRB92155.001	06/03/92	39	1
LRB92155.002	06/03/92	36	
LRB92155.003	06/03/92	73	2
LRB92156.002	06/04/92	14	3
LRB92156.003	06/04/92	54	
LRB92156.001	06/04/92	23	4
LRB92156.004	06/04/92	40	
LRB92156.005	06/04/92	60	5
1993			
LRB93158.001	06/07/93	61	1

Table A1.7 (Continued) PIT tag release group information. The table includes release group information, release group identification code, number of individuals observed at McNary Dam (MCJ), and the cohort number assigned to the group.

<i>species: chinook run type: fall</i> <i>rearing type: wild release site: Mid Colum.</i>			
Release Group	Release Date	# obs'd at MCJ	group #
LRB93159.001	06/08/93	81	2
LRB93159.002	06/08/93	115	3
LRB93160.001	06/09/93	75	4
LRB93160.002	06/09/93	118	5
LRB93160.003	06/15/93	120	6

Table A1.8 PIT tag release group information. The table includes release group information, release group identification code, number of individuals observed at Lower Granite Dam (GRJ), and the cohort number assigned to the group.

<i>species: chinook run type: fall</i> <i>rearing type: wild release site: Snake River</i>		
Release Group	Release Date	# obs'd at GRJ
1991		
WPC91149.R17	05/29/91	1
WPC91150.G29	05/30/91	3
WPC91150.R16	05/30/91	1
WPC91150.R17	05/30/91	0
WPC91155.G35	06/04/91	2
WPC91155.G38	06/04/91	0
WPC91157.G29	06/06/91	1
WPC91157.G42	06/06/91	2
WPC91162.G29	06/11/91	1
WPC91162.G42	06/11/91	3
WPC91162.G50	06/11/91	1
WPC91163.G26	06/12/91	2
WPC91163.G35	06/12/91	1

Table A1.8 (Continued) PIT tag release group information. The table includes release group information, release group identification code, number of individuals observed at Lower Granite Dam (GRJ), and the cohort number assigned to the group.

<i>species: chinook run type: fall</i> <i>rearing type: wild release site: Snake River</i>		
Release Group	Release Date	# obs'd at GRJ
WPC91164.G26	06/13/91	2
WPC91164.G29	06/13/91	0
WPC91169.G32	06/18/91	0
WPC91169.G42	06/18/91	2
WPC91170.G26	06/19/91	1
WPC91170.G29	06/19/91	0
WPC91175.G26	06/24/91	1
WPC91175.G42	06/24/91	2
WPC91176.G42	06/25/91	6
1992		
WPC92113.G48	04/23/92	1
WPC92119.229	04/29/92	0
WPC92119.248	04/29/92	0
WPC92119.B51	04/29/92	1
WPC92120.G48	04/30/92	3
WPC92120.G62	04/30/92	1
WPC92134.232	05/14/92	0
WPC92134.254	05/13/92	1
WPC92134.262	05/13/92	1
WPC92135.274	05/14/92	0
WPC92135.280	05/14/92	0
WPC92135.282	05/14/92	2
WPC92140.280	05/19/92	0
WPC92140.282	05/19/92	2
WPC92141.229	05/20/92	1
WPC92141.248	05/20/92	2
WPC92141.A42	05/20/92	1
WPC92141.B42	05/20/92	1
WPC92142.B51	05/21/92	2
WPC92147.A51	05/26/92	2
WPC92148.282	05/27/92	3
WPC92148.290	05/27/92	0
WPC92148.G62	05/27/92	5
WPC92148.G74	05/27/92	0

Table A1.8 (Continued) PIT tag release group information. The table includes release group information, release group identification code, number of individuals observed at Lower Granite Dam (GRJ), and the cohort number assigned to the group.

<i>species: chinook</i> <i>run type: fall</i> <i>rearing type: wild</i> <i>release site: Snake River</i>		
Release Group	Release Date	# obs'd at GRJ
WPC92148.G90	05/27/92	0
WPC92149.A42	05/28/92	1
WPC92149.B42	05/28/92	2
WPC92153.G62	06/01/92	3
WPC92154.232	06/02/92	0
WPC92154.B42	06/02/92	1
WPC92154.G50	06/02/92	3
WPC92156.A51	06/04/92	1
1993		
WPC93138.G61	05/18/93	3
WPC93139.229	05/19/93	3
WPC93139.B42	05/19/93	2
WPC93139.G29	05/19/93	1
WPC93139.G47	05/19/93	3
WPC93139.G51	05/19/93	1
WPC93144.226	05/25/93	1
WPC93144.229	05/25/93	3
WPC93144.G29	05/25/93	5
WPC93144.G34	05/25/93	7
WPC93145.A51	05/25/93	1
WPC93145.B42	05/25/93	1
WPC93146.G58	05/26/93	1
WPC93146.G63	05/26/93	0
WPC93146.R11	05/26/93	2
WPC93147.G28	05/27/93	4
WPC93147.G29	05/27/93	2
WPC93147.G34	05/26/93	5
WPC93147.G37	05/27/93	1
WPC93147.G47	05/27/93	1
WPC93147.G53	05/27/93	2
WPC93152.G29	06/01/93	10
WPC93152.G34	06/01/93	4
WPC93153.226	06/02/93	4
WPC93153.229	06/02/93	0

Table A1.8 (Continued) PIT tag release group information. The table includes release group information, release group identification code, number of individuals observed at Lower Granite Dam (GRJ), and the cohort number assigned to the group.

<i>species: chinook</i> <i>run type: fall</i> <i>rearing type: wild</i> <i>release site: Snake River</i>		
Release Group	Release Date	# obs'd at GRJ
WPC93153.232	06/02/93	4
WPC93153.A51	06/02/93	1
WPC93153.B42	06/02/93	2
WPC93153.G33	06/02/93	1
WPC93153.G37	06/02/93	1
WPC93153.G41	06/02/93	1
WPC93153.R03	06/02/93	3
WPC93153.R14	06/02/93	2
WPC93154.254	06/03/93	1
WPC93154.R76	06/03/93	1
WPC93155.G27	06/04/93	1
WPC93155.G30	06/04/93	1
WPC93155.G31	06/04/93	1
WPC93155.R53	06/04/93	0
WPC93159.E34	06/08/93	1
WPC93159.E37	06/08/93	0
WPC93159.E41	06/08/93	1
WPC93159.E43	06/08/93	3
WPC93159.W34	06/08/93	6
WPC93159.W35	06/08/93	1
WPC93159.W37	06/08/93	1
WPC93159.W41	06/08/93	9
WPC93159.W42	06/08/93	10
WPC93159.W44	06/08/93	1
WPC93159.W47	06/08/93	2
WPC93159.W50	06/08/93	1
WPC93160.226	06/09/93	3
WPC93160.229	06/09/93	3
WPC93160.A51	06/09/93	3
WPC93160.B42	06/09/93	1
WPC93160.G32	06/09/93	1
WPC93160.R08	06/09/93	1
WPC93160.R13	06/09/93	1
WPC93160.R19	06/09/93	2

Table A1.8 (Continued) PIT tag release group information. The table includes release group information, release group identification code, number of individuals observed at Lower Granite Dam (GRJ), and the cohort number assigned to the group.

<i>species: chinook</i> <i>run type: fall</i> <i>rearing type: wild</i> <i>release site: Snake River</i>		
Release Group	Release Date	# obs'd at GRJ
WPC93160.R92	06/09/93	2
WPC93161.G58	06/10/93	2
WPC93161.R63	06/10/93	0
WPC93162.E29	06/11/93	13
WPC93162.W24	06/11/93	4
WPC93166.E61	06/15/93	2
WPC93166.E62	06/15/93	1
WPC93166.E63	06/15/93	2
WPC93166.E64	06/15/93	1
WPC93166.E66	06/15/93	2
WPC93167.229	06/16/93	8
WPC93167.232	06/16/93	2
WPC93167.A51	06/16/93	3
WPC93167.R07	06/16/93	2
WPC93167.R09	06/16/93	1
WPC93167.R15	06/16/93	3
WPC93167.R18	06/16/93	1
WPC93168.E42	06/17/93	4
WPC93168.W34	06/16/93	0
WPC93168.W40	06/17/93	1
WPC93168.W47	06/17/93	2
WPC93169.E28	06/18/93	2
WPC93169.E29	06/18/93	6
WPC93169.W24	06/18/93	2
WPC93169.W32	06/18/93	1
WPC93169.W33	06/18/93	2
WPC93173.229	06/22/93	2
WPC93173.232	06/22/93	1
WPC93173.A51	06/22/93	2
WPC93174.254	06/23/93	3
WPC93174.R12	06/23/93	1
WPC93175.E36	06/24/93	4
WPC93175.E39	06/24/93	1
WPC93175.E50	06/24/93	4

Table A1.8 (Continued) PIT tag release group information. The table includes release group information, release group identification code, number of individuals observed at Lower Granite Dam (GRJ), and the cohort number assigned to the group.

<i>species: chinook</i> <i>run type: fall</i> <i>rearing type: wild</i> <i>release site: Snake River</i>		
Release Group	Release Date	# obs'd at GRJ
WPC93175.W34	06/24/93	3
WPC93175.W35	06/24/93	2
WPC93175.W53	06/24/93	1
WPC93175.W54	06/24/93	1
WPC93180.A42	06/29/93	1
WPC93180.A51	06/29/93	9
WPC93181.E48	06/30/93	1
WPC93181.E49	06/30/93	1
WPC93181.E50	06/30/93	1
WPC93181.E52	06/30/93	2
WPC93181.E54	06/30/93	1
WPC93188.226	07/07/93	1
WPC93195.226	07/14/93	2

Table A1.9 PIT tag release group information. The table includes release group information, release group identification code, number of individuals observed at Lower Granite Dam (GRJ), and the cohort number assigned to the group.

<i>species: steelhead</i> <i>rearing type: wild</i> <i>release site: Snake Trap</i>			
Release Group	Release Date	# obs'd at GRJ	cohort #
1989			
EWB89106.SNK	04/16/89	16	1
EWB89107.SNK	04/17/89	21	
EWB89108.SNK	04/18/89	27	
EWB89109.SNK	04/19/89	43	2

Table A1.9 (Continued) PIT tag release group information. The table includes release group information, release group identification code, number of individuals observed at Lower Granite Dam (GRJ), and the cohort number assigned to the group.

<i>species: steelhead rearing type: wild</i> <i>release site: Snake Trap</i>			
Release Group	Release Date	# obs'd at GRJ	cohort #
EWB89110.SNK	04/20/89	26	3
EWB89111.SNK	04/21/89	40	
EWB89112.SNK	04/22/89	45	4
EWB89113.SNK	04/23/89	40	5
EWB89114.SNK	04/24/89	24	
EWB89115.SNK	04/25/89	37	6
EWB89116.SNK	04/26/89	26	
EWB89117.SNK	04/27/89	15	7
EWB89118.SNK	04/28/89	17	
EWB89119.SNK	04/29/89	17	
EWB89120.SNK	04/30/89	18	8
EWB89121.SNK	05/01/89	30	
EWB89122.SNK	05/02/89	29	9
EWB89123.SNK	05/03/89	34	
EWB89124.SNK	05/04/89	40	10
EWB89125.SNK	05/05/89	39	
EWB89126.SNK	05/06/89	79	11
EWB89127.SNK	05/07/89	117	12
EWB89128.SNK	05/08/89	8	
EWB89129.SNK	05/09/89	80	13
EWB89130.SNK	05/10/89	87	14
EWB89131.SNK	05/11/89	25	15
EWB89132.SNK	05/12/89	37	
EWB89133.SNK	05/13/89	20	16
EWB89134.SNK	05/14/89	13	
EWB89135.SNK	05/15/89	14	
1990			
EWB90107.PS	04/17/90	18	1
EWB90107.SNK	04/17/90	7	
EWB90108.SNK	04/18/90	36	
EWB90109.SNK	04/19/90	51	2
EWB90111.SNK	04/21/90	69	3
EWB90112.SNK	04/22/90	72	4
EWB90113.SNK	04/23/90	52	5

Table A1.9 (Continued) PIT tag release group information. The table includes release group information, release group identification code, number of individuals observed at Lower Granite Dam (GRJ), and the cohort number assigned to the group.

<i>species: steelhead rearing type: wild</i> <i>release site: Snake Trap</i>			
Release Group	Release Date	# obs'd at GRJ	cohort #
EWB90114.SNK	04/24/90	111	6
EWB90115.SNK	04/25/90	86	7
EWB90116.SNK	04/26/90	95	8
EWB90118.SNK	04/28/90	66	9
EWB90119.SNK	04/29/90	55	10
EWB90120.SNK	04/30/90	50	11
EWB90121.SNK	05/01/90	49	12
EWB90122.SNK	05/02/90	27	
EWB90123.SNK	05/03/90	45	13
EWB90124.SNK	05/04/90	27	
EWB90125.SNK	05/05/90	53	14
EWB90126.SNK	05/06/90	80	15
EWB90127.SNK	05/07/90	146	16
EWB90128.SNK	05/08/90	87	17
EWB90129.SNK	05/09/90	55	18
EWB90130.SNK	05/10/90	36	19
EWB90131.SNK	05/11/90	16	
EWB90132.SNK	05/12/90	23	20
EWB90133.SNK	05/13/90	45	
EWB90134.SNK	05/14/90	50	21
EWB90135.SNK	05/15/90	17	22
EWB90136.SNK	05/16/90	27	
EWB90137.SNK	05/17/90	30	23
EWB90138.SNK	05/18/90	11	
EWB90139.SNK	05/19/90	20	
EWB90145.SNK	05/25/90	32	24
EWB90146.SNK	05/26/90	28	
EWB90148.SNK	05/28/90	41	25
EWB90149.SNK	05/29/90	16	
EWB90150.SNK	05/30/90	62	26
EWB90152.SNK	06/01/90	36	27
EWB90153.SNK	06/02/90	22	
1991			
EWB91116.SNK	04/26/91	57	1

Table A1.9 (Continued) PIT tag release group information. The table includes release group information, release group identification code, number of individuals observed at Lower Granite Dam (GRJ), and the cohort number assigned to the group.

<i>species: steelhead rearing type: wild</i> <i>release site: Snake Trap</i>			
Release Group	Release Date	# obs'd at GRJ	cohort #
EWB91117.SNK	04/27/91	50	2
EWB91118.SNK	04/28/91	49	3
EWB91119.SNK	04/29/91	26	4
EWB91120.PS	04/30/91	2	
EWB91120.SNK	04/30/91	18	
EWB91121.SNK	05/01/91	14	
EWB91125.SNK	05/05/91	5	5
EWB91126.SNK	05/06/91	7	
EWB91127.SNK	05/07/91	42	6
EWB91128.SNK	05/08/91	21	
EWB91129.SNK	05/09/91	47	7
EWB91130.SNK	05/10/91	360	
EWB91131.SNK	05/11/91	188	8
EWB91132.SNK	05/12/91	113	9
EWB91133.SN0	05/12/91	126	10
EWB91133.SNK	05/13/91	59	11
EWB91134.SNK	05/14/91	84	12
EWB91135.SNK	05/15/91	56	13
EWB91137.SNK	05/17/91	85	14
EWB91138.SNK	05/18/91	152	15
EWB91139.SNK	05/19/91	339	16
EWB91140.SNK	05/20/91	51	17
EWB91143.SNK	05/23/91	32	18
EWB91144.SNK	05/24/91	26	
EWB91145.SNK	05/25/91	55	19
EWB91146.SNK	05/26/91	35	20
EWB91147.SNK	05/27/91	21	
1992			
EWB92109.SNK	04/18/92	24	1
EWB92110.SNK	04/19/92	37	
EWB92112.SNK	04/21/92	58	2
EWB92113.SNK	04/22/92	38	3
EWB92114.SNK	04/23/92	26	
EWB92116.SNK	04/25/92	67	4

Table A1.9 (Continued) PIT tag release group information. The table includes release group information, release group identification code, number of individuals observed at Lower Granite Dam (GRJ), and the cohort number assigned to the group.

<i>species: steelhead rearing type: wild</i> <i>release site: Snake Trap</i>			
Release Group	Release Date	# obs'd at GRJ	cohort #
EWB92119.SNK	04/28/92	64	5
EWB92121.SNK	04/30/92	72	6
EWB92122.SNK	05/01/92	180	7
EWB92123.SNK	05/02/92	154	8
EWB92124.SNK	05/03/92	69	9
EWB92125.SNK	05/04/92	44	10
EWB92126.SNK	05/05/92	44	11
EWB92127.SNK	05/06/92	54	12
EWB92128.SNK	05/07/92	40	13
EWB92129.SNK	05/08/92	61	14
EWB92130.SNK	05/09/92	88	15
EWB92131.SNK	05/10/92	90	16
EWB92132.SNK	05/11/92	60	17
EWB92133.SNK	05/12/92	29	18
EWB92134.SNK	05/13/92	13	
1993			
EWB93110.SNK	04/20/93	12	1
EWB93111.SNK	04/21/93	10	
EWB93112.SNK	04/22/93	16	
EWB93114.SNK	04/24/93	23	2
EWB93115.SNK	04/25/93	28	3
EWB93116.SNK	04/26/93	23	
EWB93117.SNK	04/27/93	39	4
EWB93118.SNK	04/28/93	50	
EWB93119.SNK	04/29/93	57	5
EWB93120.SNK	04/30/93	50	6
EWB93121.SNK	05/01/93	87	7
EWB93122.SNK	05/02/93	85	8
EWB93123.SNK	05/03/93	72	9
EWB93124.SNK	05/04/93	217	10
EWB93125.SN2	05/05/93	97	11
EWB93125.SNK	05/05/93	253	12
EWB93126.SNK	05/06/93	59	13
EWB93127.SNK	05/07/93	236	14

Table A1.9 (Continued) PIT tag release group information. The table includes release group information, release group identification code, number of individuals observed at Lower Granite Dam (GRJ), and the cohort number assigned to the group.

<i>species: steelhead rearing type: wild</i> <i>release site: Snake Trap</i>			
Release Group	Release Date	# obs'd at GRJ	cohort #
EWB93128.SNK	05/08/93	93	15
EWB93129.SNK	05/09/93	40	16
EWB93130.SNK	05/10/93	66	17
EWB93131.SNK	05/11/93	36	18
EWB93132.SNK	05/12/93	49	
EWB93133.SN2	05/13/93	84	19
EWB93133.SNK	05/13/93	61	20

Appendix 2. Cohort covariates

Table A2.1 Data used in the regressions in chapter 5, section 4. These cohorts are the Snake River trap run-of-the-river spring chinook. The cohort numbers correspond to the ones in Table A1.1 through Table A1.3. The parameters are those reported in Table 4.4. The last two columns are the covariate values and are average values for the cohort.

cohort	parameters		date of release	ave. flow (kcfs)
	r	σ		
1989				
1	3.70	5.84	97.8	84.6
2	3.30	6.02	99.3	87.5
3	3.16	7.58	100.4	87.0
4	4.04	7.29	101.4	87.3
5	4.93	6.95	102.4	87.8
6	5.14	8.07	103.4	89.7
7	5.81	7.50	104.4	92.3
8	5.09	7.94	105.3	95.4
9	7.24	9.99	106.4	96.5
10	7.49	10.13	107.5	98.6
11	8.01	11.40	108.4	100.5
12	8.64	11.89	109.4	102.5
13	8.97	11.94	110.4	105.7
14	9.16	12.01	111.4	105.9
15	7.80	9.34	112.3	101.0
16	8.15	8.51	113.4	95.9
17	6.51	12.40	114.5	91.8
18	6.84	8.68	115.4	88.7

Table A2.1 (Continued) Data used in the regressions in chapter 5, section 4. These cohorts are the Snake River trap run-of-the-river spring chinook. The cohort numbers correspond to the ones in Table A1.1 through Table A1.3. The parameters are those reported in Table 4.4. The last two columns are the covariate values and are average values for the cohort.

cohort	parameters		date of release	ave. flow (kcfs)
	r	σ		
19	7.47	7.79	116.4	87.3
20	6.93	8.85	117.4	89.2
21	8.57	8.88	118.9	88.5
22	10.26	8.34	121.2	90.7
23	11.53	15.05	129.4	110.5
1990				
1	5.30	7.55	99.7	51.3
2	8.50	7.61	107.4	65.0
3	8.13	9.11	108.1	65.6
4	8.85	8.14	109.3	67.3
5	6.34	11.55	110.4	68.1
6	6.27	9.83	111.4	68.4
7	6.21	10.51	112.3	68.2
8	5.55	9.72	113.3	66.7
9	5.16	9.78	114.4	65.4
10	4.54	8.88	115.9	63.6
11	6.29	6.03	118.6	63.2
12	5.75	7.06	121.3	65.9
13	10.34	9.47	128.5	83.3
1991				

Table A2.1 (Continued) Data used in the regressions in chapter 5, section 4. These cohorts are the Snake River trap run-of-the-river spring chinook. The cohort numbers correspond to the ones in Table A1.1 through Table A1.3. The parameters are those reported in Table 4.4. The last two columns are the covariate values and are average values for the cohort.

cohort	parameters		date of release	ave. flow (kcfs)
	r	σ		
1	2.94	4.83	98.5	55.8
2	3.28	4.11	99.3	56.7
3	3.38	4.72	100.3	57.3
4	3.59	4.82	102.3	59.8
5	3.05	5.33	105.4	64.5
6	4.04	6.16	107.4	65.6
7	4.39	5.44	108.4	66.0
8	3.62	6.08	109.4	64.6
9	4.89	8.34	112.4	66.1
10	5.11	8.06	113.3	64.9
11	6.63	12.43	116.3	61.1
12	6.29	7.91	116.3	60.8
13	5.49	6.69	117.3	60.1
14	5.62	6.00	119.4	59.1
15	9.92	11.14	130.0	78.3
1992				
1	3.94	5.61	98.6	37.3
2	3.73	6.53	99.6	39.0
3	3.95	6.57	105.6	46.8
4	4.59	7.35	112.6	51.8
5	5.45	6.21	115.2	55.1
6	5.36	9.96	122.7	72.5
1993				

Table A2.1 (Continued) Data used in the regressions in chapter 5, section 4. These cohorts are the Snake River trap run-of-the-river spring chinook. The cohort numbers correspond to the ones in Table A1.1 through Table A1.3. The parameters are those reported in Table 4.4. The last two columns are the covariate values and are average values for the cohort.

cohort	parameters		date of release	ave. flow (kcfs)
	r	σ		
1	3.65	6.57	99.5	64.6
2	3.76	5.14	100.4	64.0
3	3.57	5.22	101.3	64.1
4	3.48	5.31	102.3	64.0
5	3.61	4.20	103.7	64.0
6	4.38	4.91	106.1	64.0
7	5.59	6.75	109.8	65.2
8	5.48	6.40	111.4	66.4
9	6.27	7.25	112.6	66.4
10	7.14	6.52	114.1	67.5
11	7.47	7.10	115.1	69.2
12	8.37	6.84	116.4	71.2
13	8.09	7.07	117.4	73.8
14	8.29	7.42	118.4	76.3
15	9.71	8.16	119.4	78.2
16	10.34	8.67	120.4	82.5
17	10.83	5.91	121.6	88.0
18	11.41	7.41	122.4	90.8
19	13.55	7.94	123.4	95.4
20	12.97	12.31	124.5	100.9
21	11.08	10.02	125.4	102.6
22	10.65	10.10	126.4	102.5
23	9.16	10.54	127.3	105.9

Table A2.1 (Continued) Data used in the regressions in chapter 5, section 4. These cohorts are the Snake River trap run-of-the-river spring chinook. The cohort numbers correspond to the ones in Table A1.1 through Table A1.3. The parameters are those reported in Table 4.4. The last two columns are the covariate values and are average values for the cohort.

cohort	parameters		date of release	ave. flow (kcfs)
	r	σ		
24	9.20	8.36	128.4	107.6
25	9.67	7.24	130.0	117.0

Table A2.2 Data used in the regressions in chapter 5, section 4. These cohorts are the Clearwater trap run-of-the-river spring chinook. The cohort numbers correspond to the ones in Tables A1.4 through A1.6. The parameters estimates were obtained using the methods described in chapter 4. The last two columns are the covariate values and are average values for the cohort.

cohort	parameters		date of release	ave. flow (kcfs)
	r	σ		
1989				
1	2.54	5.52	89.0	78.0
2	2.34	9.30	90.2	78.9
3	2.52	7.71	91.9	80.3
4	2.49	6.49	93.4	82.9
5	2.54	6.30	94.8	84.6
6	3.15	9.60	97.0	85.0
7	4.17	10.58	103.0	90.4
8	4.28	10.64	105.9	96.2
9	7.39	6.67	144.2	63.1

Table A2.2 (Continued) Data used in the regressions in chapter 5, section 4. These cohorts are the Clearwater trap run-of-the-river spring chinook. The cohort numbers correspond to the ones in Tables A1.4 through A1.6. The parameters estimates were obtained using the methods described in chapter 4. The last two columns are the covariate values and are average values for the cohort.

cohort	parameters		date of release	ave. flow (kcfs)
	r	σ		
10	7.50	7.39	145.3	63.2
11	9.51	7.92	150.5	69.3
1990				
1	2.47	5.71	89.4	49.5
2	2.52	5.98	90.3	50.1
3	2.95	6.55	91.9	50.8
4	3.19	7.34	93.8	52.7
5	2.55	5.77	95.7	56.3
6	3.04	8.50	98.8	56.5
7	4.04	8.29	99.9	55.4
8	3.46	9.24	101.9	58.9
9	3.32	6.63	103.8	63.1
10	3.23	6.62	105.5	65.2
11	4.10	10.27	106.4	65.4
12	4.50	11.17	107.8	66.2
13	6.03	8.59	123.0	69.9
14	7.80	3.86	138.1	48.0
15	9.40	3.85	140.0	50.5
16	11.25	4.33	141.3	54.1
17	13.46	9.60	142.9	60.4
18	12.03	11.03	144.5	71.8
1991				

Table A2.2 (Continued) Data used in the regressions in chapter 5, section 4. These cohorts are the Clearwater trap run-of-the-river spring chinook. The cohort numbers correspond to the ones in Tables A1.4 through A1.6. The parameters estimates were obtained using the methods described in chapter 4. The last two columns are the covariate values and are average values for the cohort.

cohort	parameters		date of release	ave. flow (kcfs)
	r	σ		
1	2.68	5.64	94.0	54.0
2	2.26	3.30	95.5	57.5
3	2.49	4.04	96.4	57.0
4	2.19	4.73	97.4	58.6
5	2.60	5.02	98.3	57.6
6	2.84	4.60	99.3	58.2
7	2.84	5.31	100.4	59.5
8	2.74	4.33	101.4	60.5
9	2.62	4.55	101.8	61.0
10	3.01	4.87	103.1	61.9
11	3.05	5.71	104.9	63.9
12	3.31	5.29	106.3	64.3
13	3.19	5.46	107.3	64.3
14	4.12	6.99	108.3	65.8
15	4.18	6.78	109.3	65.0
16	4.06	7.37	110.0	65.5
17	4.21	8.62	111.3	65.0
18	4.41	7.16	112.4	64.4
19	4.54	8.43	113.4	64.7
20	4.92	8.21	114.4	63.1
21	5.18	8.07	116.4	60.4
22	4.22	6.32	116.4	61.3

Table A2.2 (Continued) Data used in the regressions in chapter 5, section 4. These cohorts are the Clearwater trap run-of-the-river spring chinook. The cohort numbers correspond to the ones in Tables A1.4 through A1.6. The parameters estimates were obtained using the methods described in chapter 4. The last two columns are the covariate values and are average values for the cohort.

cohort	parameters		date of release	ave. flow (kcfs)
	r	σ		
23	8.21	10.13	129.0	78.4
24	7.34	7.27	130.4	82.4
25	6.74	8.52	131.5	84.4
1992				
1	2.19	3.68	82.4	28.2
2	2.26	3.52	83.4	28.0
3	2.08	3.37	80.9	28.4
4	2.72	4.58	85.8	25.8
5	2.72	4.25	87.8	27.9
6	2.94	4.45	89.8	30.2
7	3.10	5.03	91.9	33.8
8	3.51	5.51	94.0	35.9
9	3.92	5.61	95.3	36.4
10	3.48	7.03	96.5	37.8
11	3.69	5.42	97.4	38.9
12	3.23	5.28	98.4	41.0
13	3.29	5.92	99.9	42.5
14	3.18	5.39	101.4	45.0
15	2.95	5.76	102.3	47.2
16	2.94	5.02	103.3	48.4
17	3.19	5.84	104.4	49.3
18	3.10	6.89	105.3	50.0

Table A2.2 (Continued) Data used in the regressions in chapter 5, section 4. These cohorts are the Clearwater trap run-of-the-river spring chinook. The cohort numbers correspond to the ones in Tables A1.4 through A1.6. The parameters estimates were obtained using the methods described in chapter 4. The last two columns are the covariate values and are average values for the cohort.

cohort	parameters		date of release	ave. flow (kcfs)
	r	σ		
19	3.42	6.40	106.1	49.9
20	2.50	6.59	107.3	53.6
21	3.41	5.21	108.3	53.0
22	3.06	5.97	109.8	54.8
23	3.46	7.17	111.8	55.5
24	4.69	7.30	113.3	55.6
25	4.69	6.82	114.4	57.3
26	4.56	8.46	115.7	58.5
27	4.35	8.80	119.2	65.4
28	4.98	10.62	120.3	67.7
29	4.72	8.67	121.3	69.5
30	6.20	13.84	127.4	66.5
31	7.41	12.94	140.6	50.5
32	9.80	12.50	145.7	53.5
33	7.91	11.15	147.8	52.5
34	6.75	13.90	149.7	45.8
35	8.41	11.93	151.6	44.7
1993				
1	2.99	5.75	100.5	66.9
2	2.57	5.31	101.9	70.9
3	3.94	5.56	106.3	66.6
4	4.86	6.69	110.8	69.2

Table A2.2 (Continued) Data used in the regressions in chapter 5, section 4. These cohorts are the Clearwater trap run-of-the-river spring chinook. The cohort numbers correspond to the ones in Tables A1.4 through A1.6. The parameters estimates were obtained using the methods described in chapter 4. The last two columns are the covariate values and are average values for the cohort.

cohort	parameters		date of release	ave. flow (kcfs)
	r	σ		
5	4.70	7.45	112.9	73.3
6	5.04	7.83	114.8	77.0
7	5.18	7.77	116.9	82.4
8	6.23	9.26	121.2	96.1

Appendix 3. Computer code

A3.1. Introduction

This appendix contains computer code for selective algorithms. All algorithms are written in the C programming language, “traditional” or Kernighan and Ritchie (1978) version. I compiled the code with a Sun C compiler, but other compilers will also be compatible.

A3.2. Analysis of continuous travel time data

This first section contains the code to undertake the analysis of travel time data performed in chapter 4. The code is contained in 5 files, and a data file must be supplied. Before providing the code, I will briefly discuss the structure of the files and the routines contained within. I will also provide a sample data file and the output generated from the code with the sample data file.

`main.c` – contains the routine `main()` that controls the program by calling other routines. This routine also reads in the data file.

`mle.c` – contains the routines `r_mle()` and `sig_mle()` that compute maximum likelihood estimates of r and σ .

`conf_int.c` – contains the routines `r_mle()` and `sig_mle()` that determine $(1 - \alpha) \cdot 100$ percent confident intervals for the parameters and prints them out.

`cumulative.c` – contains the routine `cumulative()` that converts the travel time data to cumulative travel time based on the model and estimates parameters.

`chi.c` – contains the routine `chi()` that performs the goodness-of-fit test and prints out the results. This routine must be provided with a vector of cumulative travel times.

main.c

```

#include <stdio.h>

floatr_mle();
floatsig_mle();
void confidence_intervals();
floatcumulative();
void chi();

void main()
{
    float length; /* length of the reach */
    int num; /* number of individuals */
    char junk[12]; /* place to put header info from data file */
    float* tt_vec; /* vector to store travel time data */
    float* cum_tt_vec; /* vector for values from tt cdf */
    int i; /* increment for tt vector */
    floatr, sig; /* model parameters */
    float alpha; /* 1 - alpha is width of conf. intervals */
    int pars; /* # of parameters used in the model */
    FILE* data; /* pointer to data file */

    data = fopen("tt.data", "r");

    fscanf(data, "%s%f", junk, junk, &length);
    fscanf(data, "%s%d", junk, junk, &num);
    fscanf(data, "%s", junk, junk);

    /* allocate memory for the travel times vectors */
    tt_vec = (float *) malloc(num*sizeof(float));
    cum_tt_vec = (float *) malloc(num*sizeof(float));

    /* read in travel times from data file */
    for(i = 0; i < num; ++i)
        fscanf(data, "%f", &tt_vec[i]);

    /* compute maximum likelihood estimates */
    r = r_mle(tt_vec, length, num);
    sig = sig_mle(tt_vec, length, num);
    printf("mle r = %6.3f\n", r);
    printf("mle sig = %6.3f\n", sig);

    /* 95% confidence interval */
    alpha = 0.05;
    confidence_intervals(r, sig, length, num, alpha);

    /* X-squared goodness-of-fit test */
    /* the test needs values from the cumulative dist. func. */

```

```

for(i = 0; i < num; ++i)
    cum_tt_vec[i] = cumulative(r, sig, length, tt_vec[i]);

pars = 2; /* number of parameters used by the model */
chi(cum_tt_vec, pars, num);

fclose(data);
}

```

mle.c

```

#include <math.h>

/* computes maximum likelihood estimate for the parameter r */
/* based on the travel time data */
float    r_mle(tt_vec, pool_length, num)
    float    *tt_vec;    /* vector of travel times for group */
    float    pool_length;
    int      num;        /* number of individuals in group */
{
    float    tt_bar = 0; /* average travel time */
    int      i;

    for (i = 0; i < num; ++i){
        tt_bar += tt_vec[i];
    }

    tt_bar = tt_bar/num;

    return(pool_length/tt_bar);
}

/* computes maximum likelihood estimate for the parameter sigma */
/* based on the travel time data */
float    sig_mle(tt_vec, pool_length, num)
    float    *tt_vec;
    float    pool_length;
    int      num;
{
    float    tt_bar = 0; /* arithmetic mean */
    float    tt_recip = 0; /* harmonic mean */
    int      i;

    for (i = 0; i < num; ++i){
        tt_bar += tt_vec[i];
    }
}

```

```

        tt_recip += 1.0/tt_vec[i];
    }
    tt_bar = tt_bar/num;
    tt_recip = tt_recip/num;

    return(pool_length * sqrt(tt_recip - (1.0/tt_bar)));
}

```

conf int.c

```

#include <math.h>
#include <stdio.h>

/* This routine is passed the maximum likelihood estimates for r */
/* and sigma, reach length, number of fish and alpha. It prints */
/* 100*(1-alpha) percent confidence intervals for the parameters */
/* r and sigma. The appropriate quantiles of the Student's t and */
/* chi-square are obtained from S-plus, which is provided with */
/* the degrees of freedom. */

void    confidence_intervals(r, s, L, num, alpha)
    float    r, s; /* mles of r and sigma */
    float    L; /* reach length */
    int      num; /* number of individuals */
    float    alpha; /* 1-alpha is length of C.I. */
{
    float    r_min, r_max; /* min and max of r C.I. */
    float    sig_min, sig_max; /* min and max of sigma C.I. */
    float    a, b; /* quantiles used in C.I. calc. */
    char     junk[10]; /* junk from input file */
    FILE     *iptr, *optr; /* input and output files */

    /* provide degrees of freedom and alpha for S-plus routine */
    optr = fopen(".quant_info", "w");
    fprintf(optr, "%d\t%f\n", num - 1, alpha);
    fclose(optr);

    /* execute S-plus routine that prints quantiles to a file */
    system("S < quantile.s > /dev/null");

    /* open file and read in (1.0-alpha/2)th quantile of t dist. */
    iptr = fopen(".quantile", "r");
    fscanf(iptr, "%s%f", junk, &a);

    /* compute max and min values of r C.I. */
    r_min = r*(1.0 - a*sqrt((s*s)/(r*L*(num-1))));

```

```

r_max = r*(1.0 + a*sqrt((s*s)/(r*L*(num-1))));

/* print r C.I. */
printf("%4.1f percent confidence interval for r:\n",
       100*(1.0-alpha));
printf("(%6.2f,%6.2f)\n", r_min, r_max);

/* read (alpha/2)th and (1-alpha/2)th quantiles of chi-sq.
dist. */
fscanf(iptr,"%s%f", junk, &a);
fscanf(iptr,"%s%f", junk, &b);

/* compute max and min values of sig C.I. */
sig_min = s*sqrt((float)(num)/a);
sig_max = s*sqrt((float)(num)/b);

/* print sigma C.I. */
printf("%4.1f percent confidence interval for sigma:\n",
       100*(1.0-alpha));
printf("(%6.2f,%6.2f)\n", sig_min, sig_max);
}

```

cumulative.c

```

#include <math.h>
#include "input.h"

#define pi3.1415

/* phi is the cumulative distribution for a standard normal */
float phi(x)
float x;
{
    return(0.5 + erf(x/sqrt(2.0))/2);
}

/* this routine returns a value from the cumulative distribution */
/* of the basic travel time model. The routine must be passed */
/* the model parameters and the travel time. The procedure for */
/* generating the value is described in appendix 4.a */
float cumulative(r, sig, L, t)
    float r, sig, L; /* model parameters */
    float t; /* travel time */
{
    float mu, lam; /* reparameterization */
    float first, second;

```

```

double      y, z;
double      z2, z4;
double      fac1, fac2;
float       d0 = 0.2316419;
float       d1 = 0.319381530;
float       d2 = -0.356563782;
float       d3 = 1.781477937;
float       d4 = -1.821255978;
float       d5 = 1.330274429;
float       qz, qz2, qz4;

mu = L/r;
lam = L/sig;

y = lam*(t-mu)/(mu*sqrt(t));
z = lam*(t+mu)/(mu*sqrt(t));

if (z<4){
    qz = 1/(1+d0*z);
    qz2 = qz*qz;
    qz4 = qz2*qz2;

    fac1 = (exp(-(y*y)/2))/(sqrt(2*pi));
    fac2 = (d1*qz + d2*qz2 + d3*qz2*qz
            + d4*qz4 + d5*qz4*qz);
}
if (z>=4){
    z2 = z*z;
    z4 = z2*z2;

    fac1 = (exp(-(y*y)/2))/(sqrt(2*pi))/z;
    fac2 = 1 - 1/z2 + 3/z4 - 3*5/(z2*z4) + 3*5*7/(z4*z4)
            - 3*5*7*9/(z4*z4*z2) + 3*5*7*9*11/(z4*z4*z4)
            - 3*5*7*9*11*13/(z4*z4*z4*z2);
}
second = fac1*fac2;
first = phi(y);

return(first + second);
}

```

chi.c

```

#include <math.h>
#include <stdio.h>

```

```

float    gammp(); /* This routine is from Numerical Recipes in C */
          /* Press, et al. 1988 */

void     chi(cum_vec, params, num_fish)
float    *cum_vec; /* vector cdf values of tt dist. */
int      params; /* number of parameters estimated */
int      num_fish; /* number of individuals */
{
  int     num_bins; /* number of bins */
  float   bin_width; /* width of each bin */
  float   expect; /* expected individuals per bin */
  int     *obs; /* vector of observed individuals */
  int     i; /* counter */
  float   X = 0.0; /* chi square statistic */
  float   prob; /* chi square probability */
  int     df; /* degrees of freedom */

  /* num_bins is determined by Mann-Wald calculation */
  num_bins = (int)(3.76*pow((float)(num_fish), 0.4) );

  bin_width = 1.0/num_bins;
  expect = bin_width*num_fish;

  /* allocate memmory for vector of observed values and set */
  /* each element to zero */
  obs = (int *) malloc(num_bins*sizeof(int));
  bzero((char *) obs, num_bins*sizeof(float));

  /* determine which bin each individual falls into */
  for ( i = 0; i < num_fish; ++i)
    ++obs[(int)(cum_vec[i]/bin_width)];

  /* compute chi square statistic */
  for ( i = 0; i < num_bins; ++i)
    X += ((expect-obs[i])*(expect-obs[i]))/expect;

  df = num_bins - params - 1;

  /* compute percentile of chi-square distribution */
  prob = gammp((float)(df)/2.0, X/2.0);

  printf("\nX-squared goodness-of-fit test\n");
  printf("X-squared = %7.3f\n", X);
  printf("degrees of freedom = %3d\n", df);
  printf("p = %7.3f\n", 1.0 - prob);
}

```

sample data file

```

reach length: 52.0
num fish: 57
travel times:
15.74 12.06 30.63 24.79 17.54
26.39 14.87 9.25 4.83 12.32
14.61 9.08 20.34 7.74 16.98
3.99 10.69 23.38 20.02 19.74
22.66 24.62 20.62 18.24 22.48
10.76 12.01 9.99 6.34 21.47
18.09 22.25 15.74 13.68 5.11
10.35 10.41 22.41 8.21 36.66
21.45 13.17 18.64 18.69 11.85
20.57 34.52 15.73 9.46 37.39
21.53 92.03 33.30 21.67 21.94
21.45 8.23

```

program output

```

mle r = 2.773
mle sig = 7.251

95.0 percent confidence interval for r:
( 2.33, 3.22)
95.0 percent confidence interval for sigma:
( 6.18, 8.97)

X-squared goodness-of-fit test
X-squared = 22.263
degrees of freedom = 15
p = 0.101

```

A3.3. inverse Gaussian random variate

The details of this procedure are contained in Chapter 4, appendix d.

Inverse gaussian random variate

```
#include <math.h>
```

```

double drand48();
void srand48();

/* returns a random variate from the standard normal */
/* distribution. Taken from Numerical Recipes in C. */
double normal()
{
    static int iset = 0;
    static double gset;
    double fac, r, v1, v2;

    if (iset == 0){
        do {
            v1 = 2.0 * drand48() - 1.0;
            v2 = 2.0 * drand48() - 1.0;
            r = v1*v1 + v2*v2;
        } while (r >= 1.0);
        fac = sqrt(-2.0 * log((float)r)/(float)r);
        gset = v1 * fac;
        iset = 1;
        return v2*fac;
    } else {
        iset = 0;
        return gset;
    }
}

/* returns a random variate from the Inverse Gaussian */
/* distribution. Details of the algorithm are contained in */
/* appendix 4.d. */
float travel(mu,lam)
    float mu, lam; /* model parameters */
{
    float n, v, w, c, x;
    float p;

    n = normal();
    v = n*n;
    w = mu*v;
    c = mu/(2.0*lam);

    x = mu + c*(w - sqrt(w*(4.0*lam + w)));
    p = mu/(mu + x);

    if (p > drand48()) return(x);
    else return(mu*mu/x);
}

```